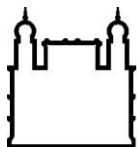**INSTITUTO CARLOS CHAGAS**

DOUTORADO EM BIOCIÊNCIAS E BIOTECNOLOGIA

FERNANDA TOMIOTTO PELLISSIER

CARACTERIZAÇÃO DE CÉLULAS E MEDIADORES ENVOLVIDOS NA PATOGÊNESE DA LESÃO CAUSADA POR *LEISHMANIA AMAZONENSIS* EM MODELO EXPERIMENTAL

CURITIBA
2021

Ministério da Saúde

FIOCRUZ
Fundação Oswaldo Cruz

INSTITUTO CARLOS CHAGAS
Doutorado em Biociências e Biotecnologia

FERNANDA TOMIOTTO PELLISSIER

CARACTERIZAÇÃO DE CÉLULAS E MEDIADORES ENVOLVIDOS NA PATOGÊNESE DA LESÃO CAUSADA POR *LEISHMANIA AMAZONENSIS* EM MODELO EXPERIMENTAL

Tese apresentada ao Programa de Pós-Graduação em Biociências e Biotecnologia do Instituto Carlos Chagas como parte dos requisitos para obtenção do título de Doutora em Biociências e Biotecnologia.

Orientador: Dr. Wander Rogério Pavanelli
Co-orientador: Dr. Juliano Bordignon

CURITIBA
2021

Tomiotto Pellissier, Fernanda.

Caracterização de células e mediadores envolvidos na patogênese da lesão causada por *Leishmania amazonensis* em modelo experimental / Fernanda Tomiotto Pellissier. - Curitiba, 2021.
176 f.

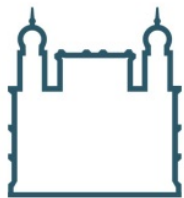(Doutorado) – Instituto Carlos Chagas, Pós-Graduação em Biociências e Biotecnologia, 2021.

Orientador: Wander Rogério Pavanelli .
Co-orientador: Juliano Bordignon .

Bibliografia: Inclui Bibliografias.

1. Leishmaniose.. 2. Macrófagos. . 3. Arginase-1. 4. iNOS.. 5. Colágeno. I. Título.

Ata da Sessão Pública de exame de tese para obtenção do grau de Doutora em

Biociências e Biotecnologia.

Aos 03 dias do mês de março de dois mil e vinte um, às 9:00 horas, através de teleconferência https://us02web.zoom.us/j/5953384663?pwd=NEo3T09MTEFZSlFHeEJHMzhMTEFhQT09 , reuniu-se a Banca Examinadora designada pelo Colegiado do Programa de Pós-Graduação em Biociências e Biotecnologia, composta pelos Professores: Dra. Letusa Albrecht, Dra. Carolina Panis e Dra. Ivete Conchon Costa, com a finalidade de julgar a tese da candidata **Fernanda Tomiotto Pellissier**, intitulada: **"CARACTERIZAÇÃO DE CÉLULAS E MEDIADORES ENVOLVIDOS NA PATOGÊNESE DA LESÃO CAUSADA POR LEISHMANIA AMAZONENSIS EM MODELO EXPERIMENTAL",** sob a orientação de Dr. Wander Rogério Pavanelli e Co -orientação de Dr. Juliano Bordignon, para obtenção do grau de **Doutora** em Biociências e Biotecnologia. A candidata teve até 45 (quarenta e cinco) minutos para a apresentação, e cada examinador teve um tempo máximo de arguição de 30 (trinta) minutos, seguido de 30 (trinta) minutos para resposta do (a) candidato(a) ou de 60 (sessenta) minutos quando houve diálogo na arguição. O desenvolvimento dos trabalhos seguiu o roteiro de sessão de defesa, estabelecido pela Coordenação do Programa, com abertura, condução e encerramento da sessão solene de defesa feito pelo(a) Presidente **Dra. Letusa Albrecht.** Após haver analisado o referido trabalho e arguido a candidata, os membros da banca examinadora deliberaram pela:

(X) Aprovação da tese por unanimidade

( ) Aprovação somente após satisfazer as exigências de modificações no prazo fixado pela banca (não superior a noventa dias).

( ) Reprovação da tese

 Na forma regulamentar foi lavrada a presente ata que é abaixo assinada pelos membros da banca, na ordem acima determinada, e pela candidata.

Curitiba, 03 de março de 2021

Dra. Dra. Letusa Albrecht – ICC/PR

Dra. Dra. Carolina Panis – UNIOESTE

Dra. Dra. Ivete Conchon Costa – UEL

Candidato(a): Fernanda Tomiotto Pellissier

+55(41)3316-3230
Rua Prof. Algacyr Munhoz Mader, 3775 - CIC 81350-010 Curitiba/PR, Brasil

Ministério da Saúde
FIOCRUZ - PARANÁ
Instituto Carlos Chagas

iv

À minha eternamente amada avó
Ilma Rossi Tomiotto.

AGRADECIMENTOS

À Deus, quem me trouxe até aqui, me instruiu e colocou pessoas maravilhosas ao meu redor. Ao Senhor, minha eterna gratidão.

Ao meu orientador, Dr. Wander Rogério Pavanelli, que me acolheu em seu laboratório no meu primeiro ano de graduação. Professor, depois de tantos anos trabalhando juntos, só posso te agradecer. Você acompanhou meu crescimento e fez parte dele. Obrigada pelos conselhos, incentivo e até pelas brigas durante todos estes anos. Isso tudo contribuiu muito para o meu desenvolvimento profissional e pessoal.

Ao meu co-orientador, Dr. Juliano Bordignon por toda a disponibilidade e prestatividade. Obrigada por não medir esforços sempre que precisei, pelas revisões críticas e orientações ao longo dos últimos quatro anos.

À minha banca de acompanhamento, Drª. Letusa Albrecht e Dr. Guilherme Ferreira Silveira, que foram essenciais no direcionamento deste trabalho. Obrigada pela mentoria e por todas as discussões.

À Drª. Ivete Conchon Costa, que me abriu as portas de seu laboratório e me recebeu de braços abertos. Obrigada por tantos ensinamentos, conselhos e incentivos, ter a senhora do meu lado é uma grande honra. Obrigada por me ensinar também tanto sobre a profissão da docência, sua paixão é uma inspiração para mim.

À Drª. Milena Menegazzo Miranda Sapla pela amizade, apoio e pelo papel fundamental no desenvolvimento de todas as etapas deste trabalho. Obrigada pela companhia nas noites de experimentos, pelos fim de semana escrevendo comigo e por me ensinar tanto.

À Drª. Idessania Nazareth Costa pela oportunidade de trabalhar com toxoplasmose e ampliar meus horizontes, por confiar em meu trabalho e capacidade durante todos esses anos.

À banca examinadora composta pela Drª. Letusa Albrecht, Drª. Ivete Conchon Costa e Drª. Carolina Panis, bem como à banca suplente composta pela Drª. Pryscilla Fanini Wowk e Dr. Guilherme Ferreira Silveira, por aceitarem participar desse momento.

Aos colegas de laboratório que foram parte ativa na construção de minha vida acadêmica e deixaram a rotina mais leve e divertida. Em especial à Ms. Manoela Gonçalves, Ms. Taylon Felipe Silva, Ms. Ana Carolina Jacob, Ms. Mariana Detoni, Ms. Raquel Sanfelice e Ms. Virgínia Concato. Agradeço também à minha querida Ms.

Não andem ansiosos por coisa alguma, mas em tudo, pela oração e súplicas, e com ação de graças, apresentem seus pedidos a Deus.
E a paz de Deus, que excede todo o entendimento, guardará os seus corações e as suas mentes em Cristo Jesus.

Filipenses 4:6,7

RESUMO

A leishmaniose cutânea é uma doença infecciosa zoonótica com ampla distribuição mundial. Parasitos do gênero *Leishmania* são os agentes etiológicos da doença, sendo que diferentes espécies podem desencadear manifestações clínicas que variam desde infecções autocuráveias à lesões crônicas desfigurantes. Os macrófagos são as células hospedeiras finais dos parasitos, e células chave para o direcionamento da resposta imune que culmina em manifestações clínicas. M1 e M2 são os dois principais fenótipos de macrófagos. M1 é um subtipo pró-inflamatório com propriedades microbicidas, e M2 é um subtipo antiinflamatório/regulador que está relacionado à resolução da inflamação e reparo tecidual. No entanto, o entendimento da resposta imune efetiva à infecção por esses protozoários ainda apresenta muitas lacunas, cuja compreensão pode ser fundamental para o potencial desenvolvimento de drogas e vacinas. Assim, investigamos as moléculas e mediadores locais envolvidos no desenvolvimento da lesão cutânea em modelos experimentais de suscetibilidade (BALB/c) e resistência parcial (C57BL/6) à infecção por *Leishmania amazonensis*. Verificou-se que camundongos BALB/c apresentaram pior evolução da doença em comparação com camundongos C57BL/6, com maior carga parasitária e níveis elevados de IL-6, enquanto C57BL/6 apresentaram maiores níveis de INF-γ e O_2^- após 11 semanas de infecção. Um pico de macrófagos locais foi observado após 24h de infecção em ambas as linhagens de camundongos estudadas, seguido por um novo aumento após 240h apenas em camundongos C57BL/6. Quando os marcadores de macrófagos M1 e M2 (iNOS, MHC-II, CD206 e arginase-1 [Arg-1]) foram analisados, foi identificado um aumento pronunciado nos níveis de Arg-1 em BALB/c após 11 semanas de infecção, enquanto em C57BL/6 houve predomínio de marcadores M2 coincidindo com um segundo pico de infiltração macrofágica em 240h, e com maior deposição de colágeno tipo III e resolução da lesão. Para confirmar que os resultados obtidos estavam relacionados à presença de macrófagos e sua capacidade de controlar a infecção, foi realizada a transferência adotiva de macrófagos peritoneais de C57BL/6 para BALB/c infectados. Os dados obtidos na 11ª semana revelaram que a transferência de macrófagos promoveu redução do edema e do número de parasitos no local da lesão, além de reduzir os níveis de Arg-1 sem afetar os níveis de iNOS. Assim, pode-se concluir que camundongos C57BL/6 têm uma melhor evolução da infecção causada por *L. amazonensis*, baseada em um balanço entre inflamação e resposta antioxidante, coincidindo com maior deposição de colágeno e melhor reparo tecidual, enquanto camundongos BALB/c apresentam elevados níveis de Arg-1 nos tempos tardios de infecção, marcador relacionado ao desenvolvimento e gravidade da doença. A pior evolução parece estar envolvida com o recrutamento de macrófagos ricos em Arg-1, uma vez que a transferência adotiva de macrófagos de camundongos C57BL/6 para BALB/c resultou em melhor evolução de lesão, com menores níveis de Arg-1.

Palavras-chave: Leishmaniose; Macrófagos; M1; M2; Arginase-1; iNOS; Colágeno.

ABSTRACT

Cutaneous leishmaniasis is a zoonotic infectious disease with broad world distribution. *Leishmania* parasites are the etiologic agents of the disease, and different species can trigger clinical manifestations ranging from self-curing infections to disfiguring chronic lesions. Macrophages are the final host cells for the parasites and key cells for the immune response and clinical manifestations. M1 and M2 are the two main macrophage phenotypes. M1 is a pro-inflammatory subtype with microbicidal properties, and M2 is an anti-inflammatory/regulatory subtype related to inflammation resolution and tissue repair. However, the understanding of the effective immune response to *Leishmania* infection still has many gaps, which may be fundamental to the potential development of drugs and vaccines. Thus, we investigated the molecules and local mediators involved in the development of the skin lesion in experimental models of susceptibility (BALB/c) and partial resistance (C57BL/6) to *Leishmania amazonensis* infection. BALB/c mice had a worse disease outcome compared to C57BL/6 mice, with almost 15 times higher parasitic load, ulcerated lesion formation, and higher levels of IL-6, while C57BL/6 presented higher levels of INF-γ and O_2^- after 11 weeks of infection and no lesion ulcerations. A peak of local macrophages was observed after 24h of infection in both studied mice strains, followed by a further increase after 240h only in C57BL/6 mice. When the M1 and M2 macrophage markers (iNOS, MHC-II, CD206, and arginase-1 [Arg-1]) were analyzed, we found that in BALB/c there was a pronounced increase in Arg-1 levels after 11 weeks of infection, whereas in C57BL/6 there was an initial predomination of markers from both profiles, followed by an M2 predominance, that coincided with the second peak of macrophage infiltration, 240h after the infection, greater deposition of type III collagen and lesion resolution. To confirm that the results obtained were related to the presence of macrophages and their ability to control the infection, we carried out an adoptive transfer of these cells from C57BL/6 to infected BALB/c. The data obtained at the 11th week revealed that the adoptive transfer of macrophages promoted a reduction in edema and number of parasites at the lesion site, besides inducing lower levels of Arg-1 without affecting the iNOS levels. Thus, C57BL/6 mice have a more effective response against *L. amazonensis*, based on a balance between inflammation and antioxidant response, coinciding with better tissue repair, while BALB/c mice have an excessive Arg-1 production in late infection times, which is related to the development of disease severity. The worst evolution seems to be involved with the recruitment of Arg-1 related macrophages, since the adoptive transfer of macrophages from C57BL/6 mice to BALB/c resulted in better outcomes, with lower levels of Arg-1.

Keywords: Leishmaniasis; Macrophages; M1; M2; Arginase-1; iNOS; Collagen.

LISTA DE ILUSTRAÇÕES

LISTA DE TABELAS

SUMÁRIO

1. INTRODUÇÃO

1.1. Capítulo 1

Polarização de Macrófagos na Leishmaniose: Ampliando os Horizontes
Macrophage Polarization in Leishmaniasis: Broadening Horizons

Fernanda Tomiotto-Pellissier, Bruna Taciane da Silva Bortoleti, João Paulo Assolini, Manoela Daiele Gonçalves, Amanda Cristina Machado Carloto, Milena Menegazzo Miranda-Sapla, Ivete Conchon-Costa, Juliano Bordignon, Wander Rogério Pavanelli

As Leishmanioses são um grupo de doenças causadas por parasitos de mais de 20 espécies do gênero *Leishmania*, transmitidas aos seres humanos pela picada de flebotomíneos infectados. Mais de 700.000 novos casos são registrados anualmente, com 20.000 a 30.000 mortes anuais. As doenças se manifestam como diferentes formas clínicas, refletindo principalmente a diversidade de espécies do parasito e a resposta imune do hospedeiro.

Macrófagos são as principais células hospedeiras do parasito e a chave no desencadeamento de uma resposta protetora ou prejudicial do hospedeiro frente à infecção. Nas últimas décadas foi descrita a plasticidade de macrófagos em relação ao tipo de resposta desenvolvida, sendo subdivididos em dois grupos, denominados M1 e M2. Macrófagos M1, ou ativados classicamente, são aqueles detentores de características pró-inflamatórias, com grande potencial microbicida, enquanto macrófagos M2, ou alternativamente ativados, são células com características anti-inflamatória/regulatória.

Apesar dos avanços no conhecimento do papel de macrófagos M1 e M2 em diferentes doenças infecciosas, ainda pouco é descrito sobre suas funções no

desenvolvimento da Leishmaniose. Neste sentido, foi realizada uma extensa busca na literatura, visando a compilação dos dados envolvendo leishmanioses e polarização macrofágica, subdividida nas seguintes seções:

1) Introdução – consistindo em uma apresentação das Leishmanioses, suas manifestações clínicas, epidemiologia, ciclo biológico do parasito e resposta imune desenvolvida pelo hospedeiro.

2) Uma visão geral sobre macrófagos M1 e M2 – tratando das funções básicas dos macrófagos e interação com células da imunidade inata e adaptativa, seguida por discussão da plasticidade de macrófagos e polarização em M1 e M2. Além disso, esta seção trata das funções de macrófagos M1 e M2, bem como as citocinas, quimiocinas, fatores de transcrição, receptores, genes transcritos e interação celular de cada subtipo.

3) Interação da saliva do vetor com as células imunes – descrevendo o papel da saliva do inseto vetor no estabelecimento e curso da infecção, modulando a resposta imune e o padrão de moléculas dos macrófagos.

4) Macrófagos M1 e M2 na Leishmaniose – onde são apresentados os estudos *in vitro* e *in vivo* que correlacionam diretamente a o papel de macrófagos polarizados (M1/M2) na infecção por *Leishmania*, ou indiretamente, tratando da importância de moléculas envolvidas na polarização frente à infecção. Além disso, são apresentados trabalhos que sugerem estratégias terapêuticas para modular moléculas-chave no controle da atividade celular, induzindo determinado padrão de resposta. Nesta seção foram considerados estudos envolvendo as espécies de *Leishmania* que causam as formas viscerais e cutânea da doença.

A referida revisão bibliográfica, publicada no periódico *Frontiers in Immunology* trata de maneira ampla o estado da arte da temática da presente tese de doutorado "Modulação Macrofágica na Leishmaniose". Desta forma, a mesma, diante da aprovação do colegiado da Pós-Graduação em Biociências e Biotecnologia e da banca de Qualificação, constitui o capítulo primeiro da presente tese de doutorado, substituindo o capítulo tradicionalmente intitulado "Introdução".

Macrophage Polarization in Leishmaniasis: Broadening Horizons

Fernanda Tomiotto-Pellissier [1,2], Bruna Taciane da Silva Bortoleti [1,2], João Paulo Assolini [2], Manoela Daiele Gonçalves [3], Amanda Cristina Machado Carloto [2], Milena Menegazzo Miranda-Sapla [2], Ivete Conchon-Costa [2], Juliano Bordignon [1,4*] and Wander Rogério Pavanelli [1,2*]

[1] Biosciences and Biotechnology Postgraduate Program, Carlos Chagas Institute (ICC), Fiocruz, Curitiba, Brazil, [2] Laboratory of Immunoparasitology, Department of Pathological Sciences, State University of Londrina, Londrina, Brazil, [3] Laboratory of Biotransformation and Phytochemistry, Department of Chemistry, State University of Londrina, Universitary Hospital, Londrina, Brazil, [4] Laboratory of Molecular Virology, Carlos Chagas Institute (ICC), Fiocruz, Curitiba, Brazil

Leishmaniasis is a vector-borne neglected tropical disease that affects more than 700,000 people annually. *Leishmania* parasites cause the disease, and different species trigger a distinct immune response and clinical manifestations. Macrophages are the final host cells for the proliferation of *Leishmania* parasites, and these cells are the key to a controlled or exacerbated response that culminates in clinical manifestations. M1 and M2 are the two main macrophage phenotypes. M1 is a pro-inflammatory subtype with microbicidal properties, and M2, or alternatively activated, is an anti-inflammatory/regulatory subtype that is related to inflammation resolution and tissue repair. The present review elucidates the roles of M1 and M2 polarization in leishmaniasis and highlights the role of the salivary components of the vector and the action of the parasite in the macrophage plasticity.

Keywords: classical macrophage, non-classical macrophage, vector saliva, *Leishmania*, immunomodulation, chemokine

INTRODUCTION

Leishmaniasis is a broad term that is used for a group of vector-borne diseases caused by species of protozoan parasites of the *Leishmania* genus of which 18 spp. are pathogenic to humans (1). The disease presents in five main clinical forms: visceral leishmaniasis (VL, or kala-azar), cutaneous leishmaniasis (CL), mucocutaneous leishmaniasis (MCL), diffuse cutaneous leishmaniasis (DCL) and post-kala-azar dermal leishmaniasis (PKDL) (2). All types of leishmaniases are transmitted to an animal or human reservoir through the bite of female infected phlebotomine sand flies, which infect a range of 70 animal species, including humans, rodents, and canids in their transmission cycle (3).

The World Health Organization (WHO) classifies leishmaniasis as a neglected tropical disease because it is directly linked to economically disadvantaged populations in tropical regions (2). A total of 700,000 to one million cases of leishmaniasis occur annually in 102 countries, areas or territories worldwide, with 20,000–30,000 deaths (3).

The high prevalence of this disease is directly influenced by the success of long host–parasite coevolutionary process in which parasites *Leishmania* have the ability to manipulate the vertebrate immune system in their favor, through the synthesis of parasites molecules, but also by vector saliva molecules, which are injected into the blood-feeding site during transmission (4).

The *Leishmania* parasites exhibit a biological digenetic life cycle with variable morphology that alternates between two main distinct developmental stages: the free-living flagellated promastigote form found in the midgut of phlebotomine sandfly vectors and the obligate intracellular aflagellated amastigotes in phagolysosomal vesicles of the vertebrate phagocytic cells, mainly into macrophages (5, 6).

During the blood feeding of the infected sandfly, which inoculates the host with metacyclic promastigotes and a large portion of the salivary content of the insect. Phlebotomine saliva is composed of pharmacologically active components with anti-hemostatic, chemotactic and immunomodulatory properties, that directly influence the parasite infection process modulating the local immune response (7). At the site of the bite occurs a rapid and intense neutrophil infiltration after inoculation, followed by monocytes/macrophages (8, 9).

Neutrophils primarily phagocytize most (80–90%) of the parasites and produce chemokines and cytokines that recruit and activate different cell types to regulate the development of the adaptive immune response during *Leishmania* sp. infection (8). Neutrophils are important components of the initial immune response against *Leishmania* parasites, even though there are currently contradictory findings on their role in the *Leishmania* infection.

Although the effective participation of neutrophils in the elimination of the parasite has been reported for *L. braziliensis, L. amazonensis* (10–15) and *Leishmania donovani* (16), collectively, most of these studies reported that the leishmanicidal action of neutrophils is clearly insufficient to control the establishment of infection and the development of the disease [reviewed in (17)].

Subversion of neutrophil killing functions by *Leishmania* is a strategy that allows parasite spreading in the host with a consequent infection evolution, transforming the primary protective role of neutrophils into a deleterious one. Neutrophils do not eliminate the parasite but act as "Trojan horses," becoming late apoptotic and rapidly internalized by macrophages and dendritic cells, increasing the infectivity and persistence of the parasite (18, 19).

Macrophages play a dual role in *Leishmania* infection. These cells are responsible for the destruction of internalized parasites but also provide a safe place for *Leishmania* replication. Therefore, macrophages are key to disease progression and the success or failure of the infection depends on the interplay between infecting *Leishmania* species and the type and magnitude of the host's immune response. Both of these factors are closely related to the clinical forms of leishmaniasis (20, 21).

Abbreviations: Arg, arginase; CL, cutaneous leishmaniasis; IL, interleukin; IFNγ, interferon gamma; IGF1, insulin-like growth factor 1; iNOS, inducible nitric oxide synthase; LPS, lipopolysaccharide; Max, maxadilan; MCL, mucocutaneous leishmaniasis; mTOR, mammalian target of rapamycin; NO, nitric oxide; PKDL, post-kala-azar dermal leishmaniasis; PPAR, proliferator-activated receptors; PSG, promastigote secretory gel; ROS, reactive oxygen species; SGE, salivary gland extract; SGH, salivary gland homogenate; SGL, salivary gland lysate; TACI, transmembrane activator and calcium modulator and cyclophilin ligand interactor; TGFβ, transforming growth factor beta; Th, T helper; TLR, toll like receptor; TNFα, tumor necrosis factor alpha; Treg, T regulatory; and VL, visceral leishmaniasis.

Macrophages are normally at rest as naïve macrophages (M0), but the microenvironment in which these cells are found provides different signals that activate them and lead to the development of functionally distinct macrophage's phenotype, toward "classically activated" (M1) or "alternatively activated" (M2) with different disease outcomes (22, 23). Therefore, the activation of M1 macrophages by Th1 lymphocyte subpopulation, which produces various cytokines, primarily interferon gamma (IFN-γ) and tumor necrosis factor-alpha (TNF-α) is crucial for the elimination of this intracellular pathogen via the triggering of an oxidative burst. The host cells increase the production of reactive oxygen species (ROS), including superoxide, hydrogen peroxide, and hydroxyl radicals, and nitric oxide (NO), which exhibit high microbicidal capacity (20, 22).

In contrast, the activation of Th2 lymphocytes, which produce IL-4 and IL-13 cytokines, induces the M2 profile caracterized by polyamine biosynthesis via activation of the enzyme arginase (arg) and production of urea and *L*-ornithine, which are beneficial for *Leishmania* intramacrophage growth favoring parasite survival in the infected macrophages and disease progression (22, 24).

Different *Leishmania* species trigger distinct immune responses (25). These responses are far beyond the classical Th1/Th2 paradigm (26) and increase the interest in understanding the role of M1 and M2 macrophages in the context of different *Leishmania* species infection. The immunomodulatory influence of the saliva of different leishmaniasis vectors should also be considered in the differential recruitment/activation of macrophages subtypes.

It is known how important macrophages are in the resistance or susceptibility to *Leishmania* infection, therefore we reviewed the impact of macrophage plasticity and M1 and M2 phenotypes on infection outcome. We also consider the role of vector saliva, which is a well-established immunomodulatory element in the *Leishmania* infection, in macrophage plasticity and phenotype.

M1 AND M2 MACROPHAGES: AN OVERVIEW

Macrophages are phagocytic cells that are found in several tissues. In innate immunity, macrophages are responsible primarily for the control of pathogens and in adaptive immunity, this cell participates in the recognition, processing, and presentation of antigens to T cells (27). Macrophages interact with T and B cells via intercellular contact and the production of molecules and mediators to participate in the inflammatory response and tissue repair (27).

Two main macrophages phenotypes are known, M1 and M2 (28). The M1, or the classically activated macrophage, is a pro-inflammatory subtype that exhibits microbicidal properties (29). The M2, or the alternatively activated macrophage, is an anti-inflammatory/regulatory subtype that plays a role in the resolution of inflammation and tissue repair (30). The polarization of macrophages into M1 and M2 phenotypes is

4

dependent on the signals provided by the microenvironment (28, 30, 31).

The designations M1 and M2 originated from Th1 and Th2 cytokine patterns and are associated with the change in macrophage phenotypes (32). Macrophage subtypes also differ in the production of cytokines, chemokines and other mediators and the expression of receptors, surface molecules, and transcription factors, which can act as specific markers to aid in the identification and function of these cells (27, 29, 32–34).

M1 macrophages are characterized by a high production of pro-inflammatory cytokines (TNF-α, IL-1β, IL-6, IL-12, IL-18, IL-23, and Type 1 IFN), high phagocytosis rate, and the production of reactive oxygen and nitrogen species and act to control intracellular pathogens. This macrophage subtype plays a role in tumor control, and it may be involved in autoimmune diseases and tissue damage (7, 27, 34–39).

M1 macrophages constitute the first line of defense against intracellular pathogens and induce the development of the Th1 response via IL-12 secretion (40, 41). The polarization of M1 macrophages may be primarily due to the presence of lipopolysaccharide (LPS), IFN-γ or TNF-α. Granulocyte-macrophage colony-stimulating factor (GM-CSF) may also result in the differentiation and maintenance of the M1 phenotype (41, 42). Ruan et al. (43) demonstrated that complement system activation is also related to M1 polarization.

M1 polarization activates transcription factors, such as AP1, STATs, NFκBp65 and IRFs, which lead to the expression of pro-inflammatory genes, costimulatory molecules and chemokines to attract various immune cells (**Table 1**) (7, 27, 34–39). IRF4 and IRF5 are involved in the polarization of M1 and M2 macrophages, but the role of IRFs in M2 polarization is not completely clear (44).

The alternatively activated macrophages, or M2, exhibit an anti-inflammatory/immunoregulatory phenotype that is related to tissue remodeling and repair, resistance to some parasites and the promotion of tumor growth (30, 45, 46). M2 was initially characterized by the expression of mannose receptor (CD206), but a range of markers and mediators produced by these cells were described, including important chemokines for the recruitment of different cells (**Table 1**) (37, 45, 47).

Different stimuli, such as IL-4/IL-13, IL-10, TGF-β, M-CSF, vitamin D3, and immunocomplexes, induce M2 macrophages (48, 49). Other cytokines, such as IL-21 and IL-33, may also act on macrophage polarization and maintenance to an M2 phenotype (50–52). Li et al. (52) demonstrated that IL-21 reduced the expression of CD86, iNOS, TLR-4, and IL-6 and TNF-α production via STAT3 phosphorylation. IL-33 amplifies IL-13-induced M2 polarization (50, 51).

The classification of M2 macrophages was recently expanded and subdivides these cells into four subtypes, M2a, M2b, M2c, and M2d, according to stimulus and function (23, 45). M2a macrophages are polarized by macrophage colony-stimulating factor (M-CSF) and IL-4 or IL-13. This subtype is characterized by arg-1, IL-10, and SOCS3 expression and produces CCL24, CCL17, and CCL22, which are responsible for the recruitment of eosinophils, basophils and Th2 cells. These cells are involved

in allergic reactions, parasite death and encapsulation, the promotion of fibrogenesis, tissue repair and cell proliferation (53–55).

The M2b phenotype is induced by the combination of immunocomplexes with IL-1βRa/TLR ligands, apoptotic cells or LPS. These cells secrete a large amount of IL-10 and inflammatory mediators, such as TNF-α and IL-6, and express iNOS (30, 53). M2b macrophages secrete the CCL1 chemokine, which results in the infiltration of eosinophils, Th2 lymphocytes and regulatory T cells (Tregs) (56). Therefore, M2b macrophages act as an immunoregulator and trigger activation of the Th2 response (23, 53).

M2c macrophage polarization results from IL-10, TGF-β and glucocorticoids (38, 57, 58). This subtype produces IL-10, TGF-β, CXCL13, CCL16, and CCL18, which leads to the down-regulation of pro-inflammatory cytokines and an increase in the recruitment of eosinophils and naïve T cells. M2c cells express high levels of arg-1, CD163, CD206, scavenger receptors, TLR1, TLR8, FPR1, CCR2, and CCR5, and this subtype is involved in tissue regeneration and angiogenesis (53–55, 59).

The M2d macrophage phenotype is involved in the inhibition of the immune response and the promotion of angiogenesis (60). These cells are induced by IL-6, toll-like receptor (TLR) ligands and adenosine A_{2A} receptor agonists (60, 61). Stimulation with adenosine may result in the polarization of M1 macrophages to M2d (53, 61). This phenotype expresses high levels of IL-10, VEGF, and iNOS and secretes CCL5, CXCL10, and CXCL6 and low levels of IL-12 and TNF-α (53, 60–63).

Signals of the microenvironment are of great importance of the change in the polarization state of macrophages, and the programming from one phenotype to another is closely related to the activation of specific transcription factors and microRNAs (miRNAs) (64, 65). miRNAs are small molecules of non-coding RNAs which can act on gene expression at the post-transcriptional level (64), regulating some important transcription factors in the M1 and M2 phenotypes (66, 67).

Li et al. (67) reviewed the role of various miRNAs which participate in the regulation and polarization of macrophages in murine and human models. The miRNAs miRNA-9, miRNA-146a, miRNA-146b, miRNA-124, miRNA-181a, miRNA let-7c, miRNA-93, and miRNA-210 act to suppress the M1 and promote M2 phenotype. On the other hand, miRNA-27a, miRNA-130a, miRNA-130b, miRNA-155, miRNA-21, miRNA-19a-3p, miRNA-23a, miRNA-125a, miRNA-125b, miRNA-26a, miRNA-26b, and miRNA-720 act on transcription factors involved in the promotion of M1 phenotype and M2 suppression [reviewed in (67)].

Although we discussed above on the macrophage polarization of M0 to M1 or M2, it is known that macrophages have high plasticity and can be repolarized or reprogrammed under specific stimuli, in other words, M1 macrophages can differentiate into M2, and vice versa (40, 68). M2 macrophage may be repolarized more quickly than M1 macrophages, and this repolarization can occur through exposure of TLR ligands such as LPS and/or IFN-γ, or by expression of miRNAs such as miR-155 (69, 70). Van den Bossche et al. (71) showed that exposure of M1 macrophages

TABLE 1 | Chemokines differentially produced by M1 and M2 macrophages and their role in cell recruitment.

M1 macrophages		M2 macrophages	
Chemokines	**Cell recruitment**	**Chemokines**	**Cell recruitment**
CXCL1	Neutrophils	CXCL13	B cells
CXCL2	Granulocytes, polymorphonuclear	CCL1	Monocytes, Th2 and Treg cells
CXCL3	Neutrophils	CCL16	Monocytes and lymphocytes
CXCL5	Neutrophils	CCL17	Th2 cells
CXCL8	Neutrophils	CCL18	Th2 cells
CXCL9	Activated T cells	CCL22	Th2 and Treg cells
CCL2	Monocytes, memory T cells and NK	CCL24	Eosinophils and basophils
CCL3	Monocytes, T lymphocytes and polymorphonuclear cells		
CCL4	Monocytes, T lymphocytes and polymorphonuclear cells		
CCL11	Eosinophils		
CX3CL1	T cells and monocytes		

CCL, CC-chemokine ligand; CXCL, CXC-chemokine ligand; NK, natural killer cells.

to IL-4 is not able to reprogram the macrophages to M2 (71). However, the miRNAs can suppress the M1 phenotype and promote the polarization to M2 as commented above (67).

INTERACTION OF VECTOR SALIVA WITH IMMUNE CELLS

Among over 800 species of phlebotomines recorded, 98 are proven or suspected vectors of human leishmaniases; these include 42 *Phlebotomus* species in the Old World and 56 *Lutzomyia* species in the New World (all: Diptera: Psychodidae) (72). It is known that through the insect bite, vector saliva plays an important role in the establishment of *Leishmania* infection by increasing the infectivity of the parasite and modulating the host immune response (73, 74). Arthropod saliva contains anti-inflammatory, chemotactic and anti-hemostatic components that influence the course of parasite transmission to the host (7, 75, 76).

Most studies of the role of vector saliva in disease course were performed prior to the establishment of the M1 and M2 macrophage concept. Therefore, these works do not use this nomenclature. However, they investigated molecules that are involved in the plastic response of macrophages. These molecules are discussed below.

Some groups produced extracts, homogenates, sonicates and salivary lysates to elucidate the function of vector saliva in *Leishmania* transmission and infection (**Table 2**). We review the literature and assemble the results of different groups to provide an overview of the function of saliva.

Saliva contains molecules that induce a long-lasting erythema, which facilitates the obtaining of blood from capillaries in the host tissue (79). Vector saliva may facilitate cell recruitment via the promotion of vasodilation (79, 80, 92). The recruited cells include neutrophils, eosinophils and macrophages. Neutrophils may be attracted by the presence of several mediators, such as LTB$_4$, and the role of these cells as a "Trojan horse" favors the establishment of infection (80, 92). The role of eosinophils is

controversial, and whether these cells promote or suppress the infection is not well known (80, 95).

Some studies observed that vector saliva increased macrophages recruitment to the site of infection because of the modulation of chemotactic factors, such as CCL2/MCP-1, CCR2 and PGE$_2$ (80, 92). Although some studies have shown the participation of lipid mediators such as PGE$_2$ and LTB$_4$ in cell migration (73, 92), the role of these lipid mediators acting in the polarization or recruitment of a specific profile of macrophages is uncertain, differing between cell types and models studied (28, 96–98).

Vector saliva plays an important immunomodulatory role and favors the M2 profile in different manners. Vector saliva induces IL-10 to promote a regulatory response (81, 89, 90), and it is related to the activation of a Th2 response via the increase in IL-4 and IL-6 synthesis (85, 87) Rohousov et al. (88). Besides that, the salivary components reducing the M1 related parameters, such as the pro-inflammatory cytokines IFN-γ and IL-12, iNOS and nitric oxide (NO) (85, 86, 88, 90).

However, some studies showed the action of saliva inducing M1 parameters. C57BL/6 mice immunized with plasmids encoding salivary proteins developed a Th1 response, resulting in protection against *L. major* infection, demonstrating that saliva may provide a protective effect and conferring characteristics for the development of a vaccine against *Leishmania* (90, 99). In a clinical study, was observed that individuals from an endemic area exposed to *P. duboscqi* bite presented high serum levels of INF-γ and decrease of IL-13, IL-5, directing a Th1 profile. Nonetheless, when PBMC of those individuals were exposed to *P. duboscqi* saliva, the most presented a mixed Th1/Th2 response, without a specific polarized profile (82).

In addition to complexes containing salivary components, the biological activity of pharmacological compounds isolated from vector saliva was examined. Adenosine and adenosine monophosphatase are active compounds found in *P. papatasi* saliva, and these factors inhibit the function of dendritic cells via a PGE$_2$/IL-10-dependent mechanism to promote a tolerogenic profile that is characterized by the induction of regulatory T cells, which is also related to M2 polarization (73).

6

TABLE 2 | Salivary compounds and their effects on *Leishmania* infection.

Compound	Immunomodulatory effect		References
Promastigote secretory gel (PSG)	↑ Arg ↑ IL-1β ↑ IL-6 ↑ IL-10 ↑ TNF-α ↑ CCL2 ↑ CCL4 ↑ CCL3 ↑ CXCL2 ↑ FGFR2 ↑ EGF ↑ EGFR ↑ IGF1		(77) (78)
Salivary Gland Homogenate (SGH)	↑ MCP-1 ↑ CCR2 ↑ IL-10 ↑ Eosinophils ↑ Macrophages ↑ IFN-γ ↑ IL-13 ↑ IL-5	↓ iNOS ↓ NO ↓ IFN-γ ↓ IL-13 ↓ IL-5	(79) (80, 81) (82)
Salivary Gland Lysate (SGL)	↑ IL-4 ↑ IL-6	↓ IFN-γ ↓ IL-12 ↓ iNOS	(83, 84) (85–88)
Salivary Gland Extracts (SGE)	↑ IL-10 ↑ IL-4 ↑ CD8 ↑ INF-γ ↑ CD4	↓ NO	(89) (90)
Salivary Gland Sonicate (SGS)	↑ IL-4 ↑ PGE₂ ↑ Macrophages ↑ LTB₄	↓ IFN-γ	(91, 92)
Maxadilan (max)	↑ IL-6 ↑ IL-10 ↑ TGF-β ↑ CD86	↓ IL-1β ↓ IL-12p70 ↓ TNF-α ↓ IFN-γ ↓ CD80 ↓ CCR7	(87, 93, 94)
Adenosine	↑ IL-10 ↑ PGE₂		(73)

CCR, chemokine receptor; CD, cluster of differentiation; IFN, interferon; IL, interleukin; iNOS, inducible nitric oxide synthase; MCP-1, monocyte chemoattractant protein-1; NO, nitric oxide; PG, prostaglandin; TNF, tumor necrosis factor; TGF, transforming growth factor; CCL, chemokines; CXCL, motif chemokine ligand; FGFR, fibroblast growth factor receptor; EGF, epidermal growth factor; EGFR, epidermal growth factor; IGF, Insulin-like growth factor.

Maxadilan (Max) is a vasodilator peptide isolated from the saliva of arthropod vectors, and it reduces CD80 expression, which is responsible for T cell activation, and CCR7, which is involved in the development of adaptive immunity. Max increases CD86 expression on a subpopulation of dendritic cells, which leads to a preferential Th2 type response. Max also promotes an increased production of IL-6, IL-10, and TGF-β, and reduction of the Th1 cytokines, IL-1β, IL-12p70, TNF-α, and IFN-γ (87, 93). Max treatment of *L. major*-infected peritoneal exudate cells increased parasite load because of Th2 polarization

and decreased NO production (94). These results suggest that Max acts on M2 polarization, as demonstrated previously for total saliva.

Parasites also play an important role in vector saliva modulation because these pathogens secrete promastigote secretory gel (PSG) in the insect gut. The vector regurgitates PSG with the other salivary components at the moment of blood-feeding (77). *Leishmania mexicana*-PSG regurgitated by *L. longipalpis* exacerbates skin infection via an increase in the recruitment of macrophages to the site of infection (77). PSG also increases parasite load *in vitro* and *in vivo* via increasing arginase activity (77).

In more detail, Giraud et al. (78) demonstrated that PSG exacerbates the inflammatory phase of the early wound response (high levels of cytokines IL-1β, IL-6, IL-10, TNFα and chemokines CCL2, CCL3, CCL4, CXCL2), to induce insulin-like growth factor 1 (IGF1)-signaling and later IGF1-dependent expression of arg-1 in macrophages. As a result, the M2 macrophages promote the effective infection of the parasites in a PGS-dependent manner (78).

In this way, it is noteworthy that some works show that high levels of pro-inflammatory cytokines are induced by saliva components, leading to a Th1 profile, that can act in a host protective way. However, the most of studies inferred that the different salivary components are allied to the immunomodulatory capacity of the parasite, and these components are essential tools in the success of the infection, via the down-regulation of a pro-inflammatory response and reduction of macrophages M1, which are fundamental to parasite elimination and disease resolution. The saliva also up-regulates Th2-standard cytokines and regulatory molecules, which act in M2 polarization, facilitate the promastigote infection and increase the survival and proliferation of intracellular amastigotes (**Figure 1**).

M1 AND M2 MACROPHAGES IN *LEISHMANIA* INFECTION

The role of macrophage subsets in *Leishmania* infection was not investigated thoroughly. However, the fundamental role of these cells in the development of the lesion support an improved understanding of the M1 and M2 profiles as an important tool in the pathogenesis of leishmaniasis. *In vitro* and *in vivo* studies of the host response to *Leishmania* (**Table 3**) and therapeutic strategies for modulating key molecules that control cellular activity were performed. We discuss the studies of species that cause the visceral and cutaneous forms of the disease.

M1 and M2 Macrophages in Cutaneous Leishmaniasis (CL)

CL is the most common form of leishmaniasis, with an estimated 600,000 to 1 million new cases worldwide annually. CL causes skin lesions that leave life-long scars and serious disability, and it has become a serious public health problem (3). The primary etiological agents include the *Leishmania tropica* and *L. major*

7

FIGURE 1 | Role of saliva vectors on macrophage polarization. Vector saliva induces the recruitment of neutrophils and macrophages and acts as an immunomodulator to reduce pro-inflammatory and microbicidal molecules and improve Th2 cytokines and regulatory molecules, which lead to a M2 polarization. M2 macrophages allow for the facilitated entry of *Leishmania* promastigotes and higher survival/proliferation of intracellular amastigotes.

TABLE 3 | M1/M2 macrophages in leishmaniasis.

Model		Disease	*Leishmania* specie	References
Mouse	*in vivo*	–	*L. major*	(100)
Mouse	*in vitro*	–	*L. amazonensis*	(101)
Human	NI/*in vitro*	VL	–	(102)
Mouse	*in vitro*	VL	–	(103)
Raw	*in vitro*	–	*L. amazonensis*	(104)
Dog	NI	VL	–	(105)
Dog	NI	VL	*L. infantum*	(106)
Mathematical	–	–	–	(107)
Mouse	*in vitro*	–	*L. major*	(108)
Human	NI	PKDL	–	(109)
Mouse	*in vitro/in vivo*	CL	*L. major*	(110)
Mouse	*in vitro*	–	*L. donovani*	(111)
Mouse	*in vitro*	–	*L. major*	(112)
Mouse	*in vitro*	–	*L. mexicana*	(113)
Mouse	*in vitro*	–	*L. major/L. amazonensis*	(114)

CL, cutaneous leishmaniasis; NI, natural infection; PKDL, post-kala-azar dermal leishmaniasis; VL, visceral leishmaniasis.

species, in the Old World, and the *L. mexicana* species complex (e.g., *L. amazonensis*), and the subgenus *Viannia*, as the *L. (V.) braziliensis* species complex, in the New World (115).

Patients with CL have higher plasma levels of arg-1, TGF-β and PGE$_2$ (116), as wells as, increased arginine in lesions (117), suggesting that M2 macrophages might play a role in the pathogenesis of the disease. In this sense, an *in vitro* study demonstrated that only M2 macrophages allow for *L. major* and *L. amazonensis* growth (114). These authors demonstrated that lipophosphoglycan (LPG) and glycoprotein GP63 of the parasites acted on M2 macrophages and suppressed non-coding RNAs, which left these cells permissive to infection (114). Lee et al. (118) also demonstrated that a non-healing strain of *L. major* efficiently interacted with M2 macrophages (CD206^{hi}), which phagocytized the parasite *in vitro* and *in vivo*. However, a strain that produced self-healing lesions was less phagocytosed by M2 macrophages. The authors stated that the preferential infection of M2 cells played a crucial role in the severity of the cutaneous disease.

The role of peroxisome proliferator-activated receptors (PPARs) was investigated in infected macrophages from mouse strains resistant and susceptible to *Leishmania* infection. PPARs are ligand-activated transcription factors that are expressed in macrophages, and regulate the expression of certain genes related to the inflammatory response (119). Odegaard et al. (120) demonstrated that PPARγ-knockout mice have delayed in disease progress, with less footpad swelling and reduced parasitic burden. Importantly, genes preferentially expressed in alternatively activated macrophages, such as *arg-1*, *Mrc1*, and *Clec7a*, were also decreased in the tissue of PPARγ-knockout mice. These data strongly suggest that PPARγ is required for

acquisition and maintenance of the M2 macrophages in *L. major* model (120). Besides that, Gallardo-Soler et al. (121) showed that PPARγ and -δ ligands promote intracellular *L. major* amastigote growth in infected macrophages, and this effect is dependent on both PPAR expression and arg-1 activity, namely suggesting that PPAR ligands promote amastigote growth in M2 macrophages in an arginase-dependent manner (121).

On the other hand, PPAR expression induced the activation of the murine macrophage cell line J774A.1 via polarization toward an M1 profile, with high production of pro-inflammatory mediators (TNF-α, IL-1β, IL-6, TLR4, and ROS), and an increase in microbicide activity against *L. mexicana* (113).

The transmembrane activator and calcium modulator and cyclophilin ligand interactor (TACI) is a key molecule for plasma cell maintenance. This receptor is in the TNF family, and it is required in infections where protection depends on antibody response. Analysis of macrophage phenotype revealed that macrophages adapted the M2 phenotype in the absence of TACI. The levels of M2 markers, IL-4Rα and CD206, were significantly higher in TACI-knockout macrophages than wild-type cells. TACI-knockout mice were unable to control *L. major* infection *in vitro*, which confirms their M2 phenotype, and intradermal inoculation of *Leishmania* resulted in a more severe manifestation of the disease than in the resistant C57BL/6 strain. The transfer of WT macrophages to TACI-knockout mice significantly reduced the disease severity (110).

One fundamental role of TNF was the induction of M1 differentiation and blockade of M2 polarization in the livers of *L. major*-infected mice (100). These authors also described the role of IL-6, which did not interfere with the macrophage phenotype alone, but it was highly expressed in M2 macrophages. The authors suggested that a balance between TNF and IL-6 mediated macrophage polarization in L. *major* infection (100).

8

Vellozo et al. (122) also demonstrated that the resistance of C57BL/6 mice to *Leishmania* infection was because of their ability to mature macrophages in the peritoneum from M0 to M1. Susceptible mice (BALB/c) exhibit immature peritoneal macrophages and succumb to infection. However, both mouse strains are resistant to *L. braziliensis* infection because in both strains convert M0 to M1 macrophages in this model, despite the incomplete M1 maturation and lower iNOS expression and NO production in BALB/c mice.

The co-culture of mesenchymal stem cells and *L. major*-infected macrophages also induced an event suggestive of M1 polarization, with the induction of inflammatory cytokines and reduction of IL-10 levels (108). This strategy provides new hope for stem cell therapy in the control of *L. major* (108).

SLPI (secretory leukocyte protease inhibitor) is a potent serine protease inhibitor that exhibits antimicrobial and anti-inflammatory functions. The role of SLPI in *L. major* infected-macrophage polarization was investigated (112). SPLI-knockout macrophages produced high levels of iNOS and IFN-γ but failed to contain cutaneous *L. major* infection. This study highlights that a very strong M1 response is detrimental in *L. major* models and causes tissue injury because of exacerbated inflammation. This study suggests that a balance of M1 and M2 macrophage responses influences the outcome of innate host defense against intracellular parasites, and SLPI is critical for the coordination of this balance and the resistance to chronic leishmaniasis (112).

One study of PKDL demonstrated that monocytes from patients exhibited decreased expression of TLR-2/4 and an attenuated generation of reactive oxidative/nitrosative species (109). Patients also exhibited an increased expression of classical M2 markers (arg-1, PPARγ and CD206) in monocytes and lesional macrophages, which indicated the M2 polarization of macrophages. These subsets appeared to sustain disease chronicity, which is a hallmark of Indian PKDL (109).

Two studies showed the development of new drugs addressed the M1/M2 plasticity (101, 104). The first study demonstrated that high antimony dilutions, a homeopathic medicine, potentiated the *L. amazonensis*-induced reduction of pro-inflammatory cytokine (IL-6, IL-12, and IFN-γ) and chemokine (CCL-2 and CCL-4) production in RAW cells. The treatment also induced an increase of the parasites internalization, but there was a reduction of the acid vacuoles, which implied in less elimination of the amastigote forms. The authors suggest that this phenomenon is related to the M2 polarization and regulation of the chronic inflammation events (104).

The second study used crotoxin, which is the main component of *Crotalus durissus terrificus* venom, to treat peritoneal BALB/c mouse macrophages infected with *L. amazonensis* (101). The host cells exhibited an increase in nitric oxide, IL-6 and TNF-α production, that converged into an M1 activation profile, as suggested by their morphological changes (larger spreading), inducing leishmanicidal activity against intracellular parasites, which may be associated with a better prognosis for CL (101).

Siewe et al. (107) proposed a mathematical model that states that *Leishmania* parasite takes advantage of the immune system and invades M1 and M2 macrophages. Simulations of the model demonstrated that the number of M2 macrophages constantly

increased and M1 macrophages constantly decreased over the course of the infection, but the sum of the number of M1 and M2 cells reached a steady state, which was approximately the same as the healthy state of the host. The ratio of *Leishmania* parasites to macrophages depends homogeneously on their ratio at the time of the initial infection (107).

M1 and M2 Macrophages in Visceral Leishmaniasis (VL)

Visceral leishmaniasis is the most aggressive form of the disease, with high rates of mortality (3). Visceral leishmaniasis is generally caused by *L. donovani* and *L. infantum chagasi* species and affects internal organs, such as spleen, liver, and bone marrow (115, 123). It has been shown that blood arginase levels in VL patients are considerably increased (124), while NO levels are decreased (125). In this sense, a recent study demonstrated that monocytes/macrophages of VL patients present reduced oxidative burst and antigen presentation, with a M2 regulatory phenotype, characterized by high CD163, IL-10 and CXCL14 levels (126).

In the same direction, Silva et al. (102) demonstrated that the CD163s molecule was associated with the M2 macrophage phenotype, and it may be used as a biomarker of the clinical parameters of human VL severity. *L. donovani* also promotes the output of monocytes with a regulatory phenotype from the bone marrow that function as safe targets for the parasite (127). These data are consistent with analyses of dogs with VL, that demonstrated a higher number of M2-polarized macrophages compared to healthy dogs (106). The authors concluded that the predominance of the M2 phenotype (high CD163 labeling) in VL dogs favored the multiplication of *L. infantum* in the skin, spleen and lymph nodes (106).

Similarly, Chan et al. (128) suggest that the regulation of the macrophage phenotype is induced by the parasite, since PPAR expression is induced by parasitic infection. The authors showed that *L. donovani* activation of PPARγ promotes survival, whereas blockade of PPARγ facilitates removal of the parasite. Thus, *Leishmania* parasites harness PPARγ to sustain the M2 phenotype and increase infectivity of visceral disease (128).

A recent study has also shown the role of mammalian target of rapamycin (mTOR) in M2 macrophage polarization for *Leishmania* survival (129). The authors observed that *L. donovani*-infection activated host mTOR pathway, resulting in reduced expression of M1 macrophage markers (ROS, NO, iNOS, NOX-1, IL-12, IL-1β, and TNF-α), and increased expression of M2 macrophage markers (arg-1, IL-10, TGF-β, CD206, and CD163), favoring the *Leishmania* survival inside macrophages. Thus, they concluded that mTOR plays a crucial role in M2 macrophage polarization and parasite persistence in *L. donovani* infection (129).

These results correlated with studies performed in *L. donovani*-infected Syrian hamsters, in which the spleen environment was inflammatory with a high production of types I and II IFN. However, IFN-γ did not direct M1 macrophage polarization in this

9

FIGURE 2 | Role of M1 and M2 macrophages in *Leishmania* infection. TACI (transmembrane activator and calcium modulator and cyclophilin ligand interactor), peroxisome proliferator-activated receptors (PPARs) and mesenchymal stem cells (MSCs) participate in M1 polarization in macrophage-leishmania studies, as well as the crotoxin treatment. The epithelial and myeloid-derived serine protease inhibitor (SLPI), mammalian target of rapamycin (m-TOR) and the treatment with high diluted antimony participate in M2 polarizersion in leishmania models.

model, which allowed for parasite growth and the expression of counter-regulatory molecules, such as arg-1 (103).

A different group demonstrated that macrophages cultured from the lymph nodes of VL dogs exhibited low arg-1 activity and high NO and PGE$_2$ production compared to uninfected dogs (105). These authors suggested that M1 macrophages were participating in the immune response in the lymph nodes of these animals (105). Attenuated *L. donovani* induced innate immunity via the classical activation of macrophages (M1), with upregulation of IL-1β, TNF-α, IL-12 and downregulation of IL-10, YM1, Arg-1, and MRC-1 genes, which led to the generation of protective Th1 responses in BALB/c mice (111).

This controversy may be explained by the fact that different patterns of gene expression are found in macrophages at different time points (130). A recent study demonstrated that the early response against *L. donovani* infection was distinguished by the increase in of Th1 markers and M1-macrophage activation molecules (IFN-γ, Stat1, Cxcl9, Cxcl10, Ccr5, Cxcr3, Xcl1, and Ccl3). However, this activation was not protective because the parasitic burden increased over time. There was no marked overlap of macrophage phenotypes at intermediate times of infection, and the overexpression of these Th1/M1 markers was restored later in the chronic phase without parasitic burden control (130).

Together, these results demonstrate that there are no "good guys" and "bad guys" in the polarization of macrophages following infection by *Leishmania* parasites. Therefore, a balance between the potent microbicidal response of M1 macrophages and the potential regulation by M2 macrophages may be key to the success of overcoming leishmaniasis (**Figure 2**).

CONCLUSION

The collected works suggest that vector saliva plays an immunomodulatory effect on macrophages, which leads to the polarization of macrophages to an M2 phenotype. Therefore, vector saliva may contribute to an increase in the infectivity and persistence of the parasite during the initial periods of infection. Different *Leishmania* species exhibit virulence factors that can subvert the microbicidal mechanisms of the host to favor its proliferation because of the M2 polarization. However, M1 macrophages act during later periods of the infection and trigger an exacerbated immune response that leads to a worsening of the lesions, despite the role of these cells as powerful microbicidal agents. Therefore, a balance between the initial microbicidal response (M1) followed by a restorative response (M2) at later periods of time would provide the utmost benefit for the host. Further studies are necessary to fully elucidate the balance between these two main macrophages populations in the control of *Leishmania* infection.

AUTHOR CONTRIBUTIONS

FT-P study design, literature review, data collection and manuscript writing. BB, JA, MG, AC, and MM-S literature review, data collection and manuscript writing. IC-C and JB text correction and organization. WP study design, text correction and organization.

FUNDING

REFERENCES

1. Steverding D. The history of leishmaniasis. *Parasit Vectors* (2017) 10:82. doi: 10.1186/s13071-017-2028-5

2. World Health Organization Leishmaniasis in high-burden countries: an epidemiological update based on data reported in 2014. *Relev Epidemiol Hebd.* (2016) 91:287–96.

3. World Health Organization (2018). Leishmaniasis. Available online at: http://www.who.int/news-room/fact-sheets/detail/leishmaniasis

4. Lestinova T, Rohousova I, Sima M, de Oliveira CI, Volf P. Insights into the sand fly saliva: blood-feeding and immune interactions between sand flies, hosts, and Leishmania. *PLoS Negl Trop Dis.* (2017) 11:e0005600. doi: 10.1371/journal.pntd.0005600

5. Liu D, Uzonna JE. The early interaction of Leishmania with macrophages and dendritic cells and its influence on the host immune response. *Front Cell Infect Microbiol.* (2012) 2:83. doi: 10.3389/fcimb.2012.00083

6. Serafim TD, Coutinho-Abreu IV, Oliveira F, Meneses C, Kamhawi S, Valenzuela JG. Sequential blood meals promote *Leishmania* replication and reverse metacyclogenesis augmenting vector infectivity. *Nat Microbiol.* (2018) 3:548–55. doi: 10.1038/s41564-018-0125-7

7. Scorza BM, Carvalho EM, Wilson ME. Cutaneous manifestations of human and murine Leishmaniasis. *Int J Mol Sci.* (2017) 18:1296. doi: 10.3390/ijms18061296

8. Peters NC, Egen JG, Secundino N, Debrabant A, Kimblin N, Kamhawi S, et al. *In Vivo* imaging reveals an essential role for neutrophils in leishmaniasis transmitted by sand flies. *Science (80-).*(2008) 321:970–4. doi: 10.1126/science.1159194

9. Hurrell BP, Schuster S, Grün E, Coutaz M, Williams RA, Held W, et al. Rapid sequestration of leishmania mexicana by neutrophils contributes to the development of chronic lesion. *PLoS Pathog.* (2015) 11:e1004929. doi: 10.1371/journal.ppat.1004929

10. Carlsen ED, Jie Z, Liang Y, Henard CA, Hay C, Sun J, et al. Interactions between neutrophils and leishmania braziliensis amastigotes facilitate cell activation and parasite clearance. *J Innate Immun.* (2015) 7:354–63. doi: 10.1159/000373923

11. Falcão SAC, Weinkopff T, Hurrell BP, Celes FS, Curvelo RP, Prates DB, et al. Exposure to leishmania braziliensis triggers neutrophil activation and apoptosis. *PLoS Negl Trop Dis.* (2015) 9:e0003601. doi: 10.1371/journal.pntd.0003601

12. Guimarães-Costa AB, Nascimento MTC, Froment GS, Soares RPP, Morgado FN, Conceição-Silva F, et al. Leishmania amazonensis promastigotes induce and are killed by neutrophil extracellular traps. *Proc Natl Acad Sci USA.* (2009) 106:6748–53. doi: 10.1073/pnas.0900226106

13. Novais FO, Santiago RC, Bafica A, Khouri R, Afonso L, Borges VM, et al. Neutrophils and macrophages cooperate in host resistance against leishmania braziliensis infection. *J Immunol.* (2009) 183:8088–98. doi: 10.4049/jimmunol.0803720

14. Rochael NC, Guimarães-Costa AB, Nascimento MTC, DeSouza-Vieira TS, Oliveira MP, Garcia e Souza LF, et al. Classical ROS-dependent and early/rapid ROS-independent release of neutrophil extracellular traps triggered by leishmania parasites. *Sci Rep.* (2016) 5:18302. doi: 10.1038/srep18302

15. Tavares NM, Araújo-Santos T, Afonso L, Nogueira PM, Lopes UG, Soares RP, et al. Understanding the mechanisms controlling Leishmania amazonensis infection *in vitro*: the role of LTB4 derived from human neutrophils. *J Infect Dis.* (2014) 210:656–66. doi: 10.1093/infdis/jiu158

16. McFarlane E, Perez C, Charmoy M, Allenbach C, Carter KC, Alexander J, et al. Neutrophils contribute to development of a protective immune response during onset of infection with Leishmania donovani. *Infect Immun.* (2008) 76:532–41. doi: 10.1128/IAI.01388-07

17. Regli I, Passelli K, Hurrell B, Tacchini-Cottier F. Survival mechanisms used by some leishmania species to escape neutrophil killing. *Front Immunol.* (2017) 8:1558. doi: 10.3389/fimmu.2017.01558

18. Ribeiro-Gomes FL, Peters NC, Debrabant A, Sacks DL. Efficient capture of infected neutrophils by dendritic cells in the skin inhibits the early anti-leishmania response. *PLoS Pathog.* (2012) 8:e1002536. doi: 10.1371/journal.ppat.1002536

19. van Zandbergen G, Klinger M, Mueller A, Dannenberg S, Gebert A, Solbach W, et al. Cutting edge: neutrophil granulocyte serves as a vector for Leishmania entry into macrophages. *J Immunol.* (2004) 173, 6521–5. doi: 10.4049/jimmunol.173.11.6521

20. Scott P, Novais FO. Cutaneous leishmaniasis: immune responses in protection and pathogenesis. *Nat Rev Immunol.* (2016) 16:581–92. doi: 10.1038/nri.2016.72

21. Srivastava S, Shankar P, Mishra J, Singh S. Possibilities and challenges for developing a successful vaccine for leishmaniasis. *Parasit Vectors* (2016) 9:277. doi: 10.1186/s13071-016-1553-y

22. Arango Duque G, Descoteaux A. Macrophage cytokines: involvement in immunity and infectious diseases. *Front Immunol.* (2014) 5:491. doi: 10.3389/fimmu.2014.00491

23. Zanluqui NG, Wowk PF, Pinge-Filho P. Macrophage polarization in chagas disease. *J Clin Cell Immunol.* (2015) 6:1–6. doi: 10.4172/2155-9899.1000317

24. Muxel SM, Aoki JI, Fernandes JCR, Laranjeira-Silva MF, Zampieri RA, Acuña SM, et al. Arginine and polyamines fate in leishmania infection. *Front Microbiol.* (2017) 8:2682. doi: 10.3389/fmicb.2017.02682

25. Mendonça SCF. Differences in immune responses against Leishmania induced by infection and by immunization with killed parasite antigen: implications for vaccine discovery. *Parasit Vectors* (2016) 9:492. doi: 10.1186/s13071-016-1777-x

26. Sacks D, Noben-Trauth N. The immunology of susceptibility and resistance to leishmania major in mice. *Nat Rev Immunol.* (2002) 2:845–58. doi: 10.1038/nri933

27. Murray PJ, Wynn TA. Protective and pathogenic functions of macrophage subsets. *Nat Rev Immunol.* (2011) 11:723–37. doi: 10.1038/nri3073

28. Parisi L, Gini E, Baci D, Tremolati M, Fanuli M, Bassani B, et al. Macrophage polarization in chronic inflammatory diseases: killers or builders? *J Immunol Res.* (2018) 2018:1–25. doi: 10.1155/2018/8917804

29. Covarrubias A, Byles V, Horng T. ROS sets the stage for macrophage differentiation. *Cell Res.* (2013) 23:984–5. doi: 10.1038/cr.2013.88

30. Anderson CF, Mosser DM. A novel phenotype for an activated macrophage: the type 2 activated macrophage. *J Leukoc Biol.* (2002) 72:101–6. doi: 10.1189/jlb.72.1.101

31. Bashir S, Sharma Y, Elahi A, Khan F. Macrophage polarization: the link between inflammation and related diseases. *Inflamm Res.* (2016) 65:1–11. doi: 10.1007/s00011-015-0874-1

32. Muraille E, Leo O, Moser M. TH1/TH2 paradigm extended: macrophage polarization as an unappreciated pathogen-driven escape mechanism? *Front Immunol.* (2014) 5:603. doi: 10.3389/fimmu.2014.00603

33. Murray PJ, Allen JE, Biswas SK, Fisher EA, Gilroy DW, Goerdt S, et al. Macrophage activation and polarization: nomenclature and experimental guidelines. *Immunity* (2014) 41:14–20. doi: 10.1016/j.immuni.2014.06.008

34. Sica A, Mantovani A. Macrophage plasticity and polarization: *in vivo* veritas. *J Clin Invest.* (2012) 122:787–95. doi: 10.1172/JCI59643

35. Jablonski KA, Amici SA, Webb LM, Ruiz-Rosado J, de D, Popovich PG, Partida-Sanchez S, et al. Novel markers to delineate murine M1 and M2 macrophages. *PLoS ONE* (2015) 10:e0145342. doi: 10.1371/journal.pone.0145342

36. Lehtonen A, Ahlfors H, Veckman V, Miettinen M, Lahesmaa R, Julkunen I. Gene expression profiling during differentiation of human monocytes to macrophages or dendritic cells. *J Leukoc Biol.* (2007) 82:710–20. doi: 10.1189/jlb.0307194

37. Mantovani A, Sica A, Sozzani S, Allavena P, Vecchi A, Locati M. The chemokine system in diverse forms of macrophage activation and polarization. *Trends Immunol.* (2004) 25:677–86. doi: 10.1016/j.it,.2004.09.015

38. Mosser DM, Edwards JP. Exploring the full spectrum of macrophage activation. *Nat Rev Immunol.* (2008) 8:958–69. doi: 10.1038/nri2448

39. Szanto A, Balint BL, Nagy ZS, Barta E, Dezso B, Pap A, et al. STAT6 transcription factor is a facilitator of the nuclear receptor PPARγ-regulated gene expression in macrophages and dendritic cells. *Immunity* (2010) 33:699–712. doi: 10.1016/j.immuni.2010.11.009

40. Wang N, Liang H, Zen K. Molecular mechanisms that influence the macrophage m1-m2 polarization balance. *Front Immunol.* (2014) 5:614. doi: 10.3389/fimmu.2014.00614

11

41. Xu W, Zhao X, Daha MR, van Kooten C. Reversible differentiation of pro- and anti-inflammatory macrophages. *Mol Immunol.* (2013) 53:179–86. doi: 10.1016/j.molimm.2012.07.005

42. Finnin M, Hamilton JA, Moss ST. Characterization of a CSF-induced proliferating subpopulation of human peripheral blood monocytes by surface marker expression and cytokine production. *J Leukoc Biol.* (1999) 66:953–60. doi: 10.1002/jlb.66.6.953

43. Ruan C-C, Ge Q, Li Y, Li X-D, Chen D-R, Ji K-D, et al. Complement-mediated macrophage polarization in perivascular adipose tissue contributes to vascular injury in deoxycorticosterone acetate–salt micesignificance. *Arterioscler Thromb Vasc Biol.* (2015) 35:598–606. doi: 10.1161/ATVBAHA.114.304927

44. Chistiakov DA, Myasoedova VA, Revin VV, Orekhov AN, Bobryshev YV. The impact of interferon-regulatory factors to macrophage differentiation and polarization into M1 and M2. *Immunobiology* (2018) 223:101–11. doi: 10.1016/j.imbio.2017.10.005

45. Gordon S. Alternative activation of macrophages. *Nat Rev Immunol.* (2003) 3:23–35. doi: 10.1038/nri978

46. Gordon S, Martinez FO. Alternative activation of macrophages: mechanism and functions. *Immunity* (2010) 32:593–604. doi: 10.1016/j.immuni.2010.05.007

47. Martinez FO, Helming L, Gordon S. Alternative activation of macrophages: an immunologic functional perspective. *Annu Rev Immunol.* (2009) 27:451–83. doi: 10.1146/annurev.immunol.021908.132532

48. Pesce J, Kaviratne M, Ramalingam TR, Thompson RW, Urban JF, Cheever AW, et al. The IL-21 receptor augments Th2 effector function and alternative macrophage activation. *J Clin Invest.* (2006) 116:2044–55. doi: 10.1172/JCI27727

49. Biswas SK, Mantovani A. Macrophage plasticity and interaction with lymphocyte subsets: cancer as a paradigm. *Nat Immunol.* (2010) 11:889–96. doi: 10.1038/ni.1937

50. Hazlett LD, McClellan SA, Barrett RP, Huang X, Zhang Y, Wu M, et al. IL-33 shifts macrophage polarization, promoting resistance against *Pseudomonas aeruginosa* Keratitis. *Investig Opthalmol Vis Sci.* (2010) 51:1524–32. doi: 10.1167/iovs.09-3983

51. Kurowska-Stolarska M, Stolarski B, Kewin P, Murphy G, Corrigan CJ, Ying S, et al. IL-33 amplifies the polarization of alternatively activated macrophages that contribute to airway inflammation. *J Immunol.* (2009) 183:6469–77. doi: 10.4049/jimmunol.0901575

52. Li S, Wang W, Fu S, Wang J, Liu H, Xie S, et al. IL-21 modulates release of proinflammatory cytokines in LPS-stimulated macrophages through distinct signaling pathways. *Mediators Inflamm.* (2013) 2013:548073. doi: 10.1155/2013/548073

53. Fraternale A, Brundu S, Magnani M. Polarization and Repolarization of Macrophages. *J Clin Cell Immunol.* (2015) 6:319. doi: 10.4172/2155-9899.1000319.

54. Lu J, Cao Q, Zheng D, Sun Y, Wang C, Yu X, et al. Discrete functions of M 2a and M 2c macrophage subsets determine their relative efficacy in treating chronic kidney disease. *Kidney Int.* (2013) 84:745–55. doi: 10.1038/ki.2013.135

55. Lucey DR, Clerici M, Shearer GM. Type 1 and type 2 cytokine dysregulation in human infectious, neoplastic, and inflammatory diseases. *Clin Microbiol Rev.* (1996) 9:532–62.

56. Asai A, Nakamura K, Kobayashi M, Herndon DN, Suzuki F. CCL1 released from M2b macrophages is essentially required for the maintenance of their properties. *J Leukoc Biol.* (2012) 92:859–67. doi: 10.1189/jlb.0212107

57. Ley K, Miller YI, Hedrick CC. Monocyte and macrophage dynamics during atherogenesis. *Arterioscler Thromb Vasc Biol.* (2011) 31:1506–16. doi: 10.1161/ATVBAHA.110.221127

58. Wolfs I, Donners M, de Winther M. Differentiation factors and cytokines in the atherosclerotic plaque micro-environment as a trigger for macrophage polarisation. *Thromb Haemost.* (2011) 106:763–71. doi: 10.1160/TH11-05-0320

59. Park-Min K-H, Antoniv TT, Ivashkiv LB. Regulation of macrophage phenotype by long-term exposure to IL-10. *Immunobiology* (2005) 210:77–86. doi: 10.1016/j.imbio.2005.05.002

60. Wang Q, Ni H, Lan L, Wei X, Xiang R, Wang Y. Fra-1 protooncogene regulates IL-6 expression in macrophages and promotes the generation of M2d macrophages. *Cell Res.* (2010) 20:701–12. doi: 10.1038/cr.2010.52

61. Ferrante CJ, Pinhal-Enfield G, Elson G, Cronstein BN, Hasko G, Outram S, et al. The adenosine-dependent angiogenic switch of macrophages to an M2-like phenotype is independent of interleukin-4 receptor alpha (IL-4Rα) signaling. *Inflammation* (2013) 36:921–31. doi: 10.1007/s10753-013-9621-3

62. Csóka B, Selmeczy Z, Koscsó B, Németh ZH, Pacher P, Murray PJ, et al. Adenosine promotes alternative macrophage activation *via* A $_{2A}$ and A $_{2B}$ receptors. *FASEB J.* (2012) 26:376–86. doi: 10.1096/fj.11-190934

63. Lawrence T, Natoli G. Transcriptional regulation of macrophage polarization: enabling diversity with identity. *Nat Rev Immunol.* (2011) 11:750–61. doi: 10.1038/nri3088

64. Self-Fordham JB, Naqvi AR, Uttamani JR, Kulkarni V, Nares S. MicroRNA: dynamic regulators of macrophage polarization and plasticity. *Front Immunol.* (2017) 8:1062. doi: 10.3389/fimmu.2017.01062

65. Terry RL, Miller SD. Molecular control of monocyte development. *Cell Immunol.* (2014) 291:16–21. doi: 10.1016/j.cellimm.2014.02.008

66. Graff JW, Dickson AM, Clay G, McCaffrey AP, Wilson ME. Identifying functional MicroRNAs in macrophages with polarized phenotypes. *J Biol Chem.* (2012) 287:21816–25. doi: 10.1074/jbc.M111.327031

67. Li H, Jiang T, Li M-Q, Zheng X-L, Zhao G-J. Transcriptional regulation of macrophages polarization by MicroRNAs. *Front Immunol.* (2018) 9:1175. doi: 10.3389/fimmu.2018.01175

68. Davis MJ, Tsang TM, Qiu Y, Dayrit JK, Freij JB, Huffnagle GB, et al. Macrophage M1/M2 polarization dynamically adapts to changes in cytokine microenvironments in *Cryptococcus neoformans* infection. *MBio* (2013) 4:e00264–e00213. doi: 10.1128/mBio.00264-13

69. Mylonas KJ, Nair MG, Prieto-Lafuente L, Paape D, Allen JE. Alternatively activated macrophages elicited by helminth infection can be reprogrammed to enable microbial killing. *J Immunol.* (2009) 182:3084–94. doi: 10.4049/jimmunol.0803463

70. Stout RD, Jiang C, Matta B, Tietzel I, Watkins SK, Suttles J. Macrophages sequentially change their functional phenotype in response to changes in microenvironmental influences. *J Immunol.* (2005) 175:342–9. doi: 10.4049/jimmunol.175.1.342

71. Van den Bossche J, Baardman J, Otto NA, van der Velden S, Neele AE, van den Berg SM, et al. Mitochondrial dysfunction prevents repolarization of inflammatory macrophages. *Cell Rep.* (2016) 17:684–96. doi: 10.1016/j.celrep.2016.09.008

72. Maroli M, Feliciangeli MD, Bichaud L, Charrel RN, Gradoni L. Phlebotomine sandflies and the spreading of leishmaniases and other diseases of public health concern. *Med Vet Entomol.* (2013) 27:123–47. doi: 10.1111/j.1365-2915.2012.01034.x

73. Carregaro V, Ribeiro JM, Valenzuela JG, Souza-júnior DL. Nucleosides present on phlebotomine saliva induce immunossupression and promote the infection establishment. *PLoS Negl Trop Dis.* (2015) 9:e0003600. doi: 10.1371/journal.pntd.0003600

74. Rouhousová I, Volf P. Sand fly saliva: effects on host immune response and Leishmania transmission. *Folia Parasitol (Praha).* (2006) 53:161–71. doi: 10.14411/fp.2006.022

75. Kamhawi S. The biological and immunomodulatory properties of sand fly saliva and its role in the establishment of Leishmania infections. *Microbes Infect.* (2000) 2:1765–73. doi: 10.1016/S1286-4579(00)01331-9

76. Soares RPP, Turco SJ. Lutzomyia longipalpis (Diptera: psychodidae: phlebotominae): a review. *An Acad Bras Cienc.* (2003) 75:301–30. doi: 10.1590/S0001-37652003000300005

77. Rogers M, Kropf P, Choi B, Dillon R, Podinovskaia M, Bates P, et al. Proteophosophoglycans regurgitated by leishmania-infected sand flies target the L-arginine metabolism of host macrophages to promote parasite survival. *PLoS Pathog.* (2009) 5:e1000555. doi: 10.1371/journal.ppat.1000555

78. Giraud E, Lestinova T, Derrick T, Martin O, Dillon RJ, Volf P, et al. Leishmania proteophosphoglycans regurgitated from infected sand flies accelerate dermal wound repair and exacerbate leishmaniasis via insulin-like growth factor 1-dependent signalling. *PLoS Pathog.* (2018) 14:e1006794. doi: 10.1371/journal.ppat.1006794

12

79. Ribeiro JMC, Rossignol PA, Spielman A. Blood-finding strategy of a capillary-feeding sandfly, lutzomyia longipalpis. *Comp Biochem Physiol.* (1986) 83:683–6. doi: 10.1016/0300-9629(86)90709-7

80. Teixeira CR, Teixeira MJ, Regis BB, Santos CS, Andrade BB, Silva JS, et al. Saliva from lutzomyia longipalpis induces CC chemokine ligand 2/monocyte chemoattractant protein-1 expression and macrophage recruitment. *J Immunol.* (2005) 175:8346–53. doi: 10.4049/jimmunol.175.12.8346

81. Pushpanjali AKT, Purkait B, Jamal F, Singh MK, Ahmed G, Bimal S, et al. Direct evidence for role of anti-saliva antibodies against salivary gland homogenate of P. argentipes in modulation of protective Th1-immune response against Leishmania donovani. *Cytokine* (2016) 86:79–85. doi: 10.1016/j.cyto.2016.07.017

82. Oliveira F, Traoré B, Gomes R, Faye O, Gilmore DC, Keita S, et al. Delayed-type hypersensitivity to sand fly saliva in humans from a leishmaniasis-endemic area of mali is TH1-mediated and persists to midlife. *J Invest Dermatol.* (2013) 133:452–9. doi: 10.1038/jid.2012.315

83. Theodos CM, Ribeiro JM, Titus RG. Analysis of enhancing effect of sand fly saliva on Leishmania infection in mice. *Infect Immun.* (1991) 59:1592–8.

84. Titus RG, Ribeiro JM. Salivary gland lysates from the sand fly Lutzomyia longipalpis enhance Leishmania infectivity. *Science* (1988) 239:1306–8. doi: 10.1126/science.3344436

85. Mbow ML, Bleyenberg JA, Hall LR, Titus RG. Phlebotomus papatasi S and fly salivary gland lysate down-regulates a Th1, but up-regulates a Th2, response in mice infected with leishmania major. *J Immunol.* (1998) 161:5571–7.

86. Hall LR, Titus RG. Sand fly vector saliva selectively modulates macrophage functions that inhibit killing of Leishmania major and nitric oxide production. *J Immunol.* (1995) 155:3501–6.

87. Rogers KA, Titus RG. Immunomodulatory effects of Maxadilan and *Phlebotomus* papatasi sand fly salivary gland lysates on human primary *in vitro* immune responses. *Parasite Immunol.* (2003) 25:127–34. doi: 10.1046/j.1365-3024.2003.00623.x

88. Rohousová I, Volf P, Lipoldová M. Modulation of murine cellular immune response and cytokine production by salivary gland lysate of three sand fly species. *Parasite Immunol.* (2005) 704:469–73. doi: 10.1111/j.1365-3024.2005.00787.x

89. Norsworthy NB, Sun J, Elnaiem D, Lanzaro G, Soong L. Sand fly saliva enhances leishmania amazonensis infection by modulating interleukin-10 production. *Infect Immun.* (2004) 72:1240–7. doi: 10.1128/IAI.72.3.1240-1247.2004

90. Abdeladhim M, Ben Ahmed M, Marzouki S, Belhadj Hmida N, Boussoffara T, Belhaj Hamida N, et al. Human cellular immune response to the saliva of phlebotomus papatasi is mediated by IL-10-producing CD8+ T cells and Th1-polarized CD4+ lymphocytes. *PLoS Negl Trop Dis.* (2011) 5:e1345. doi: 10.1371/journal.pntd.0001345

91. Belkaid Y, Kamhawi S, Modi G, Valenzuela J, Noben-Trauth N, Rowton E, et al. Development of a natural model of cutaneous leishmaniasis: powerful effects of vector saliva and saliva preexposure on the long-term outcome of Leishmania major infection in the mouse ear dermis. *J Exp Med.* (1998) 188:1941–53. doi: 10.1084/jem.188.10.1941

92. Araújo-Santos T, Prates DB, Andrade BB, Nascimento DO, Clarêncio J, Entringer PF, et al. Lutzomyia longipalpis saliva triggers lipid body formation and prostaglandin E2 production in murine macrophages. *PLoS ONE Neglected Trop Dis.* (2010) 4:e873. doi: 10.1371/journal.pntd.0000873

93. Wheat WH, Pauken KE, Morris RV, Titus RG. *Lutzomyia longipalpis* salivary peptide maxadilan alters murine dendritic cell expression of CD80/86, CCR7 and cytokine secretion and reprograms dendritic cell-mediated cytokine release from cultures containing allogeneic T cells. *J Immunol.* (2008) 180:8286–98. doi: 10.4049/jimmunol.180.12.8286

94. Brodie TM, Smith MC, Morris RV, Titus RG. Immunomodulatory effects of the lutzomyia longipalpis salivary gland protein maxadilan on mouse macrophages. *Infect Immun.* (2007) 75:2359–65. doi: 10.1128/IAI.01812-06

95. Rodríguez NE, Wilson ME. Eosinophils and mast cells in leishmaniasis. *Immunol Res.* (2014) 59:129–41. doi: 10.1007/s12026-014-8536-x

96. Hosono K, Isonaka R, Kawakami T, Narumiya S, Majima M. Signaling of prostaglandin E receptors, EP3 and EP4 facilitates wound healing and lymphangiogenesis with enhanced recruitment of M2 macrophages in mice. *PLoS ONE* (2016) 11:e0162532. doi: 10.1371/journal.pone.0162532

97. Kim Y-G, Udayanga KGS, Totsuka N, Weinberg JB, Núñez G, Shibuya A. Gut dysbiosis promotes M2 macrophage polarization and allergic airway inflammation via fungi-induced PGE2. *Cell Host Microbe* (2014) 15:95–102. doi: 10.1016/j.chom.2013.12.010

98. Wang Z, Brandt S, Medeiros A, Wang S, Wu H, Dent A, et al. MicroRNA 21 is a homeostatic regulator of macrophage polarization and prevents prostaglandin E2-mediated M2 generation. *PLoS ONE* (2015) 10:e0115855. doi: 10.1371/journal.pone.0115855

99. Xu X, Oliveira F, Chang BW, Collin N, Gomes R, Teixeira C, et al. Structure and function of a "yellow" protein from saliva of the sand fly *Lutzomyia* longipalpis that confers protective immunity against Leishmania major infection. *J Biol Chem.* (2011) 286:32383–93. doi: 10.1074/jbc.M111.268904

100. Hu S, Marshall C, Darby J, Wei W, Lyons AB, Körner H. Absence of tumor necrosis factor supports alternative activation of macrophages in the liver after infection with leishmania major. *Front Immunol.* (2018) 9:1. doi: 10.3389/fimmu.2018.00001

101. Farias LHS, Rodrigues APD, Coêlho EC, Santos MF, Sampaio SC, Silva EO. Crotoxin stimulates an M1 activation profile in murine macrophages during Leishmania amazonensis infection. *Parasitology* (2017) 144:1458–67. doi: 10.1017/S0031182017000944

102. Silva RLL, Santos MB, Almeida PLS, Barros TS, Magalhães L, Cazzaniga RA, et al. sCD163 levels as a biomarker of disease severity in leprosy and visceral leishmaniasis. *PLoS Negl Trop Dis.* (2017) 11:e0005486. doi: 10.1371/journal.pntd.0005486

103. Kong F, Saldarriaga OA, Spratt H, Osorio EY, Travi BL, Luxon BA, et al. Transcriptional profiling in experimental visceral leishmaniasis reveals a broad splenic inflammatory environment that conditions macrophages toward a disease-promoting phenotype. *PLoS Pathog.* (2017) 13:e1006165. doi: 10.1371/journal.ppat.1006165

104. de Santana FR, Dalboni LC, Nascimento KF, Konno FT, Alvares-Saraiva AM, Correia MSF, et al. High dilutions of antimony modulate cytokines production and macrophage – Leishmania (L.) amazonensis interaction *in vitro*. *Cytokine* (2017) 92:33–47. doi: 10.1016/j.cyto.2017.01.004

105. Venturin GL, Chiku VM, Silva KLO, de Almeida BFM, de Lima VMF. M1 polarization and the effect of PGE $_2$ on TNF-α production by lymph node cells from dogs with visceral leishmaniasis. *Parasit Immunol.* (2016) 38:698–704. doi: 10.1111/pim.12353

106. Moreira PRR, Fernando FS, Montassier HJ, André, MR, de Oliveira Vasconcelos, R. Polarized M2 macrophages in dogs with visceral leishmaniasis. *Vet Parasitol.* (2016) 226:69–73. doi: 10.1016/j.vetpar.2016.06.032

107. Siewe N, Yakubu A-A, Satoskar AR, Friedman A. Immune response to infection by Leishmania : a mathematical model. *Math Biosci.* (2016) 276:28–43. doi: 10.1016/j.mbs.2016.02.015

108. Dameshghi S, Zavaran-Hosseini A, Soudi S, Shirazi FJ, Nojehdehi S, Hashemi SM. Mesenchymal stem cells alter macrophage immune responses to Leishmania major infection in both susceptible and resistance mice. *Immunol Lett.* (2016) 170:15–26. doi: 10.1016/j.imlet.2015.12.002

109. Mukhopadhyay D, Mukherjee S, Roy S, Dalton JE, Kundu S, Sarkar A, et al. M2 Polarization of monocytes-macrophages is a hallmark of indian post Kala-Azar dermal leishmaniasis. *PLoS Negl Trop Dis.* (2015) 9:e0004145. doi: 10.1371/journal.pntd.0004145

110. Allman WR, Dey R, Liu L, Siddiqui S, Coleman AS, Bhattacharya P, et al. TACI deficiency leads to alternatively activated macrophage phenotype and susceptibility to Leishmania infection. *Proc Natl Acad Sci USA.* (2015) 112:E4094–103. doi: 10.1073/pnas.1421580112

111. Bhattacharya P, Dey R, Dagur PK, Kruhlak M, Ismail N, Debrabant A, et al. Genetically modified live attenuated leishmania donovani parasites induce innate immunity through classical activation of macrophages that direct the Th1 response in mice. *Infect Immun.* (2015) 83:3800–15. doi: 10.1128/IAI.00184-15

112. McCartney-Francis N, Jin W, Belkaid Y, McGrady G, Wahl SM. Aberrant host defense against *Leishmania major* in the absence of SLPI. *J Leukoc Biol.* (2014) 96:917–29. doi: 10.1189/jlb.4A0612-295RR

113. Díaz-Gandarilla JA, Osorio-Trujillo C, Hernández-Ramírez VI, Talamás-Rohana P. PPAR activation induces M1 macrophage polarization via cPLA $_2$

13

-COX-2 inhibition, activating ROS production against *Leishmania mexicana*. *Biomed Res Int.* (2013) 2013:1–13. doi: 10.1155/2013/215283

114. Farrow AL, Rana T, Mittal MK, Misra S, Chaudhuri G. Leishmania-induced repression of selected non-coding RNA genes containing B-box element at their promoters in alternatively polarized M2 macrophages. *Mol Cell Biochem.* (2011) 350:47–57. doi: 10.1007/s11010-010-0681-5

115. CDC (2017). *CDC - DPDx - Leishmaniasis.*

116. França-Costa J, Weyenbergh J, Van Boaventura VS, Luz NF, Malta-Santos H, Cezar M, et al. Arginase, I., polyamine, and prostaglandin E2 pathways suppress the inflammatory response and contribute to diffuse cutaneous leishmaniasis. *J Infect Dis.* (2014) 211:426–35. doi: 10.1093/infdis/jiu455

117. Abebe T, Hailu A, Woldeyes M, Mekonen W, Bilcha K, Cloke T, et al. Local increase of arginase activity in lesions of patients with cutaneous leishmaniasis in ethiopia. *PLoS Negl. Trop. Dis.* (2012) 6:e1684. doi: 10.1371/journal.pntd.0001684

118. Lee SH, Charmoy M, Romano A, Paun A, Chaves MM, Cope FO, et al. Mannose receptor high, M2 dermal macrophages mediate nonhealing *Leishmania major* infection in a Th1 immune environment. *J Exp Med.* (2018) 215:357–75. doi: 10.1084/jem.20171389

119. Rigamonti E, Chinetti-Gbaguidi G, Staels B. Regulation of macrophage functions by PPAR-alpha, PPAR-gamma, and LXRs in mice and men. *Arterioscler Thromb Vasc Biol.* (2008) 28:1050–9. doi: 10.1161/ATVBAHA.107.158998

120. Odegaard JI, Ricardo-Gonzalez RR, Goforth MH, Morel CR, Subramanian V, Mukundan L, et al. Macrophage-specific PPARγ controls alternative activation and improves insulin resistance. *Nature* (2007) 447:1116–20. doi: 10.1038/nature05894

121. Gallardo-Soler A, Gómez-Nieto C, Campo ML, Marathe C, Tontonoz P, Castrillo A, et al. Arginase I induction by modified lipoproteins in macrophages: a peroxisome proliferator-activated receptor-gamma/delta-mediated effect that links lipid metabolism and immunity. *Mol Endocrinol.* (2008) 22:1394–402. doi: 10.1210/me.2007-0525

122. Vellozo NS, Pereira-Marques ST, Cabral-Piccin MP, Filardy AA, Ribeiro-Gomes, FL, Rigoni TS, et al. All-trans retinoic acid promotes an M1-to M2-phenotype shift and inhibits macrophage-mediated immunity to leishmania major. *Front Immunol.* (2017) 8:1560. doi: 10.3389/fimmu.2017.01560

123. de Freitas EO, Leoratti FM, de S, Freire-de-Lima CG, Morrot A, Feijó DF. The contribution of immune evasive mechanisms to parasite persistence in visceral leishmaniasis. *Front Immunol.* (2016) 7:153. doi: 10.3389/fimmu.2016.00153

124. Abebe T, Takele Y, Weldegebreal T, Cloke T, Closs E, Corset C, et al. Arginase activity - a marker of disease status in patients with visceral leishmaniasis in ethiopia. *PLoS Negl Trop Dis.* (2013) 7:e2134. doi: 10.1371/journal.pntd.0002134

125. Sarkar A, Saha P, Mandal G, Mukhopadhyay D, Roy S, Singh SK, et al. Monitoring of intracellular nitric oxide in leishmaniasis: its applicability in patients with visceral leishmaniasis. *Cytom Part A* (2011) 79A:35–45. doi: 10.1002/cyto.a.21001

126. Roy S, Mukhopadhyay D, Mukherjee S, Moulik S, Chatterji S, Brahme N, et al. An IL-10 dominant polarization of monocytes is a feature of indian visceral leishmaniasis. *Parasite Immunol.* (2018) 40:e12535. doi: 10.1111/pim.12535

127. Hammami A, Abidin BM, Charpentier T, Fabié A, Duguay A-P, Heinonen KM, et al. HIF-1α is a key regulator in potentiating suppressor activity and limiting the microbicidal capacity of MDSC-like cells during visceral leishmaniasis. *PLoS Pathog.* (2017) 13:e1006616. doi: 10.1371/journal.ppat.1006616

128. Chan MM, Adapala N, Chen C. Peroxisome proliferator-activated receptor-γ-mediated polarization of macrophages in leishmania infection. *PPAR Res.* (2012) 2012:796235. doi: 10.1155/2012/796235

129. Kumar A, Das S, Mandal A, Verma S, Abhishek K, Kumar A, et al. *Leishmania* infection activates host mTOR for its survival by M2 macrophage polarization. *Parasit Immunol.* (2018) 40:e12586. doi: 10.1111/pim.12586

130. Ontoria E, Hernández-Santana YE, González-García AC, López MC, Valladares B, Carmelo E. Transcriptional profiling of immune-related genes in leishmania infantum-infected mice: identification of potential biomarkers of infection and progression of disease. *Front Cell Infect Microbiol.* (2018) 8:197. doi: 10.3389/fcimb.2018.00197

14

2. OBJETIVOS

2.1. OBJETIVOS GERAIS

Sabendo das lacunas existentes no entendimento da imunidade protetora desenvolvida frente à infecção por *Leishmania (Leishmania) amazonensis*, o objetivo deste trabalho foi demonstrar a resposta imune diferencial estabelecida por camundongos parcialmente resistentes (C57BL/6) e susceptíveis (BALB/c) à infecção por esta espécie de protozoário.

2.2. OBJETIVOS ESPECÍFICOS

- Caracterizar a evolução da infecção nas diferentes linhagens de camundongos;
- Quantificar a produção de citocinas dos padrões Th1, Th2 e Th17;
- Analisar a produção de ânion superóxido no local da infecção;
- Quantificar o número macrófagos no local da infecção e identificar marcadores relacionados aos padrões de macrófagos M1 e M2;
- Determinar o reparo tecidual no local da infecção;
- Avaliar a transferência adotiva de macrófagos como potencial interferente no curso da infeção.

3. RESULTADOS
3.1. Capítulo 2

Susceptibilidade murina à infecção por *Leishmania amazonensis* é dependente da arginase-1 de macrófagos

Murine susceptibility to Leishmania amazonensis infection is dependent on arginase-1 of macrophages

Fernanda Tomiotto Pellissier, Milena Menegazzo Miranda-Sapla, Taylon Felipe Silva, Bruna Taciane da Silva Bortoleti, Manoela Daiele Gonçalves, Virginia Márcia Concato, Ana Carolina Jacob Rodrigues, Idessania Nazareth Costa, Carolina Panis, Ivete Conchon-Costa, Juliano Bordignon, Wander Rogério Pavanelli

Artigo com resumo aceito para a edição especial "*Cutaneous Leishmaniasis: Exploring Pathogenesis and Immunomodulatory Approaches*" do periódico *Frontiers in Cellular and Infection Microbiology* - fator de impacto 4,12 (JCR 2020)/ Qualis A1 em fevereiro de 2021 (Anexo 6.1).

A partir dos resultados compilados no capítulo 1, percebe-se que apesar dos avanços no conhecimento do papel de macrófagos M1 e M2 em diferentes doenças infecciosas, ainda pouco é descrito sobre suas funções no desenvolvimento da Leishmaniose, em especial na doença causada por *Leishmania amazonensis*, espécie presente no Brasil, principalmente nas regiões norte e nordeste.

Em infecções por parasitos desta espécie, camundongos BALB/c desenvolvem lesões e uma resposta imune predominantemente do tipo Th2, enquanto camundongos da linhagem C57BL/6 apresentam edema local sem ulcerações, e manifestam resposta imune mista Th1 e Th2, sendo considerados parcialmente resistentes à infecção. Tal resposta mista é similar à observada na leishmaniose cutânea humana, validando a relevância biológica deste modelo experimental.

Sendo assim, avaliou-se a resposta diferencial estabelecida por camundongos BALB/c e C57BL/6 frente à infecção por *L. amazonensis*. O presente trabalho é constituído de duas etapas. Na primeira, foi verificado que camundongos C57BL/6 apresentaram marcadores de ambos os perfis imunes M1 e M2, e identificada a enzima arginase-1 (Arg-1) como um possível marcador de agravamento das lesões em período crônico de infecção em camundongos BALB/c.

Na segunda parte, foi observado que a transferência adotiva de macrófagos peritoneais de C57BL/6 para BALB/c infectados promove redução do edema e do número de parasitos no local da lesão, além de reduzir os níveis de Arg-1. Assim, a pior evolução das lesões parece estar envolvida com o recrutamento de macrófagos ricos em Arg-1. Esses resultados ampliam a compreensão sobre a imunidade protetora contra *L. amazonensis*, fornecendo novos conhecimentos que podem contribuir para o desenvolvimento de intervenções de tratamento ou prevenção da leishmaniose.

Os resultados brevemente descritos acima são detalhados no capítulo 2 da presente tese de doutorado, apresentado a seguir.

Murine susceptibility to *Leishmania amazonensis* infection is dependent on arginase-1 of macrophages

Fernanda Tomiotto Pellissier[1,2,*], Milena Menegazzo Miranda-Sapla[2], Taylon Felipe Silva[2], Bruna Taciane da Silva Bortoleti[1,2], Manoela Daiele Gonçalves[3], Virginia Márcia Concato[2], Ana Carolina Jacob Rodrigues[1,2], Idessania Nazareth Costa[2], Carolina Panis[4], Ivete Conchon-Costa[2], Juliano Bordignon[1,5], Wander Rogério Pavanelli[1,2,*]

[1] Biosciences and Biotechnology Postgraduate Program, Carlos Chagas Institute (ICC), Fiocruz, Curitiba, Brazil.
[2] Laboratory of Immunoparasitology of Neglected Diseases and Cancer (LIDNC), Department of Pathological Sciences, State University of Londrina, Londrina, Brazil.
[3] Laboratory of Biotransformation and Phytochemistry, Department of Chemistry, State University of Londrina, University Hospital, Londrina, Brazil.
[4] Laboratory of Tumor Biology, State University of Western Paraná (UNIOESTE), Francisco Beltrão, Brazil.
[5] Laboratory of Molecular Virology, Carlos Chagas Institute (ICC), Fiocruz, Curitiba, Brazil.

*Correspondence:
Corresponding Authors
fernandatomiotto@gmail.com and wanderpavanelli@yahoo.com.br

Abstract

Cutaneous leishmaniasis is a zoonotic infectious disease with broad world distribution that causes a range of diseases with clinical outcomes ranging from self-healing infections to chronic disfiguring disease. The understanding of the effective immune response to this infection still has many gaps, which comprehension is fundamental to the development of drugs and vaccines. Thus, we investigated the local profile of mediators involved in the development of cutaneous leishmaniasis in experimental models of susceptibility (BALB/c) and partial resistance (C57BL/6) to *Leishmania amazonensis* infection. It was found that BALB/c mice had a worse disease outcome compared to C57BL/6 mice, with higher parasitic load, ulcerated lesion formation, and higher levels of IL-6 in infected paws. On the other hand, C57BL/6 presented higher levels of IFN-γ and superoxide anion ($^{\bullet}O_2^-$) after 11 weeks of infection and no lesion ulcerations. A peak of local macrophages was observed after 24h of infection in both studied mice strains, followed by a further increase after 240h detected only in C57BL/6 mice. Regarding M1 and M2 macrophage phenotype markers (iNOS, MHC-II, CD206, and arginase-1 [Arg-1]), we found that in BALB/c there was a pronounced increase in Arg-1 levels after 11 weeks of infection, whereas in C57BL/6 there was an initial predomination of markers from both profiles, followed by an M2 predominance, that coincided with the second peak of macrophage infiltration, 240h after the infection. Greater deposition of type III collagen and lesion resolution was also observed in C57BL/6 mice. The adoptive transfer of macrophages from C57BL/6 to infected BALB/c at the 11th week shown a reduction in both edema and the number of parasites at the lesion site, besides lower levels of Arg-1. Thus, C57BL/6 mice have a more effective response against *L. amazonensis*, based on a balance between inflammation and antioxidant response, coinciding with better tissue repair, while BALB/c mice have an excessive Arg-1 production in late infection times, which is related to the development of disease severity. The worst evolution seems to be involved with the recruitment of Arg-1 related macrophages, since the adoptive transfer of macrophages from C57BL/6 mice to BALB/c resulted in better outcomes, with lower levels of Arg-1.

1   Introduction

Leishmaniasis is a group of infectious diseases caused by species of protozoan parasites of the *Leishmania* genus, which are transmitted to animals and humans through the bite of female infected phlebotomine sand flies. The main clinical forms of the disease are cutaneous leishmaniasis (CL), visceral leishmaniasis, and mucocutaneous leishmaniasis. CL is the most common form, with estimates of 1 million new cases annually worldwide (WHO, 2020).

Considered a neglected tropical disease by the World Health Organization, leishmaniasis represents a great challenge in the pharmacological field with no experimental vaccine candidates with satisfactory progression in human trials until now (Lage et al., 2020). Additionally, the available treatment for CL present high toxicity and is not fully effective (Caridha et al., 2019). A range of factors could explain the lack of vaccines and therapeutic options against CL, like the diversity among *Leishmania* species and the complexity of the host's immune responses (Müller et al., 2018; Kaye et al., 2020). Thus, the understanding of the effective immune response to *Leishmania*-infection is fundamental to help drug discovery and vaccine development.

Since the discovery of T CD4^{+} helper 1 (Th1) and Th2 cells, experimental studies of CL have answered basic immunological questions related to the development of the lesions (Scott and Novais, 2016). It was postulated by experimental studies using *L. major* that C57BL/6 mice present a predominant Th1 response, associated with infection control, while BALB/c mice developed a Th2 response, favoring the disease progression (Sacks and Noben-Trauth, 2002; Scott and Novais, 2016). However, it is currently known that the Th1/Th2 paradigm is not valid for all *Leishmania* species.

In *L. amazonensis* infections, BALB/c mice also develop a lesion and a predominant Th2 response, however, C57BL/6 mice manifest a mixed immune response with mediators from both Th1 and Th2 patterns, being considered partially resistant to the infection (Soong, 2012; Pratti et al., 2016; Scott and Novais, 2016). This mixed response is similar to those observed in human infections, validating the biological relevance of these mice models for the study of cutaneous leishmaniasis (Soong, 2012).

Is noteworthy that *Leishmania* parasites can actively manipulate their hosts and subvert the microbicide mechanisms through the modification/delay of the development of a type 1 response (Gregory and Olivier, 2005; Rossi and Fasel, 2018; Aoki et al., 2019). These escape mechanisms have been extensively characterized and vary according to the parasite species and host genetic background (Alexander et al., 1980; Lira et al., 2000; Rosas et al., 2005; Velasquez et al., 2016; Muxel et al., 2018).

Besides this, the clinical course of *Leishmania* spp. infections is not only dependent on T cells response and involves a complex range of cells, including macrophages, the main host cells

for parasite replication. The macrophages present a dual role during the infection, providing a safe place for parasites' survival inside the parasitophorous vacuole, but also triggering an inflammatory response (cytokines production and oxidative stress response) that can control the parasite replication. Therefore, macrophages are the key cell to disease progression, and their interaction with the parasites can dictate the success or failure of the infection (Liu and Uzonna, 2012).

There are two main macrophage types described, M1 or "classically activated" and M2 or "alternatively activated" (Mills et al., 2000). M1 macrophages are activated by the Th1 lymphocyte subpopulation and produce interferon-gamma (IFN-γ) and tumor necrosis factor-alpha (TNF-α), triggering the microbicide machinery and inducing the production of reactive species, especially superoxide anion ($^{\bullet}O_2^-$) by NADPH oxidase enzyme, and nitric oxide (NO) by inducible nitric oxide synthase (iNOS), that eliminates *Leishmania* sp. parasites (Rossi and Fasel, 2018). However, intense activation of M1 macrophages in the attempt to control the infection can trigger inflammation with tissue damage and exacerbation of the lesion (Laskin et al., 2011).

On the other side, M2 macrophages are activated mainly by IL-13 and IL-4 produced by Th2 cells, which in turn activates the enzyme arginase-1 (Arg-1), culminating in the synthesis of polyamines, which allows *Leishmania* intramacrophagic replication, favoring parasite survival and disease progression (Pessenda and Santana da Silva, 2020). Meanwhile, despite the characteristics of permissiveness to infection, the M2 macrophage (and the Arg-1 activity) are also responsible for tissue remodeling and repair, and inflammation resolution (Laskin et al., 2011). As iNOS and Arg-1 share L-arginine as substrate, these enzymes represent two possible pathways of the immune response against *Leishmania* (Mills et al., 2000; Pessenda and Santana da Silva, 2020).

In this context, a balance between a potent microbicide response, combined with a resolutive and healing process seems to be the key to provide the utmost benefit for the host (Tomiotto-Pellissier et al., 2018). Nonetheless, little is known about this balance and the role of M1 and M2 related molecules in leishmaniasis, in which the understanding may be important to the potential development of drugs and vaccines.

Based on this, this work aimed to demonstrate the differential response established by susceptible (BALB/c) and partially resistant (C57BL/6) mice to *Leishmania amazonensis* infection. The results showed that BALB/c mice have a worse disease outcome compared to C57BL/6 mice, with higher levels of Arg-1. When the adoptive transfer of peritoneal macrophages from C57BL/6 to infected BALB/c was carried out, it was found a reduction in the parasite burden, lesion edema, and ulceration, concomitant with a reduction in the Arg-1 levels. Thus, the worst evolution of CL in BALB/c mice seems to be involved with the recruitment of Arg-1 related macrophages in the later times of *L. amazonensis* infection.

2 Materials and Methods

2.1. Culture of *Leishmania (L.) amazonensis*

Promastigote forms of *Leishmania (L.) amazonensis* (MHOM/BR/1989/166MJO) were maintained 199 growth medium (GIBCO, Invitrogen, USA) supplemented with 10% fetal bovine serum (FBS, GIBCO Invitrogen), 1 M Hepes, 0.1% human urine, 0.1% L-glutamine, 10 µg/mL penicillin and streptomycin (GIBCO Invitrogen) and 10% sodium bicarbonate (CAQ, Brazil) The cell cultures were maintained in an incubator-type B.O.D. at 25 °C, in 25 cm^2 flasks. In all experiments, promastigote forms were used in the stationary growth phase.

2.2. Animals and Infection

BALB/c and C57BL/6 mice weighing approximately 25–30 g and aged 6–12 weeks were kept under sterile conditions and used according to protocols approved by the Institutional Animal Care and Committee. This study was approved by the Ethics Committee for Animal Experimentation of the State University of Londrina, number 8286.2016.60.

Mice were infected on the footpad of both hind paws, subcutaneously, with 10^5 promastigote forms of *L. amazonensis/*paw. The animals were divided into groups and evaluated at 6, 24, 72, 144, and 240 hours, and 11 weeks post-infection (p.i.). Paw edema was measured weekly using a digital caliper (Starrett 799).

After the end of each time point, the animals were euthanized by intraperitoneal inoculation of 100 mg/kg ketamine (Ceva, Brazil) and 10 mg/kg xylazine (JA, Brazil) followed by cervical dislocation, and the footpads of infected paws were collected, weighed and processed for the next assays.

2.3. Parasite burden analysis

Quantitative PCR (qPCR) was performed to determine the tissue parasite load in each group. Briefly, hind paw samples were mechanically homogenized (Tissue-tearor, BioSpec) in TELT buffer (50 mM de Tris-HCl pH 8, EDTA 62,5 mM, Triton-X 4% e LiCl$_2$ 2.5 M) and DNA extraction was performed with the Easy-DNA kit (Invitrogen, USA, K1800-01) according to the manufacturer's instructions. After, it was added a solution of phenol: chloroform: isoamyl alcohol (25:24:1), and two volumes of cold ethanol (Merck, Germany) were added to the aqueous phase, and samples were stored at -20°C for 12 h. Samples were then centrifuged for 30 min at 10,000 *g*, washed with 70% ethanol, dried at room temperature, and resuspended in 10 mM Tris-HCl (pH 8.5). qPCR was performed by using GoTaq qPCR Master Mix (Promega, USA) with 100 ng total genomic DNA (gDNA). Parasite quantification was performed using AAP3 gene primer 5'-GGCGGCGGTATTATCTCGAT-3' (Forward) 5'-ACCACGAGGTAGATGACAGACA-3'

(Reverse) *Leishmania*-specific primers at 10 pM (Tellevik et al., 2014). The samples were amplified with a StepOnePlus Real-Time PCR System (Applied Biosystems, USA) under the following PCR conditions steps: 2 min at 50°C, 2 min at 95°C, 40 cycles of 15 s at 95°C, 1 min at 55°C, followed by a dissociation step of 55 - 99ºC (heating of 0.5ºC/s). The results were based on a standard curve constructed with DNA from culture samples of *L. amazonensis* promastigote forms.

2.4. Cytokines determination

Th1, Th2, and Th17 cytokines were evaluated in the supernatant of the paw homogenates. The analyzes were performed using Cytometric Beads Array (CBA) assays using a commercial kit (BD Bioscience, USA) following the manufacturer's recommendations. The concentration of each cytokine was determined regarding the standard curve generated from reading the different dilutions of the recombinant cytokine. The limit of detection for each cytokine was 0.1, 0.03, 1.4, 0.5, 0.9, 0.8 and 16.8 pg/mL, respectively for IL-2, IL-4, IL-6, IFN-γ, TNF-α, IL-17 and IL-10. The data were obtained in BD Accuri C6 flow cytometer and analyzed using FCAP Array v. 3.0.1 software.

2.5. Superoxide anion measurement

The superoxide anion ($^\bullet$O$_2^-$) production in the paw homogenates was evaluated by testing with nitroblue tetrazolium (NBT, Sigma-Aldrich, USA). For the assay, 10 μL of the sample were plated and 100 μL of the solution containing NBT (1 mg/mL) was added. After 15 minutes of reaction at room temperature, the samples were fixed with 10 μL of methanol, and the formazan, product of the reaction between NBT and $^\bullet$O$_2^-$, solubilized by the addition of 120 μL of 2M KOH (Merck). The readings were performed on a spectrophotometer (GloMax Explorer instrument, Promega) at 660 nm and the results normalized per mg of tissue.

2.6. Determination of N-acetylglucosaminidase (NAG) activity

For the indirect quantification of the presence of macrophages at the infection site, the activity of the enzyme NAG was measured. The evaluation of the cellular infiltrate in the animals' footpad samples was performed by a colorimetric method described by (Bradley et al., 1982). Briefly, the samples were collected in 50 mM potassium phosphate buffer (pH 6.0) containing 13.72 mM HTAB (hexadecyl trimethyl ammonium bromide) and stored at -20 ºC. The samples were then homogenized and centrifuged (21293 x g, 2 min, 4 ºC). The supernatant was used for the colorimetric reaction in a 96-well plate. Each aliquot of 15 μL of the sample was added to 200 μL of the reaction solution containing 52.64 mM of N-acetylglucosaminidase. The readings were

performed on a spectrophotometer (GloMax Explorer instrument, Promega) at 450 nm, and the number of macrophages per mg of tissue was determined using a standard curve.

2.7. Histological processing

For the immunohistochemistry and collagen quantification, one of the paws of each animal was fixed in 10% formalin solution and after 24 hours they were decalcified for 21 days in 5% nitric acid (Anidrol, Brazil) and then processed for inclusion in paraffin. The cuts (5 μm thick) were adhered to slides treated with poly-L-lysine (Sigma-Aldrich), washed in xylol (FMAIA, Brazil) to remove excess paraffin, and rehydrated with decreasing concentrations of alcohol.

2.8. Immunohistochemistry of lesions for iNOS, MHC-II, Arg1, and CD206 labeling

The rehydrated histological sections of paws were submitted to antigenic recovery in citrate and acetate buffer solution (pH 6) for 10 minutes in a microwave (40W, 90ºC). Endogenous peroxidase was blocked in a solution of 3% H_2O_2 (Anidrol), 10% methanol (Merck), and 0.1% tween-80 (Sigma-Aldrich) for 30 min and, subsequently, the non-specific sites blocked with PBS containing 1% FBS (GIBCO Invitrogen) for 30 min at room temperature. Then, the primary antibodies were added to the labeling of iNOS (NOS2, dilution 1:500, Santa Cruz Biotechnology, USA, Cat. SC7271), MHC-II (1:500, Santa Cruz, SC59318), arginase-1 (Arg-1, 1:600, Santa Cruz, SC18351) and CD206, 1:400, Santa Cruz, SC34577) for 2h at 37°C. Subsequently, the universal solution of secondary antibodies with biotinylated anti-rabbit, anti-mouse, and anti-goat IgG (LSAB + System-HRP, DAKO, Japan) was added for 1 hour in room temperature. After three washes with PBS, the slides containing the samples were incubated with the avidin-peroxidase (LSAB + System-HRP, DAKO, K069011-2) complex for 40 minutes at room temperature. Finally, it was added 3,3'-Diaminobenzidine (DAB, DAKO, K3468), and the counterstaining was performed with hematoxylin (Merck).

For determining a quantitative scoring, images were evaluated by using the color deconvolution tool from the Image J software (NIH, USA). Data are expressed in pixels (% of labeling in the image area).

2.9. Collagen quantification

The quantification of collagen in the paws lesion was performed by the Sirius-red staining method, assessed under polarized light through a photomicroscope (CARL ZEISS- Axio Imager A1) with a camera (HBO 100) coupled to a computer using the AxioVision software, with a 200x magnification. Five images of two sections of each animal were considered for analysis using the

Image-Pro Plus software (version 4.5). The results were expressed as a percentage of area with the presence of total collagen and type III collagen in the measured area (Miranda et al., 2015).

2.10. Adoptive transference of macrophages (ATM)

BALB/c and C57BL/6 mice were kept under the same conditions described in item 2.2.

Macrophages were recovered from the peritoneal cavity of non-infected C57BL/6 with cold PBS supplemented with 3% of FBS (GIBCO Invitrogen) and stained with antibodies F4/80-PE (dilution 1:100, Santa Cruz Biotech, SC377009 and CD11b-FITC (dilution 1:100, Santa Cruz Biotech, SC23937). The antibody staining profile was analyzed by flow cytometry (BD Accuri C6 flow cytometer) using FCAP Array v3.0.1 software.

BALB/c mice were infected on both hind paws, subcutaneously, with 10^5 promastigote forms of *L. amazonensis*/paw, and randomly divided into three groups: BALB/c ATM IP – animals who received the ATM with macrophages from C57BL/6 via intraperitoneal injection, BALB/c ATM IV – who received the ATM with macrophages from C57BL/6 via intravenous injection, and BALB/c – animals who not received ATM (n = 6/group).

At the ninth week of infection, the BALB/c ATM groups received the transference of $5x10^5$ peritoneal macrophages from C57BL/6 mice via intraperitoneal (BALB/c ATM IP) or by retro-orbital injection (BALB/c ATM IV; under anesthesia with 100 mg/kg ketamine (Ceva) and 10 mg/kg xylazine (JA) (Figure 6A). At the end of the eleventh week, the animals were euthanized as described in 2.2. The edema was measured weekly as described in item 2.2, the parasite burden analysis was performed as described in item 2.3 and the cytokines measurement was performed as item 2.4.

2.11. Enzyme-Linked Immunosorbent Assay for iNOS and Arg-1 in paws homogenate

Radioimmunoprecipitation assay buffer (RIPA lysis buffer - 140 mM sodium chloride, 1% Triton X-100, 0.1% sodium deoxycholate, 0.5% sodium dodecyl sulfate, 1 mM EDTA, 10 mM Tris, pH 8.0 and 1 mM phenylmethanesulfonyl fluoride (PMSF) was added (1 mL) to the hind paws samples, mechanically homogenized (Tissue-tearor, BioSpec), and incubated for 2h, 4ºC. The lysates were collected and centrifuged at 13,000 x *g* for 20 min at 4°C, the supernatants were transferred to a new tube and the total protein concentration was quantified in NanoVue Plus GE Healthcare (Biochrom, USA). The protein concentration of all samples was normalized to 10 µg/mL and a 50 µL aliquot was added in a 96-well ELISA plate for adsorption of proteins overnight at 4ºC, followed by incubation for 1h with blocking buffer (ELISA/ELISPOT, eBioscience, USA). The wells were washed 3x with wash buffer (PBS + 0.5% Tween 20 (Sigma-Aldrich)) and incubated with primary antibody anti-mouse iNOS (Santa Cruz Biotech, SC7271) and Arg-1 (Santa

Cruz Biotech, SC18351) at 1:500 dilutions for 1h at room temperature. The wells were washed to remove unbound antibodies, followed by the addition of universal biotinylated secondary antibody (LSAB2 System-HRP, Dako), 1h incubation, washing, and addition of streptavidin-HRP (LSAB2 System-HRP, Dako) for 1h. After the incubation time, the wells were washed 5 times and 100 µL of TMB Substrate Solution (eBioscience, 00-4201-56) was added, followed by incubation for 30 min and 100 µL of stop solution (1N sulfuric acid) was added. The plate reading was performed in a microplate reader at 450 nm (GloMax, Promega), and the results are expressed as arbitrary units.

2.12. Statistical analysis

Data were expressed as a mean ±SEM. Data were analyzed using the GraphPad Prism statistical software (GraphPad Software, Inc., USA, 500.288). Differences between the two groups were evaluated using the student's t-test. Comparisons between multiple groups were done using ANOVA, followed by Tukey's test. Differences were considered as statistically significant upon $p < 0.05$. At least five animals per group were evaluated.

3 RESULTS

3.1. BALB/c mice show worse evolution of *L.amazonensis* infection when compared to C57BL/6 mice

The evolution of *L. amazonensis* infection was analyzed by the paw lesion edema, measured weekly until the eleventh week after infection. The edema was similar on both BALB/c and C57BL/6 mice until the eighth week of infection, however, from the ninth week on, the BALB/c mice showed significantly higher edema than the C57BL/6 (Figure 1A). Also, after 11 weeks of infection, ulcerated lesions were observed in all BALB/c mice, while none of the C57BL/6 strain had ulcerations (Figure 1B).

Regarding the parasitic load, we observed that BALB/c mice showed a significantly greater amount of parasites in the infected paws than the C57BL/6 mice after 11 weeks of infection (Figure 1C).
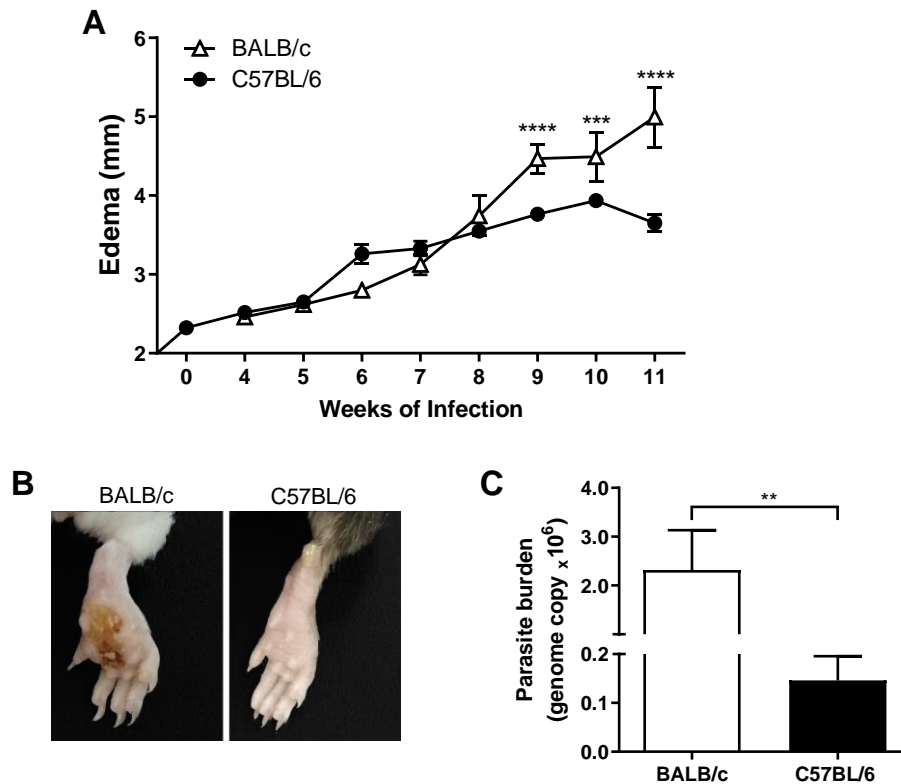
Figure 1 - Evolution of *L. amazonensis* infection in BALB/c and C57BL/6 mice. (A) BALB/c and C57BL/6 mice were infected on the hind paws with 10^5 promastigote forms of *L. amazonensis* and the edema was analyzed for 11 weeks. (B) Representative images of BALB/c and C57BL/6 mice paws 11 weeks after the infection with *L. amazonensis*. (C) Parasitic load (number of *Leishmania amazonensis* kDNA copies) determined in the mouse paw homogenate by quantitative real-time PCR after 11 weeks of infection. Data represent the mean ± SEM of 6 mice group. **Significant difference in relation to the opposite strain infected by *L. amazonensis*, $p \leq 0.01$, *** $p \leq 0.001$, **** $p \leq 0.0001$.

3.2. Cytokines are differentially produced by *L. amazonensis*-infected BALB/c and C57BL/6 mice paw

Based on the knowledge that *L. amazonensis* infection leads to a differential inflammatory response in BALB/c and C57BL/6 mice we measured the production of inflammatory cytokines in paws homogenates of infected-mice after 11 weeks. C57BL/6 mice presented higher levels of IFN-γ (Figure 2A), while BALB/c exhibited higher levels of IL-6 (Figure 2C). TNF-α levels, 11 weeks after infection, did not differ in BALB/c and C57BL/6-infeceted mice (Figure 2B). IL-2, IL-4, IL-10, and IL-17 values, as well as IFN-γ, TNF-α, and IL-6 levels at the infection times from 6 to 240h, remained below the detection limit of the technique; therefore, were not interpreted in the study.
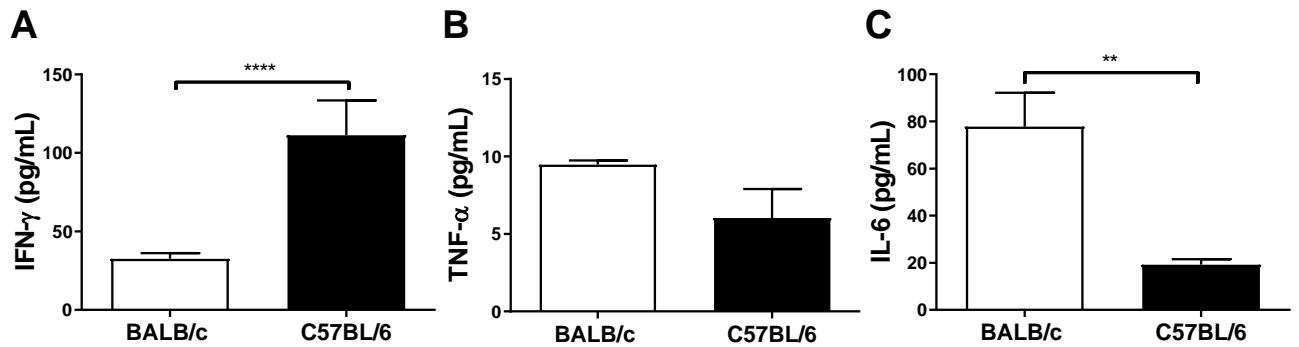
Figure 2 - Cytokines levels of BALB/c and C57BL/6 mice infected with *L. amazonensis*. Homogenates of *L. amazonensis*-infected BALB/c and C57BL/6 paws for 11 weeks were submitted to the CBA assay. (A) Measurement of IFN-γ, (B) TNF-α and (C) IL-6 levels after 11 weeks of infection. Data represent the mean ± SEM of 5 mice group. * Significant difference in relation to the opposite strain infected by *L. amazonensis*, p ≤ 0.05; ** p ≤ 0.01; *** p ≤ 0.001.

3.3. C57BL/6 mice produce higher levels of $^\bullet O_2^-$ in the infection site when compared to BALB/c mice

Aiming to understand the mechanisms involved with the early and late-stage pathogenesis of *L. amazonensis* infection in C57BL/6 and BALB/c mice strains, it was measured the $^\bullet O_2^-$ production (NBT assay) in paws homogenates. C57BL/6 mice had a higher basal production of $^\bullet O_2^-$ (0h), when compared to BALB/c mice. After infection, these radical levels were drastically reduced in both strains of mice (6h) but were restored later in the C57BL/6 mice (72h to 11 weeks). In BALB/c mice, it was observed that there was no restoration of $^\bullet O_2^-$ levels in the evaluated periods (no statistical difference between 6h and the later time points), which remained significantly lower when compared to C57BL/6 (72 to 240h) (Figure 3).
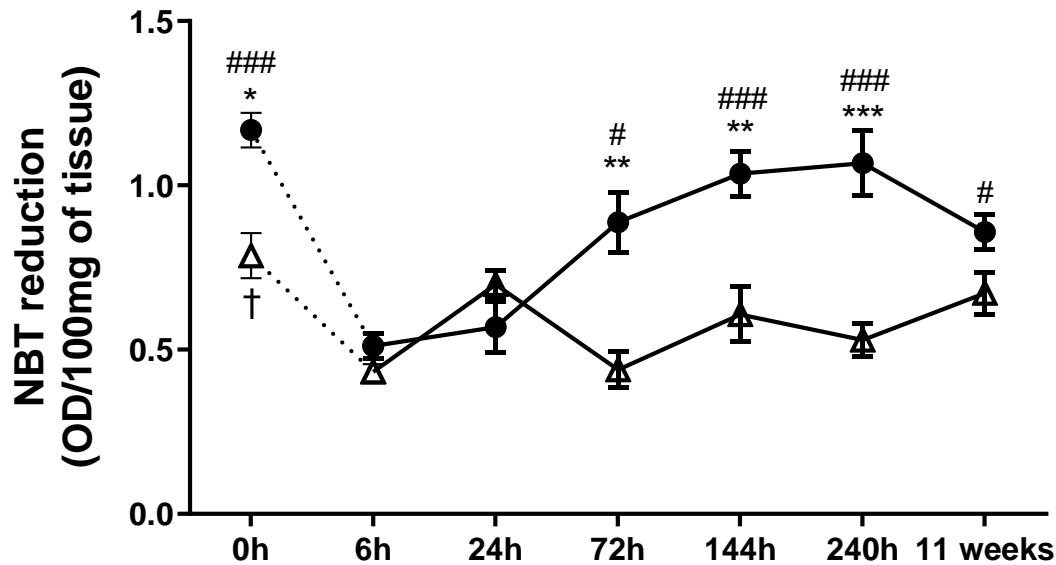
Figure 3 - Superoxide anion measured at the paws of BALB/c and C57BL/6 mice infected with *L. amazonensis*. Homogenates of BALB/c and C57BL/6 paws infected with *L. amazonensis* from 6h to 11 weeks submitted to the NBT assay. Uninfected mice were used as controls (0h). * Significant difference between mice strains infected by *L. amazonensis*, $p \leq 0.05$; ** $p \leq 0.01$, *** $p \leq 0.001$. [#]Difference in the time points *vs.* 6h within C57BL/6 mice, $p \leq 0.05$, [##]$p \leq 0.01$, [###]$p \leq 0.001$. [†]Difference in the time points *vs.* 6h within BALB/c mice, $p = 0.016$. Data represent the mean ± SEM of 5 mice group.

3.4. Macrophage infiltration and M1 and M2 markers are different between BALB/c and C57BL/6 during *L. amazonensis* infection.

To understand the dynamics of macrophage infiltration in the lesion site, we analyzed the quantity of these cells in the paws throughout the infection. It was found that in BALB/c mice, a single peak of macrophage infiltration occurs after 24 hours post *L. amazonensis* infection and that the amount of local macrophages decreases later (144h to 11 weeks). On the other hand, C57BL/6 showed two peaks of macrophage infiltration, one more initial 24h after infection, and the later one at 240h p.i. (Figure 4A).

To identify the profile of macrophages at the infection site, it was performed the immunohistochemistry assay to identify the presence of MHC-II and iNOS labeling, related to the M1 profile, and CD206and Arg-1 markers, related to the M2 phenotype. It was observed that at the beginning of infection (6h) the C57BL/6 mice show markers from both macrophages subpopulations when compared to BALB/c mice. After 24h, time point related to the first macrophage infiltration (Figure 4A), high CD206 marking was observed in C57BL/6. 72h p.i., Arg-1 was higher on C57BL/6 mice paws. After 144h, there was higher labeling for iNOS, Arg-1, and CD206 in C57BL/6 compared to BALB/c mice. In the time point that coincides with the second peak of infiltration, 240h, C57BL/6 mice presented higher marking of both Arg-1 and CD206 in

the infection site. After 11 weeks of infection, this profile was altered, with C57BL/6 presenting a greater presence of M1 markers, and BALB/c showed significantly higher levels of Arg-1 marking when compared to the C57BL/6 (Figure 4B -E, G).

We also found that, after 240h of infection, C57BL/6 mice showed a higher Arg-1/iNOS ratio than BALB/c. However, after 11 weeks of infection, this balance was reversed, with a substantial increase in the proportion of marking for Arg-1 on the BALB/c paws compared to C57BL/6 mice (Figure 4F).

Furthermore, immunohistochemical images show intense labeling Arg-1 after 11 weeks of infection is coincident with areas with vacuolated macrophages filled with parasites (Figure 4G, Figure S1). This pattern was also verified in the heatmap (Figure 4H), where it was possible to identify prominent Arg-1 labeling in BALB/c, while the levels found in C57BL/6 were more evenly distributed among the analyzed markers and times.
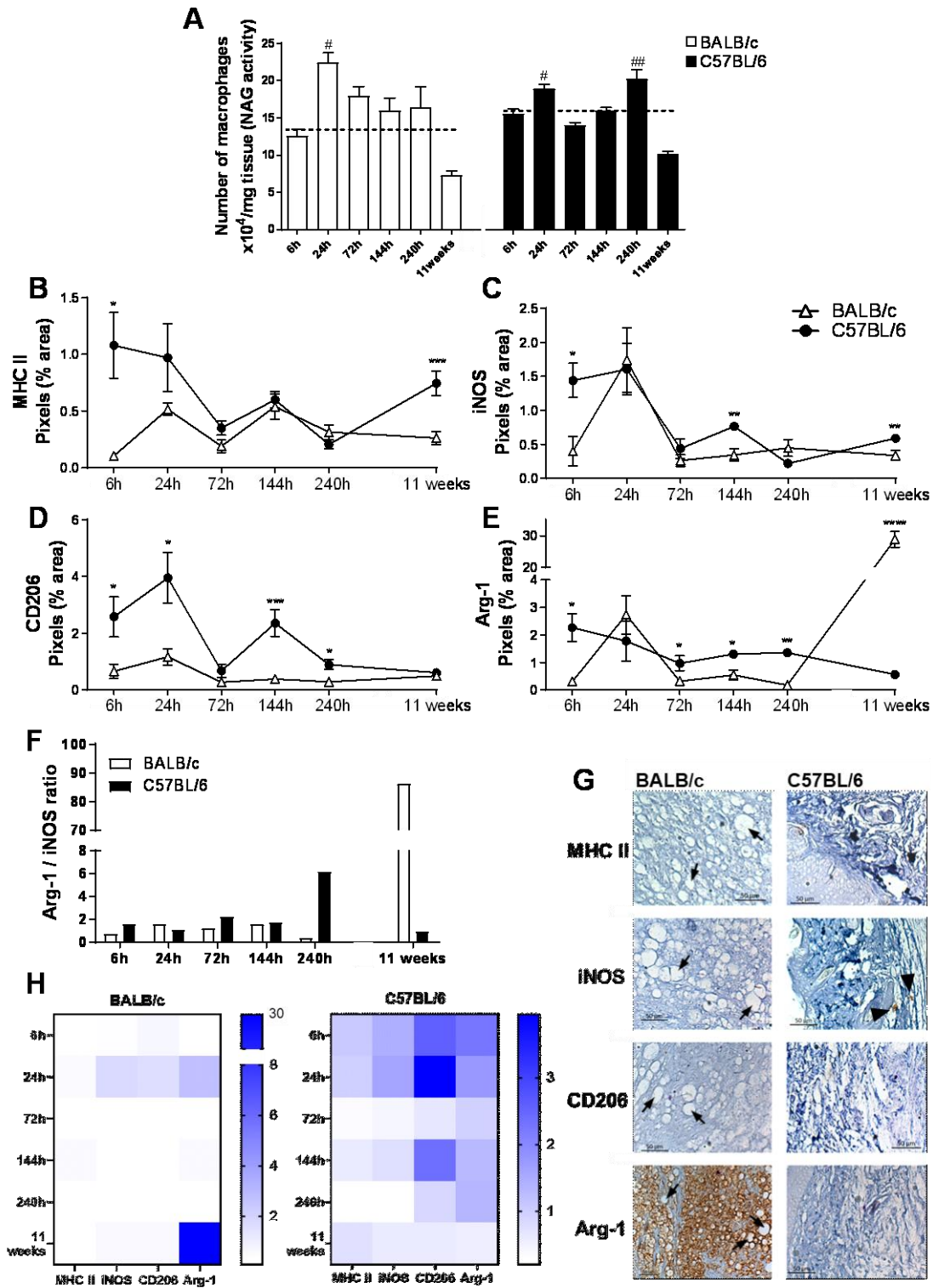
Figure 4 - Characterization of local macrophages in infected mice paws. (A) Indirect measurement of macrophages number by NAG activity. (B) Immunohistochemical quantification of MHC-II, (C) iNOS, (D) Arg-1, and (E) CD206 staining in the paw of infected mice. [#]Significant difference in relation to the non-infected mice (dashed lines), $p \leq 0.05$; [##]$p \leq 0.01$. *Significant difference between BALB/c and C57BL/6 mice infected with *L. amazonensis*, $p \leq 0.05$; **$p \leq 0.01$, ***$p \leq 0.001$, ****$p \leq 0.0001$. (F) Arg-1/iNOS ratio. (G) Representative figures of immunohistochemical labeling. The positive marking on immunohistochemistry sections

corresponds to the brown areas (arrowhead). Arrows indicate vacuolated macrophages filled with parasites. (H) Heatmap of MHC-II, iNOS, Arg-1, and CD206, in all evaluated time points. Data from A-E represent the mean ± SEM of 6 mice group

3.5. Type III collagen deposition in the site of infection is higher in C57BL/6 mice in the late stages of infection

Knowing that tissue repair is closely related to the clinical course of leishmaniasis, it was performed the identification of total collagen and the newly deposited collagen (type III) in the paws of infected mice as a readout of tissue repair (Frahs et al., 2018). From the results obtained it was possible to verify that, at 240h and 11 weeks p.i., C57BL/6 mice had significantly more total and type III collagen than BALB/c (Figure 5A and B). Besides, in C57BL/6 the amount of total collagen increased from 240h to 11 weeks of infection (Figure 5A).
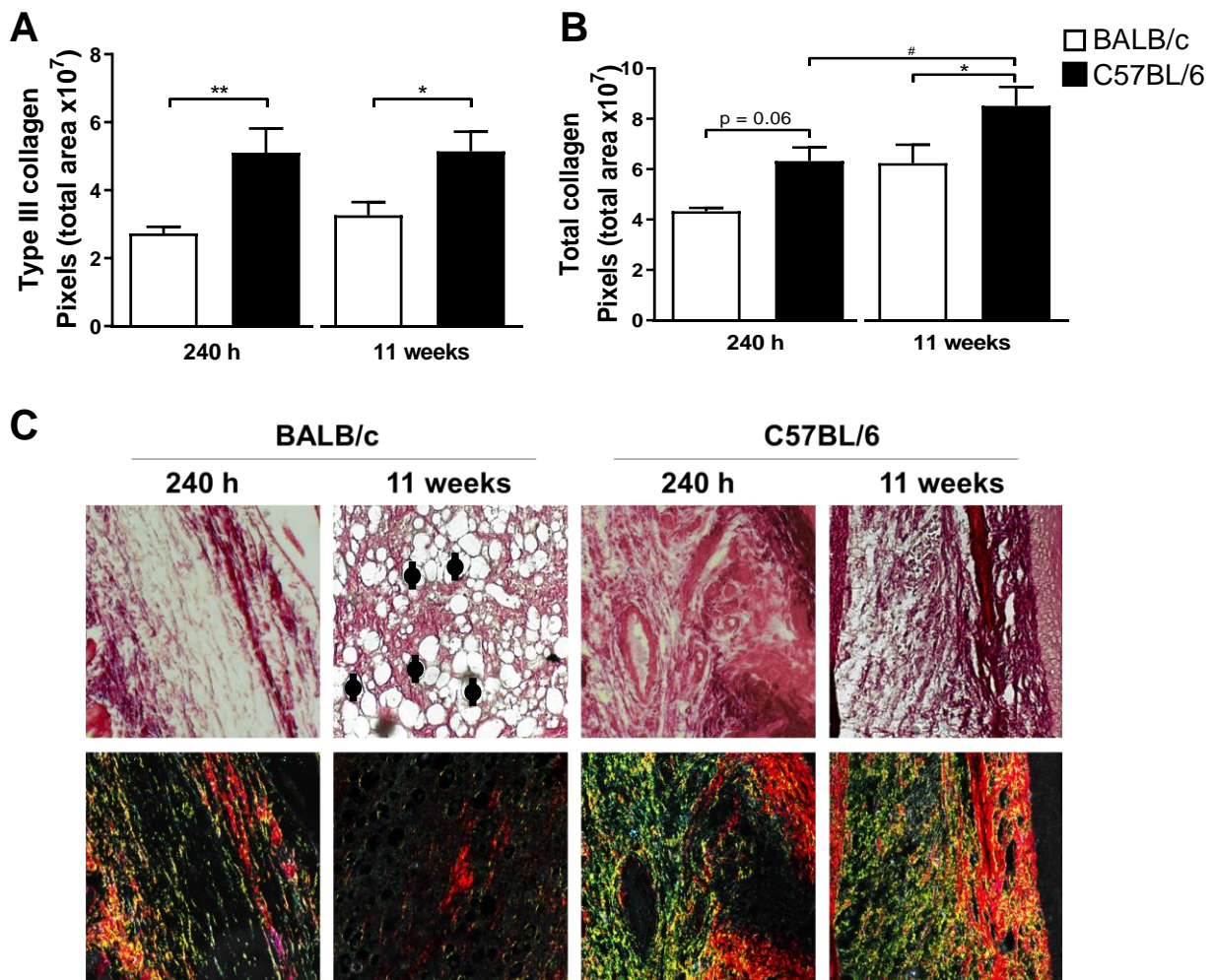
Figure 5 - Analysis of collagen in mice paws infected with *L. amazonensis*. Histological sections of the paws of *L. amazonensis*-infected BALB/c and C57BL/6 mice for 240h or 11 weeks p.i. were stained with Sirius Red to measure (A) total collagen and (B) type III collagen, using the Image-Pro Plus. * Significant difference between the mice strains infected by *L. amazonensis*, $p \leq 0.05$; ** $p \leq 0.01$, *** $p \leq 0.001$, **** $p \leq 0.0001$. [#]Significant difference of time points in C57BL/6 mice, $p \leq 0.05$. (C) Representative figures of histological sections of the paws of BALB/c and C57BL/6 mice infected by *L. amazonensis* for 240h and 11 weeks. ϕ - Indication of some

parasitophorous vacuoles. The fibers stained in red correspond to type I collagen and in yellow/green correspond to deposited type III collagen. Data from A and B represent the mean ± SEM of 6 mice group.

Figure 5C and Figure S1 show in BALB/c mice 11 weeks after infection the presence of vacuolated macrophages containing amastigotes (parasitophorous vacuoles), coinciding with areas of low labeling for type I and type III collagen. In C57BL/6 mice, after 240h, there were no visible vacuoles into macrophages and, consequently, reduction of parasites at the infection site. Also, it is notable the collagen deposition in the C57BL/6 sections, characterizing a tissue repair process.

3.6. The recruited macrophages to the site of the lesion are decisive in the evolution of edema and the arginase-1 presence

To verify the role of recruited macrophages on *L. amazonensis* lesion evolution, it was performed the adoptive transfer of macrophages (ATM) from partially resistant mice (C57BL/6) to susceptible ones (BALB/c) after 9 weeks of infection, time point in which the paw edema starts to significantly differ between the mice strains (Figure 1A and 6A). First, peritoneal cells from C57BL/6 were characterized as predominantly macrophages (F4/80$^+$/CD11b$^+$) (Figure 6B, gate strategy Figure S2). Then, we found that mice who received ATM intraperitoneal (ATM IP) presented lower paw edema and more than 250 times less parasite burden (Figure 6C, D). Besides, most ATM animals did not show any ulceration at the infection site, while BALB/c mice presented typical ulcerated lesions (Figure 6E).
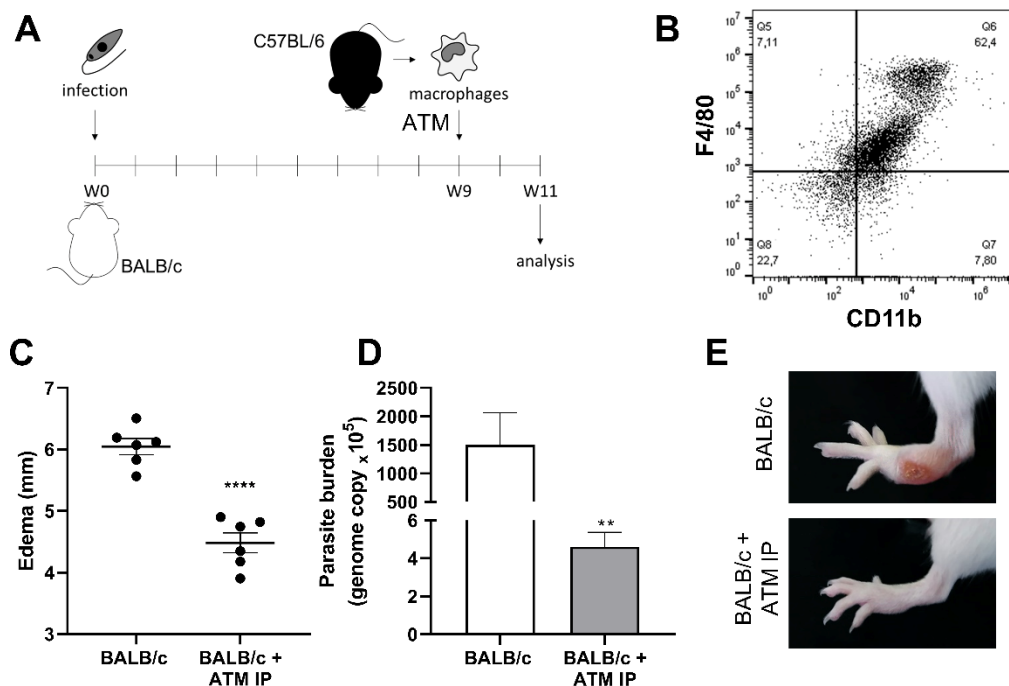
Figure 6 – Adoptive transfer of macrophages (ATM). (A) Representative scheme of the experimental design: BALB/c mice were infected with *L. amazonensis* and, after 9 weeks, they received peritoneal macrophages isolated from C57BL/6 mice intraperitoneally. (B) Dot plot showing the macrophage markers (F4/80+/CD11b+) in the peritoneal cells from non-infected C57BL/6 mice. (C) Paw edema of mice that did not receive the adoptive transfer of macrophages (BALB/c) and mice that received intraperitoneal ATM (BALB/c + ATM IP) after 11 weeks of infection. (D) Parasite burden and (E) representative photographs of mice paws after 11 weeks of infection. Data from C and D represent the mean ± SEM of 5 mice group* Significant difference in relation to the group that did not receive ATM, ** $p \le 0.01$, *** $p \le 0.001$, **** $p \le 0.0001$.

When analyzed the local cytokines at the eleventh week, ATM mice showed an increase of IFN-γ levels, while mice that did not receive ATM presented higher IL-6 levels (Figure 7A, B). It was also verified in ATM IP mice a reduction in Arg-1 levels, without significant variation in iNOS when compared to BALB/c who not received ATM (Figure 7C, D). Similar results were found when ATM was performed by intravenous route (ATM IV), with edema and Arg-1 reduction in ATM IV group, without significant difference in iNOS levels (Figure S3).
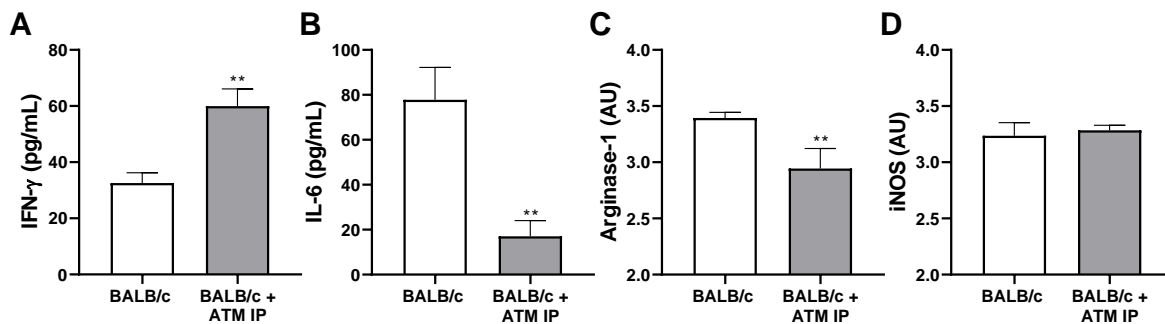
Figure 7 – Immunomodulation of ATM mice. Homogenates of *L. amazonensis*-infected BALB/c and BALB/c that received ATM via intraperitoneal paws were submitted to (A) IFN-γ and (B) IL-6 measurement by CBA assay; and (C) Arg-1 and (D) iNOS measurement by ELISA. Data represent the mean ± SEM of 5 mice group. ** Significant difference in relation to the opposite strain infected by *L. amazonensis*, $p \le 0.01$. ATM – adoptive transfer of macrophages. IP – intraperitoneal. AU – arbitrary units.

4 DISCUSSION

The pathological mechanisms that lead to cutaneous lesions caused by *L. amazonensis* infection are not yet fully understood. The present work aimed to elucidate the role of different molecules and cells, comparing the evolution of *L. amazonensis* infection in mice strains partially resistant and susceptible to infection

The most studied experimental model of cutaneous leishmaniasis is the *L. major* infection, in which the susceptibility of BALB/c mice has been correlated with the predominance of Th2 immune response, while C57BL/6 mice are resistant to infection, with a predominance of Th1 type response (Sacks and Noben-Trauth, 2002; Scott and Novais, 2016). However, this dichotomy is not identified in the disease induced by other *Leishmania* species, as *L. amazonensis* (Soong, 2012; Scott and Novais, 2016). Here, it was shown that BALB/c mice, had progressive edema from 0 to 11 weeks after *L. amazonensis* infection, with ulceration of the lesion and high local parasitic load 11 weeks p.i. On the other hand, C57BL/6 mice presented initial edema that was steadied at the later times analyzed, did not present ulcerated lesions, and had lower parasitic load compared to BALB/c.

It was also found that 11 weeks post-infection, BALB/c mice showed higher production of IL-6, which play an important role in the leishmaniasis pathogenesis, triggering the down-modulation of the microbicide molecules, and the polarization of macrophages to an M2-phenotype, that are more permissive to *Leishmania* proliferation (Hatzigeorgiou et al., 1993; Hu et al., 2018). On the other hand, C57BL/6 mice had a significant increase in IFN-γ levels after 11 weeks of infection, a key cytokine in the activation of inflammatory macrophages (M1), associated with protection in several experimental models of infection (Laskin et al., 2011), including *Leishmania* sp. (Wang et al., 1994; Sacks and Noben-Trauth, 2002).

Moreover, IFN-γ triggers the synthesis of reactive oxygen species (ROS), such as $^\bullet O_2^-$. ROS are produced by M1 macrophages, causing oxidation of lipids, proteins, and nucleic acids, with the consequent elimination of intracellular parasites (Murray and Wynn, 2011; Jafari et al., 2014). C57BL/6 mice showed higher levels of $^\bullet O_2^-$ over the infection, with lower parasitic load, explaining a better lesion evolution in this mice strain.

However, an exacerbated pro-oxidant response can be harmful to the host during *Leishmania* sp. infection, since the action of ROS are nonspecific and causes damage to the surrounding host cells, and consequently, inflammation and tissue injury (Morgado et al., 2018; Herb and Schramm, 2021). Therefore, in the presence of pro-oxidant molecules, such as $^\bullet O_2^-$, adaptive homeostasis mechanisms must be activated as a way to protect against tissue damage (Pomatto et al., 2019). Mice of the C57BL/6 strain, despite producing $^\bullet O_2^-$ in a more pronounced

manner, showed higher collagen deposition, suggesting an ability to balance the pro- and antioxidant properties, and explaining the concomitant elimination of the parasite combined with the tissue protection capacity found in C57BL/6 mice (Morgado et al., 2018).

Regarding macrophages, it was verified a peak of infiltration in the mice paws of both C57BL/6 and BALB/c mice after 24h of infection, corroborating the expected kinetics of migration of these cells (Minutti et al., 2017). However, at the beginning of the infection, there was no clear polarization of macrophages for M1 or M2 phenotype in both mice strains. These data are in accordance with the mixed Th1/Th2 profile induced by *L. amazonensis* infection (Scott and Novais, 2016), and with the findings of Ontoria et al., (2018), that verified an inconstant distribution of M1 markers throughout the infection by *L. infantum* between 1 and 8 weeks.

The results also showed that after 240h of infection there was a second peak of macrophages infiltration in the C57BL/6 mice, with higher Arg-1 and CD206 marking compared to BALB/c. This indicates that macrophages recruited at this point are predominantly M2, which play an important role in tissue remodeling and wound healing (Tomiotto-Pellissier et al., 2018). Krzyszczyk et al. (2018) showed that as the tissue begins to recover, the general population of M2 macrophages induces the migration and proliferation of fibroblasts, keratinocytes, and endothelial cells to restore the dermis, epidermis, and vasculature, respectively, by remodeling the injured tissue. In CL wounds, this remodeling is marked by the control of inflammation and an increase in the amount of collagen at the sites where the parasites have been eliminated (Baldwin et al., 2007; Miranda et al., 2015). The data are in agreement with these studies and show that collagen deposition is higher in areas with low parasitic load and tissue reorganization in the C57BL/6 mice infection.

Although there was an infiltration of M2 macrophages in 240h in C57BL/6 mice, in the later period studied, 11 weeks, there is a shift for M1 macrophages, coinciding with higher levels of IFN-γ, with less parasitic load, and no apparent lesion. On the other side, BALB/c mice had worse lesion evolution and a marked increase in Arg-1 (an M2 macrophage marker) in the later period analyzed (Muraille et al., 2014). Arginase-1 plays a fundamental role in the survival and multiplication of intracellular amastigotes of *Leishmania* sp., bypassing the amino acid L-arginine for the preferential synthesis of polyamines, fundamental for the parasite's nutrition (Muxel et al., 2018).

In vitro studies showed that *L. amazonensis*-infected BALB/c macrophages present increased L-arginine uptake and expression of arginase and arginase-related genes (Muxel et al., 2018; Aoki et al., 2019). The detrimental role of Arg-1 from macrophages on CL lesions was further confirmed by the adoptive transference of macrophages from C57BL/6 to BALB/c mice, in which it was verified that mice that received the cells presented better disease outcome, with similar features to those found in partially resistant mice. The recruited macrophages have been described

as important weapons in *Leishmania* control because the tissue-resident macrophages present oxidative deficiency compared to the recruited ones (Pessenda and Santana da Silva, 2020).

An important role for arginase in the susceptibility of mice to *L. major* infection has already been described (Kropf et al., 2005), as well as its action in *L. amazonensis* infection *in vitro*. Interestingly, skin biopsies and plasma from CL patients also present high levels of Arg-1 (reviewed in (Muxel et al., 2018)). However, until now little was known about Arg-1 in *L. amazonensis* infection *in vivo*. We showed that the participation of this enzyme in the susceptibility of animals is particularly important in later times of infection.

Peritoneal macrophages are a heterogeneous population of M0, M1, and M2 cells, which can differentiate or redifferentiate into both M1 and M2 phenotypes (Zhao et al., 2017). Besides, these cells are recruited to other tissue under infection or inflammation conditions (Cassado et al., 2015). Thus, we performed the adoptive transference of macrophages from C57BL/6 to BALB/c mice. Our results suggested the recruited macrophages have great importance in controlling susceptibility to *L. amazonensis*. The transfer of macrophages from partially resistant mice (C57BL/6) to a susceptible mouse (BALB/c) modulates the pro-*Leishmania* environment to an anti-leishmania state, with high IFN-γ and low Arg-1 levels, less parasite burden and edema, and better disease outcome.

5   CONCLUSION

Taking together the results suggest that a balance between a pro-inflammatory and microbicide M1-related and a tissue restorative M2-related response seems to provide the utmost benefit for the host. We also demonstrated the higher levels of Arg-1 in later periods of infection are related to a poor disease outcome in susceptible mice, but the transference of macrophages from partially resistant mice (C57BL/6) restore the host protection and disease control. These results expand our understanding of the protective immunity against *L. amazonensis*, providing new insights about potential interventions to treat or prevent the disease.

6   Conflict of Interest

The authors declare that the research was conducted in the absence of any commercial or financial relationships that could be construed as a potential conflict of interest.

7   Funding

8   Acknowledgments

We would like to gratefully acknowledge Dr. Letusa Albrecht and Dr. Guilherme Ferreira Silveira (ICC/FIOCRUZ) who contributed with the critical reviews, suggestions, and discussions during the execution of the present work.

9 References

Alexander, J., Brombacher, F., Peters, N., and Malchiodi, E. L. (1980). T helper1/T helper2 cells and resistance/susceptibility to Leishmania infection: is this paradigm still relevant? *Front. Immunol.* 3, 80. doi:10.3389/fimmu.2012.00080.

Aoki, J. I., Laranjeira-Silva, M. F., Muxel, S. M., and Floeter-Winter, L. M. (2019). The impact of arginase activity on virulence factors of Leishmania amazonensis. *Curr. Opin. Microbiol.* 52, 110–115. doi:10.1016/j.mib.2019.06.003.

Baldwin, T., Sakthianandeswaren, A., Curtis, J. M., Kumar, B., Smyth, G. K., Foote, S. J., et al. (2007). Wound healing response is a major contributor to the severity of cutaneous leishmaniasis in the ear model of infection. *Parasite Immunol.* 29, 501–513. doi:10.1111/j.1365-3024.2007.00969.x.

Bradley, P. P., Priebat, D. A., Christensen, R. D., and Rothstein, G. (1982). Measurement of cutaneous inflammation: Estimation of neutrophil content with an enzyme marker. *J. Invest. Dermatol.* 78, 206–209. doi:10.1111/1523-1747.ep12506462.

Caridha, D., Vesely, B., van Bocxlaer, K., Arana, B., Mowbray, C. E., Rafati, S., et al. (2019). Route map for the discovery and pre-clinical development of new drugs and treatments for cutaneous leishmaniasis. *Int. J. Parasitol. Drugs Drug Resist.* 11, 106–117. doi:10.1016/j.ijpddr.2019.06.003.

Cassado, A. A., D'Império Lima, M. R., and Bortoluci, K. R. (2015). Revisiting mouse peritoneal macrophages: Heterogeneity, development, and function. *Front. Immunol.* 6, 225. doi:10.3389/fimmu.2015.00225.

Frahs, S. M., Oxford, J. T., Neumann, E. E., Brown, R. J., Keller-Peck, C. R., Pu, X., et al. (2018). Extracellular Matrix Expression and Production in Fibroblast-Collagen Gels: Towards an In Vitro Model for Ligament Wound Healing. *Ann. Biomed. Eng.*, 1–14. doi:10.1007/s10439-018-2064-0.

Gregory, D. J., and Olivier, M. (2005). Subversion of host cell signalling by the protozoan parasite Leishmania. in *Parasitology*, S27-35. doi:10.1017/S0031182005008139.

Hatzigeorgiou, D. E., He, S., Sobel, J., Grabstein, K. H., Hafner, A., and Ho, J. L. (1993). IL-6 down-modulates the cytokine-enhanced antileishmanial activity in human macrophages. *J. Immunol.* 151, 3682–92.

Herb, M., and Schramm, M. (2021). Functions of ROS in Macrophages and Antimicrobial Immunity. *Antioxidants* 10, 313. doi:10.3390/antiox10020313.

Hu, S., Marshall, C., Darby, J., Wei, W., Lyons, A. B., and Körner, H. (2018). Absence of Tumor Necrosis Factor Supports Alternative Activation of Macrophages in the Liver after Infection with Leishmania major. *Front. Immunol.* 9, 1. doi:10.3389/fimmu.2018.00001.

Jafari, M., Shirbazou, S., and Norozi, M. (2014). Induction of Oxidative Stress in Skin and Lung of Infected BALB/C Mice with Iranian Strain of Leishmania major (MRHO/IR/75/ER). *Iran. J. Parasitol.* 9, 60–9.

Kaye, P. M., Cruz, I., Picado, A., Van Bocxlaer, K., and Croft, S. L. (2020). Leishmaniasis immunopathology—impact on design and use of vaccines, diagnostics and drugs. *Semin. Immunopathol.* 42, 247–264. doi:10.1007/s00281-020-00788-y.

Kropf, P., Fuentes, J. M., Fähnrich, E., Arpa, L., Herath, S., Weber, V., et al. (2005). Arginase and polyamine synthesis are key factors in the regulation of experimental leishmaniasis in vivo. *FASEB J.* 19, 1000–1002. doi:10.1096/fj.04-3416fje.

Krzyszczyk, P., Schloss, R., Palmer, A., and Berthiaume, F. (2018). The Role of Macrophages in Acute and Chronic Wound Healing and Interventions to Promote Pro-wound Healing Phenotypes. *Front. Physiol.* 9, 419. doi:10.3389/fphys.2018.00419.

Lage, D. P., Ribeiro, P. A. F., Dias, D. S., Mendonça, D. V. C., Ramos, F. F., Carvalho, L. M., et al. (2020). A candidate vaccine for human visceral leishmaniasis based on a specific T cell epitope-containing chimeric protein protects mice against Leishmania infantum infection. *npj Vaccines* 5, 1–13. doi:10.1038/s41541-020-00224-0.

Laskin, D. L., Sunil, V. R., Gardner, C. R., and Laskin, J. D. (2011). Macrophages and tissue injury: Agents of defense or destruction? *Annu. Rev. Pharmacol. Toxicol.* 51, 267–288. doi:10.1146/annurev.pharmtox.010909.105812.

Lira, R., Doherty, M., Modi, G., and Sacks, D. (2000). Evolution of lesion formation, parasitic load, immune response, and reservoir potential in C57BL/6 mice following high- and low-dose challenge with Leishmania major. *Infect. Immun.* 68, 5176–82.

Liu, D., and Uzonna, J. E. (2012). The early interaction of Leishmania with macrophages and dendritic cells and its influence on the host immune response. *Front. Cell. Infect. Microbiol.* 2, 83. doi:10.3389/fcimb.2012.00083.

Mills, C. D., Kincaid, K., Alt, J. M., Heilman, M. J., and Hill, A. M. (2000). M-1/M-2 Macrophages and the Th1/Th2 Paradigm. *J. Immunol.* 164, 6166–6173. doi:10.4049/jimmunol.164.12.6166.

Minutti, C. M., Knipper, J. A., Allen, J. E., and Zaiss, D. M. W. (2017). Tissue-specific contribution of macrophages to wound healing. *Semin. Cell Dev. Biol.* 61, 3–11. doi:10.1016/J.SEMCDB.2016.08.006.

Miranda, M. M., Panis, C., Cataneo, A. H. D., Da Silva, S. S., Kawakami, N. Y., Lopes, L. G. D.

F., et al. (2015). Nitric oxide and Brazilian propolis combined accelerates tissue repair by modulating cell migration, cytokine production and collagen deposition in experimental leishmaniasis. *PLoS One* 10, 1–19. doi:10.1371/journal.pone.0125101.

Morgado, F. N., de Carvalho, L. M. V., Leite-Silva, J., Seba, A. J., Pimentel, M. I. F., Fagundes, A., et al. (2018). Unbalanced inflammatory reaction could increase tissue destruction and worsen skin infectious diseases – a comparative study of leishmaniasis and sporotrichosis. *Sci. Rep.* 8, 2898. doi:10.1038/s41598-018-21277-1.

Müller, K. E., Solberg, C. T., Aoki, J. I., Floeter-Winter, L. M., and Nerland, A. H. (2018). Developing a vaccine for leishmaniasis: How biology shapes policy. *Tidsskr. den Nor. Laegeforening* 138. doi:10.4045/tidsskr.17.0620.

Muraille, E., Leo, O., and Moser, M. (2014). TH1/TH2 paradigm extended: macrophage polarization as an unappreciated pathogen-driven escape mechanism? *Front. Immunol.* 5, 603. doi:10.3389/fimmu.2014.00603.

Murray, P. J., and Wynn, T. A. (2011). Protective and pathogenic functions of macrophage subsets. *Nat. Rev. Immunol.* 11, 723–737. doi:10.1038/nri3073.

Muxel, S. M., Aoki, J. I., Fernandes, J. C. R., Laranjeira-Silva, M. F., Zampieri, R. A., Acuña, S. M., et al. (2018). Arginine and Polyamines Fate in Leishmania Infection. *Front. Microbiol.* 8, 2682. doi:10.3389/fmicb.2017.02682.

Ontoria, E., Hernández-Santana, Y. E., González-García, A. C., López, M. C., Valladares, B., and Carmelo, E. (2018). Transcriptional Profiling of Immune-Related Genes in Leishmania infantum-Infected Mice: Identification of Potential Biomarkers of Infection and Progression of Disease. *Front. Cell. Infect. Microbiol.* 8, 197. doi:10.3389/fcimb.2018.00197.

Pessenda, G., and Santana da Silva, J. (2020). Arginase and its mechanisms in Leishmania persistence . *Parasite Immunol.* 42, e12722. doi:10.1111/pim.12722.

Pomatto, L. C. D., Sun, P. Y., Yu, K., Gullapalli, S., Bwiza, C. P., Sisliyan, C., et al. (2019). Limitations to adaptive homeostasis in an hyperoxia-induced model of accelerated ageing. *Redox Biol.* 24, 101194. doi:10.1016/J.REDOX.2019.101194.

Pratti, J. E. S., Ramos, T. D., Pereira, J. C., Da Fonseca-Martins, A. M., Maciel-Oliveira, D., Oliveira-Silva, G., et al. (2016). Efficacy of intranasal LaAg vaccine against Leishmania amazonensis infection in partially resistant C57Bl/6 mice. *Parasites and Vectors* 9, 1–11. doi:10.1186/s13071-016-1822-9.

Rosas, L. E., Keiser, T., Barbi, J., Satoskar, A. A., Septer, A., Kaczmarek, J., et al. (2005). Genetic background influences immune responses and disease outcome of cutaneous L. mexicana infection in mice. *Int. Immunol.* 17, 1347–1357. doi:10.1093/intimm/dxh313.

Rossi, M., and Fasel, N. (2018). How to master the host immune system? Leishmania parasites

have the solutions! 30, 103–111. doi:10.1093/intimm/dxx075.

Sacks, D., and Noben-Trauth, N. (2002). The immunology of susceptibility and resistance to Leishmania major in mice. *Nat. Rev. Immunol.* 2, 845–858. doi:10.1038/nri933.

Scott, P., and Novais, F. O. (2016). Cutaneous leishmaniasis: immune responses in protection and pathogenesis. *Nat. Rev. Immunol.* 16, 581–592. doi:10.1038/nri.2016.72.

Soong, L. (2012). Subversion and Utilization of Host Innate Defense by Leishmania amazonensis. *Front. Immunol.* 3, 58. doi:10.3389/fimmu.2012.00058.

Tellevik, M. G., Muller, K. E., Løkken, K. R., and Nerland, A. H. (2014). Detection of a broad range of Leishmania species and determination of parasite load of infected mouse by real-time PCR targeting the arginine permease gene AAP3. *Acta Trop.* 137, 99–104. doi:10.1016/j.actatropica.2014.05.008.

Tomiotto-Pellissier, F., Bortoleti, B. T. da S., Assolini, J. P., Gonçalves, M. D., Carloto, A. C. M., Miranda-Sapla, M. M., et al. (2018). Macrophage Polarization in Leishmaniasis: Broadening Horizons. *Front. Immunol.* 9, 2529. doi:10.3389/fimmu.2018.02529.

Velasquez, L. G., Galuppo, M. K., De Rezende, E., Brandão, W. N., Peron, J. P., Uliana, S. R. B., et al. (2016). Distinct courses of infection with Leishmania (L.) amazonensis are observed in BALB/c, BALB/c nude and C57BL/6 mice. *Parasitology* 143, 692–703. doi:10.1017/S003118201600024X.

Wang, Z. E., Reiner, S. L., Zheng, S., Dalton, D. K., and Locksley, R. M. (1994). CD4+ effector cells default to the Th2 pathway in interferon gamma-deficient mice infected with Leishmania major. *J. Exp. Med.* 179, 1367–71.

WHO (2020). Leishmaniasis. Available at: https://www.who.int/news-room/fact-sheets/detail/leishmaniasis [Accessed August 11, 2020].

Zhao, Y. long, Tian, P. xun, Han, F., Zheng, J., Xia, X. xin, Xue, W. jun, et al. (2017). Comparison of the characteristics of macrophages derived from murine spleen, peritoneal cavity, and bone marrow. *J. Zhejiang Univ. Sci. B* 18, 1055–1063. doi:10.1631/jzus.B1700003.

SUPPLEMENTARY MATERIAL
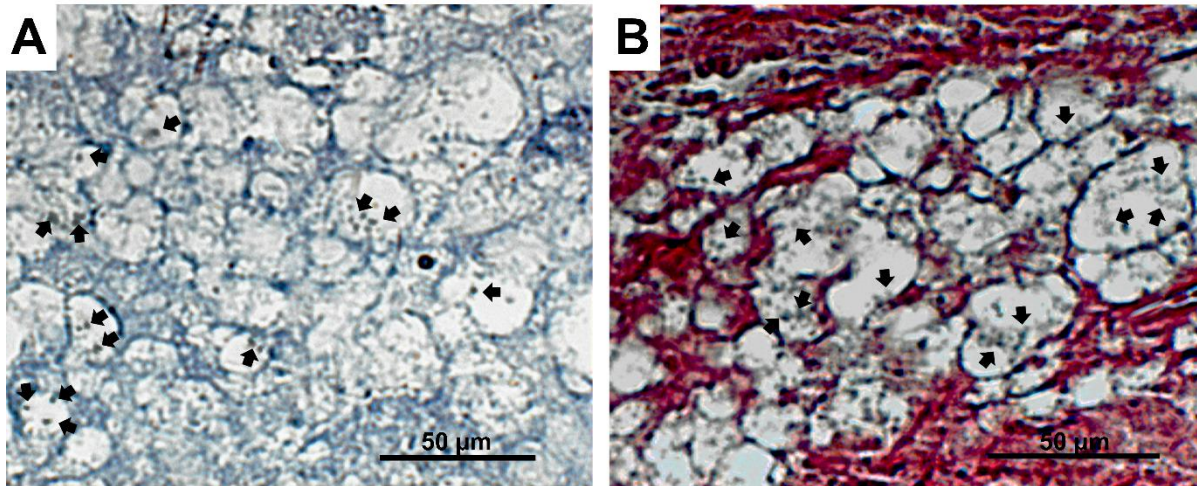
Figure S1 – Vacuolated macrophages in paws of BALB/c mice infected with *L. amazonensis* for 11 weeks. (A) Lesion areas of cuts stained with hematoxylin. (B) Lesion areas of cuts stained with Sirus Red. Both images show macrophage vacuoles filled with parasites. The arrows indicate *L. amazonensis* amastigote forms inside parasitophorous vacuoles. Scale bar indicates 50 μm.
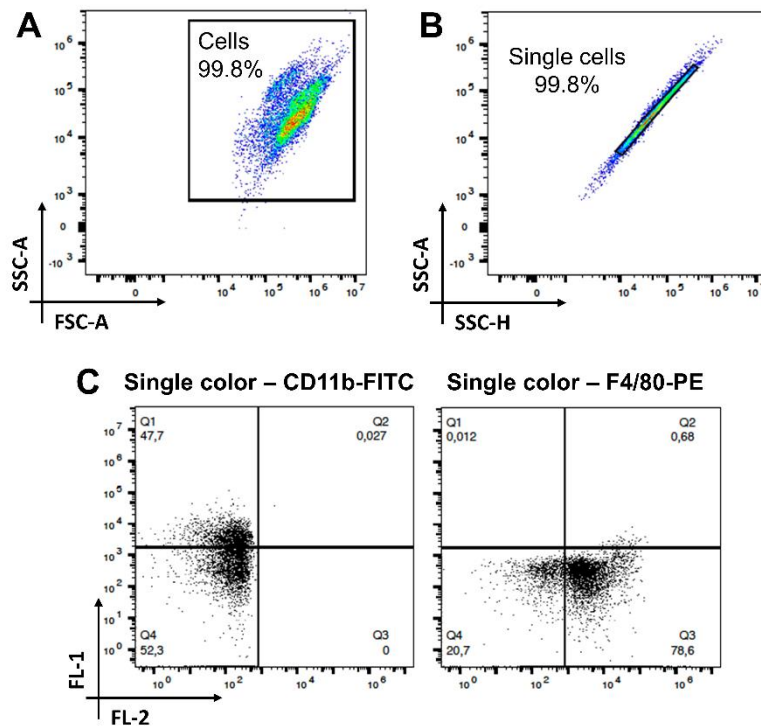
Figure S2 – Flow cytometry gating strategy for macrophages. (A) Cells were first identified by a forward scatter (FSC) and side scatter (SSC) gate. (B) Gating strategy for identifying singlets (single cells). (C) Single-color compensation controls for each fluorophore. Flow cytometry plots are shown in logarithmic format.
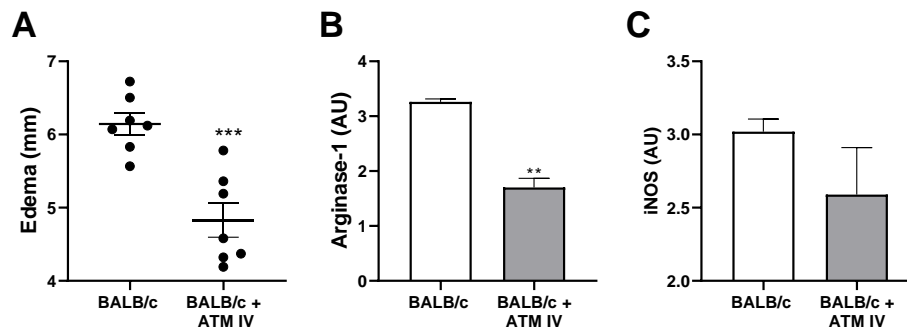
Figure S3 – Analysis of intravenous ATM. (A) Paw edema of mice that did not receive adoptive transfer of macrophages (BALB/c) and mice that received intravenous ATM (BALB/c + ATM IV) after 11 weeks of infection. Paws homogenates of were submitted to (B) Arg-1 levels. (C) iNOS levels. Data represent the mean ± SEM of 5 mice group. ** Significant difference in relation to the group that did not receive ATM $p \leq 0.01$, *** $p \leq 0.001$. ATM – adoptive transfer of macrophages. IV – intravenous. AU – arbitrary units.

4. CONCLUSÕES

- Fatores de virulência dos parasitos atuam no favorecimento do desenvolvimento de macrófagos M2, que são permissivos à infecção e proliferação de *Leishmania.*

- Macrófagos M1, apesar de seu potencial leishmanicida, também podem contribuir com o desenvolvimento das lesões ao induzirem uma resposta inflamatória exacerbada que provoca danos ao tecido.

- Em modelos experimentais de suscetibilidade (BALB/c) e resistência parcial (C57BL/6) à infecção por *Leishmania amazonensis* não há um claro predomínio de macrófagos M1 ou M2 no local da infecção.

- A pior evolução das lesões parece estar envolvida com o recrutamento de macrófagos ricos em arginase-1 em camundongos suscetíveis.

- Um equilíbrio entre uma resposta pró-inflamatória e microbicida relacionada ao perfil M1 e uma resposta de reparo tecidual relacionada ao perfil M2 parecem fornecer o maior benefício para o hospedeiro.

- Esses resultados ampliam a compreensão sobre a imunidade protetora contra *L. amazonensis*, fornecendo novos conhecimentos que podem contribuir para o desenvolvimento de intervenções de tratamento ou prevenção da leishmaniose.

5. REFERÊNCIAS

ABDELADHIM, M. et al. Human Cellular Immune Response to the Saliva of Phlebotomus papatasi Is Mediated by IL-10-Producing CD8+ T Cells and Th1-Polarized CD4+ Lymphocytes. **PLoS Neglected Tropical Diseases**, v. 5, n. 10, p. e1345, out. 2011.

ABEBE, T. et al. Local Increase of Arginase Activity in Lesions of Patients with Cutaneous Leishmaniasis in Ethiopia. **PLoS Neglected Tropical Diseases**, v. 6, n. 6, p. e1684, jun. 2012.

ABEBE, T. et al. Arginase Activity - A Marker of Disease Status in Patients with Visceral Leishmaniasis in Ethiopia. **PLoS Neglected Tropical Diseases**, v. 7, n. 3, p. e2134, mar. 2013.

ALEXANDER, J. et al. T helper1/T helper2 cells and resistance/susceptibility to Leishmania infection: is this paradigm still relevant? **Frontiers in Immunology**, v. 3, p. 80, 17 abr. 1980.

ALLMAN, W. R. et al. TACI deficiency leads to alternatively activated macrophage phenotype and susceptibility to Leishmania infection. **Proceedings of the National Academy of Sciences of the United States of America**, v. 112, n. 30, p. E4094-103, jul. 2015.

ALVAR, J.; CROFT, S.; OLLIARO, P. Chemotherapy in the Treatment and Control of Leishmaniasis. In: **Advances in parasitology**. [s.l: s.n.]. v. 61p. 223–274.

ANDERSON, C. F.; MOSSER, D. M. A novel phenotype for an activated macrophage: the type 2 activated macrophage. **Journal of leukocyte biology**, v. 72, n. 1, p. 101–6, jul. 2002.

AOKI, J. I. et al. **The impact of arginase activity on virulence factors of Leishmania amazonensisCurrent Opinion in Microbiology**Elsevier Ltd, , dez. 2019.

ARANGO DUQUE, G.; DESCOTEAUX, A. Macrophage Cytokines: Involvement in Immunity and Infectious Diseases. **Frontiers in Immunology**, v. 5, p. 491, out. 2014.

ARAÚJO-SANTOS, T. et al. Lutzomyia longipalpis Saliva Triggers Lipid Body Formation and Prostaglandin E2 Production in Murine Macrophages. **PLOS ONE Neglected Tropical Disease**, v. 4, n. 11, p. 1–9, 2010.

ASAI, A. et al. CCL1 released from M2b macrophages is essentially required for the maintenance of their properties. **Journal of Leukocyte Biology**, v. 92, n. 4, p. 859–867, out. 2012.

BALDWIN, T. et al. Wound healing response is a major contributor to the severity of cutaneous leishmaniasis in the ear model of infection. **Parasite Immunology**, v. 29, n. 10, p. 501–513, out. 2007.

BASHIR, S. et al. Macrophage polarization: the link between inflammation and related diseases. **Inflammation Research**, v. 65, n. 1, p. 1–11, 14 jan. 2016.

BHATTACHARYA, P. et al. Genetically Modified Live Attenuated Leishmania donovani Parasites Induce Innate Immunity through Classical Activation of Macrophages That Direct the Th1 Response in Mice. **Infection and Immunity**, v. 83, n. 10, p. 3800–3815, out. 2015.

BRADLEY, P. P. et al. Measurement of cutaneous inflammation: Estimation of

neutrophil content with an enzyme marker. **Journal of Investigative Dermatology**, v. 78, n. 3, p. 206–209, 1 mar. 1982.

BRODIE, T. M. et al. Immunomodulatory Effects of the Lutzomyia longipalpis Salivary Gland Protein Maxadilan on Mouse Macrophages. **Infection and Immunity**, v. 75, n. 5, p. 2359–2365, 2007.

CARIDHA, D. et al. Route map for the discovery and pre-clinical development of new drugs and treatments for cutaneous leishmaniasis. **International Journal for Parasitology: Drugs and Drug Resistance**, v. 11, p. 106–117, 1 dez. 2019.

CARLSEN, E. D. et al. Interactions between Neutrophils and Leishmania braziliensis Amastigotes Facilitate Cell Activation and Parasite Clearance. **Journal of innate immunity**, v. 7, n. 4, p. 354–63, 2015.

CARREGARO, V. et al. Nucleosides Present on Phlebotomine Saliva Induce Immunossuppression and Promote the Infection Establishment. **PLOS Neglected Tropical Diseases**, v. 9, p. 1–21, 2015.

CASSADO, A. A.; D'IMPÉRIO LIMA, M. R.; BORTOLUCI, K. R. **Revisiting mouse peritoneal macrophages: Heterogeneity, development, and functionFrontiers in Immunology**Frontiers Media S.A., , 19 maio 2015. Disponível em: <www.frontiersin.org>. Acesso em: 20 fev. 2021

CDC. **CDC - DPDx - Leishmaniasis**.

CHAN, M. M.; ADAPALA, N.; CHEN, C. Peroxisome Proliferator-Activated Receptor-γ-Mediated Polarization of Macrophages in Leishmania Infection. **PPAR Research**, v. 796235, n. 11, 2012.

CHISTIAKOV, D. A. et al. The impact of interferon-regulatory factors to macrophage differentiation and polarization into M1 and M2. **Immunobiology**, v. 223, n. 1, p. 101–111, jan. 2018.

COVARRUBIAS, A.; BYLES, V.; HORNG, T. ROS sets the stage for macrophage differentiation. **Cell Research**, v. 23, n. 8, p. 984–985, ago. 2013.

CSÓKA, B. et al. Adenosine promotes alternative macrophage activation *via* A $_{2A}$ and A $_{2B}$ receptors. **The FASEB Journal**, v. 26, n. 1, p. 376–386, jan. 2012.

DAMESHGHI, S. et al. Mesenchymal stem cells alter macrophage immune responses to Leishmania major infection in both susceptible and resistance mice. **Immunology Letters**, v. 170, p. 15–26, fev. 2016.

DAVIS, M. J. et al. Macrophage M1/M2 polarization dynamically adapts to changes in cytokine microenvironments in Cryptococcus neoformans infection. **mBio**, v. 4, n. 3, p. e00264-13, jun. 2013.

DE FREITAS, E. O. et al. The Contribution of Immune Evasive Mechanisms to Parasite Persistence in Visceral Leishmaniasis. **Frontiers in Immunology**, v. 7, p. 153, abr. 2016.

DE SANTANA, F. R. et al. High dilutions of antimony modulate cytokines production and macrophage – Leishmania (L.) amazonensis interaction in vitro. **Cytokine**, v. 92, p. 33–47, abr. 2017.

DÍAZ-GANDARILLA, J. A. et al. PPAR Activation Induces M1 Macrophage Polarization via cPLA $_2$ -COX-2 Inhibition, Activating ROS Production against *Leishmania mexicana*. **BioMed Research International**, v. 2013, p. 1–13, 2013.

FALCÃO, S. A. C. et al. Exposure to Leishmania braziliensis Triggers Neutrophil Activation and Apoptosis. **PLOS Neglected Tropical Diseases**, v. 9, n. 3, p. e0003601, mar. 2015.

FARIAS, L. H. S. et al. Crotoxin stimulates an M1 activation profile in murine macrophages during Leishmania amazonensis infection. **Parasitology**, v. 144, n. 11, p. 1458–1467, set. 2017.

FARROW, A. L. et al. Leishmania-induced repression of selected non-coding RNA genes containing B-box element at their promoters in alternatively polarized M2 macrophages. **Molecular and Cellular Biochemistry**, v. 350, n. 1–2, p. 47–57, abr. 2011.

FERRANTE, C. J. et al. The Adenosine-Dependent Angiogenic Switch of Macrophages to an M2-Like Phenotype is Independent of Interleukin-4 Receptor Alpha (IL-4Rα) Signaling. **Inflammation**, v. 36, n. 4, p. 921–931, ago. 2013.

FINNIN, M.; HAMILTON, J. A.; MOSS, S. T. Characterization of a CSF-induced proliferating subpopulation of human peripheral blood monocytes by surface marker expression and cytokine production. **Journal of leukocyte biology**, v. 66, n. 6, p. 953–60, dez. 1999.

FRAHS, S. M. et al. Extracellular Matrix Expression and Production in Fibroblast-Collagen Gels: Towards an In Vitro Model for Ligament Wound Healing. **Annals of Biomedical Engineering**, p. 1–14, jun. 2018.

FRANÇA-COSTA, J. et al. Arginase I, Polyamine, and Prostaglandin E 2 Pathways Suppress the Inflammatory Response and Contribute to Diffuse Cutaneous Leishmaniasis. 2014.

FRATERNALE, A.; BRUNDU, S.; MAGNANI, M. Polarization and Repolarization of Macrophages. **Journal of Clinical and Cellular Immunology**, v. 06, n. 02, p. 1–10, dez. 2015.

GALLARDO-SOLER, A. et al. Arginase I induction by modified lipoproteins in macrophages: a peroxisome proliferator-activated receptor-gamma/delta-mediated effect that links lipid metabolism and immunity. **Molecular endocrinology (Baltimore, Md.)**, v. 22, n. 6, p. 1394–402, jun. 2008.

GIRAUD, E. et al. Leishmania proteophosphoglycans regurgitated from infected sand flies accelerate dermal wound repair and exacerbate leishmaniasis via insulin-like growth factor 1-dependent signalling. **PLOS Pathogens**, v. 14, n. 1, p. e1006794, jan. 2018.

GORDON, S. Alternative activation of macrophages. **Nature Reviews Immunology**, v. 3, n. 1, p. 23–35, jan. 2003.

GRAFF, J. W. et al. Identifying Functional MicroRNAs in Macrophages with Polarized Phenotypes. **Journal of Biological Chemistry**, v. 287, n. 26, p. 21816–21825, jun. 2012.

GREGORY, D. J.; OLIVIER, M. **Subversion of host cell signalling by the protozoan parasite Leishmania**. Parasitology. **Anais**...mar. 2005Disponível em: <http://www.ncbi.nlm.nih.gov/pubmed/16281989>. Acesso em: 5 mar. 2020

GUIMARÃES-COSTA, A. B. et al. Leishmania amazonensis promastigotes induce and are killed by neutrophil extracellular traps. **Proceedings of the National Academy of Sciences of the United States of America**, v. 106, n. 16, p. 6748–53,

abr. 2009.

HALL, L. R.; TITUS, R. G. Sand fly vector saliva selectively modulates macrophage functions that inhibit killing of Leishmania major and nitric oxide production. **Journal of Immunology**, v. 155, n. 7, p. 3501–3506, 1995.

HAMMAMI, A. et al. HIF-1α is a key regulator in potentiating suppressor activity and limiting the microbicidal capacity of MDSC-like cells during visceral leishmaniasis. **PLoS pathogens**, v. 13, n. 9, p. e1006616, set. 2017.

HATZIGEORGIOU, D. E. et al. IL-6 down-modulates the cytokine-enhanced antileishmanial activity in human macrophages. **Journal of immunology (Baltimore, Md. : 1950)**, v. 151, n. 7, p. 3682–92, out. 1993.

HAZLETT, L. D. et al. IL-33 Shifts Macrophage Polarization, Promoting Resistance against *Pseudomonas aeruginosa* Keratitis. **Investigative Opthalmology & Visual Science**, v. 51, n. 3, p. 1524, mar. 2010.

HERB, M.; SCHRAMM, M. Functions of ROS in Macrophages and Antimicrobial Immunity. **Antioxidants**, v. 10, n. 2, p. 313, 19 fev. 2021.

HOSONO, K. et al. Signaling of Prostaglandin E Receptors, EP3 and EP4 Facilitates Wound Healing and Lymphangiogenesis with Enhanced Recruitment of M2 Macrophages in Mice. **PLOS ONE**, v. 11, n. 10, p. e0162532, out. 2016.

HU, S. et al. Absence of Tumor Necrosis Factor Supports Alternative Activation of Macrophages in the Liver after Infection with Leishmania major. **Frontiers in Immunology**, v. 9, p. 1, jan. 2018.

HURRELL, B. P. et al. Rapid Sequestration of Leishmania mexicana by Neutrophils Contributes to the Development of Chronic Lesion. **PLOS Pathogens**, v. 11, n. 5, p. 1–23, 2015.

JABLONSKI, K. A. et al. Novel Markers to Delineate Murine M1 and M2 Macrophages. **PLOS ONE**, v. 10, n. 12, p. e0145342, dez. 2015.

JAFARI, M.; SHIRBAZOU, S.; NOROZI, M. Induction of Oxidative Stress in Skin and Lung of Infected BALB/C Mice with Iranian Strain of Leishmania major (MRHO/IR/75/ER). **Iranian journal of parasitology**, v. 9, n. 1, p. 60–9, mar. 2014.

KAMHAWI, S. The biological and immunomodulatory properties of sand fly saliva and its role in the establishment of Leishmania infections. **Microbes and Infection**, v. 2, n. 14, p. 1765–1773, 2000.

KAYE, P. M. et al. **Leishmaniasis immunopathology—impact on design and use of vaccines, diagnostics and drugsSeminars in Immunopathology**Springer, , 1 jun. 2020. Disponível em: <https://doi.org/10.1007/s00281-020-00788-y>. Acesso em: 20 fev. 2021

KIM, Y.-G. et al. Gut dysbiosis promotes M2 macrophage polarization and allergic airway inflammation via fungi-induced PGE_2. **Cell host & microbe**, v. 15, n. 1, p. 95–102, jan. 2014.

KONG, F. et al. Transcriptional Profiling in Experimental Visceral Leishmaniasis Reveals a Broad Splenic Inflammatory Environment that Conditions Macrophages toward a Disease-Promoting Phenotype. **PLOS Pathogens**, v. 13, n. 1, p. e1006165, jan. 2017.

KROPF, P. et al. Arginase and polyamine synthesis are key factors in the regulation

of experimental leishmaniasis in vivo. **The FASEB Journal**, v. 19, n. 8, p. 1000–1002, 5 jun. 2005.

KRZYSZCZYK, P. et al. The Role of Macrophages in Acute and Chronic Wound Healing and Interventions to Promote Pro-wound Healing Phenotypes. **Frontiers in physiology**, v. 9, p. 419, 2018.

KUMAR, A. et al. *Leishmania* infection activates host mTOR for its survival by M2 macrophage polarization. **Parasite Immunology**, p. e12586, set. 2018.

KUROWSKA-STOLARSKA, M. et al. IL-33 Amplifies the Polarization of Alternatively Activated Macrophages That Contribute to Airway Inflammation. **The Journal of Immunology**, v. 183, n. 10, p. 6469–6477, nov. 2009.

LAGE, D. P. et al. A candidate vaccine for human visceral leishmaniasis based on a specific T cell epitope-containing chimeric protein protects mice against Leishmania infantum infection. **npj Vaccines**, v. 5, n. 1, p. 1–13, 1 dez. 2020.

LAWRENCE, T.; NATOLI, G. Transcriptional regulation of macrophage polarization: enabling diversity with identity. **Nature Reviews Immunology**, v. 11, n. 11, p. 750–761, nov. 2011.

LEE, S. H. et al. Mannose receptor high, M2 dermal macrophages mediate nonhealing *Leishmania major* infection in a Th1 immune environment. **The Journal of Experimental Medicine**, v. 215, n. 1, p. 357–375, jan. 2018.

LEHTONEN, A. et al. Gene expression profiling during differentiation of human monocytes to macrophages or dendritic cells. **Journal of Leukocyte Biology**, v. 82, n. 3, p. 710–720, set. 2007.

LESTINOVA, T. et al. Insights into the sand fly saliva: Blood-feeding and immune interactions between sand flies, hosts, and Leishmania. **PLOS Neglected Tropical Diseases**, v. 11, n. 7, p. e0005600, jul. 2017.

LEY, K.; MILLER, Y. I.; HEDRICK, C. C. Monocyte and Macrophage Dynamics During Atherogenesis. **Arteriosclerosis, Thrombosis, and Vascular Biology**, v. 31, n. 7, p. 1506–1516, jul. 2011.

LI, H. et al. Transcriptional Regulation of Macrophages Polarization by MicroRNAs. **Frontiers in Immunology**, v. 9, p. 1175, maio 2018.

LI, S. et al. IL-21 modulates release of proinflammatory cytokines in LPS-stimulated macrophages through distinct signaling pathways. **Mediators of inflammation**, v. 2013, p. 548073, dez. 2013.

LIRA, R. et al. Evolution of lesion formation, parasitic load, immune response, and reservoir potential in C57BL/6 mice following high- and low-dose challenge with Leishmania major. **Infection and immunity**, v. 68, n. 9, p. 5176–82, set. 2000.

LIU, D.; UZONNA, J. E. The early interaction of Leishmania with macrophages and dendritic cells and its influence on the host immune response. **Frontiers in cellular and infection microbiology**, v. 2, n. June, p. 83, 2012.

LU, J. et al. Discrete functions of M 2a and M 2c macrophage subsets determine their relative efficacy in treating chronic kidney disease. **Kidney International**, v. 84, n. 4, p. 745–755, out. 2013.

LUCEY, D. R.; CLERICI, M.; SHEARER, G. M. Type 1 and type 2 cytokine dysregulation in human infectious, neoplastic, and inflammatory diseases. **Clinical**

microbiology reviews, v. 9, n. 4, p. 532–62, out. 1996.

MANTOVANI, A. et al. The chemokine system in diverse forms of macrophage activation and polarization. **Trends in Immunology**, v. 25, n. 12, p. 677–686, dez. 2004.

MAROLI, M. et al. Phlebotomine sandflies and the spreading of leishmaniases and other diseases of public health concern. **Medical and Veterinary Entomology**, v. 27, n. 2, p. 123–147, [s.d.].

MARTINEZ, F. O.; HELMING, L.; GORDON, S. Alternative Activation of Macrophages: An Immunologic Functional Perspective. **Annual Review of Immunology**, v. 27, n. 1, p. 451–483, abr. 2009.

MBOW, M. L. et al. Phlebotomus papatasi Sand Fly Salivary Gland Lysate Down-Regulates a Th1, but Up-Regulates a Th2, Response in Mice Infected with Leishmania major. **The Journal of Immunology**, v. 161, p. 5571–5577, 1998.

MCCARTNEY-FRANCIS, N. et al. Aberrant host defense against *Leishmania major* in the absence of SLPI. **Journal of Leukocyte Biology**, v. 96, n. 5, p. 917–929, nov. 2014.

MCFARLANE, E. et al. Neutrophils contribute to development of a protective immune response during onset of infection with Leishmania donovani. **Infection and immunity**, v. 76, n. 2, p. 532–41, fev. 2008.

MENDONÇA, S. C. F. Differences in immune responses against Leishmania induced by infection and by immunization with killed parasite antigen: implications for vaccine discovery. **Parasites & vectors**, v. 9, n. 1, p. 492, set. 2016.

MINUTTI, C. M. et al. Tissue-specific contribution of macrophages to wound healing. **Seminars in Cell & Developmental Biology**, v. 61, p. 3–11, 1 jan. 2017.

MIRANDA, M. M. et al. Nitric oxide and Brazilian propolis combined accelerates tissue repair by modulating cell migration, cytokine production and collagen deposition in experimental leishmaniasis. **PLoS ONE**, v. 10, n. 5, p. 1–19, 2015.

MOREIRA, P. R. R. et al. Polarized M2 macrophages in dogs with visceral leishmaniasis. **Veterinary Parasitology**, v. 226, p. 69–73, ago. 2016.

MORGADO, F. N. et al. Unbalanced inflammatory reaction could increase tissue destruction and worsen skin infectious diseases – a comparative study of leishmaniasis and sporotrichosis. **Scientific Reports**, v. 8, n. 1, p. 2898, 13 dez. 2018.

MOSSER, D. M.; EDWARDS, J. P. Exploring the full spectrum of macrophage activation. **Nature Reviews Immunology**, v. 8, n. 12, p. 958–969, dez. 2008.

MUKHOPADHYAY, D. et al. M2 Polarization of Monocytes-Macrophages Is a Hallmark of Indian Post Kala-Azar Dermal Leishmaniasis. **PLOS Neglected Tropical Diseases**, v. 9, n. 10, p. e0004145, out. 2015.

MÜLLER, K. E. et al. Developing a vaccine for leishmaniasis: How biology shapes policy. **Tidsskrift for den Norske Laegeforening**, v. 138, n. 3, 25 dez. 2018.

MURAILLE, E.; LEO, O.; MOSER, M. TH1/TH2 paradigm extended: macrophage polarization as an unappreciated pathogen-driven escape mechanism? **Frontiers in immunology**, v. 5, p. 603, 2014.

MURRAY, H. W. et al. Advances in leishmaniasis. **The Lancet**, v. 366, n. 9496, p. 1561–1577, out. 2005.

MURRAY, P. J. et al. Macrophage Activation and Polarization: Nomenclature and Experimental Guidelines. **Immunity**, v. 41, n. 1, p. 14–20, jul. 2014.

MURRAY, P. J.; WYNN, T. A. Protective and pathogenic functions of macrophage subsets. **Nature Reviews Immunology**, v. 11, n. 11, p. 723–737, 14 nov. 2011.

MUXEL, S. M. et al. Arginine and Polyamines Fate in Leishmania Infection. **Frontiers in microbiology**, v. 8, p. 2682, 2018.

MYLONAS, K. J. et al. Alternatively Activated Macrophages Elicited by Helminth Infection Can Be Reprogrammed to Enable Microbial Killing. **The Journal of Immunology**, v. 182, n. 5, p. 3084–3094, mar. 2009.

NORSWORTHY, N. B. et al. Sand Fly Saliva Enhances Leishmania amazonensis Infection by Modulating Interleukin-10 Production. **Infection and Immunity**, v. 72, n. 3, p. 1240–1247, 2004.

NOVAIS, F. O. et al. Neutrophils and Macrophages Cooperate in Host Resistance against Leishmania braziliensis Infection. **The Journal of Immunology**, v. 183, n. 12, p. 8088–8098, dez. 2009.

ODEGAARD, J. I. et al. Macrophage-specific PPARγ controls alternative activation and improves insulin resistance. **Nature**, v. 447, n. 7148, p. 1116–1120, jun. 2007.

OLIVEIRA, F. et al. Delayed-Type Hypersensitivity to Sand Fly Saliva in Humans from a Leishmaniasis-Endemic Area of Mali Is TH1-Mediated and Persists to Midlife. **Journal of Investigative Dermatology**, v. 133, n. 2, p. 452–459, fev. 2013.

ONTORIA, E. et al. Transcriptional Profiling of Immune-Related Genes in Leishmania infantum-Infected Mice: Identification of Potential Biomarkers of Infection and Progression of Disease. **Frontiers in cellular and infection microbiology**, v. 8, p. 197, 2018.

PARISI, L. et al. Macrophage Polarization in Chronic Inflammatory Diseases: Killers or Builders? **Journal of Immunology Research**, v. 2018, p. 1–25, 2018.

PARK-MIN, K.-H.; ANTONIV, T. T.; IVASHKIV, L. B. Regulation of macrophage phenotype by long-term exposure to IL-10. **Immunobiology**, v. 210, n. 2–4, p. 77–86, ago. 2005.

PESCE, J. et al. The IL-21 receptor augments Th2 effector function and alternative macrophage activation. **The Journal of clinical investigation**, v. 116, n. 7, p. 2044–55, jul. 2006.

PESSENDA, G.; SANTANA DA SILVA, J. Arginase and its mechanisms in Leishmania persistence . **Parasite Immunology**, v. 42, n. 7, p. e12722, abr. 2020.

PETERS, N. C. et al. In Vivo Imaging Reveals an Essential Role for Neutrophils in Leishmaniasis Transmitted by Sand Flies. **Science**, v. 321, n. 5891, p. 970–974, ago. 2008.

POMATTO, L. C. D. et al. Limitations to adaptive homeostasis in an hyperoxia-induced model of accelerated ageing. **Redox Biology**, v. 24, p. 101194, 1 jun. 2019.

PRATTI, J. E. S. et al. Efficacy of intranasal LaAg vaccine against Leishmania amazonensis infection in partially resistant C57Bl/6 mice. **Parasites and Vectors**, v.

9, n. 1, p. 1–11, 6 out. 2016.

PUSHPANJALI, A. K. T. et al. Direct evidence for role of anti-saliva antibodies against salivary gland homogenate of P . argentipes in modulation of protective Th1-immune response against Leishmania donovani. **Cytokine**, v. 86, p. 79–85, 2016.

RATH, M. et al. Metabolism via Arginase or Nitric Oxide Synthase: Two Competing Arginine Pathways in Macrophages. **Frontiers in immunology**, v. 5, p. 532, 2014.

REGLI, I. B. et al. Survival mechanisms used by some Leishmania species to escape neutrophil killing. **Frontiers in Immunology**, v. 8, n. NOV, 2017.

RIBEIRO-GOMES, F. L. et al. Efficient Capture of Infected Neutrophils by Dendritic Cells in the Skin Inhibits the Early Anti-Leishmania Response. **PLoS Pathogens**, v. 8, n. 2, p. e1002536, 16 fev. 2012.

RIBEIRO, J. M. C.; ROSSIGNOL, P. A.; SPIELMAN, A. Blood-Finding Strategy Of A Capillary-Feeding Sandfly, Lutzomyia longipalpis. **Comp. Biochem. Physiol.**, v. 83, n. 4, p. 683–686, 1986.

RIGAMONTI, E.; CHINETTI-GBAGUIDI, G.; STAELS, B. Regulation of macrophage functions by PPAR-alpha, PPAR-gamma, and LXRs in mice and men. **Arteriosclerosis, thrombosis, and vascular biology**, v. 28, n. 6, p. 1050–9, jun. 2008.

ROCHAEL, N. C. et al. Classical ROS-dependent and early/rapid ROS-independent release of Neutrophil Extracellular Traps triggered by Leishmania parasites. **Scientific Reports**, v. 5, n. 1, p. 18302, nov. 2016.

RODRÍGUEZ, N. E.; WILSON, M. E. Eosinophils and mast cells in leishmaniasis. **Immunologic research**, v. 59, n. 1–3, p. 129–141, 2014.

ROGERS, K. A.; TITUS, R. G. Immunomodulatory effects of Maxadilan and Phlebotomus papatasi sand fly salivary gland lysates on human primary in vitro immune responses. **Parasite Immunology**, v. 25, n. 3, p. 127–134, 2003.

ROGERS, M. et al. Proteophosophoglycans Regurgitated by Leishmania-Infected Sand Flies Target the L-Arginine Metabolism of Host Macrophages to Promote Parasite Survival. **PLoS pathogens**, v. 5, n. 8, p. 1–14, 2009.

ROHOUSOVÁ, I.; VOLF, P.; LIPOLDOVÁ, M. Modulation of murine cellular immune response and cytokine production by salivary gland lysate of three sand fly species. **Parasite Immunology**, v. 704, p. 469–473, 2005.

ROSAS, L. E. et al. Genetic background influences immune responses and disease outcome of cutaneous L. mexicana infection in mice. **International Immunology**, v. 17, n. 10, p. 1347–1357, 1 out. 2005.

ROSSI, M.; FASEL, N. How to master the host immune system? Leishmania parasites have the solutions! [s.d.].

ROUHOUSOVÁ, I.; VOLF, P. Sand fly saliva: Effects on host immune response and Leishmania transmission. **Folia parasitologica**, v. 53, p. 161–171, 2006.

ROY, S. et al. An IL-10 dominant polarization of monocytes is a feature of Indian Visceral Leishmaniasis. **Parasite Immunology**, v. 40, n. 7, p. e12535, jul. 2018.

RUAN, C.-C. et al. Complement-Mediated Macrophage Polarization in Perivascular Adipose Tissue Contributes to Vascular Injury in Deoxycorticosterone Acetate–Salt

MiceSignificance. **Arteriosclerosis, Thrombosis, and Vascular Biology**, v. 35, n. 3, p. 598–606, mar. 2015.

SACKS, D.; NOBEN-TRAUTH, N. The immunology of susceptibility and resistance to leishmania major in mice. **Nature Reviews Immunology**, v. 2, n. 11, p. 845–858, nov. 2002a.

SACKS, D.; NOBEN-TRAUTH, N. The immunology of susceptibility and resistance to Leishmania major in mice. **Nature Reviews Immunology**, v. 2, n. 11, p. 845–858, nov. 2002b.

SARKAR, A. et al. Monitoring of intracellular nitric oxide in leishmaniasis: Its applicability in patients with visceral leishmaniasis. **Cytometry Part A**, v. 79A, n. 1, p. 35–45, jan. 2011.

SCAPINI, P. et al. The neutrophil as a cellular source of chemokines. **Immunological Reviews**, v. 177, n. 1, p. 195–203, out. 2000.

SCORZA, B. M.; CARVALHO, E. M.; WILSON, M. E. Cutaneous Manifestations of Human and Murine Leishmaniasis. **International journal of molecular sciences**, v. 18, n. 6, jun. 2017.

SCOTT, P.; NOVAIS, F. O. Cutaneous leishmaniasis: immune responses in protection and pathogenesis. **Nature Reviews Immunology**, v. 16, n. 9, p. 581–592, set. 2016a.

SCOTT, P.; NOVAIS, F. O. Cutaneous leishmaniasis: immune responses in protection and pathogenesis. **Nature Reviews Immunology**, v. 16, n. 9, p. 581–592, 18 set. 2016b.

SELF-FORDHAM, J. B. et al. MicroRNA: Dynamic Regulators of Macrophage Polarization and Plasticity. **Frontiers in immunology**, v. 8, p. 1062, 2017.

SICA, A.; MANTOVANI, A. Macrophage plasticity and polarization: in vivo veritas. **The Journal of clinical investigation**, v. 122, n. 3, p. 787–95, mar. 2012.

SIEWE, N. et al. Immune response to infection by Leishmania : A mathematical model. **Mathematical Biosciences**, v. 276, p. 28–43, jun. 2016.

SILVA, R. L. L. et al. sCD163 levels as a biomarker of disease severity in leprosy and visceral leishmaniasis. **PLOS Neglected Tropical Diseases**, v. 11, n. 3, p. e0005486, mar. 2017.

SOARES, R. P. P.; TURCO, S. J. Lutzomyia longipalpis (Diptera: Psychodidae: Phlebotominae): a review. **Anais da Academia Brasileira de Ciências**, v. 75, n. 3, p. 301–330, 2003.

SOONG, L. Subversion and Utilization of Host Innate Defense by Leishmania amazonensis. **Frontiers in immunology**, v. 3, p. 58, 2012.

SRIVASTAVA, S. et al. Possibilities and challenges for developing a successful vaccine for leishmaniasis. **Parasites & Vectors**, v. 9, n. 1, p. 277, dez. 2016.

STAURENGO-FERRARI, L. et al. Trans-Chalcone Attenuates Pain and Inflammation in Experimental Acute Gout Arthritis in Mice. **Frontiers in pharmacology**, v. 9, p. 1123, 2018.

STEVERDING, D. The history of leishmaniasis. **Parasites {&} Vectors**, v. 10, n. 1, p. 82, 2017.

STOUT, R. D. et al. Macrophages sequentially change their functional phenotype in response to changes in microenvironmental influences. **Journal of immunology (Baltimore, Md. : 1950)**, v. 175, n. 1, p. 342–9, jul. 2005.

SZANTO, A. et al. STAT6 Transcription Factor Is a Facilitator of the Nuclear Receptor PPARγ-Regulated Gene Expression in Macrophages and Dendritic Cells. **Immunity**, v. 33, n. 5, p. 699–712, nov. 2010.

TAVARES, N. M. et al. Understanding the mechanisms controlling Leishmania amazonensis infection in vitro: the role of LTB4 derived from human neutrophils. **The Journal of infectious diseases**, v. 210, n. 4, p. 656–66, ago. 2014.

TEIXEIRA, C. R. et al. Saliva from Lutzomyia longipalpis Induces CC Chemokine Ligand 2/Monocyte Chemoattractant Protein-1 Expression and Macrophage Recruitment. **Journal of immunology**, v. 175, n. 12, p. 8346–53, 2005.

TERRY, R. L.; MILLER, S. D. Molecular control of monocyte development. **Cellular Immunology**, v. 291, n. 1–2, p. 16–21, set. 2014.

TOMIOTTO-PELLISSIER, F. et al. Macrophage Polarization in Leishmaniasis: Broadening Horizons. **Frontiers in immunology**, v. 9, n. October, p. 2529, 2018.

VAN DEN BOSSCHE, J. et al. Mitochondrial Dysfunction Prevents Repolarization of Inflammatory Macrophages. **Cell Reports**, v. 17, n. 3, p. 684–696, out. 2016.

VAN ZANDBERGEN, G. et al. Cutting edge: neutrophil granulocyte serves as a vector for Leishmania entry into macrophages. **Journal of immunology (Baltimore, Md. : 1950)**, v. 173, n. 11, p. 6521–5, dez. 2004.

VELASQUEZ, L. G. et al. Distinct courses of infection with Leishmania (L.) amazonensis are observed in BALB/c, BALB/c nude and C57BL/6 mice. **Parasitology**, v. 143, n. 6, p. 692–703, 2016.

VELLOZO, N. S. et al. All-Trans retinoic acid promotes an M1-to M2-phenotype shift and inhibits macrophage-mediated immunity to Leishmania major. **Frontiers in Immunology**, v. 8, n. NOV, 2017.

VENTURIN, G. L. et al. M1 polarization and the effect of PGE $_2$ on TNF-α production by lymph node cells from dogs with visceral leishmaniasis. **Parasite Immunology**, v. 38, n. 11, p. 698–704, nov. 2016.

WANG, N.; LIANG, H.; ZEN, K. Molecular mechanisms that influence the macrophage m1-m2 polarization balance. **Frontiers in immunology**, v. 5, p. 614, 2014a.

WANG, N.; LIANG, H.; ZEN, K. Molecular Mechanisms That Influence the Macrophage M1â€"M2 Polarization Balance. **Frontiers in Immunology**, v. 5, p. 614, nov. 2014b.

WANG, Q. et al. Fra-1 protooncogene regulates IL-6 expression in macrophages and promotes the generation of M2d macrophages. **Cell Research**, v. 20, n. 6, p. 701–712, jun. 2010.

WANG, Z. et al. MicroRNA 21 is a homeostatic regulator of macrophage polarization and prevents prostaglandin E2-mediated M2 generation. **PloS one**, v. 10, n. 2, p. e0115855, 2015.

WANG, Z. E. et al. CD4+ effector cells default to the Th2 pathway in interferon gamma-deficient mice infected with Leishmania major. **The Journal of experimental**

medicine, v. 179, n. 4, p. 1367–71, abr. 1994.

WHEAT, W. H. et al. Lutzomyia longipalpis salivary peptide maxadilan alters murine dendritic cell expression of CD80/86, CCR7 and cytokine secretion and reprograms dendritic cell-mediated cytokine release from cultures containing allogeneic T cells. **Journal Immunology**, v. 180, n. 12, p. 8286–8298, 2009.

WHO. **Leishmaniasis**. Disponível em: <https://www.who.int/news-room/fact-sheets/detail/leishmaniasis>. Acesso em: 11 ago. 2020.

WHO - WORLD HEALTH ORGANIZATION. Leishmaniasis in high-burden countries: an epidemiological update based on data reported in 2014. **Releve epidemiologique hebdomadaire**, v. 91, n. 22, p. 287–96, jun. 2016.

WHO - WORLD HEALTH ORGANIZATION. **Leishmaniasis**.

WOLFS, I.; DONNERS, M.; DE WINTHER, M. Differentiation factors and cytokines in the atherosclerotic plaque micro-environment as a trigger for macrophage polarisation. **Thrombosis and Haemostasis**, v. 106, n. 11, p. 763–771, nov. 2011.

XU, W. et al. Reversible differentiation of pro- and anti-inflammatory macrophages. **Molecular Immunology**, v. 53, n. 3, p. 179–186, mar. 2013.

XU, X. et al. Structure and function of a "yellow" protein from saliva of the sand fly Lutzomyia longipalpis that confers protective immunity against Leishmania major infection. **The Journal of biological chemistry**, v. 286, n. 37, p. 32383–93, set. 2011.

ZANLUQUI, N. G.; WOWK, P. F.; PINGE-FILHO, P. Macrophage Polarization in Chagas Disease. **Journal of Clinical and Cellular Immunology**, v. 06, n. 02, p. 1–6, abr. 2015.

ZHAO, Y. LONG et al. Comparison of the characteristics of macrophages derived from murine spleen, peritoneal cavity, and bone marrow. **Journal of Zhejiang University: Science B**, v. 18, n. 12, p. 1055–1063, 1 dez. 2017.

6. ANEXOS
6.1. COMPROVANTE DE ACEITE

Izabel Galhardo Demarchi (Via FrontiersIn) <noreply@frontiersin.org>
Responder a: Izabel Galhardo Demarchi <i.g.demarchi@ufsc.br>
Para: Fernanda Tomiotto-Pellissier <fernandatomiotto@gmail.com>

1 de dezembro de 2020 18:24

frontiers

Your Research Topic abstract was accepted

Dear Dr Tomiotto-Pellissier,

Many thanks for contributing to the Research Topic "**Cutaneous Leishmaniasis: Exploring Pathogenesis and Immunomodulatory Approaches**" with your abstract "**Mice susceptibility to Leishmania amazonensis is dependent on arginase-1 of macrophages**".

We are pleased to inform you that your abstract has been accepted by the Guest Editors. Congratulations on your achievement!

To move forward, please submit your manuscript no later than 29 March 2021 via the following link **Cutaneous Leishmaniasis: Exploring Pathogenesis and Immunomodulatory Approaches**.

When submitted, your manuscript will undergo Frontiers collaborative peer-review process, through which authors can directly interact with editors and reviewers in a fully-online, dedicated review forum. If accepted, your article will be published immediately and become freely accessible to all readers. Your paper will be indexed in relevant repositories, and as an author in Frontiers, you retain the copyright to your own papers and figures. You will also have access to advanced article-level metrics to track your impact.

All articles published incur a publishing fee, allowing us to make articles free to read and download.**Find more information on article fees**.

Should you have any questions, please do not hesitate to contact us.

We look forward to receiving your manuscript!

Best Regards,

Your Frontiers in Cellular and Infection Microbiology team

Frontiers | Editorial Office - Journal Development Team

6.2. OUTRAS PRODUÇÕES REALIZADAS DURANTE O DOUTORADO
6.2.1. Artigo 1

Inhibitory Activity of *Caryocar coriaceum* Wittm. Pulp and Peel Fruit Extract Against Promastigote and Amastigote forms of *Leishmania amazonensis*: *in-vitro* and *in-silico* approaches

Fernanda Tomiotto-Pellissier[a,b,*], Daniela Ribeiro Alves[c,f], Selene Maia de Morais[c], Bruna Taciane da Silva Bortoleti[a,b], Manoela Daiele Gonçalves[d], Taylon Felipe Silva[b], Eliandro Reis Tavares[e], Lucy Megumi Yamauchi[e], Idessania Nazareth Costa[b], Emmanuel Silva Marinho[f], Marcia Machado Marinho[g], Ivete Conchon-Costa[b], Milena Menegazzo Miranda-Sapla[b], Wander Rogério Pavanelli[a,b,*]

[a]Biosciences and Biotechnology Postgraduate Program, Carlos Chagas Institute (ICC), Fiocruz.
[b]Department of Pathology Science, Center of Biological Sciences, State University of Londrina.
[c]Department of Natural Sciences, Ceará State University.
[d]Department of Chemistry, Center of Exact Sciences, State University of Londrina.
[e]Department of Microbiology, Center of Biological Sciences, State University of Londrina.
[f]Theoretical and Electrochemical Chemistry Group, Faculty of Philosophy Dom Aureliano Matos, State University of Ceará.
[g]Iguatu Faculty of Education, Science and Letters, State University of Ceará.
* Corresponding authors.

1

1 **Inhibitory Activity of *Caryocar coriaceum* Wittm. Pulp and Peel Fruit Extract Against**

2 **Promastigote and Amastigote forms of *Leishmania amazonensis*: an *in vitro* and *in silico***

3 **approach**

4

5 Fernanda Tomiotto-Pellissier[a,b,*], Daniela Ribeiro Alves[c,f], Selene Maia de Morais[c], Bruna Taciane

6 da Silva Bortoleti[a,b], Manoela Daiele Gonçalves[d], Taylon Felipe Silva[b], Eliandro Reis Tavares[e], Lucy

7 Megumi Yamauchi[e], Idessania Nazareth Costa[b], Emmanuel Silva Marinho[f], Marcia Machado

8 Marinho[g], Ivete Conchon-Costa[b], Milena Menegazzo Miranda-Sapla[b], Wander Rogério Pavanelli[a,b,*]

9

10 [a]Biosciences and Biotechnology Postgraduate Program, Carlos Chagas Institute (ICC), Fiocruz,

11 Curitiba. Paraná, Brazil.

12 [b]Department of Pathology Science, Center of Biological Sciences, State University of Londrina,

13 Londrina, Paraná, Brazil.

14 [c]Department of Natural Sciences, Ceará State University, Fortaleza, Ceará, Brazil.

15 [d]Department of Chemistry, Center of Exact Sciences, State University of Londrina, Londrina, Paraná,

16 Brazil.

17 [e]Department of Microbiology, Center of Biological Sciences, State University of Londrina, Londrina,

18 Paraná, Brazil.

19 [f]Theoretical and Electrochemical Chemistry Group, Faculty of Philosophy Dom Aureliano Matos,

20 State University of Ceará, Limoeiro do Norte, Ceará, Brazil.

21 [g]Iguatu Faculty of Education, Science and Letters, State University of Ceará, Iguatu, Ceará, Brazil.

22

23 * Corresponding author. Laboratory of Immunopathology of Neglected Diseases, Center of

24 Biological Sciences, State University of Londrina, Celso Garcia Rod, PR-445, Km380, Londrina,

25 Paraná, Brazil. Phone number: +55 43 33714539. Zip Code: 86057970. Orcid 0000-0002-7273-8237.

26 E-mail address: fernandatomiotto@gmail.com / wanderpavanelli@yahoo.com.br

27 **ABSTRACT**

28 Leishmaniasis is a group of neglected diseases caused by parasites of *Leishmania* genus.

29 The treatment of Leishmaniasis represents a great challenge, because the available drugs

30 present high toxicity and none of them has been shown to be fully effective. *Caryocar* is

31 a botanical genus rich in phenolic compounds, which leaves extracts have already been

32 described by its antileishmanial action. Thus, we investigated the effect of pulp and peel

33 extracts of the *Caryocar coriaceum* fruit on promastigote and amastigote forms of

34 *Leishmania amazonensis*. Both extracts had antipromastigote effect after 24, 48 and 72 h

35 and this effect was by apoptosis-like process induction, with reactive oxygen species

36 (ROS) production, damage to the mitochondria and plasma membrane, and

37 phosphatidylserine exposure. Knowing that the fruit extracts did not alter the viability of

38 macrophages, we observed that the treatment reduced the infection of these cells.

39 Thereafter, in the *in vitro* infection context, the extracts showed antioxidant proprieties,

40 by reducing NO, ROS and MDA levels. In addition, both peel and pulp extracts up-

41 regulated Nrf2/HO-1/Ferritin expression and increase the total iron bound in infected

42 macrophages, which culminates in a depletion of available iron for *L. amazonensis*

43 replication. *In silico*, the molecular modeling experiments showed that the three

44 flavonoids presented in the *C. coriaceum* extracts can act as synergistic inhibitors of

45 *Leishmania* proteins, and compete for the active site. Also, there is a preference for rutin

46 at the active site due to its greater interaction binding strength.

47

48 **Keywords:** Ferritin; Heme oxygenase-1; Leishmaniasis; Nrf2; Oxidative stress; Nitric

49 oxide; Docking molecular.

50

51

52   GRAPHICAL ABSTRACT

53
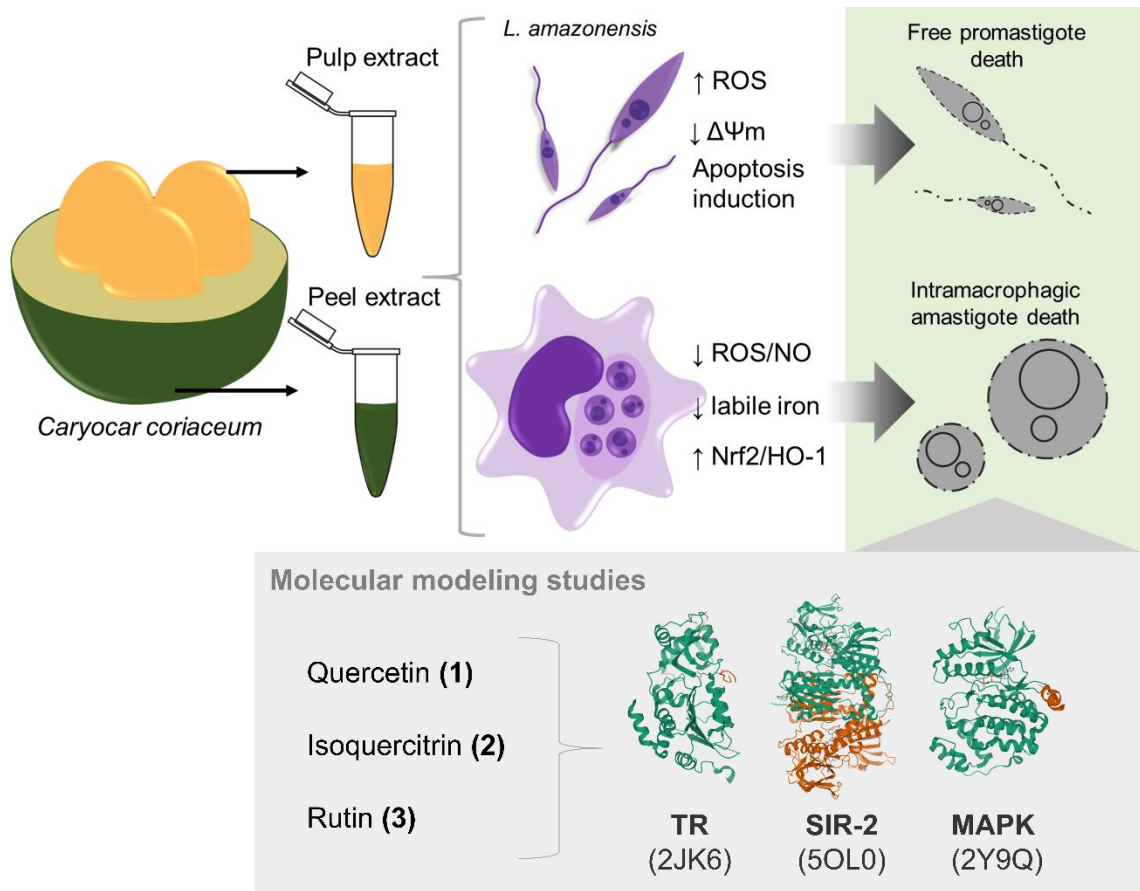
1 INTRODUCTION

55   Leishmaniasis is a group of diseases caused by parasitic protozoa of the

56 *Leishmania* genus transmitted through the bite of phlebotomine insects. The World

57 Health Organization (WHO) categorizes it as a neglected tropical disease since 350

58 million people in 102 countries worldwide are at risk of developing one of the disease

59 clinical forms (WHO, 2018). The macrophages are the main host cells to *Leishmania*

60 parasites whose machinery eliminates the parasites. However, the parasite can evade the

61 macrophage responses, persist on the host, and develop the disease (reviewed in: Rossi

62 and Fasel, 2018). Additionally, amastigote forms can survive inside macrophages

63 depending on the host's labile iron uptake regarding its metabolism, virulence, and

64 multiplication [3,4].

65   Nuclear factor transcription factor (erythroid-derived-2)-like 2 (NRF2) finely

66 controls iron metabolism in macrophages and acts on genes involved in heme synthesis,

67 hemoglobin catabolism, iron storage, and exportation [5]. Also, the NRF2/ heme

68 oxygenase-1 (HO-1)/ ferritin signaling cascade is important to *Leishmania amazonensis*

69 proliferation controlling by culminating in iron storage and, consequently, unavailability

70 of parasite uptake (Cataneo et al., 2019; Miranda-Sapla et al., 2019; Tomiotto-Pellissier

71 et al., 2018).

72   Leishmaniasis treatment represents a great challenge considering that the

73 available drugs have high toxicity and are yet to prove fully effective. Relapses,

74 therapeutic failure, and resistance to treatment are factors that motivate the search for

75 drugs with leishmanicidal actions that are more effective and less toxic to the patient [9].

76   *Caryocar* is a botanical genus belonging to the Caryocaraceae family distributed

77 through South and Central America in the vegetation type of Cerrado. The use of the

78 fruits encompasses the production of food, cosmetics as well as the scope of folk

79   medicine. Rich in phenolic compounds, these extracts have been described as potent

80   antioxidants, in addition to having anti-inflammatory, antineoplastic, and antimicrobial

81   effects [10–13]. The description of these extracts also appeared regarding its activity

82   against *Leishmania amazonensis* (Alves et al., 2017; Paula-Ju et al., 2006; Tomiotto-

83   Pellissier et al., 2018).

84   Previous studies demonstrated that leaf extracts of *Caryocar coriaceum* Wittm,

85   rich in flavonoids, have leishmanicidal activity (Tomiotto-Pellissier et al., 2018), but the

86   possible action mechanisms of fruit extracts on extra or intracellular parasite was not

87   evaluated.

88   Given this context, this study aimed at investigating the leishmanicidal effect of

89   *C. coriaceum.* fruit pulp and peel extracts on promastigote and amastigote *Leishmania*

90   *(Leishmania) amazonensis* forms, including an *in silico* experiment investigating the

91   main constituents of plant extracts quercetin, isoquercitrin and rutin.

92

93   **2   MATERIALS AND METHODS**

94   **2.1   Pulp and peel extracts of *Caryocar coriaceum* Wittm.**

95   The extracts of *C. coriaceum* Wittm. were kindly supplied by Dr. Selene Maia de

96   Morais of the State University of Ceará and obtained as previously described [15].

97   Briefly, peel and pulp of *C. coriaceum* Wittm. mature fruits were obtained at the Campus

98   of the State University of Ceará (UECE) (lat.: −3.792222; long.: −38.556111), Fortaleza,

99   Brazil, and were identified by Prisco Bezerra Herbarium under the code EAC57060. The

100   extracts were obtained by cold maceration with 96% ethanol, at 12 h cycle of light for 7

101   days. Filtration of the supernatant and evaporation of the solvent at reduced pressure in a

102   rotary evaporator led to crude ethanol extracts of *C. coriaceum.* fruit pulp and fruit peel.

103

104 **2.2 Extracts characterization by HPLC**

105   The identification and quantification of flavonoids on peel and pulp were

106 performed by high-performance liquid chromatography (HPLC) with SHIMADZU liquid

107 chromatography coupled to a SCL-10AVP controller system, UV-VIS detector SPD-

108 10AVP, and isocratic pump LC-10ATVP. The software LC Solution software was used

109 to record the chromatograms and measure peak areas. The column used was a Shimadzu

110 analytical CLC-ODS M (C-18) of 25 cm.

111   The calibration curve was constructed using the standards rutin, isoquercitrin, and

112 quercetin injected at different concentrations (0.25; 0.05; 0.025 and 0.005 mg.mL^{-1}) into

113 the liquid chromatography. The flow rate was 1.8 mL per minute for quercetin and 1.25

114 ml per minute to rutin both at a wavelength of 350 nm and a mobile phase of 20%

115 acetonitrile and 80% solution of H_3PO_4 pH buffer 2.8. The linear regression equation was

116 obtained by using the Microsoft Office Excel 2010 program.

117   The chromatographic profile of flavonoids rutin, quercetin, and isoquercitrin, the

118 chosen standards, was obtained preparing ethanolic solutions at a concentration of 0.5

119 mg.mL^{-1}. As a mobile phase, the same solution was used for the calibration curve at the

120 same wavelength and flow rate of 1.80 mL per minute.

121

122 **2.3 *Leishmania (Leishmania) amazonensis* maintenance**

123   *L. (L.) amazonensis* (MHOM/BR/1989/166MJO) promastigotes forms of were

124 maintained in culture medium 199 (GIBCO) pH 7.18-7.22 supplemented with 10% fetal

125 bovine serum (FBS) (GIBCO), 10 mM-HEPES buffer, 0.1% human urine, 0.1% L-

126 glutamine, 10U/mL-penicillin and 10μg/mL-streptomycin (GIBCO) and 10% sodium

127 bicarbonate. The cell culture was maintained at 25°C in a 25 cm^2 culture flask. All

128 experiments used promastigote forms at the stationary growth phase.

129

130 **2.4 Antipromastigote assay**

131   *L. amazonensis* promastigote forms (10^6 cells/mL) were treated with *C.*

132 *coriaceum.* extracts 25, 50 and 100 μg/mL. Parasites were counted on a Neubauer

133 chamber after 24, 48, and 72h of treatment. *L. amazonensis* promastigote maintained in

134 the culture medium was used as a control, DMSO 0.01% was used as a vehicle, and

135 amphotericin B (AMB) 1μM was used as a positive control.

136

137 **2.5 Scanning electron microscopy of promastigote forms**

138   Scanning electron microscopy of promastigotes forms was performed according

139 to [16]. Briefly, the parasites (10^6) were treated with 50 μg/mL of pulp and peel extracts

140 for 24 h, processed, and analyzed through scanning electron microscopy (FEI QUANTA

141 200 scanning electron microscope). The length of the promastigote forms was analyzed

142 in the Image-Pro Plus software, based on the 8000 - 10500x magnification images

143 obtained. At least three images of each condition were subjected to measurement.

144

145 **2.6 Mechanism of action determination on promastigote forms**

146   To determine the mechanism of action of the *C. coriaceum.* extracts on

147 promastigote forms, the parasites (10^6 cells/mL) were treated for 24h with 50 μg/mL of

148 the extracts, and different parameters were accessed as previously described by our group

149 (Tomiotto-Pellissier et al., 2018). Briefly, the inner mitochondrial membrane potential

150 was investigated by incubation with tetramethylrhodamine ethyl ester (TMRE) (Sigma);

151 phospholipids (PS) exposure was detected by Annexin-V FITC (Invitrogen); the cellular

152 membrane integrity was evaluated by propidium iodide (PI) (Sigma); and the reactive

153 oxygen species (ROS) were analyzed by a permeant probe diacetate 2',7'-

154   dichlorofluorescein (H₂DCFDA) (Sigma). All the analyses were performed on a

155   fluorescence microplate reader (Victor X3, PerkinElmer).

156

157   **2.7   Co-determination of annexin V and propidium iodide label**

158   Promastigotes (10^6 cells/mL) were washed and resuspended in 100 μL of assay

159   buffer 1x (Santa Cruz Biotechnology), followed by the addition of a mix containing 1 μL

160   of annexin-V FITC and 5 μL of PI (Santa Cruz Biotechnology). A total of 10,000 events

161   were acquired in a BD Accuri™ C6 flow cytometer. The labeling was analyzed as

162   previously described (Doroodgar et al., 2016; Tomiotto-Pellissier et al., 2018).

163

164   **2.8   Ethics Committee**

165   BALB/c mice were kindly provided by the Carlos Chagas Institute (ICC)/Fiocruz,

166   Curitiba, Brazil. The animals (25-30 g and 6-8 weeks) were kept under sterile conditions

167   and used according to protocols approved by the Institutional Animal Care and

168   Committee. This study was approved by the Ethics Committee for Animal

169   Experimentation of the State University of Londrina (13134.2016.62).170.

170

171   **2.9   Viability of peritoneal exudate cells**

172   The cytotoxic effects of *C. coriaceum* extracts on peritoneal exudate cells (PEC)

173   were tested based on mitochondrial oxidation of MTT (3-(4,5-dimethylthiazol-2-yl)-2,5-

174   diphenyltetrazolium bromide) (Sigma) assay described by [16,18]. Briefly, 5×10^5

175   cells/mL were recovered from the peritoneal cavity of BALB/c and the adherent cells

176   were incubated with 25, 50, and 100 µg/mL of pulp or peel extract and cultured for 24 h.

177   After this period, MTT (5 mg/mL) was added for 3 h and the plates were read in a

178   spectrophotometer (Thermo Scientific, Multiskan GO) at 550 nm.

179

2.10 Anti-amastigote assay

181   PEC ($5x10^5$ cells/mL) were obtained as previously described. The adherent cells

182 were infected with *L. amazonensis* promastigotes of ($1x10^6$ cells/mL) for 2h. After, the

183 non-internalized parasites were washed with PBS and the infected cells treated with the

184 extracts (25, 50 or 100 µg/mL), RPMI 1640 medium (control), DMSO 0.01% (vehicle)

185 or AMB 1µM (positive control) for 24h (37°C, 5% CO_2). After this, the cells were stained

186 with Giemsa (Laborclin) and 20 fields analyzed through an optical microscope (Olympus

187 BX41, Olympus Optical Co).

188

2.11 Promastigote recovery test

190   Promastigotes recovery assay was performed as previously described by

191 (Tomiotto-Pellissier et al., 2018). In brief, adherent PEC were infected with *L.*

192 *amazonensis* and treated with concentrations of *C. coriaceum* extracts. After 24 h of

193 treatment, it was induced the differentiation of intracellular viable amastigotes into

194 promastigote free forms. Free promastigotes recovered (FPR) were counted on a

195 Neubauer chamber for three consecutive days.

196

2.12 Malondialdehyde (MDA) Levels Measurement

198   MDA levels were determined through a High-Performance Chromatography

199 (HPLC) according to Tomiotto-Pellissier et al., 2018. The analyses were conducted using

200 an Alliance e2695 HPLC (Waters) equipped with a SecurityGuard ODS-C18 (4×3.0

201 mm, Phenomenex), C18 reverse-phase column (Eclipse XDBC18; 4.6×250 mm, 5 µm,

202 Agilent) as well as a photodiode array detector (Photodiode ArrayDetector (PDA), 2998)

203 using Empower 2 software (Waters).

204

2.13 Determination of iron concentration and total bound iron

205

206   The determination of iron concentration in supernatants of the anti-amastigote

207   assay was performed utilizing the method adapted by our group [8]. Briefly, in pH 4.5

208   and in the presence of ascorbic acid, it occurs the release of iron bound to transferrin. The

209   resulting product (Fe^{2+}) forms a complex measured using a biochromatic endpoint

210   technique (600, 700nm). The test principle for the total bound iron is similar: all available

211   sites of iron-binding in transferrin were saturated. In pH 8.6, only saturated iron in excess,

212   unbound, is available to be reduced to ferric iron by ascorbic acid forming a complex.

213   The subsequent addition of acid (pH 4.5) releases the iron bound to transferrin, this

214   supplemental iron is reduced to ferric iron by ascorbic acid, forming an increased amount

215   of complex. The increase in absorbance during the change of pH 8.6 to pH 4.5 is

216   proportional to the concentration of iron-bound.

217

218   **2.14 Relative quantification of Nrf2, ferritin and HO-1 mRNA**

219   The mRNA expression levels quantification for nuclear factor erythroid 2–related

220   factor 2 (Nrf2), ferritin, and heme-oxygenase 1 (HO-1) genes were performed following

221   Tomiotto-Pellissier et al. (2018) using the Total RNA Isolation System kit (Promega)

222   following the manufacturer's procedure.

223

224   **2.15 Statistical analysis**

225   Data were expressed as a mean ± SEM. At least three independent experiments

226   were performed, each with duplicate datasets. Data were analyzed using the GraphPad

227   Prism statistical software (GraphPad Software, Inc., USA, 500.288). Significant

228   differences between the groups were determined through one-way ANOVA, followed by

229 Tukey's test for multiple comparisons. Differences were considered statistically

230 significant upon p≤0.05.

231

232 **2.16 *In sílico* antileishmanial evaluation**

233 2.16.1 Ligands preparation

234 The chosen ligands were: quercetin (1), isoquercitrin (2) and rutin (3). The control

235 molecules were phosphoaminophosphonic acid-adenylate ester (4), L-peptide linking

236 cellular tumor antigen p53 (5), flavin-adenine dinucleotide sulfate (6) and amphotericin

237 b (7). Their respective two-dimensional structures were obtained from the virtual

238 repository PubChem© (https://pubchem.ncbi.nlm.nih.gov/). In order to use molecules in

239 their best potential energy state for the simulation of molecular docking, they were

240 optimized by the semi-empirical parametric method 7 (PM7) of molecular mechanics

241 [19–21] with the MOPAC® software and converted to ligand.mol2.

242

243 2.16.2 Target protein preparation

244 Human ERK2 complexed with a Mitogen-Activated Protein Kinase docking

245 peptide (MAPK) (PDB: 2Y9Q) [22], Silent Information Regulator 2 related protein 1

246 (SIR) (PDB: 5OL0) [23] and Trypanothione Reductase (TR) (PDB: 2JK6) [24] biological

247 targets of *Leishmania* sp. and was reported from the RCSB© protein data bank

248 (https://www.rcsb.org/) in protein format .pdb. The structures were filed in the Protein

249 Data Bank, determined from X-ray diffraction, with a resolution of 1.55Å, 1.99Å and

250 2.95Å, respectively. Furthermore the file was loaded into UCSF Chimera® software [25]

251 for all residues remotion and polar hydrogens additions for producing favorable

252 protonation states [26,27] and preparing the target for submission to the molecular

253 docking test.

254   2.16.3 Molecular docking study

255   After the ligand and protein preparation stage, the molecules were finally

256   subjected   to   molecular   docking   simulation   by   the   SwissDock   server

257   (http://www.swissdock.ch/docking#) [28,29] from the Molecular Modeling Group from

258   Swiss Institute of Bioinformatics (SIB) (https://www.sib.swiss/). The .zip files received

259   from the online server were downloaded and processed in the UCSF Chimera® software,

260   where the curcumins interaction and distance analyzes were performed, in comparison

261   with the catalytic sites occupied by the control ligands (4)-(6). 4 is the inhibitor described

262   from the characterization of MAPK (PDB: 2Y9Q) [22], *5* is the SIR (PDB: 5OL0)

263   inhibitor [23] and 6 is TR (PDB: 2JK6) inhibitor described [24], (7) is a drug considered

264   as positive controls described in the literature [30–32]. The detailed analysis of the

265   intermolecular interactions between the tested compounds and the residues of the MAPK,

266   SIR and TR catalytic sites was done by obtaining the theoretical values of H-bond donors

267   and acceptors of the ligands and their respective acid dissociation constants (pKa),

268   calculated in the software MarvinSketch® [33], where it was possible to predict the micro-

269   species formed from the ligands under physiological actions (approximately pH 7.4)

270   [34,35]. The data obtained from the analysis were plotted on the Morpheus® online

271   statistical tool (https://software.broadinstitute.org/morpheus/), where heat maps were

272   generated to identify the ligand-residue interaction and similarity profiles by the statistical

273   test Pearson. The types of linker-residue interactions, as well as the figures, were

274   generated using the Discovery Studio® [36].

275

276   **3   RESULTS**

277 **3.1** *Caryocar coriaceum* **Wittm. composition**

278   The chromatographic analysis of the *C. coriaceum.* fruit extracts showed that both

279 extracts, pulp, and peel, presented the flavonoids rutin and isoquercitrin. However, only

280 the pulp extract showed a small peak corresponding to quercetin (Figure 1).

281

282 **3.2   Peel and pulp extracts exert an anti-promastigote effect on *L. amazonensis***

283   We assessed the antileishmanial effect of pulp and peel extracts by determining

284 the number of viable parasites. All tested concentrations of the extracts proved a

285 significant reduction of *L. amazonensis* proliferation from 24h ($p \leq 0.01$), 48h ($p \leq 0.001$),

286 and 72h ($p \leq 0.001$) when compared to both the control and vehicle groups (Figure 2A).

287   Figure 2B shows the following difference between the concentrations: 100 µg/mL

288 dose was more effective at reducing *L. amazonensis* proliferation than 25 µg/mL in 24

289 and 48h ($p \leq 0.05$ and $p \leq 0.01$, respectively) for pulp extract, and in 24, 48 and 72h for peel

290 extract ($p \leq 0.05$, $p \leq 0.01$ and $p \leq 0.01$, respectively). After 48h of pulp extract treatment,

291 100 µg/mL had different results than 25 and 50 µg/mL ($p \leq 0.01$); after 72h, no difference

292 appeared between the concentrations of this extract. In addition, the effect proved not

293 time-dependent for both extracts ($p > 0.05$). Considering the similar results, we conducted

294 further experiments by investigating the effect of treatments on promastigote forms using

295 the intermediate concentration (50 µg/mL) at 24h.

296

297 **3.3   Apoptosis-like mechanism induced by *C. coriaceum* extracts**

298   Upon the verification of the leishmanicidal action of the extracts, we sought to

299 elucidate the death mechanisms induced by these treatments and found that pulp and peel

300 extracts enhanced the ROS levels ($p \leq 0.001$), reduced the mitochondrial membrane

301 potential ($\Delta\Psi$m) ($p \leq 0.0001$), induced PS exposition ($p \leq 0.0001$), and damaged the plasma

302 membrane (p≤0.001) (Figure 3A-D). Enhanced ROS levels, induced PS exposition and

303 PI labeling proved higher in peel-treated than in pulp-treated parasites (p≤0.0001).

304   We performed an annexin V/ PI co-staining in treated promastigote forms to

305 differentiate the cell death mechanisms. The annexin V+ parasites showed an increase of

306 7.34 and 10.6% after treatment using pulp and peel, respectively, concerning the control,

307 while the PI+ cells enhanced in 7.8% for pulp and 1.48% for peel extract. Lastly, the

308 annexin V+/PI+ promastigotes proved 28.4 and 24.9% higher in the pulp and peel treated

309 parasites, respectively, when compared to the control, indicating that most of the treated

310 promastigote forms underwent late apoptosis-like death in both conditions (Figure 3F and

311 G).

312   Moreover, we found that extracts acted in the morphology of promastigote forms

313 since the extracts promoted a significant reduction on cell body (p≤0.05), flagellum

314 (p≤0.05), and total length (p≤0.001) (Figure 4A). Besides that, pulp extract induced

315 blebbing (apoptotic bodies) formation on the parasite membrane (Figure 4C), and both

316 extracts acted on the rounding, shrinking, and double flagella formation on *Leishmania*

317 (Figure 4D-F) after 24h of treatment using 50 μg/mL.

318

319 **3.4** *C. coriaceum* **extracts act in intracellular amastigote forms without**

320   **cytotoxicity to host cells**

321   Considering the effects of *C. coriaceum.* pulp and peel extracts on promastigote

322 forms, we performed experiments to verify their possible action on intracellular

323 amastigotes. Initially, we found that the tested concentrations of both extracts (25 to 100

324 μg/mL) did not interfere with the viability of host cells (macrophages) (Figure 5A)

325 (p≥0.99), but they were subsequently able to significantly reduce the percentage of

326 infected macrophages (Figure 5B) and amastigote forms by macrophage (Figure 5C)

327 when compared to the control (p≤0.05) – not different between them or AMB.

328   To confirm the infection reduction, we performed a recovery assay of

329 promastigotes forms by subjecting the culture of amastigote-infected macrophages to

330 ideal conditions to differentiate viable amastigotes in free promastigote forms. All tested

331 concentrations reduced the percentage of recovery promastigotes forms after 48 and 72h

332 of culture (Figure 5D and E) (p≤0.05). After 48h, none of the treatments differed from

333 AMB and neither did the concentrations of 50 and 100μM of pulp and 100μM of peel

334 extract after 72h. Considering the similar effect of the different concentrations, we applied

335 the lowest concentration to carry out the following experiments.

336

337 **3.5   Pulp and peel *C. coriaceum* extracts act as an antioxidant on *L. amazonensis*-**

338   **infected macrophages**

339   Seeking to understand the mechanisms involved in the elimination of intracellular

340 parasites, we analyzed the production of reactive species which are important to the

341 response against *Leishmania* parasites. Surprisingly, our results demonstrated that

342 infected cells treated with *C. coriaceum.* pulp and peel extracts (25 μg/mL) showed lower

343 NO and ROS production. The treatment using extracts acted as antioxidants, which is

344 reinforced with lower lipid peroxidation indicated when measuring the lipid peroxidation

345 metabolite MDA (Figure 6A, B, and C, respectively) in infected macrophages when

346 compared to the control (p≤0.05).

347

348 **3.6** *C. coriaceum* **pulp and peel extracts modulate iron pool of infected**

349 **macrophages**

350 Still aiming at understanding the parasites death pathway, we investigated the

351 levels of iron and total binding iron capacity and found data indicating that the treatment

352 using pulp and peel extracts did not alter the total iron concentration in *L. amazonensis*-

353 infected macrophages (Figure 7A) ($p \geq 0.2$), but increased iron-bound (Figure 7B) when

354 compared to the control ($p \leq 0.001$) and decreased iron labile bioavailability. We found a

355 sharper increase in total iron-bound capacity for the peel extract treatment ($p \leq 0.001$).

356

357 **3.7** *C. coriaceum* **fruit extracts induce Nrf2, HO-1 and Ferritin expression**

358 Considering that the treatments using the extracts induced an antioxidant action

359 and concomitant higher iron-bound, we investigated the cascade involving the

360 transcription factor Nrf2, HO-1 enzyme, and protein ferritin (Figure 8). Our results

361 showed that both pulp and peel extracts were able to up-regulate the expression of the

362 three genes investigated (Nrf2, HO-1, and ferritin) when compared to the control

363 ($p \leq 0.01$). Also, we found that the pulp extract caused more pronounced effects than the

364 peel extract in the expression analysis of HO-1 and Nrf2 ($p \leq 0.01$).

365

366 **3.8** **Molecular docking**

367 The energy binding/affinity energy (ΔG) of the compounds (1), (2) and (3) were

368 strongest (lower than -6 kcal/mol) than the controls (4), (5) and (6) as it has an affinity

369 energy greater than -5 kcal/mol (Figure 9). Highlighting the bests results with all proteins

370 evaluated for the (3) compound, rutin, with high abundance in all extracts here proposed.

371 The (7) compound did it did not bind with the proteins evaluated here ($\Delta G > -3$), indicating

372 that its mechanism of action potentially acts on other pathways. The ligands proposed

373   here do not connect at the proposed active sites [22–24], but perform high molecular

374   strength interactions with their respective amino acids, as we will see below.

375   The ligand (4), MAPK's proposed inhibitor [22], strongly connects with 10 amino

376   acids (AA) by conventional hydrogen bonds with binding distances from 2.58 to 3.29 Å,

377   the strongest bonds are with ALA35, ASP106, ASP111, GLN105, GLY37, LYS114 and

378   LYS54. However, this compound has bonds with average interaction forces at G34

379   (carbon hydrogen bond; 3.69 Å), ARG67 and LYS151 (electrostatic salt bridges; 2.85 to

380   3.44 Å), and weak Pi hydrophobic bonds (4.15 to 5.44 Å) with ALA52, ILE31, LEU156

381   and VAL39.

382   As well, (5) compound, SIR's proposed inhibitor [23], has higher eletrostatic salt

383   bridge binding (2.74 Å) with ASP196, strong conventional hydrogen bonds with 10 AA

384   distances up from 2.58 to 3.29 Å, the most important ones are ALA35, ASP106, ASP111,

385   GLY37, LYS54, SER153 and TYR36. Also, this compound poorly connects GLY34 AA

386   with carbon hydrogen bond (3.69 Å) and pi-alkyl bonds with ALA52, ILE31, LEU156

387   and VAL39 (3.87 to 5.44 Å).

388   The (6) compound, TR's proposed inhibitor [24], performs strong conventional

389   hydrogen bonds with 15 AA, most importantly at ALA47, ASP327, ASP35, GLY127,

390   GLY286, LYS60, THR39, THR51 and TYR221 of TR receptor distances up from 2.56

391   to 3.01Å. Also, this ligand achieves average carbon hydrogen bonds with the residues of

392   ALA159, GLY11, GLY13, GLY161, GLY50, MET333, PRO336 and THR160 of TR

393   receptor from 3.11 to 3.73Å. With PHE203, TYR198 and VAL36 fulfill hydrophobic pi-

394   alkyl interactions and with CYS57 pi-sulfur binding. Yet, amide-pi stacked connections

395   with GLY56 were performed.

396   Regarding the behavior of the binding energies of the compounds (1), (2) and (3)

397   evaluated in this work, despite all of it demonstrated better binding energy than all the

398   controls, its binding with AA of each target were also better than the controls, as we can

399   demonstrate at supplementary figures, in which the better compound (3) were

400   demonstrated.

401   Regarding the interaction between the ligands and the MAPK protein (Figure S1),

402   each interest compound occupies a different site, as seen. The better binding compound

403   was (3), with ΔG=-7.682 kcal/mol, followed by (2) and (1) with -6.925 and -6.352,

404   respectively. For (3) the better bindings distances (lower values) ligand-residues were

405   ASP251, ASP291, PHE296 and SER246 with 1.88 to 2.84 Å, with conventional hydrogen

406   bonds; followed by carbon hydrogen bonds with LEU244 (2.54 Å), LYS272 (2.65 Å) and

407   LYS292 (2.72 Å). The weak bindings was with LYS300, pi-alkyl binding, with 3.57 Å.

408   The (2) compound also performs strong conventional hydrogen bonds with ARG91,

409   ASP20, GLN355 and GLY22 at distances from 2.05 to 3.01 Å. Also performing weak pi-

410   alkyl binding with ILE90, PRO23 and PRO356 at distances from 3.02 to 4.86 Å. Strong

411   conventional hydrogen bonds also are presents with interactions (1) compound and

412   MAPK residues with PHE329 at 2.75 Å and electrostatic pi-cation bond with LYS330 at

413   2.93 Å. Weak pi-alkyl binding were find with ALA325, ALA327 and ARG77 at distances

414   from 4.12 to 5.10 Å.

415   The interaction between the ligands and the SIR protein (Figure S2), each interest

416   compound also occupies a different site, as seen. Again, the better binding compound was

417   (3), with ΔG=-9.393 kcal/mol, followed by (2) and (1) with -8.038 and -8.608,

418   respectively. For (3) the strongest bindings were conventional hydrogen bonds with

419   GLU243, ILE48, GLN124 and HIS144 with 1.96 to 3.03 Å. The weak bindings was with

420   ILE126, ALA40, PHE74, ASP50 and HIS204 acting as pi-pi, alkyl or pi-alkyl binding,

421   with 3.20 to 5.30 Å distances. Strong conventional hydrogen bonds also are presents with

422   interactions (2) compound and SIR residues with ASN186, ASN193, HIS156 and

423   LYS184 at 1.88 to 3.30 Å distances and carbon hydrogen bond with GLU192 at 2.32 Å.

424   Weak pi-alkyl binding were find with PRO195 and ALA197 at distances from 4.59 and

425   5.36 Å. The (1) compound also performs strong conventional hydrogen bonds with

426   ASP127 and PHE100 at distances from 1.96 and 2.33 Å. Also performing weak pi-sigma

427   and pi-alkyl binding with ALA132 and PRO97 at distances from 3.51 and 4.77 Å,

428   respectively.

429   After molecular docking simulation, it was found that all ligands (1) quercetin,

430   (2) isoquercitrin and (3) rutin occupy the same catalytic site of interaction of TR (Figure

431   S3). The better bind energy, or affinity energy, was find with this target. Once again, the

432   better binding compound was (3), with ΔG= -10.216 kcal/mol, followed by (2) and (1)

433   with -7.701 and -6.969, respectively. The strongest bindings relations between (3) and

434   TR residues were conventional hydrogen bonds with ASP453, THR457, CYS444 and

435   CYS469 with 2.47 to 3.62 Å; followed by carbon hydrogen bond at SER440 with 3.63 Å

436   distance. The (2) compound also performs strong conventional hydrogen bonds with

437   CYS469 at distances from 2.31 Å; and carbon hydrogen bonds with PHE454 and THR457

438   at distances from 2.50 and 3.04 Å. Also performing average force pi binding with

439   CYS444 at distance 2.75 Å. Also, (1) ligand interacts with strong conventional hydrogen

440   bond at SIR residues with VAL460 at 2.60 Å distance and weak pi-alkyl binding with

441   ALA465 at 4.22 Å distance.

442   For the construction of the analysis by heatmap, statistical Pearson's analyzes

443   were carried out in order to be able to show the topology of the amino acids that suffered

444   interaction with each proposed ligand. As evidenced, for the MAPK and SIR targets, each

445   ligand fixed in a different protein cavity (Figure 10). As the ligands (2) and (3) are

446   modifications of the ligand (1), these data demonstrate a high degree of their interaction

447   with the entire protein surface, corroborating the results obtained *in vitro*.

448   Still in Figure 10, with respect to the data shown in C, it can be seen that the

449   behavior of the compounds has a slight modification by formation of clusters. Thus, they

450   remain in another area than that of the proposed control, but are clustered in a region.

451   Interestingly, in relation to the control sites and the ligands there is a set of preserved AA

452   residues that only become evident when the residues are compared with each other, in

453   light of Pearson's statistical similarity. This data leads us to infer that, for compounds with

454   a flavonoid structure, potentially the most important preserved binding site of AA are

455   CYS444, CYS469, PHE454 and THR457.

456   When comparing the ligands in terms of their similarity, the formation of clusters

457   of AA residues can be identified. It is important to mention that the grouped substances

458   can act competitively with the molecules of the same site (Figure 10C) and in a synergistic

459   way with molecules of different sites (Figure 10A, B).

460

461   **4   DISCUSSION**

462   Over the past few decades, limitations have emerged regarding the use of synthetic

463   drugs – high toxicity, side effects, high costs – generating great interest in the

464   ethnobotanical research [37]. In the case of leishmaniasis, the current therapy can cause

465   serious side effects such as hepatotoxicity, nephrotoxicity, cardiotoxicity [9], which

466   arouses interest in natural compounds targeting minor damage to the patient.

467   Recent studies conducted by our group as well as other researchers have shown

468   that extracts from leaves of *Caryocar* genus plants act on different microorganisms,

469   including *Leishmania amazonensis* (Alves et al., 2017; Paula-Ju et al., 2006; Tomiotto-

470   Pellissier et al., 2018). Our group also demonstrated an inhibitory effect of both the pulp

471   and peel *C. coriaceum* extracts on *Leishmania amazonensis* promastigote forms [15].

472   However, until now no information has been achieved on the possible action mechanisms

473   of these extracts on the extra and intracellular parasite.

474   The present study showed the action of *C. coriaceum.* fruit ethanol extracts

475   ranging from 25 to 100 μg/mL on *L. amazonensis* promastigotes. These results

476   corroborate with our previous work, which defined IC_{50} of 30 (±5) and 38 (±13) μg/mL

477   for pulp and peel extracts, respectively [15]. Furthermore, we demonstrated the ability of

478   the extracts to increase ROS levels, molecules with different cellular functions which in

479   excess can trigger organelles damage and consecutively cellular death [38].

480   In this sense, it was also found mitochondrial membrane damage upon lower

481   ΔΨm. Mitochondrial integrity is essential for parasite survival since trypanosomatids

482   have a single mitochondrion [38]. Considering that mitochondrial dysfunction and

483   reactive oxygen species production can lead to cell death by apoptosis [39], we

484   investigated such process by applying annexin V labeling. Similarly to the extracts

485   (Tomiotto-Pellissier et al., 2018), the effect of fruit extracts also increased both annexin

486   V and PI marking.

487   Aiming at differentiating the death type in necrotic, apoptotic, and late-apoptotic,

488   we performed a co-staining analyzed through flow cytometry. We verified that most of

489   the parasites were in the double-positive zone indicating the predominance of the late-

490   apoptotic process. This death type was previously described for *Leishmania* parasites

491   treated with different compounds [16,17]. The morphological changes found in the

492   parasite reinforce such results, since bleb formation, cell length reduction, and cellular

493   shrinkage are typical signs of apoptotic death [39].

494   We used the next experimental set to elucidate whether the fruit extracts would be

495   able to act on intracellular amastigote forms, which is more resistant and represent a

496   challenging target since the compound needs to diffuse through the host cell structures to

497 act on the parasite [40]. Firstly, it was found that the pulp and peel of *C. coriaceum.*

498 extracts were not toxic to the macrophages, the major host cell for *Leishmania* parasites.

499 Previous results showed a selectivity index for the parasite (macrophage/ promastigote

500 forms) of approximately 9 and 12 for pulp and peel, respectively [15]. Subsequently, it

501 was demonstrated the ability of the extracts to improve the elimination of intracellular

502 amastigotes, similarly to those found in *C. coriaceum.* leaf extracts (Tomiotto-Pellissier

503 et al., 2018). Finally, it was investigated the mechanisms involved in such elimination as

504 follows below.

505 The main effector of molecules in the intracellular pathogen elimination is known

506 to be reactive nitrogen species (RNS) and reactive oxygen species (ROS). In contrast,

507 RNS and ROS are also responsible for tissue damage in leishmaniasis [2]. Given the

508 importance of these molecules to the infection course, it was investigated their effects in

509 the studied model and the levels of ROS and RNS were lower upon treatment.

510 This corroborates the previous results regarding the antioxidant effect of the *C.*

511 *coriaceum.* fruit extracts using 2,2-diphenyl-1-picrylhydrazyl (DPPH) methodology [15].

512 Additionally, antioxidant capacity is intrinsically related to the presence of phenols and

513 flavonoids, such as isoquercitrin, quercetin, and rutin, present in the extracts studied,

514 contributing to radical scavenging potential [41].

515 We investigated the iron metabolism after discarding the hypothesis of oxidative

516 stress is responsible for eliminating the parasite. *Leishmania* parasites use the host's labile

517 iron pool and depend on this metal uptake for its replication and survival [3,4]. Thus, the

518 higher iron-bound caused by *C. coriaceum.* fruit extracts treatment made iron unavailable

519 to the parasite and decreased macrophage infection rate.

520 Aiming at corroborating such hypothesis, it was verified the cascade involving

521 Nrf2/HO-1/ferritin complexes for being directly related to both the antioxidant capacity

522 and iron metabolism [42]. While on the one hand, Nrf2 activation may be a weapon of *L.*

523 *amazonensis* to block oxidative stress and persist in the host [43], on the other hand, it

524 can induce transcription of downstream genes, such as HO-1, acting on iron metabolism

525 by inducing ferritin expression. Finally, ferritin plays an important role in free iron

526 capture reducing its availability to intracellular parasites [42,44]. Still, overall antioxidant

527 balance can be a powerful ally to protect against tissue injury caused by leishmaniasis

528 [45].

529 Methanolic and ethanolic extracts of *C. coriaceum.* leaves up-regulate Nrf2

530 transcription, HO-1, and ferritin genes, however, when assessing oxidative mediators,

531 fruit and peel extracts appeared to be more effective as they reduced MDA and ROS

532 levels more effectively, as well as generating lower NO formation, whereas leaf extracts

533 did not influence this mediator production (Tomiotto-Pellissier et al., 2018).

534 Notably, similar results were found with compounds trans-chalcone (intermediate

535 in the synthesis of flavonoids) [7] and quercetin [8]. Both had a direct effect on

536 promastigote forms of *L. amazonensis* inducing an apoptosis-like death pattern and action

537 on intracellular amastigote forms by inducing NRF2 and iron unavailability to parasite

538 metabolism. Therefore, these effects can be due at least partially, to the presence of rutin,

539 isoquercitrin, and quercetin present in *C. coriaceum* extracts.

540 All three flavonoids presented in the *C. coriaceum* extracts can act as synergistic

541 inhibitors of MAPK and SIR proteins, and these compounds also tend to compete for the

542 active TR site. MAPK proteins in host cells are related to an induction of pro-

543 inflammatory response [46], while in *Leishmania*, they are involved in the regulation of

544 flagella length, playing an important role in disease transmission [47]. Both of these

545 features were found in the *in vitro* experiments, reinforcing the importance of the

546 flavonoids of *C. coriaceum* extracts in acting on these proteins.

547   The proteins belonging to the SIR family have been implicated in the regulation

548   of a number of biological processes, such as gene silencing, DNA repair, cell cycle,

549   metabolism, and apoptosis. In *Leishmania* parasites, SIR has emerged as a promising drug

550   target, due to its participation in the parasite survival, proliferation, drug resistence and

551   infectivity [23,48–50].

552   TR is considered to be one of the best targets to find new anti-Leishmanial drugs.

553   This enzyme is the main detoxifying system against oxidative damage found in

554   trypanosomatids and thus is important for parasite's infectivity and survival, but absent

555   in the human host [24,51]. In our study, it was found a competitive interaction of

556   flavonoids for the active TR site, with a preference for rutin due to its greater interaction

557   binding strength. The results found in the *in silico* analysis corroborate the results found

558   in the *in vitro* experiments, as well as the metabolic pathway for the elimination of the

559   pathogen proposed.

560   Together, our data demonstrate for the first time that pulp and peel extracts from

561   the *C. coriaceum* fruit can induce death of *L. amazonensis* promastigotes through

562   apoptosis-like mechanisms and act on intracellular amastigote forms by activating the

563   Nrf2/HO-1/ferritin pathway, consecutively reducing iron availability for parasite

564   survival,. Furthermore, both treatments induced an antioxidant response, which is

565   important to protect against the tissue damage caused by leishmaniasis. The *in silico*

566   evaluations corroborate the data found *in vitro*, showing a predictive action of the

567   flavonoids present in the extract on essential *Leishmania* proteins.

568

571

6   CONFLICT OF INTERESTS

573   The authors declared that there is no conflict of interest.

574

7   FUNDING

578

8   AUTHOR CONTRIBUITION

580   FTP - study design, carrying out experiments on *Leishmania* parasites, data

581   analysis and scientific writing. DRA, SMM, ESM and MMM - collecting and identifying

582   plants, performing extractions, characterization of extracts and *in silico* evaluations.

583   BTSB and MDG - microscopy experiments and antioxidant tests. TFS - data analysis and

584   scientific writing. ERT and LMY - conducting, interpreting and analyzing molecular

585   biology experiments. INC and ICC - critical data analysis and review of scientific writing.

586   MMMS and WRP - experimental design, critical data analysis and review of scientific

587   writing.

9   REFERENCES

1.   WHO World Health Organization - Leishmaniasis. *WHO* 2018.

2.   Rossi, M.; Fasel, N. How to master the host immune system? Leishmania parasites have the solutions! *Int. Immunol.* **2018**, *30*, 103–111.

3.   Zaidi, A.; Singh, K.P.; Ali, V. Leishmania and its quest for iron: An update and overview. *Mol. Biochem. Parasitol.* **2017**, *211*, 15–25.

4.   Das, N.K.; Biswas, S.; Solanki, S.; Mukhopadhyay, C.K. *Leishmania donovani* depletes labile iron pool to exploit iron uptake capacity of macrophage for its intracellular growth. *Cell. Microbiol.* **2009**, *11*, 83–94.

5.   Kerins, M.J.; Ooi, A. The Roles of NRF2 in Modulating Cellular Iron Homeostasis. *Antioxid. Redox Signal.* **2018**, *29*, 1756–1773.

6.   Tomiotto-Pellissier, F.; Alves, D.R.; Miranda-Sapla, M.M.; de Morais, S.M.; Assolini, J.P.; da Silva Bortoleti, B.T.; Gonçalves, M.D.; Cataneo, A.H.D.; Kian, D.; Madeira, T.B.; et al. Caryocar coriaceum extracts exert leishmanicidal effect acting in promastigote forms by apoptosis-like mechanism and intracellular amastigotes by Nrf2/HO-1/ferritin dependent response and iron depletion: Leishmanicidal effect of Caryocar coriaceum leaf ex. *Biomed. Pharmacother.* **2018**, *98*, 662–672.

7.   Miranda-Sapla, M.M.; Tomiotto-Pellissier, F.; Assolini, J.P.; Carloto, A.C.M.; Bortoleti, B.T. da S.; Gonçalves, M.D.; Tavares, E.R.; Rodrigues, J.H. da S.; Simão, A.N.C.; Yamauchi, L.M.; et al. trans-Chalcone modulates Leishmania amazonensis infection in vitro by Nrf2 overexpression affecting iron availability. *Eur. J. Pharmacol.* **2019**, *853*, 275–288.

8.   Cataneo, A.H.D.; Tomiotto-Pellissier, F.; Miranda-Sapla, M.M.; Assolini, J.P.; Panis, C.; Kian, D.; Yamauchi, L.M.; Colado Simão, A.N.; Casagrande, R.; Pinge-

613   Filho, P.; et al. Quercetin promotes antipromastigote effect by increasing the ROS

614   production and anti-amastigote by upregulating Nrf2/HO-1 expression, affecting

615   iron availability. *Biomed. Pharmacother.* **2019**, *113*, 108745.

616 9. Alvar, J.; Croft, S.; Olliaro, P. Chemotherapy in the Treatment and Control of

617   Leishmaniasis. In *Advances in parasitology*; 2006; Vol. 61, pp. 223–274.

618 10. Baptista, A.; Gonçalves, R.V.; Bressan, J.; Pelúzio, M. do C.G. Antioxidant and

619   Antimicrobial Activities of Crude Extracts and Fractions of Cashew (Anacardium

620   occidentale L.), Cajui (Anacardium microcarpum), and Pequi (Caryocar

621   brasiliense C.): A Systematic Review. *Oxid. Med. Cell. Longev.* **2018**, *2018*, 1–13.

622 11. Colombo, N.B.R.; Rangel, M.P.; Martins, V.; Hage, M.; Gelain, D.P.; Barbeiro,

623   D.F.; Grisolia, C.K.; Parra, E.R.; Capelozzi, V.L. Caryocar brasiliense camb

624   protects against genomic and oxidative damage in urethane-induced lung

625   carcinogenesis. *Brazilian J. Med. Biol. Res.* **2015**, *48*, 852–862.

626 12. de Figueiredo, P.R.L.; Oliveira, I.B.; Neto, J.B.S.; de Oliveira, J.A.; Ribeiro, L.B.;

627   de Barros Viana, G.S.; Rocha, T.M.; Leal, L.K.A.M.; Kerntopf, M.R.; Felipe,

628   C.F.B.; et al. Caryocar coriaceum Wittm. (Pequi) fixed oil presents hypolipemic

629   and anti-inflammatory effects in vivo and in vitro. *J. Ethnopharmacol.* **2016**, *191*,

630   87–94.

631 13. Palmeira, S.M.; Silva, P.R.P.; Ferrão, J.S.P.; Ladd, A.A.B.L.; Dagli, M.L.Z.;

632   Grisolia, C.K.; Hernandez-Blazquez, F.J. Chemopreventive effects of pequi oil

633   (Caryocar brasiliense Camb.) on preneoplastic lesions in a mouse model of

634   hepatocarcinogenesis. *Eur. J. Cancer Prev.* **2016**, *25*, 299–305.

635 14. Paula-Ju, W. de; Rocha, F.H.; Donatti, L.; Fadel-Picheth, C.M.T.; Weffort-Santos,

636   A.M. Leishmanicidal, antibacterial, and antioxidant activities of Caryocar

637   brasiliense Cambess leaves hydroethanolic extract. *Rev. Bras. Farmacogn.* **2006**,

638   *16*, 625–630.

639   15.   Alves, D.R.; Maia de Morais, S.; Tomiotto-Pellissier, F.; Miranda-Sapla, M.M.;

640   Vasconcelos, F.R.; Silva, I.N.G. da; Araujo de Sousa, H.; Assolini, J.P.; Conchon-

641   Costa, I.; Pavanelli, W.R.; et al. Flavonoid Composition and Biological Activities

642   of Ethanol Extracts of *Caryocar coriaceum* Wittm., a Native Plant from Caatinga

643   Biome. *Evidence-Based Complement. Altern. Med.* **2017**, *2017*, 1–7.

644   16.   Bortoleti, B.T. da S.; Gonçalves, M.D.; Tomiotto-Pellissier, F.; Miranda-Sapla,

645   M.M.; Assolini, J.P.; Carloto, A.C.M.; de Carvalho, P.G.C.; Cardoso, I.L.A.;

646   Simão, A.N.C.; Arakawa, N.S.; et al. Grandiflorenic acid promotes death of

647   promastigotes via apoptosis-like mechanism and affects amastigotes by increasing

648   total iron bound capacity. *Phytomedicine* **2018**, *46*, 11–20.

649   17.   Doroodgar, M.; Delavari, M.; Doroodgar, M.; Abbasi, A.; Taherian, A.A.;

650   Doroodgar, A. Tamoxifen Induces Apoptosis of Leishmania major Promastigotes

651   in Vitro. *Korean J. Parasitol.* **2016**, *54*, 9–14.

652   18.   Mosmann, T. Rapid colorimetric assay for cellular growth and survival:

653   Application to proliferation and cytotoxicity assays. *J. Immunol. Methods* **1983**,

654   *65*, 55–63.

655   19.   Stewart, J.J.P. Optimization of parameters for semiempirical methods VI: More

656   modifications to the NDDO approximations and re-optimization of parameters. *J.*

657   *Mol. Model.* **2013**, *19*, 1–32.

658   20.   Marinho, M.M.; Castro, R.R.; Marinho, E.S. Utilização do método semi-empírico

659   PM7 para caracterização do fármaco atalureno: HOMO, LUMO, MESP. *Rev.*

660   *Expressão Católica Saúde* **2016**, *1*, 177–184.

661   21.   Almeida-Neto, F.W.Q.; da Silva, L.P.; Ferreira, M.K.A.; Mendes, F.R.S.; de

662   Castro, K.K.A.; Bandeira, P.N.; de Menezes, J.E.S.A.; dos Santos, H.S.; Monteiro,

663   N.K.V.; Marinho, E.S.; et al. Characterization of the structural, spectroscopic,

664   nonlinear optical, electronic properties and antioxidant activity of the N-{4'-[(E)-

665   3-(Fluorophenyl)-1-(phenyl)-prop-2-en-1-one]}-acetamide. *J. Mol. Struct.* **2020**,

666   *1220*, 128765.

667   22. Garai, A.; Zeke, A.; Gogl, G.; Toro, I.; Fordos, F.; Blankenburg, H.; Barkai, T.;

668   Varga, J.; Alexa, A.; Emig, D.; et al. Specificity of Linear Motifs That Bind to a

669   Common Mitogen-Activated Protein Kinase Docking Groove. *Sci. Signal.* **2012**,

670   *5*, ra74–ra74.

671   23. Ronin, C.; Costa, D.M.; Tavares, J.; Faria, J.; Ciesielski, F.; Ciapetti, P.; Smith,

672   T.K.; MacDougall, J.; Cordeiro-da-Silva, A.; Pemberton, I.K. The crystal structure

673   of the Leishmania infantum Silent Information Regulator 2 related protein 1:

674   Implications to protein function and drug design. *PLoS One* **2018**, *13*, e0193602.

675   24. Baiocco, P.; Colotti, G.; Franceschini, S.; Ilari, A. Molecular Basis of Antimony

676   Treatment in Leishmaniasis. *J. Med. Chem.* **2009**, *52*, 2603–2612.

677   25. Pettersen, E.F.; Goddard, T.D.; Huang, C.C.; Couch, G.S.; Greenblatt, D.M.;

678   Meng, E.C.; Ferrin, T.E. UCSF Chimera - A visualization system for exploratory

679   research and analysis. *J. Comput. Chem.* **2004**, *25*, 1605–1612.

680   26. Melo Lucio, F.N.; Da Silva, J.E.; Marinho, E.M.; Da Silva Mendes, F.R.; Marinho,

681   M.M.; Marinho, E.S. methylcytisine alcaloid potentially active against dengue

682   virus: a molecular docking study and electronic structural characterization. *Int. J.*

683   *Res. -GRANTHAALAYAH* **2020**, *8*, 221–236.

684   27. Jin, Z.; Du, X.; Xu, Y.; Deng, Y.; Liu, M.; Zhao, Y.; Zhang, B.; Li, X.; Zhang, L.;

685   Peng, C.; et al. Structure of Mpro from SARS-CoV-2 and discovery of its

686   inhibitors. *Nature* **2020**, *582*, 289–293.

687   28. Grosdidier, A.; Zoete, V.; Michielin, O. SwissDock, a protein-small molecule

688   docking web service based on EADock DSS. *Nucleic Acids Res* **2011**, *39*, 270–

689   277.

690 29. Grosdidier, A.; Zoete, V.; Michielin, O. Fast docking using the CHARMM force

691   field with EADock DSS. *J. Comput. Chem.* **2011**, *32*, 2149–2159.

692 30. Pandey, R.K.; Kumbhar, B.V.; Sundar, S.; Kunwar, A.; Prajapati, V.K. Structure-

693   based virtual screening, molecular docking, ADMET and molecular simulations to

694   develop benzoxaborole analogs as potential inhibitor against Leishmania donovani

695   trypanothione reductase. *J. Recept. Signal Transduct.* **2017**, *37*, 60–70.

696 31. Shokri, A.; Abastabar, M.; Keighobadi, M.; Emami, S.; Fakhar, M.; Teshnizi, S.H.;

697   Makimura, K.; Rezaei-Matehkolaei, A.; Mirzaei, H. Promising antileishmanial

698   activity of novel imidazole antifungal drug luliconazole against Leishmania major:

699   In vitro and in silico studies. *J. Glob. Antimicrob. Resist.* **2018**, *14*, 260–265.

700 32. Nieto-Meneses, R.; Castillo, R.; Hernández-Campos, A.; Maldonado-Rangel, A.;

701   Matius-Ruiz, J.B.; Trejo-Soto, P.J.; Nogueda-Torres, B.; Dea-Ayuela, M.A.;

702   Bolás-Fernández, F.; Méndez-Cuesta, C.; et al. In vitro activity of new N-benzyl-

703   1H-benzimidazol-2-amine derivatives against cutaneous, mucocutaneous and

704   visceral Leishmania species. *Exp. Parasitol.* **2018**, *184*, 82–89.

705 33. Csizmadia, P. MarvinSketch and MarvinView: Molecule Applets for the World

706   Wide Web.; 2019; p. 1775.

707 34. Atkins, P.; Jones, L.; Laverman, L. *Princípios de Química: Questionando a Vida*

708   *Moderna e o Meio Ambiente*; 7th ed.; Bookman Editora: São Paulo, 2018;

709 35. Nelson, D.L.; Cox, M.M. *Princípios de Bioquímica de Lehninger*; 7th ed.; Artmed:

710   Porto Alegre, 2018;

711 36. Biovia, D.S.; Berman, H.M.; Westbrook, J.; Feng, Z.; Gilliland, G.; Bhat, T.N.;

712   Richmond, T.J. Dassault Systèmes BIOVIA, Discovery Studio Visualizer. *J.*

713   *Chem. Phys.* **2000**, *17*.

714   37.   Odonne, G.; Houël, E.; Bourdy, G.; Stien, D. Treating leishmaniasis in Amazonia:

715   A review of ethnomedicinal concepts and pharmaco-chemical analysis of

716   traditional treatments to inspire modern phytotherapies. *J. Ethnopharmacol.* **2017**,

717   *199*, 211–230.

718   38.   Fidalgo, L.M.; Gille, L. Mitochondria and trypanosomatids: Targets and drugs.

719   *Pharm. Res.* **2011**, *28*, 2758–2770.

720   39.   Jiménez-Ruiz, A.; Alzate, J.; MacLeod, E.; Lüder, C.G.; Fasel, N.; Hurd, H.

721   Apoptotic markers in protozoan parasites. *Parasit. Vectors* **2010**, *3*, 104.

722   40.   Kima, P.E. The amastigote forms of Leishmania are experts at exploiting host cell

723   processes to establish infection and persist. *Int. J. Parasitol.* **2007**, *37*, 1087–96.

724   41.   Kaurinovic, B.; Vastag, D. Flavonoids and Phenolic Acids as Potential Natural

725   Antioxidants. In *Antioxidants* ; IntechOpen, 2019.

726   42.   Loboda, A.; Damulewicz, M.; Pyza, E.; Jozkowicz, A.; Dulak, J. Role of Nrf2/HO-

727   1 system in development, oxidative stress response and diseases: an evolutionarily

728   conserved mechanism. *Cell. Mol. Life Sci.* **2016**, *73*, 3221–47.

729   43.   Vivarini, Á. de C.; Calegari-Silva, T.C.; Saliba, A.M.; Boaventura, V.S.; França-

730   Costa, J.; Khouri, R.; Dierckx, T.; Dias-Teixeira, K.L.; Fasel, N.; Barral, A.M.P.;

731   et al. Systems Approach Reveals Nuclear Factor Erythroid 2-Related Factor

732   2/Protein Kinase R Crosstalk in Human Cutaneous Leishmaniasis. *Front.*

733   *Immunol.* **2017**, *8*, 1127.

734   44.   Kasai, S.; Mimura, J.; Ozaki, T.; Itoh, K. Emerging Regulatory Role of Nrf2 in

735   Iron, Heme, and Hemoglobin Metabolism in Physiology and Disease. *Front. Vet.*

736   *Sci.* **2018**, *5*, 242.

737   45.   Ozbilge, H.; Aksoy, N.; Kilic, E.; Saraymen, R.; Yazar, S.; Vural, H. Evaluation

738 of Oxidative Stress in Cutaneous Leishmaniasis. *J. Dermatol.* **2005**, *32*, 7–11.

739 46. Soares-Silva, M.; Diniz, F.F.; Gomes, G.N.; Bahia, D. The Mitogen-Activated

740 Protein Kinase (MAPK) Pathway: Role in Immune Evasion by Trypanosomatids.

741 *Front. Microbiol.* **2016**, *7*, 183.

742 47. Raj, S.; Saha, G.; Sasidharan, S.; Dubey, V.K.; Saudagar, P. Biochemical

743 characterization and chemical validation of Leishmania MAP Kinase-3 as a

744 potential drug target. *Sci. Rep.* **2019**, *9*, 1–11.

745 48. Mittal, N.; Muthuswami, R.; Madhubala, R. The mitochondrial SIR2 related

746 protein 2 (SIR2RP2) impacts Leishmania donovani growth and infectivity. *PLoS*

747 *Negl. Trop. Dis.* **2017**, *11*, e0005590.

748 49. Vergnes, B.; Sereno, D.; Tavares, J.; Cordeiro-Da-Silva, A.; Vanhille, L.;

749 Madjidian-Sereno, N.; Depoix, D.; Monte-Alegre, A.; Ouaissi, A. Targeted

750 disruption of cytosolic SIR2 deacetylase discloses its essential role in Leishmania

751 survival and proliferation. *Gene* **2005**, *363*, 85–96.

752 50. Purkait, B.; Singh, R.; Wasnik, K.; Das, S.; Kumar, A.; Paine, M.; Dikhit, M.;

753 Singh, D.; Sardar, A.H.; Ghosh, A.K.; et al. Up-regulation of silent information

754 regulator 2 (Sir2) is associated with amphotericin B resistance in clinical isolates

755 of Leishmania donovani. *J. Antimicrob. Chemother.* **2014**, *70*, 1343–1356.

756 51. Turcano, L.; Torrente, E.; Missineo, A.; Andreini, M.; Gramiccia, M.; Di Muccio,

757 T.; Genovese, I.; Fiorillo, A.; Harper, S.; Bresciani, A.; et al. Identification and

758 binding mode of a novel Leishmania Trypanothione reductase inhibitor from high

759 throughput screening. *PLoS Negl. Trop. Dis.* **2018**, *12*, e0006969.

760

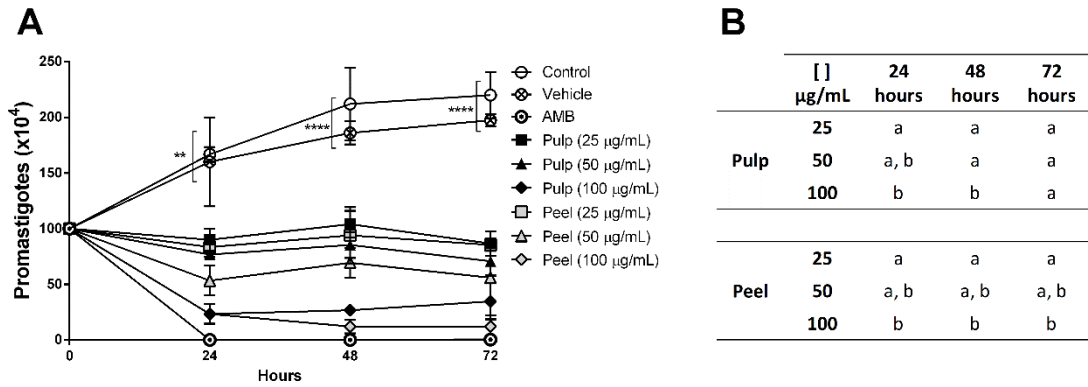761

762

763   **FIGURE LIST**
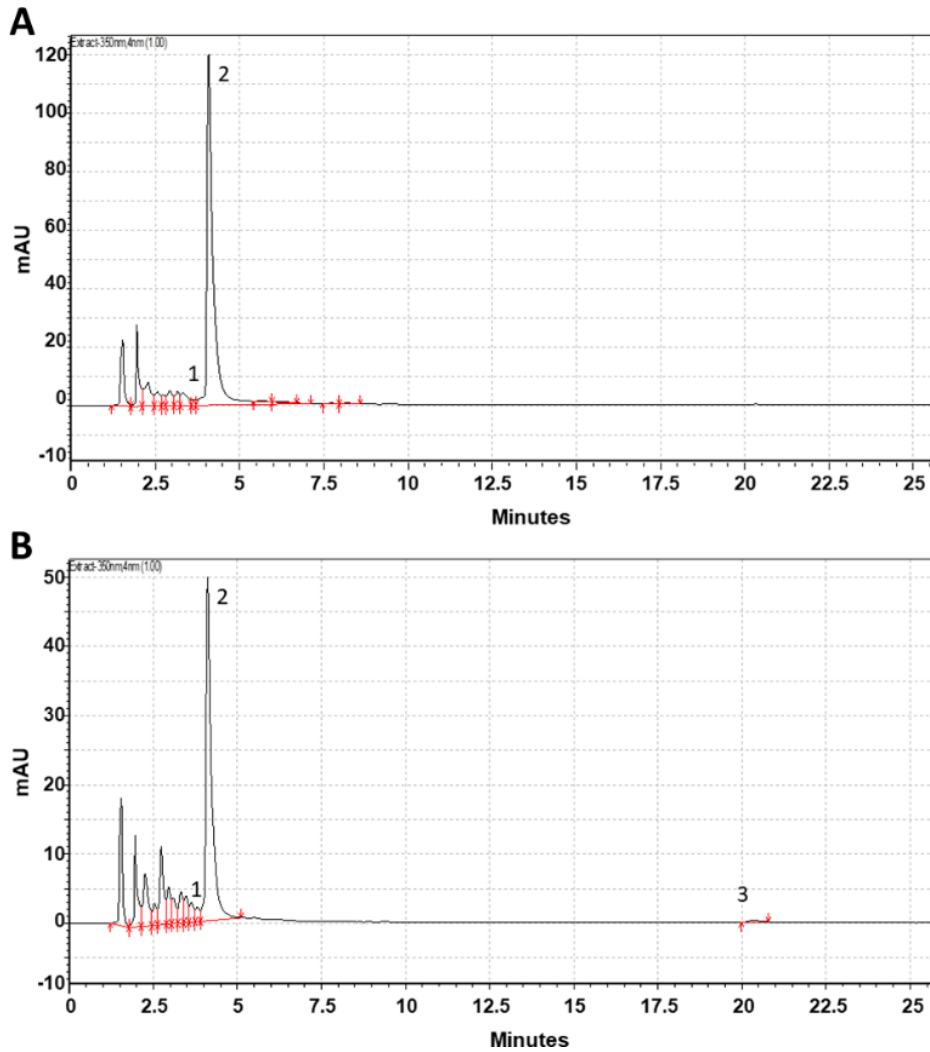
764

765   **Fig. 1 Characterization of *C. coriaceum* Wittm. fruit extracts.** The (A) pulp and (B)

766   peel extracts were analised by HPLC with Shimadzu analytical CLC-ODS M (C-18) of

767   25 cm column. The calibration curve was constructed using the standards rutin (1),

768   isoquercitrin (2) and quercetin (3) at 0.25; 0.05; 0.025 or 0.005mg/mL. The flow rate was

769   1.8 mL per minute for quercetin and 1.25 ml per minute to rutin both in a wavelength of

770   350 nm and a mobile phase of 20% acetonitrile and 80% solution of H3PO4 pH buffer

771   2.8.

772

773

A

B

	[ ] µg/mL	24 hours	48 hours	72 hours
	25	a	a	a
Pulp	50	a, b	a	a
	100	b	b	a
	25	a	a	a
Peel	50	a, b	a, b	a, b
	100	b	b	b

774

775 **Fig. 2 Antipromastigote effect of *C. coriaceum* Wittm. fuit extracts.** *L. amazonensis*

776 promastigotes forms were subjected to *Caryocar coriaceum* Wittm. pulp or peel extracts

777 treatment (25–100 µg/mL). (A) The parasite viability was assessed at 0, 24 and 48h. As

778 control was used non-treated parasites, as vehicle control was used DMSO 0.02% and as
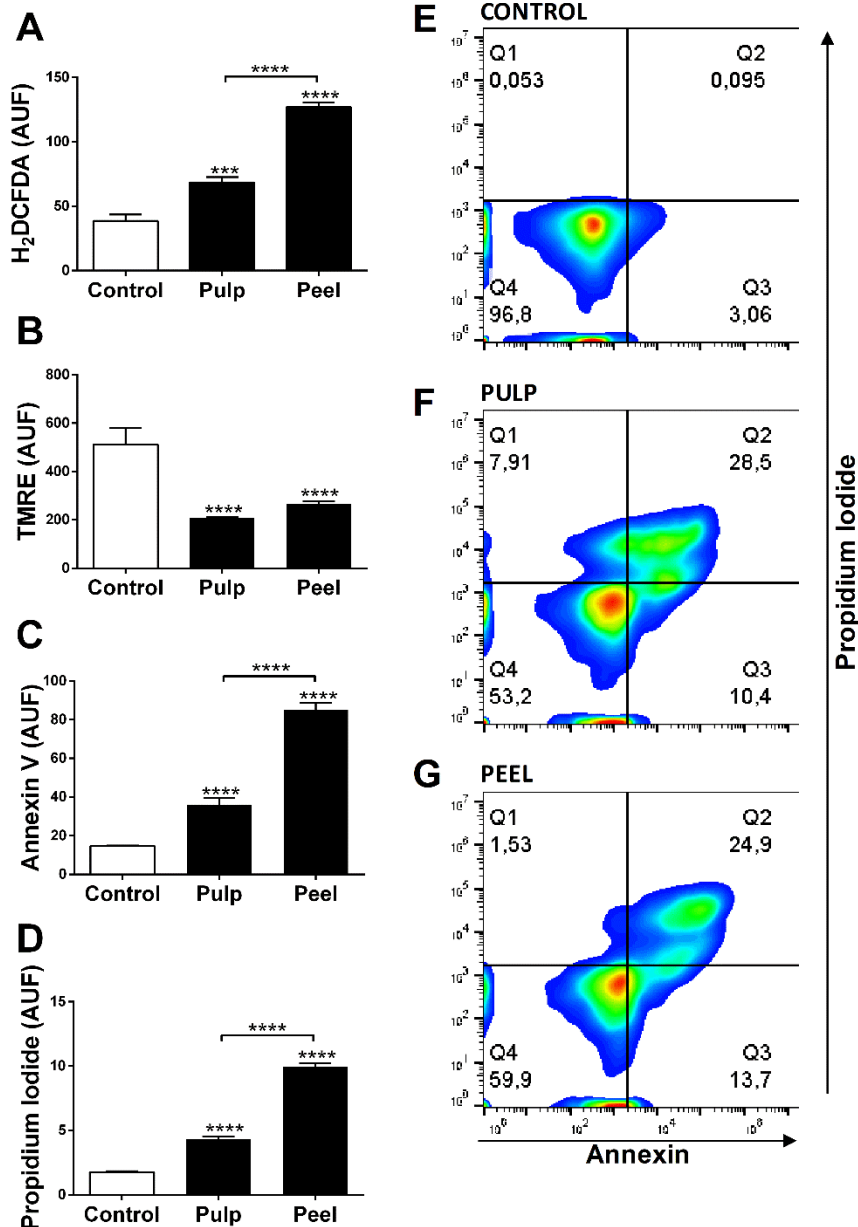
779 a positive control was used amphotericin B (AMB) 1 µM. (B) Detailed statistical analysis

780 between the treatments. Groups that not share the same letter are significantly different.

781 The values represent the mean ± SEM of three independent experiments performed in

782 duplicate. ** Significant difference compared to the control group (p≤0.01),

783 ****(p≤0.001).

Fig 3 *C. coriaceum* Wittm. extracts induce late apoptotic-like death process in *L. amazonensis* promastigote forms. (A) H₂DCFDA probe was used for reactive species of oxygen measurement, (B) TMRE assay for fluorometric analysis of the mitochondrial membrane potential, (C) Annexin V labeling for phosphatidylserine exposition evaluation, and (D) propidium iodide staining for the analyses of plasma membrane integrity. Data represent the mean ± SEM of three independent experiments performed in duplicate. *** Significant difference in relation to control (p ≤ 0.01), **** (p ≤ 0.01). Co-

791   staining of Annexin V and PI of untreated (E), pulp-treated (F) and peel-treated (G)

792   parasites. Typical pseudocolor plots of at least three independent experiments are shown.
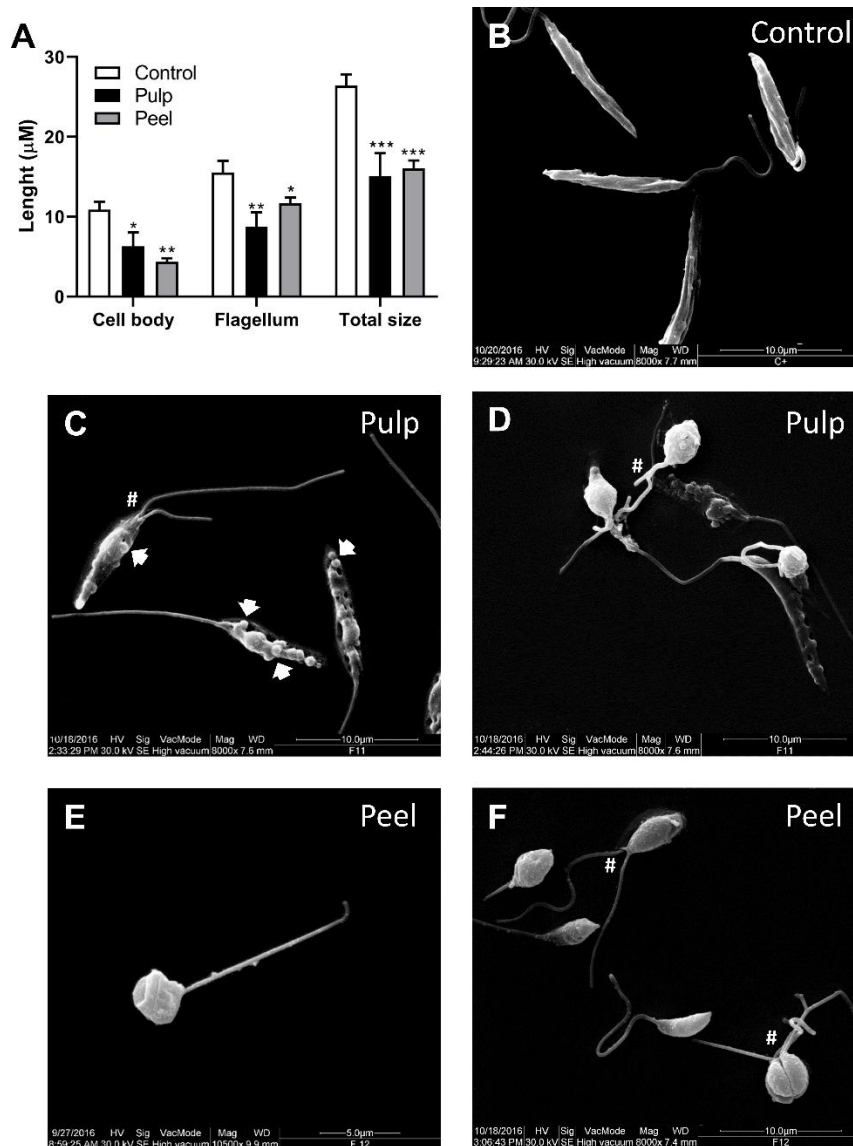
794   **Fig 4 Morphological changes of treated *L. amazonensis* promastigote forms.** (A) Cell

795   body, flagellum and total promastigote lengths were measured thought scanning electron

796   microscopy images by Image-Pro Plus software. At least three images of each condition

797   were subjected to measurement. The values represent the mean ± SEM of at least three

798   independent measurements. *Significant difference compared to the control (p≤0.05),

799   **(p≤0.01), ***(p≤0.001). (B) Scanning electron microscopy image of *L. amazonensis*

800   promastigote forms without treatment (control), and promastigotes treated for 24h at 25°C

801   with pulp (C and D) or peel (E and F) extract (50µg/mL) (B). Arrows indicate the blebbing

802   (apoptotic bodies) formation on parasite membrane. # indicate the double flagella

803   formation.
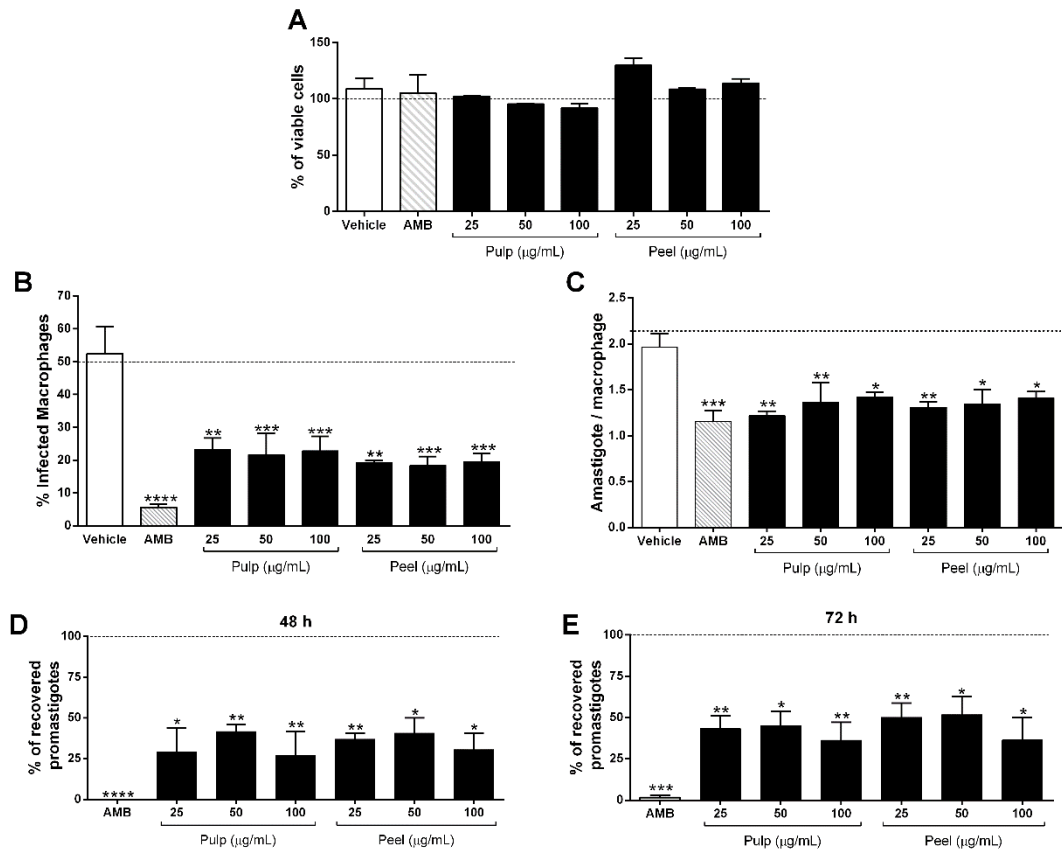
804

805   **Fig 5 Cytotoxic and antiamastigote effect of pulp and peel *C. coriaceum* Wittm.**

806   **extracts.** (A) Peritoneal BALB/c macrophages were submitted to a 24 h-treatment using

807   25, 50 and 100 µg/mL of pulp and peel extracts and viability analyzed through MTT

808   assay. (B) *L. amazonensis*-infected macrophages submitted to 25, 50 and 100 µg/mL of

809   pulp and peel extracts or DMSO 0.02% (vehicle) were assessed as the percentage of

810   infected macrophages and (C) amount of amastigotes per macrophage. Culture medium

811   and AMB (1 µM) were used as negative and positive controls. (D) 48h and (E) 72h

812   incubation of the *L. amazonensis*-infected macrophages using medium 199. The number

813   of recovered parasites was measured in Neubauer chamber. The dashed lines indicates

814   the infected control group without treatment (100%). The values represent the mean ±

815   SEM of three independent experiments performed in duplicate. *Significant difference

816   compared to the control (p≤0.05),**(p≤0.01), ***(p≤0.001).

817
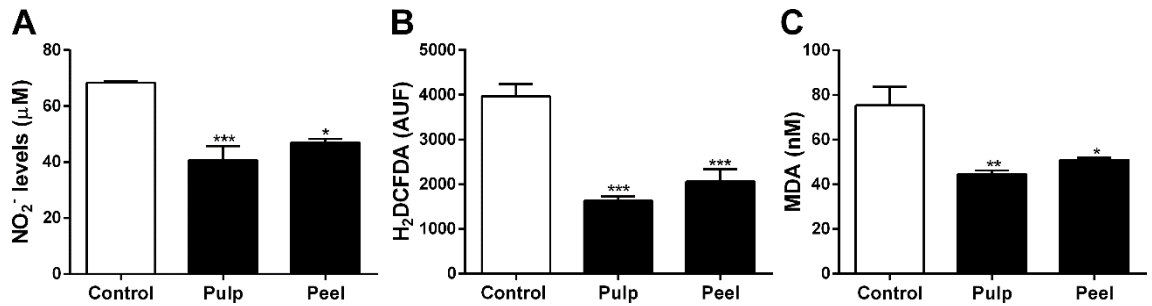
819 **Fig 6 *Caryocar coriaceum* Wittm. extracts reduces the NO, ROS and MDA levels.** *L.*

820 *amazonensis*-infected macrophages after 24h treatment with *C. coriaceum* Wittm. pulp

821 and peel extracts at 25μg/mL were submitted to (A) nitrite measurement by Griess

822 method; (B) reactive oxygen species (ROS) measurement by fluorescent probe

823 H_2DCFDA; (C) malondialdehyde (MDA) measurement through HPLC. The values

824 represent the mean ± SEM of three independent experiments performed in duplicate.

825 Control represents infected non-treated cells. *Significant difference compared to control

826 (p≤0.05), ** (p≤0.01), *** (p≤0.001).

827

828
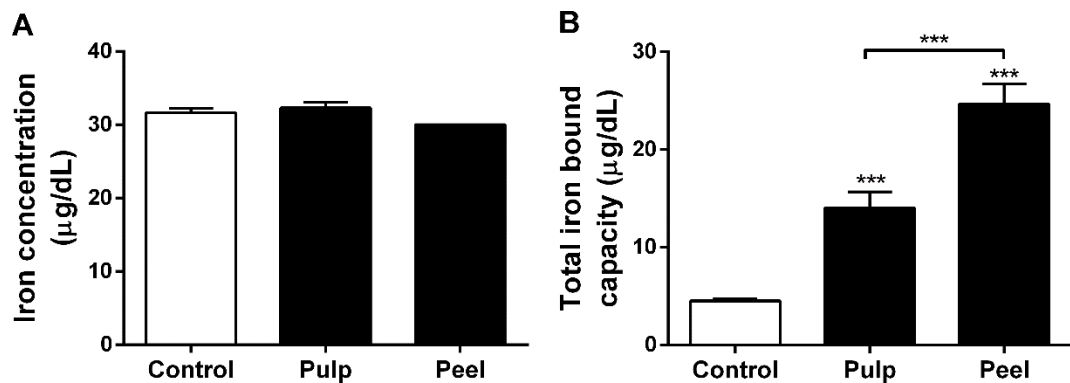
830 **Fig 7 *Caryocar coriaceum* Wittm. extracts treatment enhancing the total bound iron**

831 **capacity in *L. amazonensis*-infected macrophages.** The culture recovery supernatants

832 were used to determinate the (A) labile iron concentration and (B) total iron bound

833 capacity utilizing the Dimension® automated system. Data represent the mean ± SEM of

834 three independent experiments. *** Significant difference compared to control (p≤0.001).

835
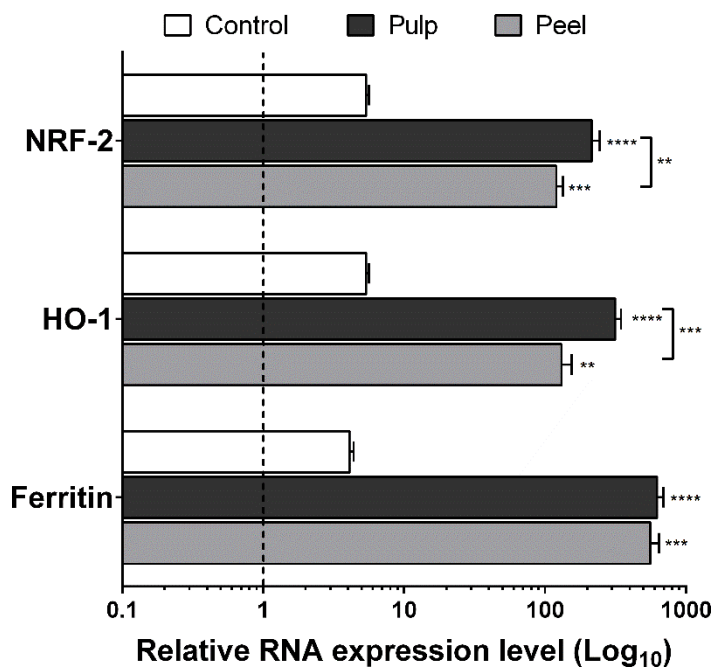
836

837

838 **Fig 8 *Caryocar coriaceum* Wittm. extracts treatment upregulates Nrf2, heme**

839 **oxigenase-1, and ferritin RNAm expression.** Real-time RT-PCR quantitative mRNA

840 analyses were performed to quantify the expression of Nrf2, HO-1, and ferritin in

841 peritoneal macrophages infected with *L. amazonensis* and treated 25μg/mL of pulp and

842 peel extracts. The dashed line represents the uninfected control. Data represent the mean

843 ± SEM of three independent experiments. **Significant difference compared to the

844 control (p≤0.01), ***(p≤0.001),**** (p≤0.0001).

845

846

41
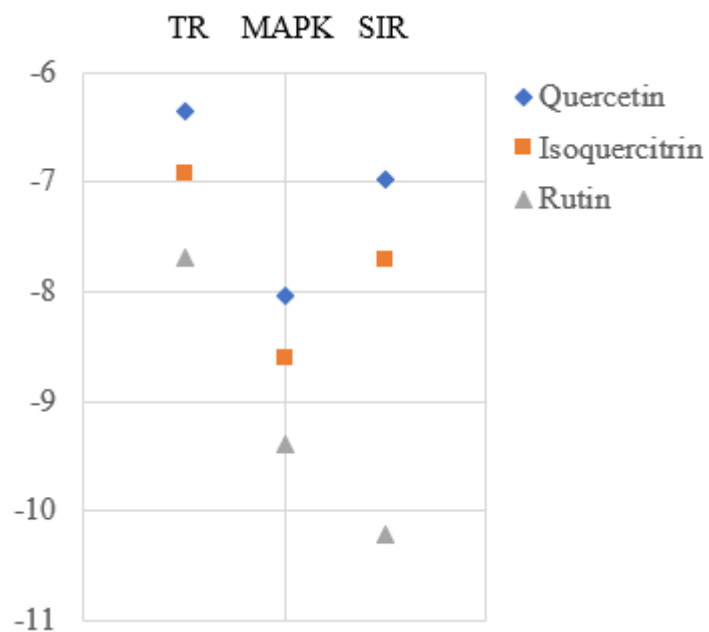
Fig 9 Energy binding (kcal/mol) of (1) quercetin (◆, blue diamond), (2) isoquercitrin (■, orange square) and (3) rutin (▲, grey triangle) with MAPK (PDB: 2Y9Q), SIR (PDB: 5OL0) and TR (PDB: 2JK6) biological targets of *Leishmania* sp.
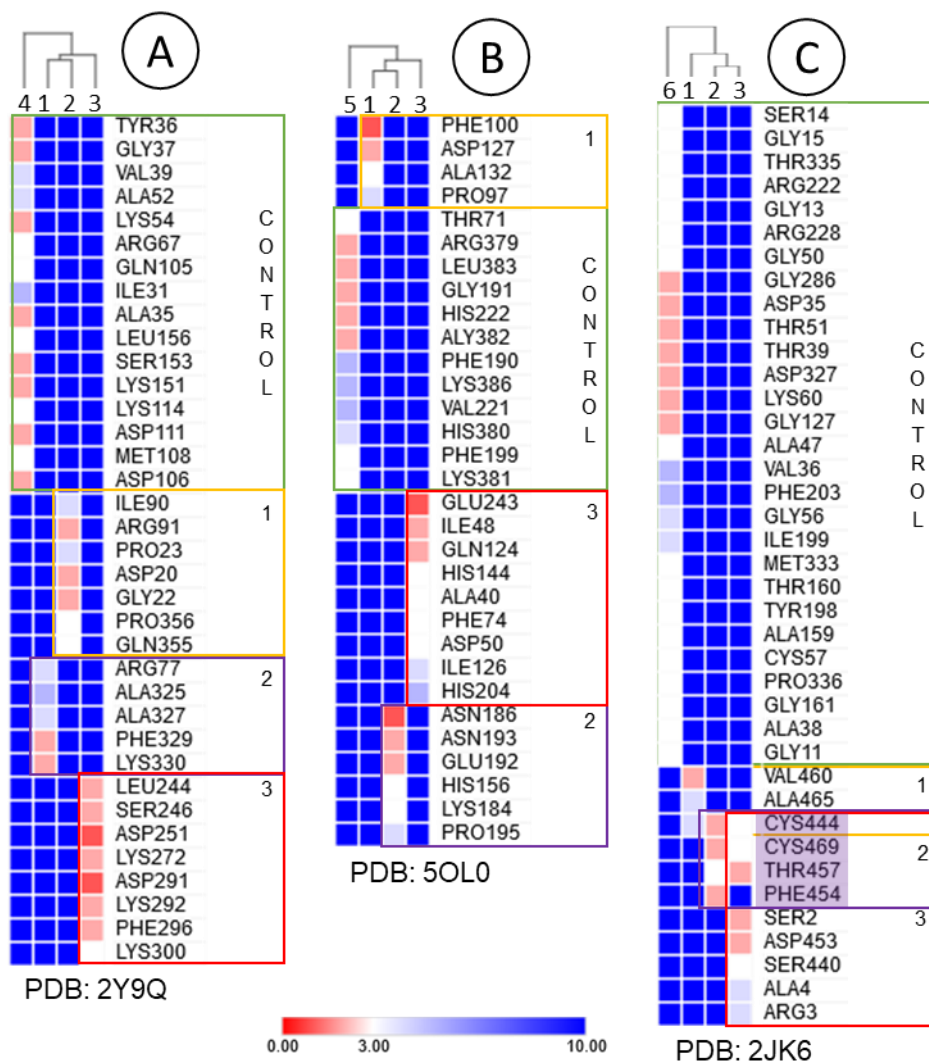
Fig 10 Heatmap panel illustrating statistically regarding interactions of minimum binding energy of test ligands and parameters of molecular interaction with target proteins MAPK (2Y9Q), SIR (5OL0) and TR (2JK6). In all graphics, the closer to 0 (red) the interaction force is more determinant and intense, the closer to 10 (blue) the greater the distance and the interaction force is negligible. Clusters of each ligand evidenced by colors, (control) green; (1) yellow; (2) blue and (3) red. Preserved residues highlighted by squares shaded by purple.

6.2.2. Artigo 2

Oregano (*Origanum vulgare*) essential oil presents drug-likeness proprieties and anti-*Leishmania* activity without triggering an inflammatory response

Artigo submetido à revista *Phytomedicine* (Qualis A1).

Fernanda Tomiotto-Pellissier[a,b,#,*], Bruna Taciane da Silva Bortoleti[a,b,*], Ana Flávia Marques Ganaza[b], Ana Carolina Quasne[b], Beatriz Ricci[b], Pedro Vinicius Dolce e Carvalho[b], Gustavo Henrique Della Colleta[b], Danielle Lazarin-Bidóia[b,c], Taylon Felipe Silva[b], Manoela Daiele Gonçalves[d], Virgínia Márcia Concato[b], Renata Katsuko Takayama Kobayashi[e], Idessania Nazareth Costa[b], Wander Rogério Pavanelli[a,b], Ivete Conchon-Costa[b], Milena Menegazzo Miranda-Sapla[b#]

[a]Graduate Program in Biosciences and Biotechnology, Carlos Chagas Institute (ICC), Fiocruz, Curitiba, Paraná, Brazil.
[b]Department of Pathological Sciences, State University of Londrina, PR, Brazil.
[c]Department of Basic Health Sciences, State University of Maringá, Maringá, Paraná 87020-900, Brazil.
[d]Department of Chemistry, Center of Exact Sciences, State University of Londrina, Londrina, Paraná, Brazil.
[e]Department of Microbiology, State University of Londrina, Londrina, Paraná, Brazil.
*Authors with an equivalent contribution.
#Corresponding authors.

Oregano (*Origanum vulgare*) essential oil presents drug-likeness proprieties and anti-*Leishmania* activity without triggering an inflammatory response

Fernanda Tomiotto-Pellissier[a,b,*,1], Bruna Taciane da Silva Bortoleti[a,b,1], Ana Flávia Marques Ganaza[a], Ana Carolina Quasne[a], Beatriz Ricci[a], Pedro Vinicius Dolce e Carvalho[a], Gustavo Henrique Della Colleta[a], Danielle Lazarin-Bidóia[a,c], Taylon Felipe Silva[a], Manoela Daiele Gonçalves[d], Virgínia Márcia Concato[a], Renata Katsuko Takayama Kobayashi[e], Idessania Nazareth Costa[a], Wander Rogério Pavanelli[a,b], Ivete Conchon-Costa[a], Milena Menegazzo Miranda-Sapla[a]**

[a]Department of Pathological Sciences, State University of Londrina, Paraná, Brazil.
[b]Graduate Program in Biosciences and Biotechnology, Carlos Chagas Institute (ICC), Fiocruz, Curitiba, Paraná, Brazil.
[c]Department of Basic Health Sciences, State University of Maringá, Maringá, Paraná, Brazil.
[d]Department of Chemistry, Center of Exact Sciences, State University of Londrina, Londrina, Paraná, Brazil.
[e]Department of Microbiology, State University of Londrina, Londrina, Paraná, Brazil.

[1] Equal contribution.

*Corresponding author: Fernanda Tomiotto-Pellissier - Department of Pathology Science, Center of Biological Sciences, State University of Londrina, Celso Garcia Cid Highway - Pr 445 Km 380 Cx. Postal 10.011 - Campus Universitário, 86057-970, Paraná, Brazil.
E-mail: fernandatomiotto@gmail.com
Phone: +554333714539

**Co-corresponding author: Milena Menegazzo Miranda-Sapla - Department of Pathology Science, Center of Biological Sciences, State University of Londrina, Celso Garcia Cid Highway - Pr 445 Km 380 Cx. Postal 10.011 - Campus Universitário, 86057-970, Paraná, Brazil.
E-mail: milenamenegazzo@yahoo.com.br
Phone: +554333714539

34   **ABSTRACT**

35   **Background:** Leishmaniasis is a neglected disease complex with high incidences in developing countries, for which

36   the available drugs present high toxicity and low efficacy. Thus, the search for new drugs is necessary and urgent.

37   The oregano essential oil (OEO) from *Origanum vulgare*, presents several biological effects, including the inhibitory

38   effect on *Leishmania amazonensis*. However, until now the mechanisms of action of OEO on promastigote or

39   intracellular amastigote forms of *Leishmania* species have not been studied.

40   **Purpose:** To investigate the effect of OEO on leishmaniasis through *in silico*, *in vitro,* and *in vivo* approaches.

41   **Methods:** This study assessed the drug-likeness prediction of OEO main components *in silico*, the leishmanicidal

42   activity against promastigotes and amastigote-infected macrophages, as well its microbicide and

43   immunomodulatory mechanisms *in vitro*, and the *in vivo* effect of OEO local treatment on *L. amazonensis*-infected

44   mice.

45   **Results:** We demonstrated that OEO main components are good candidates for the development of a drug according

46   to the *in silico* study. *In vitro*, OEO acted on promastigote forms, triggering a combination of autophagic, apoptotic,

47   and necrotic events, as well as on intramacrophagic amastigote forms, without trigger a pro-inflammatory response,

48   showing reduced levels of TNF-α, reactive oxygen species, and nitric oxide. *In vivo* studies confirmed the OEO

49   anti-leishmanial potential, once the treatment reduced the lesions of infected mice. Computational docking analysis

50   also suggested an interaction between *Leishmania* arginase and the main OEO component, carvacrol, proposing one

51   of the probable antileishmanial targets of OEO.

52   **Conclusion:** Our study provided new perspectives to the OEO treatment, showing its *in silico, in vitro,* and *in vivo*

53   effect against *L. amazonensis*, and providing satisfactory support for further studies of new prototypes of

54   antileishmanial drugs.

55   **Key-words:** Leishmaniasis; natural product; TNF-α; reactive oxygen species; nitric oxide, *in vivo*.

56

57   **Abbreviations:** AMB – amphotericin B, AUF – arbitrary units of fluorescence, DCF – dichlorofluorescein, DMSO

58   - dimethyl sulfoxide, FBS – fetal bovine serum, FSC-A – forward scatter-area, H$_2$DCFDA – diacetate 2',7'-

59   dichlorofluorescein probe, IC$_{50}$ - the half-maximal inhibitory concentration, MTT – 3-(4,5-dimethylthiazol-2-yl)-

60   2,5- diphenyltetrazolium bromide, MDC – monodansylcadaverine, NO – nitric oxide, OEO - oregano essential oil,

61   PBS – phosphate buffered saline, PI – propidium iodide, ROS – reactive oxygen species, SEM – scanning electron

62   microscopy, SEM – scanning electron microscopy, TMRE – tetramethylrhodamine ethyl ester probe, TNF – tumor

63   necrosis factor.

64

65

66

2

102

INTRODUCTION

Leishmaniasis is a neglected disease with high incidences in developing countries, with more than 1 billion people living in endemic areas at risk of infection, and with 700,000 to 1 million new cases annually. The disease is caused by protozoa of the *Leishmania* genus and transmitted through the bite of female phlebotomine insects (WHO, 2020). These parasites have a digenetic life cycle where the free-flagellated procyclic promastigote form undergoes differentiation to enter into an infective metacyclic stage in the sandfly, and finally, after infection, differentiates into the disease-causing rounded amastigotes, the obligate intracellular form (Burza et al., 2018).

In humans, the clinical manifestation of the disease is dependent on the interplay between the parasite species, vector biology, and the host's immune response ranging from the cutaneous (CL) to the visceral forms (VL) (Aruleba et al., 2020). The parasite developed different immunomodulatory strategies that are essential for infection establishment, hence, an appropriate inflammatory/immune response, defined by its ability to achieve the delicate balance between the removal of *Leishmania* parasites and the minimization of pathology, is one of the major goals for drug discovery [4].

Although there has been considerable progress in the development of treatment for VL, and several novel compounds are currently in pre-clinical and clinical development for this clinical form, for CL there have been limited advances in drug research and development, and the available treatment is based on drugs that present high toxicity, relapses, therapeutic failure, and resistance (Alvar et al., 2006).

Several products of natural origin have been studied for their therapeutic potential in leishmaniasis (Singh et al., 2014), with great interest in essential oils that possess a wide variety of hydrophobic compounds with antimicrobial potential. The ability to diffuse across cell membranes certainly gives those molecules some advantage in targeting intracellular microbes, being a valuable research option for the search of bioactive compounds (Bakkali et al., 2008).

In this sense, the oregano essential oil (OEO), extracted from *Origanum vulgare*, has attracted attention due to its biological effects as the broad antibacterial, antifungal, antiparasitic and antioxidant effect [9]. Regarding the antiparasitic effect of OEO, it includes the inhibitory effect on *Leishmania amazonensis* (Sanchez-Suarez et al., 2013; Teles et al., 2019). However, until now the mechanisms of action of OEO on promastigote or intracellular amastigote forms of *Leishmania* species have not been studied.

The antimicrobial proprieties of OEO have been associated with the presence of different chemical classes of compounds, and potent interactions between the OEO components have been reported, suggesting an improved efficacy of the mixture when compared to the isolated compounds (Bassolé and Juliani, 2012). Moreover, a mixture of molecules with antimicrobial activity could minimize the selection of resistant strains.

In the present work, we demonstrated that OEO containing carvacrol, thymol, γ-terpinene, p-cymene, and β-caryophyllene as the main components is a good candidate for drug development according to the *in silico* study, acting against *L. amazonensis in vitro* and *in vivo*. OEO presented action on promastigote forms, triggering a combination of autophagic, apoptotic, and necrotic events, as well as in amastigote forms, without trigger a pro-inflammatory response. The results were confirmed by the reduction of lesions on *in vivo* studies. Computational

3

103

103 docking analysis also suggested the arginase-carvacrol interactions by spontaneous binding proposing one of the

104 probable antileishmanial targets of OEO.

105

106 **MATERIALS AND METHODS**

107 **Animals and Ethics Committee**

108 BALB/c weighing approximately 25–30 g and aged 6–8 weeks were kept under sterile conditions and used

109 according to protocols approved by the Institutional Animal Care and Committee. This study was approved by the

110 Ethics Committee for Animal Experimentation of the State University of Londrina 8595.2018.89.

111

112 **Culture of *Leishmania (L.) amazonensis***

113 Promastigote forms of *Leishmania (Leishmania) amazonensis* ((MHOM/BR/1989/166MJO) were maintained

114 in culture medium 199 (GIBCO Invitrogen) supplemented with 10% fetal bovine serum-FBS (GIBCO Invitrogen),

115 1 M Hepes, 0.1% human urine, 0.1% L-glutamine, 10 µg/mL penicillin and streptomycin (GIBCO® Invitrogen)

116 and 10% sodium bicarbonate. The cell cultures were maintained in an incubator-type B.O.D. at 25 °C, in 25 cm^2

117 flasks. In all experiments, promastigote forms were used in the stationary growth phase.

118

119 **Oregano essential oil**

120 Oregano (*Origanum vulgare*) essential oil (OEO) was obtained from Ferquima Industry and Commerce of

121 Essential Oils (São Paulo, Brazil). This oil was extracted by steam distillation and its density (0.954 g/mL) and

122 composition (main components: carvacrol, thymol, γ-terpinene, p-cymene, and β-caryophyllene) were described in

123 a technical report (CAS number 84012-24-8, batch 224). A stock solution of 50% OEO was prepared in

124 dimethylsulfoxide (DMSO, Sigma-Aldrich; v/v). The maximum DMSO concentration in assays was 0.01%.

125

126 **Drug-likeness prediction of OEO main components**

127 The carvacrol, thymol, γ-terpinene, p-cymene, and β-caryophyllene structure *in silico* study was carried out to

128 evaluate theoretical drug-likeness parameters related to oral bioavailability and absorption, distribution, metabolism,

129 excretion, and toxicity (ADMET) properties. The predictions were calculated in admetSAR software

130 (http://lmmd.ecust.edu.cn/admetsar2/) according to Lipinski's rule of five (Ro5) [22] followed by the additional rule

131 proposed by Veber [23]. ADMET properties predictions were also calculated according to (Cheng et al., 2012).

132

133 **Antipromastigote assay**

134 *Leishmania amazonensis* promastigote forms (10^6 cells/mL) were treated with a serial concentration of OEO

135 (3.12, 6.25, 12.5, 25, 50, and 100 µg/mL) for 24 h at 25 °C, and the parasites were counted on a Neubauer chamber.

136 Promastigote forms maintained in the culture medium were used as a control, DMSO 0.01% was used as a vehicle,

137 and amphotericin B (AMB) 1µM was used as a positive control. The 50% inhibitory concentration of the parasites

138 (IC$_{50}$) curve was calculated by logarithmic non-linear regression to the dose-response curve from the data obtained.

139

4

Viewability of peritoneal macrophages

Peritoneal macrophages (5×10^5 cells/mL) were recovered from the peritoneal cavity of BALB/c mice with cold PBS supplemented with 3% of FBS and then cultured in 24-well plates with 200 μL of RPMI 1640 medium (10% FBS) for 2 h (37 °C, 5% CO_2). Adherent cells were incubated with OEO (3.12, 6.25, 12.5, 25, 50, and 100 μg/mL) cultured for 24 h under the same conditions. After this period, MTT (3-(4,5-dimethylthiazol-2-yl)-2,5-diphenyltetrazolium bromide) (Sigma-Aldrich) (5 mg/mL) was added for 4 h. Cells under the same conditions without treatment were used as control; DMSO 0.01% was the vehicle, and the positive control was H_2O_2 0.4%. The plates were read using a spectrophotometer (Thermo Scientific, Multiskan GO) at 550 nm. The results were expressed as a percentage of viability compared to the control group.

Analysis of hemolytic activity

Sheep blood was collected with heparin (Ethics Committee for Animal Experimentation of State University of Londrina: 82862016.60) and the toxicity on erythrocytes evaluated as previously described (Bortoleti et al., 2018). PBS was used with negative control and Triton X 1% as a positive control for hemolysis.

Scanning electron microscopy (SEM) of promastigote forms

The morphological changes of *L. amazonensis* promastigote forms were evaluated by SEM as previously described (Tomiotto-Pellissier et al., 2018).

The length of the promastigote forms (flagellum, cell body, and total length) was analyzed in the Image-Pro Plus software, based on the 10,000x magnification images obtained. At least three images of each condition were subjected to measurement.

Determination of the parasites cell size

L. amazonensis promastigote forms (10^6 cells/ml) were treated with OEO-IC_{50p} and incubated for 24 h at 24°C, harvested, and washed with PBS. Subsequently, the parasites were analyzed using a BD Accuri C6 flow cytometer (BD Biosciences, San Jose, CA), as previously described (Tomiotto-Pellissier et al., 2018). Parasites maintained in the culture medium were used as a control and DMSO 0.01% was used as vehicle control.

Mechanism of action determination on *L. amazonensis* promastigote forms

To determine the mechanism of action of OEO, 10^6 promastigote forms were treated for 24 h with IC_{50p} and $2xIC_{50p}$, and different parameters were assessed as previously described by our group (Concato et al., 2020; Tomiotto-Pellissier et al., 2018). Briefly, the inner mitochondrial membrane potential was investigated by incubation with tetramethylrhodamine ethyl ester (TMRE) (Sigma-Aldrich); the reactive oxygen species (ROS) were analyzed by a permeant probe diacetate 2',7'-dichlorofluorescein diacetate (H_2DCFDA) (Sigma-Aldrich), and the lipid droplets detection was performed by labeling with Nile red (Sigma-Aldrich). To verify the death type, we performed autophagic vacuoles quantification by monodansylcadaverine (MDC) (Sigma-Aldrich), phosphatidylserine exposition by annexin-V, and verification of cell membrane integrity by propidium iodide labeling.

5

177   As positive controls were used carbonyl cyanide m-chlorophenylhydrazone, H_2O_2, camptothecin, and
178   digitonin (all from Sigma) respectively for TMRE, DCF, annexin-V, and propidium iodide analysis, and 24h-
179   parasites cultivated with PBS for Nile Red and MDC.

180

181 **Anti-amastigote assay**

182   Peritoneal macrophages ($5x10^5$ cells/mL) were obtained as previously described. The adherent cells were
183   infected with *L. amazonensis* promastigotes ($2.5 x10^6$ cells/mL) for 2 h. After, the non-internalized parasites were
184   washed with PBS and the infected cells treated with OEO (3.12, 6.25, 12.5, 25, 50 and 100 μg/mL), RPMI 1640
185   medium (control), DMSO 0.01% (vehicle) or AMB 1 μM (positive control) for 24 h (37 °C, 5% CO_2). After this,
186   the cells were stained with Giemsa (Laborclin), analyzed as (Bortoleti et al., 2018). The supernatant was stored for
187   further analysis.

188

189 **Determination of nitrite as estimative of nitric oxide (NO) levels**

190   NO was determined through the Griess method. Briefly, supernatant aliquots (60 μL) of the anti-amastigote
191   assay were centrifuged at 2370×g for 2 min and a 50 μL of the supernatant was added with 50 μL of Griess reagent
192   (1% sulfanilamide and 0.1% of N-(1-Naphthyl) ethylenediamine in orthophosphoric acid (H_3PO_4) 5%). After 10
193   min incubation at room temperature, the samples were placed in 96-well microplates. A calibration curve was made
194   using dilutions of $NaNO_2$, and the absorbance was determined at 550 nm on a microplate reader (Thermo Scientific,
195   Multiskan GO).

196

197 **Reactive oxygen species (ROS) generation by macrophages**

198   The ROS generation of peritoneal macrophages ($5×10^5$ cells/mL - infected and treated under the same conditions
199   described in the anti-amastigote assay) was evaluated as described in (Tomiotto-Pellissier et al., 2018).

200

201 **Cytokines measurement**

202   The supernatants obtained in the anti-amastigote assay were used to determine the levels of TNF-α, IL-6 e IL-
203   10 using eBioscience commercial kits capture enzyme-linked immune sorbent assay (ELISA) (San Diego, CA,
204   USA), according to the manufacturer's instructions.

205

206 ***In vivo* analysis of OEO treatment**

207   BALB/c mice (n = 4 per group) were anesthetized and infected at the base of the tail, subcutaneously, with 10^5
208   promastigote forms of *L. amazonensis*. After the appearance of the lesion in all mice, 100 days post-inoculation
209   (p.i.), the daily treatment started on groups as follows: vehicle group- applications of base gel, OEO group - gel
210   containing OEO 0.2% at the lesion site (0.5 g - applied in circular movements), and positive control group -
211   intraperitoneal injection (i.p.) of glucantime 20 mg/Kg/day. Non-treated animals were used as control. After five
212   weeks of treatment, the animals were anesthetized and euthanized following the approved protocols.

6

213   The lesions were measured weekly after the onset of treatment using a digital caliper (Starrett 799). Data were

214   expressed as (final lesion size) - (initial lesion size) for each animal.

215

Statistical analysis

216

217   Data were expressed as a mean ±SEM. Data were analyzed using the GraphPad Prism statistical software

218   (GraphPad Software, Inc., USA, 500.288). Significant differences between the groups were determined through

219   one-way ANOVA, followed by Tukey's test for multiple comparisons. Differences were considered as statistically

220   significant upon $p < 0.05$. At least three independent experiments were performed, each with duplicate datasets.

221

Molecular modeling analysis

222

223   The crystal structure of *Leishmania mexicana* arginase (ARG; PDB 4IU5) was used for docking calculations

224   (D'Antonio et al., 2013). The carvacrol two-dimensional structure was obtained from the virtual repository

225   PubChem (https://pubchem.ncbi.nlm.nih.gov/) and converted to ligand.mol2.

226   Before of test, ions, co-crystallized ligands, and water molecules not relevant to the system structure were

227   removed from the target. The protein binding site for molecular docking was centered between Mg^{2+} at x: 15.141,

228   y: -15.1248, z: -5.40 for calculations as previously described (Camargo et al., 2020).

229   The types of ligand-residue interactions, as well as the figures, were generated using the Discovery Studio

230   Visualizer (Dassault Systèmes BIOVIA, Discovery Studio Modeling Environment, Release 2017, San Diego:

231   Dassault Systèmes, 2016).

232   The protein and ligand preparation was performed using AutoDockTools (ADT) v. 1.5.6 (Morris et al., 2009).

233   The polar hydrogens were added to the protein and atoms charges of protein and ligand are assigned by Kolman and

234   Gasteiger methods, respectively. The dimensions of the grid box were determined as 40x50x38 $Đ^3$ (Camargo et al.,

235   2020). Molecular docking calculations were carried out considering the Lamarckian Genetic algorithm implemented

236   in Autodock. Scoring functions with 10 iterative runs were performed.

237

RESULTS

238

Drug-likeness assessment of main components of OEO

239

240   Knowing that the main components of the tested OEO are carvacrol (71%), thymol (3%), γ-terpinene (4.5%),

241   p-cymene (3.5%), and β-caryophyllene (4%) (Figure 1), our first aim was to verify the drug-likeness theoretical

242   potential of those compounds through an *in silico* study. The studied compounds did not present any violation of

243   Lipinski's and Veber's rules, suggesting a good chance of drug-likeness and oral bioavailability (Table 1).

244   Moreover, ADMET properties were analyzed through admetSAR and reported in Table S1. The results predict

245   that the main components of OEO present potential human intestinal absorption, caco2 cell, and blood-brain barrier

246   permeability, human oral bioavailability, non-inhibitor of OATP2B1, MATE, OCT2, BASEP as well as most of the

247   CYPs, besides to no inhibition promiscuity with the main five CYP isoforms (CYP1A2, CYP2C19, CYP2C9,

248   CYP2D6, and CYP3A4). Also, the compounds were predicted as non-carcinogenic, non-mutagenic, non-inductor

7

of micronucleus, and non-hepatotoxic. Regarding the acute oral toxicity, all compounds presented degree III, that is, slightly toxic and slightly irritating predictions (Table S1).

On the other side, the compounds also were predicted as OATP1B1 and OATP1B3 inhibitors, with possible effects in eye corrosion and/or irritation. Also, carvacrol and thymol are possible CYP1A2 inhibitors. Besides that, the prediction shows subcellular localization of carvacrol and thymol in the mitochondria, while γ-terpinene, p-cymene, and β-caryophyllene in the lysosomes (Table S1).

Table S2 shows the predictive values of the *in silico* study. We found good values for water solubility and low oral toxicity. Concerning the binding to plasma proteins, γ-terpinene, p-cymene and β-caryophyllene presented low predicted values (<85%), while carvacrol and thymol presented higher predictions (≥90%).

OEO exerts leishmanicidal effect against promastigote forms of *L. amazonensis in vitro* without cytotoxic effect for macrophages

The direct effect of OEO on promastigote forms of *L. amazonensis* was evaluated by the parasite proliferation. OEO treatment was able to reduce the viability of the parasites at all concentrations evaluated (3.12-100 μg/mL) when compared to control and DMSO ($p \leq 0.0001$) (Figure 2A), exhibiting an IC_{50p} value of 16 (± 0.06) μg/mL (Table 2). This concentration and twice the value ($2xIC_{50p}$) were used for the following experiments in promastigote forms.

Besides that, the cytotoxic effect of OEO on erythrocytes and macrophages (the main host cells for *Leishmania* sp.) was evaluated. We found that the concentrations up to 100 μg/mL were not able to reduce the viability of sheep erythrocytes and BALB/c mice peritoneal macrophages (Figure 2B, C). Also, the cytotoxic value for 50% of the cells (CC_{50}) was established as 188.2 (± 10) μg/mL. The selectivity index of OEO in promastigote forms was calculated from the IC_{50} and CC_{50} values, obtaining a value of 11.7 (Table 2).

OEO induces morphological changes and reduction in the cell volume of promastigote forms

The morphological changes of OEO-treated *L. amazonensis* promastigote forms were analyzed by SEM. Untreated (Figure 3A,B) and vehicle-treated (0.01% DMSO) parasites (Figure 3C) showed an elongated body, smooth cell membrane, and all its extracellular structure preserved. Treatment with OEO-IC_{50p} for 24 h induced roughness on the surface of the parasite, reduced cell body size, presence of two flagella, and leakage of cytoplasmic content (Figure 3D-I).

Moreover, from the analysis of the images, we could verify that the IC_{50p} OEO-treatment reduced the flagellum, cell body, and total cell size after 24 h concerning the control (Figure 3J). Confirming these data, the flow cytometry analysis showed a reduction in the cell size in both, IC_{50p} and $2xIC_{50p}$ concentrations, without differences between the used doses (Figure 3K).

OEO treatment promotes death process in *L. amazonensis* promastigote forms by a combination of autophagic, apoptotic, and necrotic events

8

Our next objective was to identify the mechanisms involved in the death of the parasites. The results showed that OEO treatment in both concentrations was able to induce ROS production in parasites and cause mitochondrial depolarization when compared to the control (Figure 4A,B). We also found that treatment with OEO induced the accumulation of neutral lipid droplets and the formation of the autophagic vacuoles when compared to the respective controls. In both parameters, $2xIC_{50p}$ showed greater fluorescence than IC_{50p} (Figure 4C,D).

Besides, the cell death mechanism triggered by the OEO-treatment involved apoptosis-like death by marking the externalization of phosphatidylserine, as well as the involvement of plasma membrane damage due to the staining of the treated parasites with PI, which diffuses across permeable membranes and binds to nucleic acids (Figure 4E–F).

OEO treatment induces *L. amazonensis* amastigotes elimination from infected macrophages

As OEO showed no toxicity in murine peritoneal macrophages at concentrations of 3.12 - 100 μg/mL, we investigated its action against intramacrophagic amastigotes. We observed that concentrations of 6.25, 12.5, 25, 50, and 100 μg/mL of OEO significantly reduced the total amount of amastigotes and the percentage of infected macrophages (Figure 5A, B), while the concentrations of 12.5, 25, 50 and 100 μg/mL also induced a reduction in the number of amastigotes by macrophages when compared to the control (Figure 5C). Thus, concentrations of 12.5 - 100 μg/mL were chosen for the next set of experiments.

Based on the results, we obtained a value of 17.2 μg/mL for the IC_{50} of intracellular amastigote forms, from which a selectivity index of 10.9 times was calculated to peritoneal macrophages (Table 4).

OEO treatment down-modulates ROS, NO, and TNF-α levels in *L. amazonensis*-infected macrophages

Knowing that OEO induces the elimination of intramacrophagic amastigote forms, we studied the immunomodulation caused by the treatment. Our data demonstrated that OEO treatment (12.5 - 100 μg/mL) significantly reduced the production of ROS and NO when compared to the control (Figure 6A,B). Likewise, the highest concentrations, 50 and 100 μg/mL, also significantly reduced TNF-α levels when compared to the control (Figure 6C). The levels of IL-6 and IL-10 did not differ from the control or each other (data not shown).

In vivo **activity of OEO treatment**

Once the *in vitro* effect of OEO was showed, its potential action in *L. amazonensis*-infected mice was investigated. For this, BALB/c mice were infected and topically treated for five weeks with 0.2% OEO-based gel after the lesion appearance. The lesion size measurements showed that the control, vehicle, and positive control (glucantime) groups increased the lesion size over time, demonstrated by positive values. The OEO treatment was able to reduce the lesion sizes (negative values), presenting smaller lesions than all other groups (Figure 7). It is important to note that the OEO-treatment was more effective in the tissue repair process than the standard drug (glucantime), in which, despite the treated lesions showed smaller size when compared to the negative control and vehicle, was not able to reduce the size of the injuries, but only delayed its development.

9

Molecular docking of OEO

To gain insights into the OEO mechanism of action against *Leishmania amazonensis*, we predicted the interaction of carvacrol, the main constituent of OEO, with *Leishmania* arginase (ARG) by molecular docking. We found ARG-carvacrol interactions in the active site of the enzyme, with common hydrogen-bonding interactions with Asp141 residue, besides π-π stacking and π-alkyl interaction with His139 (Figure 8). Also, it was provided the binding energy of ARG-carvacrol complex of −6.1±0.33 kcal/mol, suggesting a spontaneous binding between the molecules. Thus, ARG enzyme was identified as one of the probable antileishmanial target of OEO.

DISCUSSION

Available drugs for leishmaniasis treatment are unsatisfactory due to their high toxicity and low efficacy (Alvar et al., 2006). Thus, the search for new drugs is necessary and urgent. In this context, our study provided new perspectives on OEO action in experimental leishmaniasis.

Drug discovery is a long and expensive process. In the past decade, from hundreds of drug candidates, only a few reached the market due to the high failure rate at the clinical trial stage, mainly due to the lack of efficacy and high toxicity (Cheng et al., 2012). Thus, to predict the influence of the chemical structure on the oral absorption of a compound by analyzing pharmacokinetic parameters is important for the development of a candidate with good chances to become a drug [22]. Also, the absorption, distribution, metabolism, excretion, and toxicity (ADMET) properties of drug candidates play key roles in drug discovery. Thus, *in silico* studies have become a useful, effective, and low-cost tool for studying drug candidates (Cheng et al., 2012).

We performed *in silico* studies to assess theoretical drug-likeness parameters and we found that none of Lipinski's and Veber's rules (Lipinski, 2004; Veber et al., 2002) were violated for the main compounds of OEO: carvacrol, thymol, γ-terpinene, p-cymene, and β-caryophyllene. In the same way, the OEO components proved favorable predictions to most of the ADMET properties calculated.

Is noteworthy that we found good values for water solubility, since more than 80% of the drugs on the market have a logS value greater than -4 ("logS Calculation - Osiris Property Explorer," n.d.), and low oral toxicity, being classified as degree III (LD_{50} >500) (Yang et al., 2018). Concerning the binding to plasma proteins, γ-terpinene, p-cymene, and β-caryophyllene presented low predicted values, while carvacrol and thymol presented higher predictions. As a general rule, minimally protein-bound drugs (<85%) penetrate tissues better than those that are highly protein-bound (≥90%), but clearance of such drugs is also higher (Johnson-Davis and Dasgupta, 2016).

Such results are important because poor ADMET properties are among the main reasons for the failure of drug candidates during clinical trials (Cheng et al., 2012). The DNDi also postulated that an ideal leishmaniasis treatment should occur orally, safely, effectively, at a low cost, and over a short period. A possible lead drug to be used should be *in vitro* non-cytotoxic, with a selectivity index ≥10 (Ioset et al., 2009). Therefore, taking together the results obtained for OEO components *in silico* and the SI obtained *in vitro* are indicative that OEO is a good drug candidate for leishmaniasis.

Aiming to understand the effect of OEO, we investigated the *in vitro* mechanisms of action on *L. amazonensis* promastigote forms. We demonstrated the ability of OEO to increase ROS levels, molecules with

10

359 different biological functions which in excess in the cells can trigger organelles damage and consequently, cellular
360 death (Menna-Barreto, 2019).

361   In this sense, we also found mitochondrial membrane damage upon the reduction of membrane potential.
362 Mitochondrial integrity is essential for parasite survival since trypanosomatids have unique mitochondrion. Also,
363 both ROS and mitochondrial dysfunction are inducers of lipid droplet accumulation, a hallmark of cellular stress
364 (Menna-Barreto, 2019). Thus, we can infer that OEO treatment induced ROS production, causing mitochondrial
365 damage and accumulation of lipid droplets, which culminates in cell stress and promastigote death.

366   Confirming this data, we found autophagic vacuole formation, phosphatidylserine exposure, and cellular
367 membrane damage on the treated parasites. Autophagy is a biological pathway associated with cell recycling through
368 the removal of damaged cell components, which can be activated in the presence of cell stress, forming autophagic
369 vacuoles. When continuous induction of autophagy occurs, it can progress to the cell death of the parasites (Menna-
370 Barreto, 2019).

371   Apoptosis-like cell death has been related to the leishmanicidal mechanism of different compounds. Besides,
372 the promastigote membrane permeabilization, indicated by marking with propidium iodide, can be indicative of
373 both: late-apoptotic and necrotic cell death (Bortoleti et al., 2018; Tomiotto-Pellissier et al., 2018).

374   These results were confirmed by morphological changes in the promastigotes. Roughness on the surface of
375 the parasite, reduction in cell body size, presence of two flagella, and leakage of cytoplasmic content are evident
376 signals of cell death. Similar morphological alterations were found by our group in OEO-treated *S. aureus*
377 (Scandorieiro et al., 2016). Our data are still in accord with the prediction of the *in silico* study, which showed that
378 the main components of OEO accumulate in mitochondria or lysosomes, two organelles intrinsically related to
379 autophagy and apoptosis (Menna-Barreto, 2019).

380   Knowing the mechanisms involved with promastigote forms death, we investigated the OEO action on
381 amastigote-infected macrophages and lesions development in *L. amazonensis*-infected mice. First, we found that
382 the concentrations used were not toxic to macrophages, the main host cells of *Leishmania* sp. [4]. Then, we found
383 that treatment with OEO was able to reduce the rate of macrophage infection *in vitro* and the lesion size *in vivo*.
384 Amastigotes are resistant forms of these parasites, which have complex defense mechanisms that allow their survival
385 in the hostile intramacrophagic environment (Alvar et al., 2006), therefore a potential drug for leishmaniasis must
386 have the ability to act in these evolutionary forms.

387   The immune response against *L. amazonensis* is complex and naturally involves a pro-inflammatory
388 response with TNF-α production that activates macrophages to ROS and NO synthesis, and consequent parasite
389 elimination [4]. However, the excessive pro-inflammatory response is also responsible for tissue damage and disease
390 persistence (Rossi and Fasel, n.d.). OEO was able to reduce *in vitro* the levels of ROS, NO, and TNF-α with
391 concomitant parasite elimination showing a parasite clearance without trigger inflammation. Also, OEO was able
392 to induce tissue repair in the *in vivo* context.

393   Our data corroborate with (Chuang et al., 2018) who found that the ethanolic extract of *Origanum vulgare*
394 suppressed the inflammatory response, reducing the TNF-α production in an inflammation model induced by

11

Propionibacterium acnes. Likewise, (Mahran et al., 2019) also identified a reduction in TNF-α levels in a gamma-ray stress induction model after the treatment with carvacrol and thymol.

We further predicted that the main OEO component, carvacrol, is capable of binding in the active site of ARG suggesting that it could inhibit this target. In *Leishmania* parasites, ARG is involved in regulating several biological functions, such as replication, growth, differentiation, infectivity, and persistence (Pessenda and Santana da Silva, 2020). Thus, this result provided new evidence that OEO can directly act on intramacrophagic amastigotes, inducing parasite elimination.

CONCLUSION

Taking together, our data demonstrated that OEO is a good candidate for the development of a drug according to the *in silico* study, in addition to having an *in vitro* effect both on promastigote forms, triggering death by autophagy, and in amastigote forms, without trigger a pro-inflammatory response. The anti-*Leishmania* effect was further confirmed *in vivo* by the reduction of lesions. Computational docking analysis also suggested the arginase-carvacrol interactions by spontaneous binding proposing a probable antileishmanial target of OEO. These results suggest OEO as a promising agent for further studies and the design of new prototypes of antileishmanial drugs.

CONFLICT OF INTERESTS

The authors declared that there is no conflict of interest.

REFERENCES

Alvar, J., Croft, S., Olliaro, P., 2006. Chemotherapy in the Treatment and Control of Leishmaniasis, in: Advances in Parasitology. pp. 223–274. https://doi.org/10.1016/S0065-308X(05)61006-8

Aruleba, R.T., Carter, K.C., Brombacher, F., Hurdayal, R., 2020. Can we harness immune responses to improve drug treatment in leishmaniasis? Microorganisms 8, 1–20. https://doi.org/10.3390/microorganisms8071069

Bakkali, F., Averbeck, S., Averbeck, D., Idaomar, M., 2008. Biological effects of essential oils - A review. Food Chem. Toxicol. https://doi.org/10.1016/j.fct.2007.09.106

Bassolé, I.H.N., Juliani, H.R., 2012. Essential oils in combination and their antimicrobial properties. Molecules.

12

432   https://doi.org/10.3390/molecules17043989

433   Bortoleti, B.T. da S., Gonçalves, M.D., Tomiotto-Pellissier, F., Miranda-Sapla, M.M., Assolini, J.P., Carloto,

434   A.C.M., de Carvalho, P.G.C., Cardoso, I.L.A., Simão, A.N.C., Arakawa, N.S., Costa, I.N., Conchon-Costa, I.,

435   Pavanelli, W.R., 2018. Grandiflorenic acid promotes death of promastigotes via apoptosis-like mechanism and

436   affects amastigotes by increasing total iron bound capacity. Phytomedicine 46, 11–20.

437   https://doi.org/10.1016/j.phymed.2018.06.010

438   Burza, S., Croft, S.L., Boelaert, M., 2018. Leishmaniasis. Lancet 392, 951–970. https://doi.org/10.1016/S0140-

439   6736(18)31204-2

440   Camargo, P.G., Bortoleti, B.T. da S., Fabris, M., Gonçalves, M.D., Tomiotto-Pellissier, F., Costa, I.N., Conchon-

441   Costa, I., Lima, C.H. da S., Pavanelli, W.R., Bispo, M. de L.F., Macedo, F., 2020. Thiohydantoins as anti-

442   leishmanial agents: n vitro biological evaluation and multi-target investigation by molecular docking studies. J.

443   Biomol. Struct. Dyn. https://doi.org/10.1080/07391102.2020.1845979

444   Cheng, F., Li, W., Zhou, Y., Shen, J., Wu, Z., Liu, G., Lee, P.W., Tang, Y., 2012. AdmetSAR: A comprehensive

445   source and free tool for assessment of chemical ADMET properties. J. Chem. Inf. Model. 52, 3099–3105.

446   https://doi.org/10.1021/ci300367a

447   Chuang, L. Te, Tsai, T.H., Lien, T.J., Huang, W.C., Liu, J.J., Chang, H., Chang, M.L., Tsai, P.J., 2018. Ethanolic

448   extract of origanum vulgare suppresses propionibacterium acnes-induced inflammatory responses in human

449   monocyte and mouse ear edema models. Molecules 23. https://doi.org/10.3390/molecules23081987

450   Concato, V.M., Tomiotto-Pellissier, F., Silva, T.F., Gonçalves, M.D., Bortoleti, B.T. da S., Detoni, M.B., Siqueira,

451   E. da S., Rodrigues, A.C.J., Schirmann, J.G., Barbosa-Dekker, A. de M., Costa, I.N., Conchon-Costa, I.,

452   Miranda-Sapla, M.M., Mantovani, M.S., Pavanelli, W.R., 2020. 3,3′,5,5′-tetramethoxybiphenyl-4,4′diol

453   induces cell cycle arrest in G2/M phase and apoptosis in human non-small cell lung cancer A549 cells. Chem.

454   Biol. Interact. 326, 109133. https://doi.org/10.1016/j.cbi.2020.109133

455   D'Antonio, E.L., Ullman, B., Roberts, S.C., Dixit, U.G., Wilson, M.E., Hai, Y., Christianson, D.W., 2013. Crystal

456   structure of arginase from Leishmania mexicana and implications for the inhibition of polyamine biosynthesis

457   in parasitic infections. Arch. Biochem. Biophys. 535, 163–176. https://doi.org/10.1016/j.abb.2013.03.015

458   Ioset, J.-R., Brun, R., Wenzler, T., Kaiser, M., Yardley, V., 2009. Drug Screening for Kinetoplastids Diseases: A

459   Training Manual for Screening in Neglected Diseases. STI.

460   Johnson-Davis, K.L., Dasgupta, A., 2016. Special Issues in Therapeutic Drug Monitoring in Patients With

461   Uremia, Liver Disease, and in Critically Ill Patients, in: Clinical Challenges in Therapeutic Drug Monitoring:

462   Special Populations, Physiological Conditions, and Pharmacogenomics. Elsevier Inc., pp. 245–260.

463   https://doi.org/10.1016/B978-0-12-802025-8.00011-8

464   Lipinski, C.A., 2004. Lead- and drug-like compounds: The rule-of-five revolution. Drug Discov. Today Technol.

465   https://doi.org/10.1016/j.ddtec.2004.11.007

466   logS Calculation - Osiris Property Explorer [WWW Document], n.d. URL https://www.organic-

467   chemistry.org/prog/peo/logS.html (accessed 8.14.20).

468   Mahran, Y.F., Badr, A.M., Aldosari, A., Bin-Zaid, R., Alotaibi, H.N., 2019. Carvacrol and Thymol Modulate the

13

Cross-Talk between TNF-α and IGF-1 Signaling in Radiotherapy-Induced Ovarian Failure. Oxid. Med. Cell. Longev. 2019. https://doi.org/10.1155/2019/3173745

Menna-Barreto, R.F.S., 2019. Cell death pathways in pathogenic trypanosomatids: lessons of (over)kill. Cell Death Dis. https://doi.org/10.1038/s41419-019-1370-2

Morris, G.M., Huey, R., Lindstrom, W., Sanner, M.F., Belew, R.K., Goodsell, David S. Olson, A.J., 2009. AutoDock4 and AutoDockTools4: Automated docking with selective receptor flexibility. J. Comput. Chem. 30, 2785–2791. https://doi.org/10.1002/jcc

Pessenda, G., Santana da Silva, J., 2020. Arginase and its mechanisms in Leishmania persistence . Parasite Immunol. 42, e12722. https://doi.org/10.1111/pim.12722

Rossi, M., Fasel, N., n.d. How to master the host immune system? Leishmania parasites have the solutions! https://doi.org/10.1093/intimm/dxx075

Sakkas, H., Papadopoulou, C., 2017. Antimicrobial activity of basil, oregano, and thyme essential oils. J. Microbiol. Biotechnol. https://doi.org/10.4014/jmb.1608.08024

Sanchez-Suarez, J.F., Riveros, I., Delgado, G., 2013. Evaluation of the Leishmanicidal and Cytotoxic Potential of Essential Oils Derived From Ten Colombian Plants. Iran. J. Parasitol. 8, 129–136.

Scandorieiro, S., de Camargo, L.C., Lancheros, C.A.C., Yamada-Ogatta, S.F., Nakamura, C. V., de Oliveira, A.G., Andrade, C.G.T.J., Duran, N., Nakazato, G., Kobayashi, R.K.T., 2016. Synergistic and additive effect of oregano essential oil and biological silver nanoparticles against multidrug-resistant bacterial strains. Front. Microbiol. 7. https://doi.org/10.3389/fmicb.2016.00760

Singh, N., Mishra, B.B., Bajpai, S., Singh, R.K., Tiwari, V.K., 2014. Natural product based leads to fight against leishmaniasis. Bioorganic Med. Chem. https://doi.org/10.1016/j.bmc.2013.11.048

Teles, A.M., Rosa, T.D.D.S., Mouchrek, A.N., Abreu-Silva, A.L., Da Silva Calabrese, K., Almeida-Souza, F., 2019. Cinnamomum zeylanicum, origanum vulgare, and curcuma longa essential oils: Chemical composition, antimicrobial and antileishmanial activity. Evidence-based Complement. Altern. Med. 2019. https://doi.org/10.1155/2019/2421695

Tomiotto-Pellissier, F., Alves, D.R., Miranda-Sapla, M.M., de Morais, S.M., Assolini, J.P., da Silva Bortoleti, B.T., Gonçalves, M.D., Cataneo, A.H.D., Kian, D., Madeira, T.B., Yamauchi, L.M., Nixdorf, S.L., Costa, I.N., Conchon-Costa, I., Pavanelli, W.R., 2018. Caryocar coriaceum extracts exert leishmanicidal effect acting in promastigote forms by apoptosis-like mechanism and intracellular amastigotes by Nrf2/HO-1/ferritin dependent response and iron depletion: Leishmanicidal effect of Caryocar coriaceum leaf ex. Biomed. Pharmacother. 98, 662–672. https://doi.org/10.1016/j.biopha.2017.12.083

Veber, D.F., Johnson, S.R., Cheng, H.Y., Smith, B.R., Ward, K.W., Kopple, K.D., 2002. Molecular properties that influence the oral bioavailability of drug candidates. J. Med. Chem. 45, 2615–2623. https://doi.org/10.1021/jm020017n

WHO, 2020. Leishmaniasis [WWW Document]. URL https://www.who.int/news-room/fact-sheets/detail/leishmaniasis (accessed 8.11.20).

Yang, H., Sun, L., Wang, Z., Li, W., Liu, G., Tang, Y., 2018. ADMETopt: A Web Server for ADMET

14

506   Optimization in Drug Design via Scaffold Hopping. J. Chem. Inf. Model. 58, 2051–2056.

507   https://doi.org/10.1021/acs.jcim.8b00532

508

509   **FIGURE LIST**
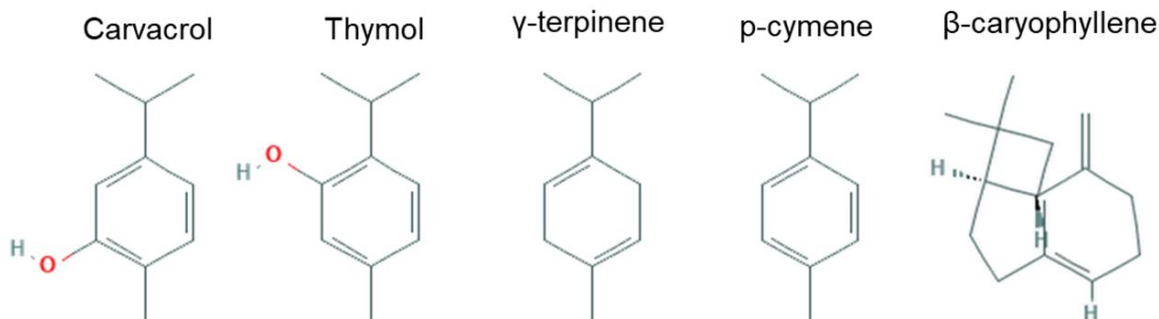
510

511   **Figure 1 – Molecular structure of the main components of OEO.** OEO composition with 71% carvacrol, 3%
512   thymol, 4.5% γ-terpinene, 3.5% p-cymene, and 4% β-caryophyllene.

513
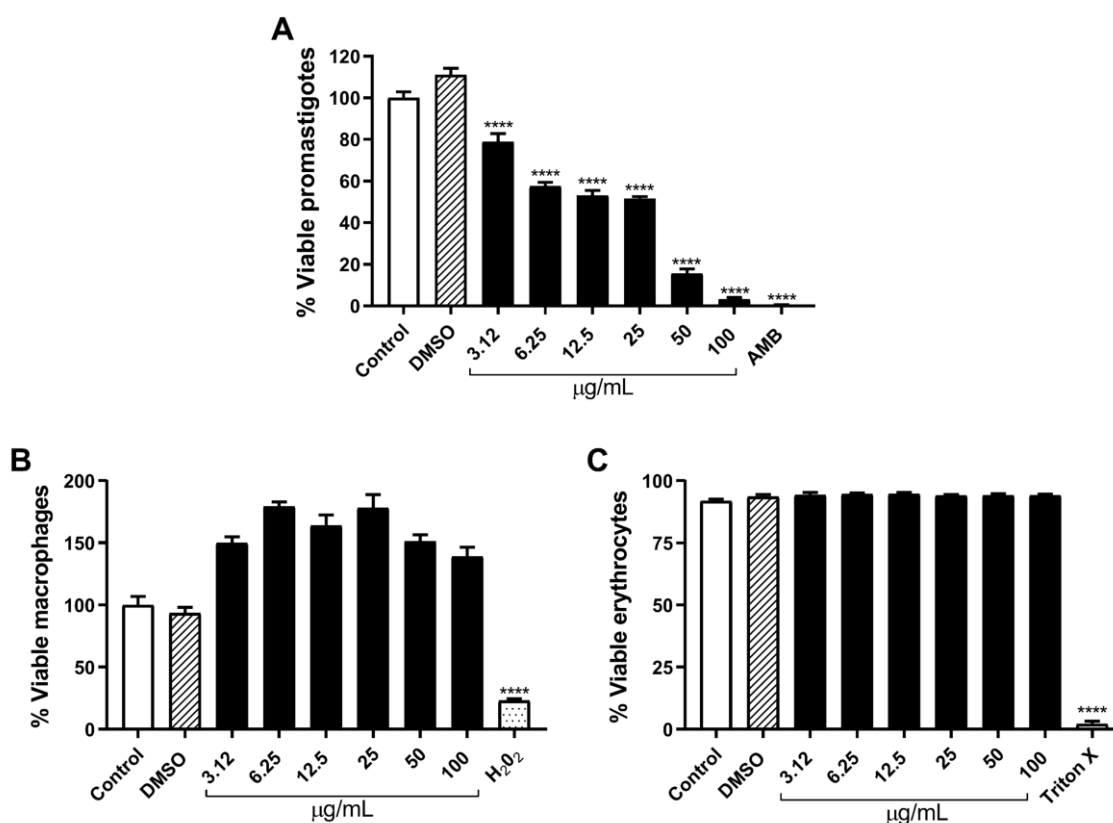
514
515   **Figure 2 – Cytotoxic effect of OEO on *L. amazonensis* promastigotes and peritoneal BALB/c macrophages.**
516   (A) *L. amazonensis* promastigote forms were treated with OEO (3.12–100 μg/mL) and the parasite viability was
517   assessed after 24 h. As control was used non-treated parasites, as vehicle control was used DMSO 0.01% and as a
518   positive control was used amphotericin B (AMB) 1 μM. (B) Viability of BALB/c peritoneal macrophages treated
519   with OEO (3.12–100 μg/mL) for 24 h by MTT assay. As control was used non-treated macrophages, as vehicle
520   control was used DMSO 0.01% and as a positive control was used H_2O_2 0.2%. (C) Viability of erythrocytes treated
521   with OEO (3.12–100 μg/mL), PBS was used as non-hemolytic control and Triton X 1% was used as a positive
522   control for hemolysis. The values represent the mean ± SEM of three independent experiments performed in
523   duplicate. ****Significant reduction compared to the control group (p≤0.0001).

15
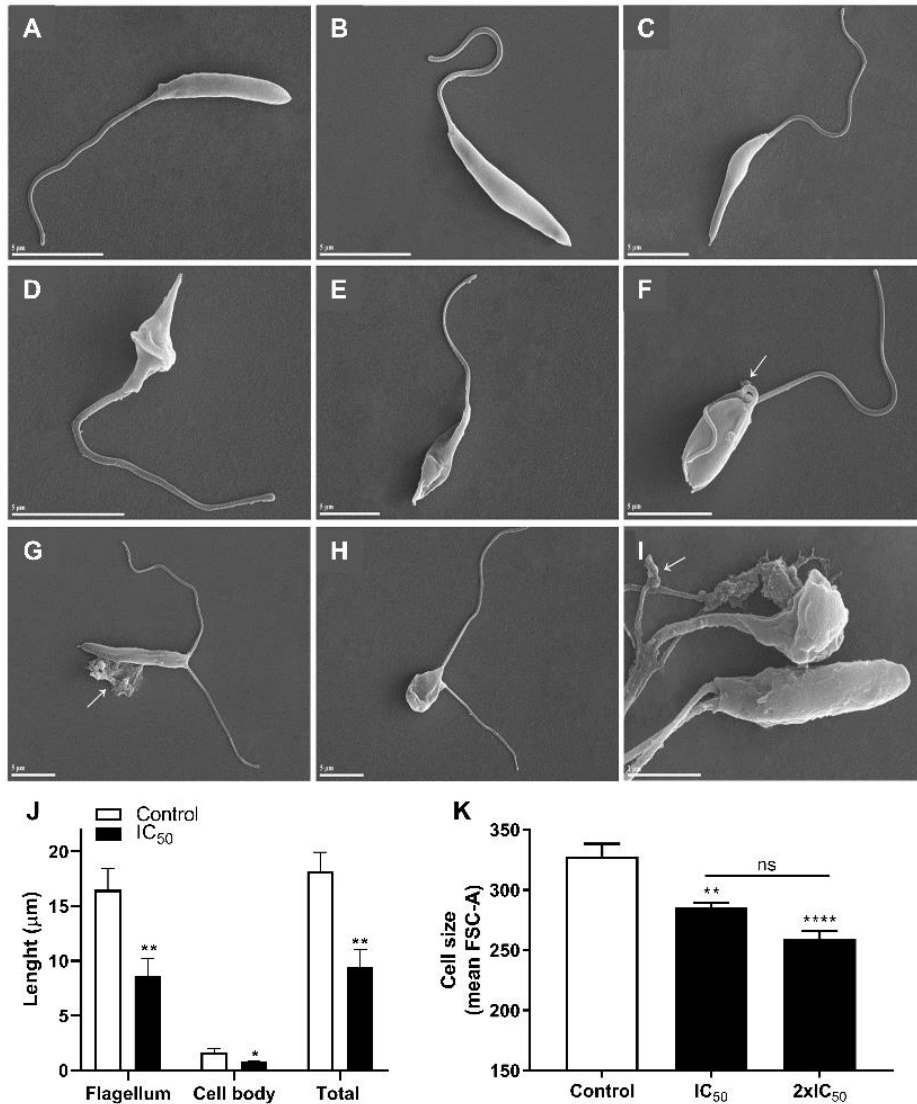
Figure 3 - Morphological changes in promastigote forms of *L. amazonensis*. The parasites were treated with IC_{50p} (16 µg/mL) of OEO for 24 h at 25 °C and analyzed by SEM. (A-B) Untreated parasites. (C) Parasites were treated with 0.01% DMSO (vehicle). (D-I) Parasites were treated with OEO IC_{50}. Arrows indicate leakage of cellular content. Scale bar = 5 µm (A-H), 2 µm (I). (J) Length of the flagellum, cell body, and total size of promastigotes were measured from SEM images using the Image Pro-plus software. (K) Flow cytometry analysis where the FSC-A was considered a function of cell size. Data represent the mean ± SEM of three independent experiments performed in duplicate. *Significant difference in relation to control ($p < 0.05$), **($p \leq 0.01$), ***($p \leq 0.001$), ****($p \leq 0.0001$).
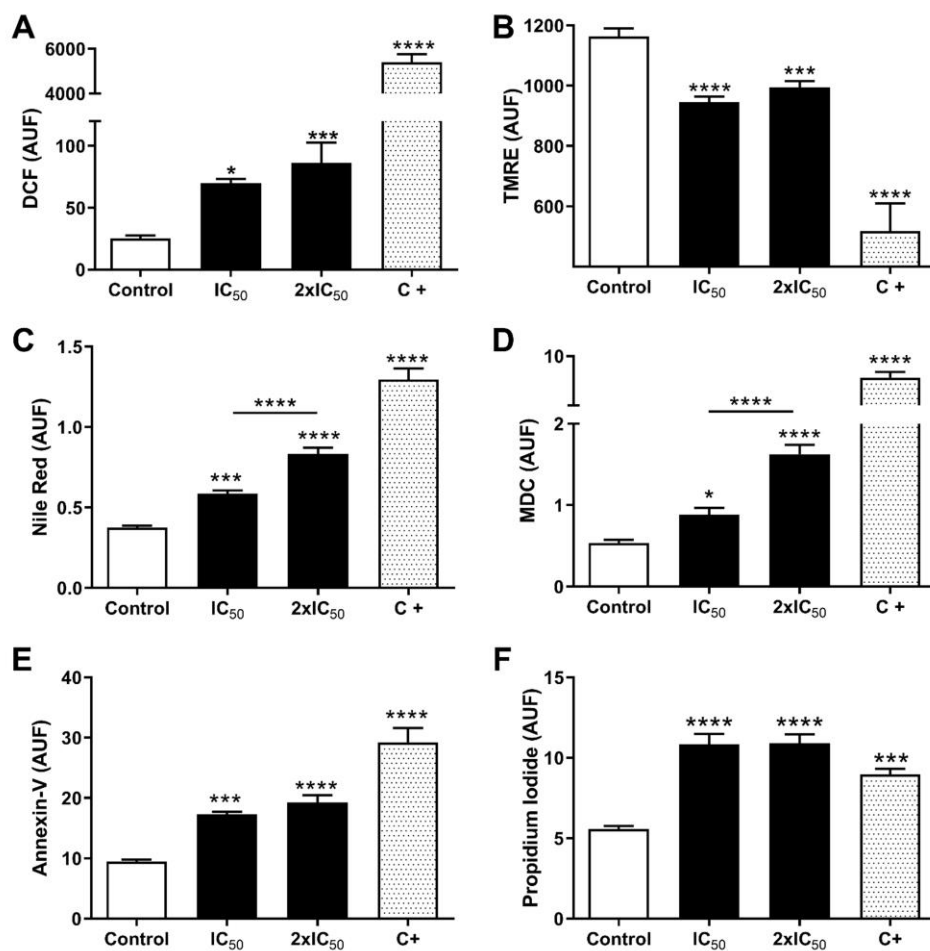
534
Figure 4 - OEO-induced death in *L. amazonensis* promastigote forms submitted to a 24 h treatment with IC$_{50p}$
535 **and 2xIC$_{50p}$.** The following methods were used for the respective assessments: (A) DCF fluorescence for reactive
536 species of oxygen measurement, (B) TMRE assay for fluorometric analysis of the mitochondrial membrane
537 potential, (C) Nile Red labeling for neutral lipid droplets accumulation labeling, and (D) monodansylcadaverine for
538 autophagic vacuoles formation, (E) annexin-V labeling for phosphatidylserine exposure detection and (F) propidium
539 iodide for membrane permeabilization. AUF – arbitrary units of fluorescence. Data represent the mean ± SEM of
540 three independent experiments performed in duplicate. *Significant difference in relation to control (p<0.05),
541 ***(p≤0.001), ****(p≤0.0001).
542
543
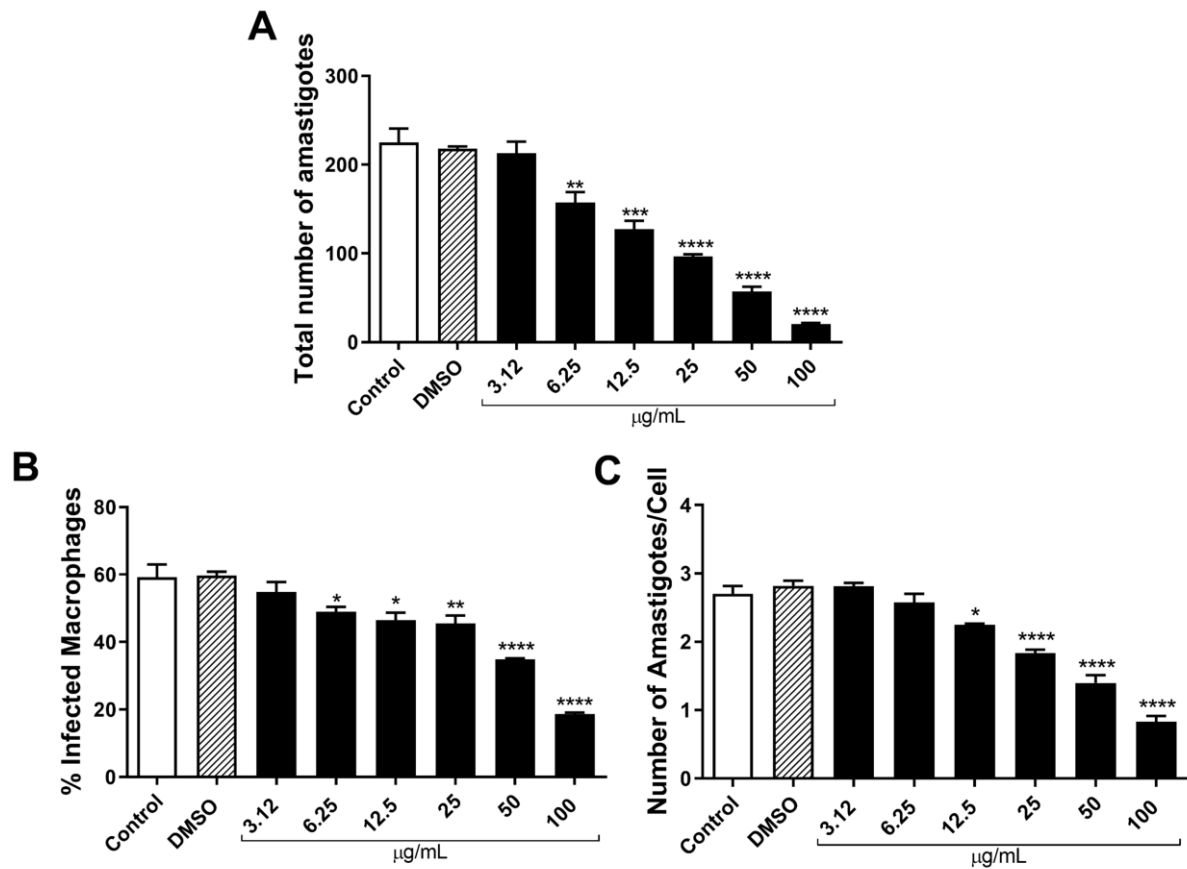
544
545 **Figure 5 - OEO-induced elimination of *L. amazonensis* intramacrophagic amastigote forms**. *L. amazonensis*-
546 infected peritoneal BALB/c macrophages were submitted to OEO treatment (3.12-100 μg/mL) or DMSO 0.01%
547 (vehicle) and were assessed as the (A) total number of amastigote forms, (B) percentage of infected macrophages,
548 and (C) number of amastigotes per macrophage. The culture medium was used as a control. The values represent
549 the mean ± SEM of three independent experiments performed in duplicate. *Significant difference compared to the
550 control ($p<0.05$), **($p \leq 0.01$), ***($p \leq 0.001$), ****($p \leq 0.0001$).
551

18

118
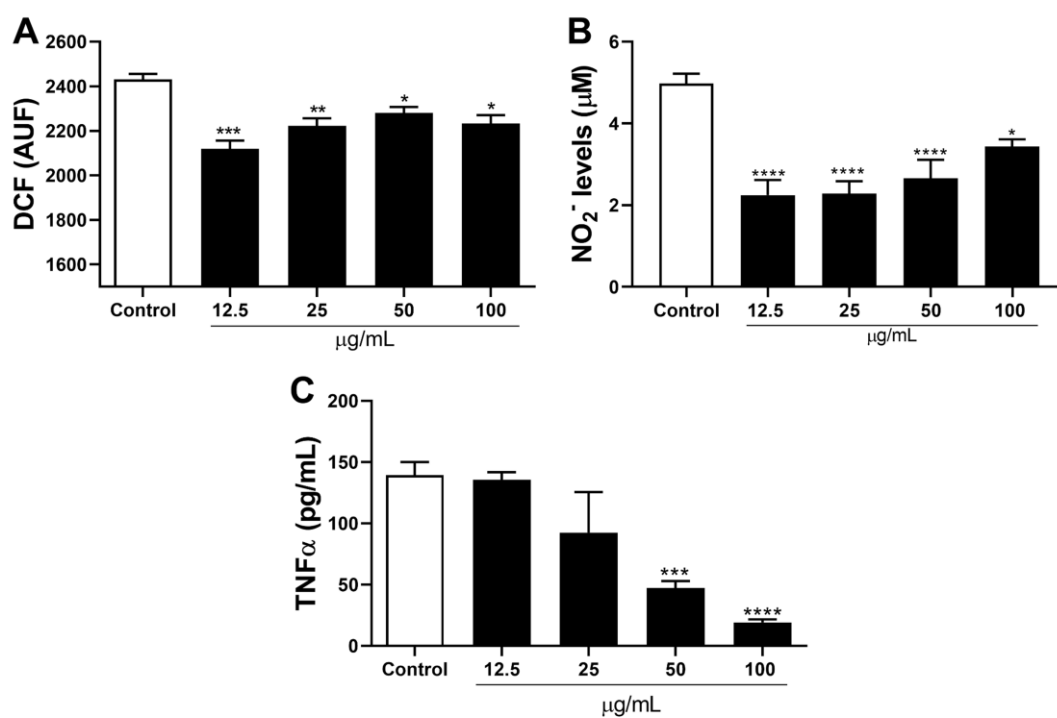
Figure 6 - Intramacrophagic *L. amazonensis* death by OEO is not dependent on ROS, NO, or TNF-α. The following methods were used for the respective assessments: (A) DCF fluorescence for reactive species of oxygen measurement, (B) Griess method for nitrite levels, and (C) ELISA for TNF-α measurement in the supernatant of culture cells. AUF – arbitrary units of fluorescence. Data represent the mean ± SEM of three independent experiments performed in duplicate. *Significant difference in relation to control ($p<0.05$), **($p \leq 0.01$), ***($p \leq 0.001$), ****($p \leq 0.0001$).
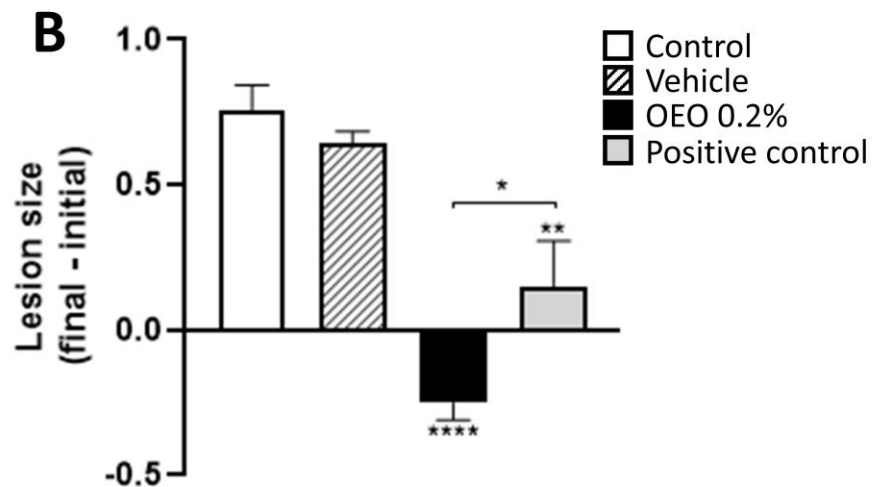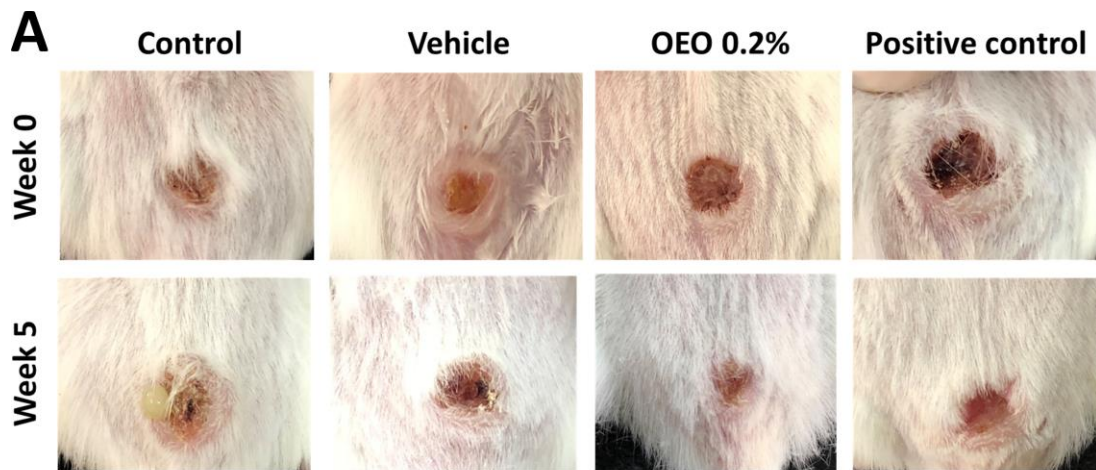
19

Figure 7 – *In vivo* activity of OEO treatment. BALB/c mice were infected in the base of the tail with *L. amazonensis* promastigotes for 100 days. After, mice were treated daily topically for five weeks or untreated (control). (A) Representative photographs of lesions before (week 0) and after (week 5) the treatments period. (B) Lesion size measurements (the initial values were subtracted from the final values). The infected groups were defined as control (untreated mice), vehicle (treated topically with the base gel), positive control (glucantime i.p., 20 mg/kg/day), or OEO (treated topically with 0.2% OEO containing gel). Data represent the mean ± SEM of lesion size for each group (n = 4). **Significant difference in relation to control and vehicle ($p \leq 0.01$), ***($p \leq 0.001$). *Significant difference between the treatments ($p < 0.05$).
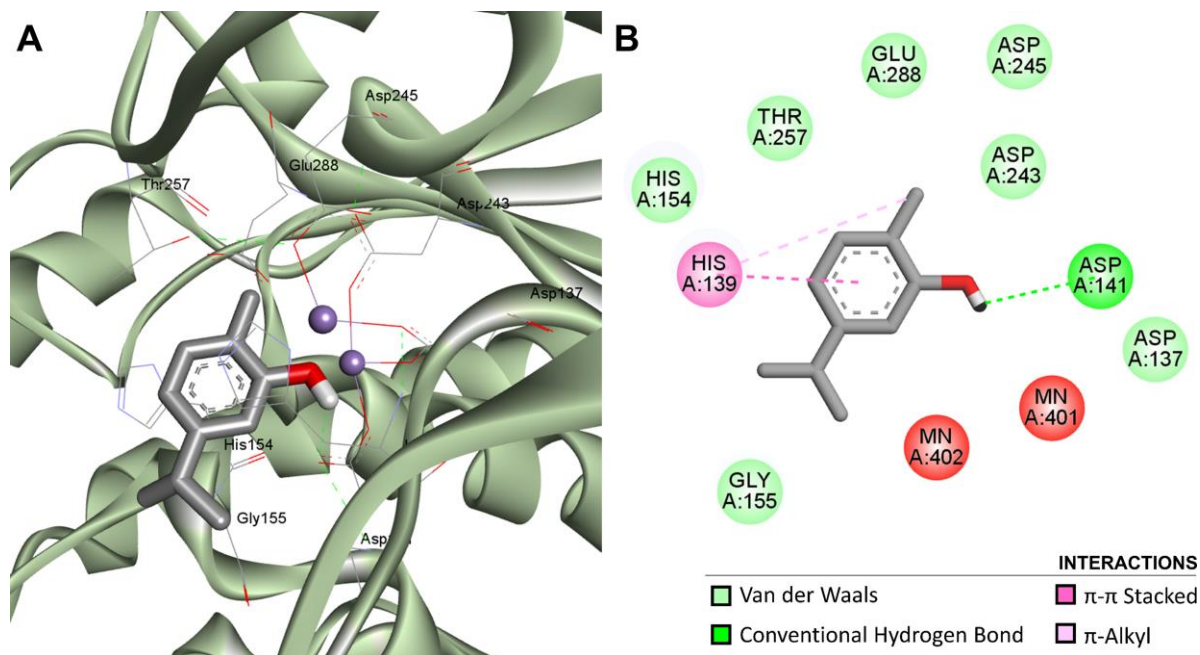
570
Figure 8 - Interaction diagrams of docking pose results of carvacrol in the active site of ARG (PDB ID: 4IU5).
(A) Putative binding profile of carvacrol (gray stick model) toward ARG active site according to the best pose.
Purple balls represent the Mn^{2+}. (B) 2D representation of residues interactions. The interactions are represented by
dashed lines.

6.2.3. Capítulo de livro

Diterpenes from plants in the breast cancer treatment: new perspectives and recent advances

> Capítulo desenvolvido para o livro *Studies in Natural Products Chemistry (Bioactive Natural Products)* da editora *Elsevier* (*status: under review*).

Fernanda Tomiotto-Pellissier[1,2]; Manoela Daiele Gonçalves[1]; Taylon Felipe Silva[1]; Virgínia Márcia Concato[1]; Bruna Taciane da Silva Bortoleti[1,2]; Nilton Syogo Arakawa[1]; Ivete Conchon-Costa[1], Wander Rogério Pavanelli[1] and Carolina Panis[1,4*]

[1] Laboratory of Immunoparasitology of neglected diseases and cancer - LIDNC, Department of Pathological Sciences, Center of Biological Sciences, State University of Londrina, Paraná, Brazil.
[2] Biosciences and Biotechnology Graduate Program, Carlos Chagas Institute (ICC), Fiocruz, Curitiba, Brazil.
[3] Laboratory of Biotransformation and Phytochemistry, Department of Chemistry, Center of Exact Sciences, State University of Londrina, Paraná, Brazil.
[4] Laboratory of Tumor Biology, State University of West Paraná, UNIOESTE, Francisco Beltrão Campus, Paraná, Brazil.
* Corresponding author.
All authors equally contributed to the manuscript.

DITERPENES FROM PLANTS IN THE BREAST CANCER TREATMENT: NEW PERSPECTIVES AND RECENT ADVANCES

Fernanda Tomiotto-Pellissier[1,2]; Manoela Daiele Gonçalves[1]; Taylon Felipe Silva[1]; Virgínia Márcia Concato[1]; Bruna Taciane da Silva Bortoleti[1,2]; Nilton Syogo Arakawa[1]; Ivete Conchon-Costa[1],Wander Rogério Pavanelli[1] and Carolina Panis [1,4*]

[1] Laboratory of Immunoparasitology of neglected diseases and cancer - LIDNC, Department of Pathological Sciences, Center of Biological Sciences, State University of Londrina, Paraná, Brazil.

[2] Biosciences and Biotechnology Graduate Program, Carlos Chagas Institute (ICC), Fiocruz, Curitiba, Brazil.

[3] Laboratory of Biotransformation and Phytochemistry, Department of Chemistry, Center of Exact Sciences, State University of Londrina, Paraná, Brazil.

[4] Laboratory of Tumor Biology, State University of West Paraná, UNIOESTE, Francisco Beltrão Campus, Paraná, Brazil.

* Corresponding author.

All authors equally contributed to the manuscript.

Abstract

A variety of plants have been a good source of therapeutic agents, mainly due to its secondary metabolites, which originate from the conversion of light energy into chemical compounds. Among these metabolites are the diterpenes, a group of structurally diverse molecules, widely distributed in nature. Diterpenes present a broad spectrum of biological activities and have been extensively studied by its antitumoral effects, with promising results.   Breast cancer is one of the most common cancers worldwide and, varying from mild and potentially curable disease to incurable manifestations using the therapy available. Therefore, the search for new drugs is urgent and necessary. We will cover in this chapter a literature update and a review regarding anti-breast cancer effects of diterpenes from plants, approaching the works published in the main databases in the period 2015-2020. The structure, mechanism of action, molecular targets, and both *in silico, in vitro*, and *in vivo* effects are presented.

Key-words: Anti-cancer; Anti-tumor; Natural Compounds; Cell Lineage; Anti-Proliferative; Metastasis; Nanotechnology; Apoptosis.

1. Introduction

Plants are complex organisms that have developed mechanisms that allow them to adapt to various stresses without harm to its cellular and developmental physiological processes, such as protection against predators (due to their bitterness), attracting pollinators, establishing symbiosis, and providing structural components for lignification of cell walls of vascular tissues. The literature shows that secondary metabolites are a central adaptation mechanism in plants (1–3).

Secondary metabolites originate from the conversion of light energy into chemical compounds, although they do not play a significant role in primary life, they are vital for plants allowing their ability to respond not only to environmental stresses but also to protect against attack by pathogens, insects, and herbivores (4). Another particularity is that these metabolites may vary according to the family, genus, or species of the plant, thus, they can be used as taxonomic markers in the botanical classification (5).

Secondary metabolites from plants can provide a range of compounds with biological activity that justifies the growing interest in the development of new drugs (6). Worldwide, approximately 25% of the drugs used are derived from plants, however, there are still over 350,000 species that have not been studied (2). Therefore, this is an area still with great possibilities of expansion and discoveries for biomedical research.

The synthesis of secondary metabolites can be carried out by different biosynthetic pathways: via malonate acetate, mevalonic acid, methylerythritol phosphate, and shikimic acid, by which the three main groups of secondary metabolites formed are phenolic compounds (biosynthesized from the shikimate pathway, containing one or more aromatic hydroxylated rings), alkaloids (nitrogenous substances, in which most are biosynthesized from amino acids) and terpenes (polymeric isoprene derivatives, biosynthesized from acetate via mevalonic acid) (7). Other groups that deserve mention are fatty acid derivatives and aromatic polyketides.

Terpenes are a large and diverse group with a wide structural variety. Having more than 60,000 known compounds (8), these structures are synthesized from isoprenoid building blocks (C5), following the "isoprene rule". The classification occurs according to the amount of isoprene in the molecule formation, such as hemiterpenes (C5), monoterpenes (C10), sesquiterpenes (C15), diterpenes (C20), sesterterpenes (C25), triterpenes (C30), and tetraterpenes (C40) (**Figure 1**) (9). The biosynthesis of terpenes in plants can occur by two pathways: via mevalonate (present in the cytosol), where it uses three units of acetyl-CoA, and via methylerythritol 4-phosphate (present in

plastids) which synthesizes isopentenyl diphosphate and dimethylallyl diphosphate in plastids (10,11).

The class of diterpenes is considered structurally diverse, widely distributed in nature, originating from the condensation of four isoprene units derived from the mevalonate or phosphate deoxylulose phosphate pathways. The latter, recently discovered, gives rise to diterpene compounds in plants. The diterpenes can be classified into different categories, the main ones being abietane, aconane, beyrane, cassiane, clerodane, gibberellane, kaurane, labdane, lathyrane, primarane, taxane, and trachylobane (**Figure 1**). In nature, they can be found in a polyoxygenated form with keto and hydroxyl groups, these are often esterified by small aliphatic or aromatic acids (12,13). Diterpenes are one of the groups most studied for their broad biological activities, such as antiprotozoal (14–16), antitumor (17–19), antioxidant (20–22), antimutagenic properties (23,24), antimicrobial (25,26). Diterpenes also have been extensively studied by their antitumoral effects, with promising results.
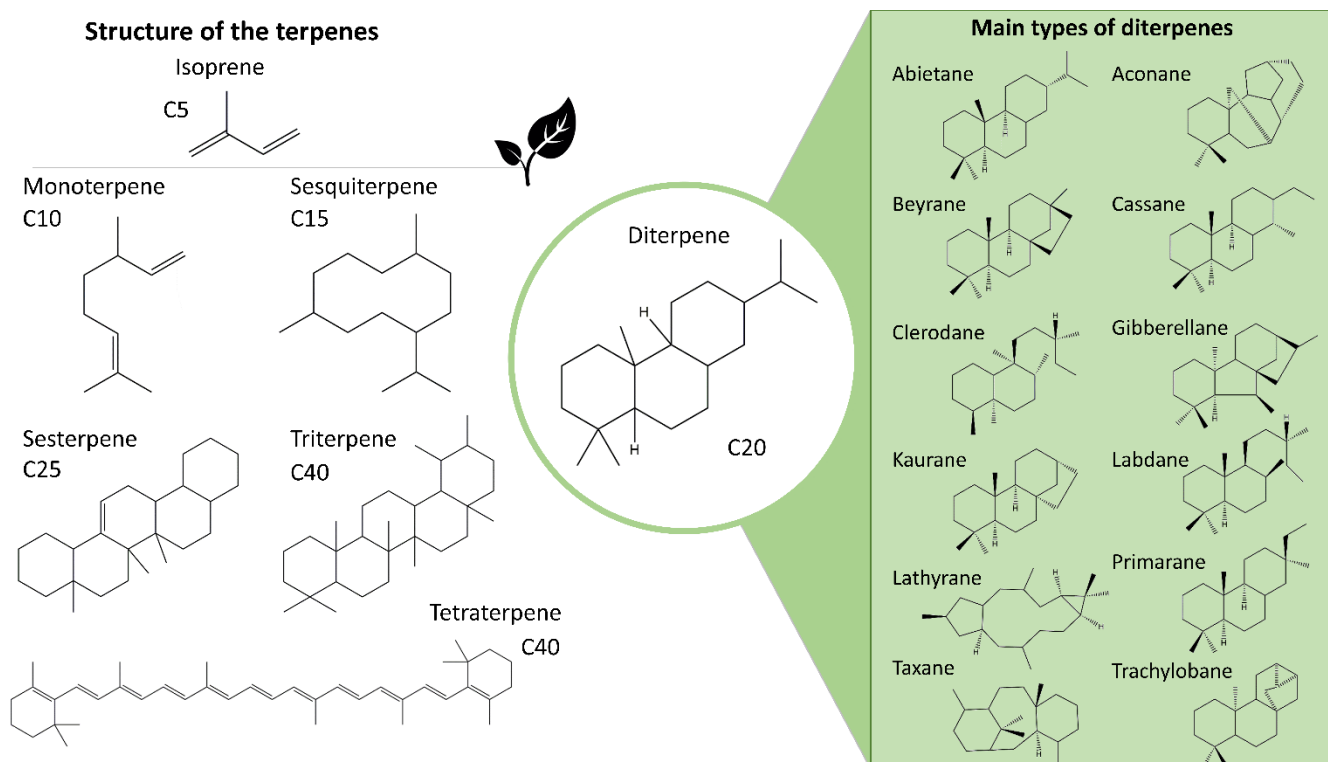
Figure 1 – Basic structure of terpenes. Terpenes are synthesized from isoprenoid building blocks (C5) and the molecules formed are classified according to the amount of isoprene in monoterpenes (C10), sesquiterpenes (C15), diterpenes (C20), sesterterpenes (C25), triterpenes (C30), and tetraterpenes (C40). The main types of diterpenes are abietane, aconane, beyrane, cassiane, clerodane, gibberellane, kaurane,labdane, lathyrane, primarane, taxane, and trachylobane.

The main example of a natural chemotherapeutic drug widely used for clinical treatment of ovarian cancer is Taxol ($C_{47}H_{51}NO_{14}$) (27). This tricyclic diterpenoid is

produced naturally in the bark and needles of *Taxus brevifolia*. It has a unique mechanism of action, promoting the assembly of tubulin in microtubules preventing the dissociation of microtubules, in addition to blocking the progression of the cell cycle, preventing mitosis by inhibiting the growth of cancer cells (28).

Breast cancer is one of the most common cancers worldwide and, depending on the time it is diagnosed, it can be early, which is considered potentially curable, and metastatic, which is considered incurable with available therapies (29). There are four main subtypes of breast cancer, that make up the majority of cases, being luminal A, which has expression of estrogen and progesterone receptors and has a slow growth rate; luminal B, which is also positive for hormone receptors, however, has a rapid growth rate; HER2 is the subtype that has a negative phenotype for hormone receptors, but has a high expression of HER2 receptors; and the fourth subtype is the triple-negative that has no expression of any of these three receptors, has an accelerated growth rate and is related to a worse prognosis. Thus, compounds that inhibit hormone-induced proliferation-inducing signaling may be effective against luminal A and B, but not against HER2 and triple-negative subtypes (30).

According to the biannual Advanced Breast Cancer Conference (ABC), systemic therapy is the first therapeutic choice in metastatic breast cancer, to promotes prolonged survival, maintaining the quality of life, mitigating symptoms, and still inhibit or reverse the development of cancer (30). Thus, new natural products that present cytotoxic activity applicable in cancer therapy are increasingly being researched (31). The main cell lines used to study breast cancer are MCF-7 (luminal A subtype); BT-474 (luminal B subtype); SKBR-3 and MDA-MD-435 (HER2 over-expression subtype); MDA-MB-231 and MCF-10 (basal subtype); and MCF-7/ADR (with multidrug resistance) (32), which will be discussed in this chapter.

According to the literature, the pharmaceutical oncology products research has 49% of medicines derived from or inspired by natural sources, such as microorganisms and marine organisms, and mainly plants (33). Thus, we will cover in this chapter updates the literature and reviews the anti-breast cancer effects of diterpenes, focusing on its chemical properties,approaching the works published in the main databases in the period 2015-2020.

2. Identification of new Diterpenes with anti-breast cancer activity

Knowing that the class of diterpenes provides compounds with important biological actions, many efforts have been concentrated on the discovery and biological characterization of new molecules of this class. This topic will address the new

diterpenes characterized by their anti-breast cancer action, the main findings are summarized in Table 1, and the detailed works are described below.

In the root bark of *Chrozophora oblongifolia*, was isolated new ent-trachylobane-3b-hydroperoxide (5) and four known compounds, ricinine (1), trimethoxy ellagic acid (2), dimethoxy ellagic acid (3), and aleurotolic acid (4). The structures of these secondary metabolites were elucidated by using different spectroscopic techniques, ^{1}H NMR, ^{13}C NMR, HSQC, HMBC, 1H-1H COSY, NOESY, HR-ESI-MS, EI-MS, and comparison with published data. Only the new compound 5 showed cytotoxicity against human breast cancer cells (MCF-7) with IC_{50} of 24.53 µM, and human hepatocyte-derived carcinoma cells (Huh-7) with IC_{50}: 34.13 µM (34).

In the leaves of *Taiwania cryptomerioides* was isolated two uncommon C37 heterodimeric diterpenoids, taicrypnacids A (1) and B (2), and a known labdane-type diterpenoid (3). To define the structures, comprehensive spectroscopic analysis, chemical conversion, X-ray crystallography, and ECD data were realized. The new compounds 1 and 2 causes cytotoxicity in human breast cancer (MCF-7) (IC_{50}: 7.4 and 9.9 µM), osteosarcoma (U-2 OS) (IC_{50}: 8.4 and 9.7 µM), and human colon carcinoma (HCT-116) (IC_{50}: 7.5 and 7.8 µM) cell lines. According to the authors, the presence of the hydroxycarbonyl group can play a crucial role in cytotoxicity, unaffected by the configurational changes in C-7 and C-14' in 1 and 2. Also, compound 1 induces an increase in intracellular Ca^{2+} concentration, ROS level, changes in the endoplasmic reticulum (ER) and mitochondria, causing cell death by activating apoptosis and autophagy. Also, compound 1 showed lower cytotoxicity to noncancerous cell line MCF-10A (35).

C18-, C19- or C20-diterpenoid alkaloids were isolated from the rhizoma of *Aconitum japonicum*, in the total of 199 natural alkaloids and their derivates isolated, 128 were non-toxic (IC_{50} > 20 or 40 µM) and 50 alkaloids present moderate antiproliferative effects (IC_{50} 10-40 µM) against five human tumor cell lines (A549, MDA-MB-231, MCF-7, KB, and MDR KB subline KB-VIN). The aconitine-type C19-diterpenoid alkaloids have been highlighted included 21 natural alkaloids, where 3 natural diterpenoid alkaloids exhibited cytotoxic activity against five human tumor cell lines A549, MDA-MB-231, MCF-7, KB, and MDR KB subline KB-VIN (Lipomesaconitine - 15 IC_{50}=17.2 ~ 21.5 µM; Lipoaconitine-16 IC_{50}= 13.7 ~ 20.3 µM; Lipomesaconitine - 17 IC_{50}: 6.0 ~ 7.3 µM) and 18 of them were inactive (IC_{50}> 20 or 40 µM), based on the results, the fatty acid ester at C-8 and the anisoyl group at C-14 found in 17 may be important to the cytotoxic activity of aconitine-type C19-diterpenoid alkaloids. (36).

Barbatin H (1), a new neo-clerodane diterpenoid, plus fifteen known analogs: scutebata P (2), scutebarbatine F (3), 6-O-nicotinoylscutebarbatine G (4), scutebata G

(5), scutebata E (6), scutebata D (7), barbatin C (8), scutebarbatine A (9), scutebarbatine G(10), scutebarbatine B (11), 6,7-di-O-acetoxybarbatin A (12), scutebata C (13), scutebata A (14), scutebar-batine X (15), and scutebata B (16) were isolated from *Scutellaria barbata*, a plant known as 'Ban zhi lian' in China. Their isolation and structures were elucidated by silica gel column, RPC18 CC, Sephadex LH-20, and preparative HPLC, characterized by NMR and HR-MS data compared to the literature. Most compounds present cytotoxicity against LoVo (colon cancer) cells. Scutebata A (14) showed significant cytotoxic activities against four tested tumor cells LoVo (IC$_{50}$: 4.57 μM), MCF-7 (IC$_{50}$: 7.68 μM), SMMC-7721 (hepatoma cancer) (IC$_{50}$: 5.31 μM) and HCT-116 (colon cancer) (IC$_{50}$: 6.23 μM). The authors suggest that the results presented by the compound, may be related to the presence of two benzoyloxy groups in C-6 and C-7, which may be closely associated with the strongest aromaticity in the benzene ring (37).

From the *Selaginella moellendorffii*, a traditional Chinese herb was isolated a new modified abietane diterpenoid (3S,4S,5R,10S)-18(4→3)-abeo-3,4,12,18-tetrahydroxy-8,11,13-abietatrien-7-one (1), and two novel dimers, selaginedorffones A (2) and B (3), featuring a new cyclohexene moiety. Their structural elucidation was realized by a combination of NMR spectroscopic analysis and ECD calculations. Selaginedorffone B (3) present cytotoxicity activity only against MCF-7 cells (IC$_{50}$ 9.0 μM), but it was inactive against SMMC-7721, SW480, HL-60, and A-549 cell lines. Also, compounds 1 and 2 were inactive against all five cancer cell lines used (38).

In the stems and twigs *Ceriops tagal*, a Chinese mangrove, four new diterpenes named tagalons A-D (1-4), comprising an isopimarane (1), two 16-nor-pimaranes (2-3), and a dolabrane (4), plus together with four known dolabranes containing a 4,18-epoxygroup, viz. tagalene I (5), 4-epitagalene I (6), tagalsin A (7), and tagalsin B (8). Their structure and the absolute configuration were elucidated by HR-ESIMS, NMR spectroscopic data and single-crystal X-ray diffraction analyses. The compound tagalene I (5) displayed potent cytotoxic effects against four human breast cancer cell lines MDA-MB-453 (IC$_{50}$ 8.97 μM), MDA-MB-231 (IC$_{50}$ 8.97 μM), SK-BR-3 (IC$_{50}$ 4.62 μM), and MT-1 (IC$_{50}$ 3.93 μM), while tagalons C (3) and D (4) exhibited cytotoxicity only against MT-1 cell line (IC$_{50}$ 3.75 and 8.07 μM) (39).

Taxus wallichiana var. mairei is a plant found southern area of the Yangtze River in China, and it was isolated a new, taxiwallinine (1), and 25 known taxane diterpenoids: taxinine J (2), 1-dehydroxy-baccatin VI (3), baccatin VI (4), 7-epi-10-deacetyltaxol (5), 10-deacetytaxol B (6), 2α, 5α, 10β- triacetoxy-14β-(2-methyl)-butyryloxy-4 (20), 11-taxadiene (7), 2α, 5α, 10β, 14β-tetra-acetoxy-4 (20), 11-taxadiene (8), 2-deacetoxyltaxinine J (9), taxinine E (10), 2α, 5α, 10β-triacetoxy-14β-propionyloxy-4 (20),

11- taxadiene (11), taxezopidine H (12), taxacin (13), 2α, 5α, 7β, 9α, 10β, 13α-hexa-acetoxy-4 (20), 11-taxadiene (14), taxuspinanane K (15), taxayuntin C (16), 7, 9, 10, 13-tetra-O-deacetylabeobacatin VI (17), baccatin V (18), baccatin IV (19), 10-deacetyl taxuyun-nanine (20), taxuspine W (21), taxin B (22), 5-dehydrotaxin B (23), 2α, 7β, 13α- triacetoxy, 5α, 9α-dihydroxy-2 (3 → 20)-abeotaxa-4 (20), 11-dien-10-one (24), 1β-hydroxybaccatin I (25) and wallifoliol (26). For the first time, the compounds 10, 12, 14, 15, 17, 21, 22, 23 were isolated from this plant. The structural elucidation was realized by HR-ESI-MS and NMR analyses. The taxiwallinine (1) and taxol has presented cytotoxicity against MCF-7 cell line (IC_{50} 20.898 µg/mL and 0.008 µg/mL) (40).

In aerial parts of *Siegesbeckia pubescens,* widely distributed in China, five new diterpenoid glycosides were isolated: Siegesides A (1), B (2), C (3), D (4), E (5), along with the known compound darutoside (6). The structural elucidation was accomplished by extensive HR-ESI-MS and NMR analysis. Siegesides A (1) showed cytotoxicity activity against MB-MDA-231 breast cancer cells (IC_{50} 0.27 µM) and the other compounds showed weak or no effects (IC_{50} >25 µM). The presence of a 15S—16 vicinal diol was an effective group for the teaching of inhibitory activities. Also, the authors showed that the number, location, and orientation of hydroxyl groups may be essential for the inhibitory effects of diterpenoids against the invasion of MB-MDA-231 cells. (41).

In the aerial parts of *Salvia leriifolia* was isolated two new (1, 2) and two known (3, 4) labdane diterpenoids, together with three other knowns compounds. The structures, confirmation, and configuration were established by 1D and 2D NMR, HR-ESI-MS, single-crystal X-ray analysis, and electronic circular dichroism spectroscopy. Compound 4 showed cytotoxicity against MCF-7 (IC_{50} 25 µM), MDA-MB231 (IC_{50} 50 µM), and DU-145 (IC_{50} 50 µM) cells. Other compounds were considerably less effective in the tumoral cell lines (IC_{50} > 10 µM) (42).

Two strobane diterpenoids, strobols A (1) and B (2), 15 new pimarane diterpenoids (3−6 and 8−18), and the known compounds kirenol (19), darutigenol (20), and ent-2β,15,16,19-tetrahydroxypimar-8(14)-ene (7) were isolated in the aerial parts of *Siegesbeckia pubescens* (Makino). The structures and configurations were established based on the interpretation of HR-ESI-MS, NMR analysis, X-ray crystallographic data, and ECD calculations. Compounds 3, 5, and 11 inhibited the EGF-induced invasion of MB-MDA-231 cells (IC_{50} 4.26, 3.45, and 9.70 µM, respectively), while other compounds have not affected MB-MDA-231 cells (IC_{50}>10 µM) (43).

Five fractions of the plant extract of *Plectranthus amboinicus* (Lour.) Spreng inhibited the viability of breast cancer MCF-7 cells, however, hexane fractions demonstrated high cytotoxic activity (average IC_{50} 8.85 µg/ml). HPLC-based

metabolic approach revealed that an abietane diterpene namely 7-acetoxy-6-hydroxyroyleanone was the main compound that contributed to the cytotoxic activity (44).

For the first time in the twigs of *Podocarpus nagi* (Podocarpaceae) was isolated two new abietane-type diterpenoids, named 1β,16-dihydroxylambertic acid (1) and 3β,16-dihydroxylambertic acid (2), along with two new ent-pimarane-type diterpenoids, name dent-2β,15,16,18-tetrahydroxypimar-8(14)-ene (3) and ent-15-oxo-2β,16,18-trihydroxypimar-8(14)-ene (4). Their structures were elucidated based on spectroscopic analyses, including 1D- and 2D-NMR, IR, CD, and HR-ESI-MS. Compounds 3 and 4 at 10 μM inhibited the proliferation of human cervical cancer HeLa cells, human lung cancer A549 cells, and human breast cancer MCF-7 cells. Also, compounds 2 and 3 inhibit NO production in LPS-stimulated RAW264.7 cells (45).

In the roots of *Euphorbia fischeriana* was isolated 23 diterpenoids (1–23), classified into five subtypes, namely, ent-rosane (1–9), ent-abietane (10–16), ent-kaurane (17), ingenane (18–22), and lathyrane (23). The chemical structures of eight new compounds, namely, euphorin A (4), B (5), C (7), D (9), E (13), F (14), G (15), and H (16) were elucidated based on extensive 1D and 2D NMR spectroscopic analyses, as well as single-crystal X-ray structure analysis. The compounds (2, 6, 7, 10, 11, 13, 16, 19, 20, 22, and 23) showed inhibitory activity on the formation of mammospheres in human breast cancer MCF-7 cells at a final concentration 10 μM. The authors suggested that an aromatic A-ring in the isolated compounds may be beneficial for the activity of ent-rosanes, and the acylation may be important for the activity of ingenanes. However, details about the action of these bioactive diterpenoids are still under investigation (46).

In *Azorella compacta* (Apiaceae), a native Chilean cushion shrub, diterpenoids were fractioned from its resin by high-speed counter-current chromatography (HSCCC). The five major compounds isolated were identified through spectroscopy as diterpenoids azorellanol (7), $13\alpha,14\alpha$-dihydroxymulin-11-en-20-oic acid (9), mulinolic acid (10), mulin-11,13-dien-20-oicacid (11), 517-acetoxy-mulinic acid (13), and new diterpenoids characterized as $13\beta,14\beta$-dihydroxymulin-11-en-20-oicacid (1), 13-epi-azorellanone (2) and 13-epi-7-deacetyl-azorellanol (3), and another four minor diterpenoids as 7-deacetyl-azorellanol (6), 13-epi-azorellanol (4), 7-acetoxy-mulin-9,12-diene (8), and 17-acetoxy-mulin-11,13-dien-20-oic (12). The structures of the new compounds were elucidated by MS, 1D–2D NMR, and molecular modeling techniques. Compounds 4, 6, 7, 8, and 11 showed good cytotoxic activity at 100 μM against MCF-7 cells. However, compound 7, was considered the most effective (IC$_{50}$ 25.64 μM). Among the azorellanes, a necessary feature for its activity is the beta acetate group at position C-7 in the skeleton for the increase of the cytotoxic effect. Besides, the alpha position of the OH group at position C-13 in the same skeleton further increases the cytotoxic effect when comparing

the cytotoxic effect of the epimers 4(OH-17 in beta position) and 7(OH-17 in alpha position (47).

In the tuber of *Icacina trichantha* were isolated seven new 17-norpimarane and (9βH)-17-norpimarane diterpenoids, icacinlactones A−G (1−7). The structures were elucidated by spectroscopic and HRMS techniques, and the absolute configuration was determined through X-ray crystallographic analysis. The known structures of icacinol, humirianthol, humirianthenolide C, and icacenone exhibited cytotoxicity, however, humirianthenolide C was the most active against MDA-MB-435 (IC$_{50}$ 0.7 μM) and MDA-MB-231 cells (IC$_{50}$ 0.7 μM) and the new icacinlactone F (6) was moderately active against MDA-MB-435 (IC$_{50}$ 6.16 μM), MDA-MB-231 (IC$_{50}$ 8.94 μM), and OVCAR3 (IC$_{50}$ 10.50 μM) cancer cell lines (48).

In the *Casearia graveolens* twigs was isolated a new clerodane diterpene, caseariagraveolin (1), together with six known compounds casearlucin G (2), casearvestrin C (3), casearvestrin B (4), caseargrewiin L (5), casearvestrin A (6) and caseamembrol B (7). Their structures were elucidated by 1H and 13C NMR, 1H-1H COSY, HMQC, HMBC, 2D NOESY, and mass spectra data. Caseariagraveolin (1) showed cytotoxicity against oral cavity KB (IC$_{50}$ 2.48 μM) and breast cancer MCF-7 (IC$_{50}$ 6.63 μM) cell lines (49).

Phytochemical investigation of the leaves of *Casearia grewiifolia* was isolated two new clerodane diterpenoids named 1 and 2 and the known compound caseanigrescen D (3). Caseagrewifolin B (2) had inhibitory activity against cancer cell lines as KB (mouth epidermal carcinoma) and HepG-2 (human liver hepatocellular carcinoma) and exhibited a significant selective inhibition in comparison with normal cells (NIH/3T3), but no effect against MCF-7 cells, while caseanigrescen D (3) was cytotoxic against four cancer cell lines KB, HepG-2, LU-1 (human lung adenocarcinoma), and also MCF-7, however, it had no selective inhibition compared with normal cells (50).

Most of the new diterpenes isolated by plants have good cytotoxicity against breast cancer cell lines, with IC$_{50}$ ranging from 0.23 to 25.64 μM, indicating a good potency. However, some new diterpenes, despite being unprecedented, were not effective against cancer cell lines.

Is the case of the study performed by He et al. (2020), which has proposed isolation of two new diterpenoid alkaloids: delphatisine D (1), chrysotrichumine A (2), and ten known diterpenoid alkaloids: sharwuphinine A (3), delphatisine A (4), lycoctonine (5), davidisine B (6), delsemine A (7), delavaine A (8), isodelpheline (9), delpheline (10), delcorine (11), del-brusine (12) and 3β,6α-dihydroxysclareolida (13), isolated from *Delphinium chrysotrichum*, a plant native to China. For the first time, a sesquiterpene compound 13 was isolated from this genus. The isolation, structure, and molecular

formula were elucidated by spectroscopic analysis as HRESIM data, ^{1}H,^{13}C NMR, DEPT, HSQC spectra, ^{1}H-^{1}H COSY, and HMBC spectrum. However, none of the new compounds present cytotoxicity against human breast cancer cell lines of MCF-7 and MDA-MB-23, and among the known ones, only compound 7 has activity against MDA-MB-23 at 100 μM (51).

In the same way, eighteen new cembrane-type diterpenoids named Boscartins (1–18) and eight known analogs isolated from *Boswellia carterii* didn't show cytotoxicity activity (IC$_{50}$>10 μM) against five human tumor cell lines: HCT-8 (human ileocecal adenocarcinoma), Bel-7402 (human hepatoma), BGC-823 (human gastric cancer), A549 (human lung epithelial), and A2780 (human ovarian cancer) (52).

From the plant, *Salvia sahendica* was isolated six compounds: as a new norditerpene (1), and known terpenoids, sclareol (2), oleanolic acid (3), β-sitosterol (4), salvigenin (5) and 3α-hydroxy-11α,12α-epoxyoleanan-28,13β-olide (6). The inedited compound showed no toxicity, but sclareol (2) and toxol revealed a moderate cytotoxic activity against the MDA-MB-231 cancer cell line (IC$_{50}$ 81.0 and 0.23 μM) (53).

Similarly, from *Akebia quinata*, one new diterpene glycoside (1) and 13 known compounds (2–14) were isolated. Compounds cyrtophyllones B (2), uncinatone (3), 3-*O*-α-l-arabinopyranosyl olean-12-en-28-oic acid (6), 3-*O*-[β-d-glucopyranosyl(1-4)-α-l-arabinopyranosyl)]olean-12-en-28-oic acid (8), and 2α,3α,23-trihydroxyoleane-12-en-28-oic acid (11) showed inhibitory effects on the PTP1B enzyme, and concentration-dependent cytotoxic effects mainly by inducing cell apoptosis on breast cancer cell lines, such as MCF7, MDA-MB-231, and tamoxifen-resistant MCF7 (MCF7/TAMR) (IC$_{50}$ ranging from 0.84 to 7.91 μM), but the new compound did not affect breast cancer cell lines. The presence of a COOH group at C-28 in triterpene compounds (6, 8, and 11) showed a significant increase in inhibitory activity against the PTP1B enzyme. Also, compound 6 showed increased activity due to having one less glucopyranosyl, which is linked to arabinopyranyl C-3′. The presence of an alcohol group at C-23 may decrease the inhibitory effects on PTP1B. (54).

Finally, eight new diterpenoids were isolated from *Kaempferia pulchra* of Myanmar: kaempulchraols A−H, and five known analogues: 9α-hydroxyisopimara-8, 15-dien-7-one, 117β,9α-dihydroxypimara-8, 15-diene, 121α,11α-dihydroxypimara-8, 15-diene, 13 sandar-acopimaradien-1α,2α-diol, and (2R)-ent-2-hydroxyisopi-mara-8, 15-diene. None of the isolated compounds present antiproliferative activity against A549, HeLa, PANC-1, PSN-1, and MDA-MB-23 human cancer cell lines, except Kaempulchraol F, that exhibited activity against the human pancreatic PSN-1 cell line (IC$_{50}$ 12.3 μM) (55).

Table 1 – The new identified diterpenes with anti-breast cancer activity.

New diterpen	Plant source	Cell line	IC$_{50}$	Ref
Delsemine A	*Delphinium chrysotrichum*	MDA-MB-23	ND	(51)
Ent-trachylobane-3b-hydroperoxide	*Chrozophora oblongifolia*	MCF-7	24.53 µM	(34)
Taicrypnacids A and B	*Taiwania cryptomerioides*	MCF-7	9.9 µM	(35)
Lipomesaconitine	*Aconitum japonicum*	MDA-MB-231 and MCF-7	20 and 19 µM	(36)
Lipoaconitine			15.5 and 16 µM	
Lipomesaconitine			6 and 6.7 µM	
Scutebata A	*Scutellaria barbata*	LoVo, MCF-7, SMMC-7721, and HCT-116	4.57 µM, 7.68 µM, 5.31 µM, and 6.23 µM	(37)
Selaginedorffone B	*Selaginella moellendorffii*	MCF-7	9.0 µM	(38)
Tagalene I	*Ceriops tagal*	MDA-MB-453 and MDA-MB-231	8.97 µM	(39)
Taxiwallinine	*Taxus wallichiana var. mairei*	MCF-7	20.89 µg/mL	(40)
Siegesides A	*Siegesbeckia pubescens*	MB-MDA-231	0.27 µM	(41)
Pimarane diterpenoid 3	*Siegesbeckia pubescens*	MB-MDA-231	4.26 µM	(43)
Pimarane diterpenoid 5			3.45 µM	
Pimarane diterpenoid 11			9.7 µM	
15,16,18-tetrahydroxypimar-8(14)-ene	*Podocarpus nagi*	MCF-7	ND	(45)
Ent-15-oxo-2β,16,18-trihydroxypimar-8(14)-ene			ND	
Euphorin C, E, and H	*Euphorbia fischeriana*	MCF-7	ND	(46)
Azorellanol	*Azorella compacta*	MCF-7	25.64 µM	(47)
Humirianthenolide C	*Icacina trichantha*	MDA-MB-435 and MDA-MB-231	0.7 µM	(48)

		MDA-MB-435 and MDA-MB-231	6.16 and 8.94 µM	
Icacinlactone F				
Casearia graveolin	*Casearia graveolens*	MCF-7	6.63 µM	(49)

IC$_{50}$: inhibitory concentration for 50% of cells, ND: non-determined.

3. Diterpenes with antiproliferative activity

The chemoprevention of breast cancer is based on chemical compounds capable of inhibiting or reversing the proliferation of cancer cells, thus, new natural products that obtain antiproliferative activity applicable in cancer therapy are increasingly being researched (31).

In the study by Lu et al., (2016) (56), it was observed that when treating two human breast cancer cell lines (AS-B145 and BT-474) with ovatodiolide (Ova) (extracted from *Anisomeles indica (L.) Kuntze*), the compound showed a reduction in the proliferation of these cells, obtaining IC$_{50}$ values of 6.55 and 4.80 µM, respectively. In addition, the authors, to enrich and analyze the self-renewal capacity of these strains, used a cluster of mammary tumor cells with stem/progenitor (mammosphere) properties and tested with the same diterpene. They observed that Ova was able to reduce the self-renewal property, to inhibit the expression of stemness genes [including octamer-binding transcription factor 4 (Oct4), Nanog and heat shock protein 27 (Hsp27) and regulate positively the regulatory factor 2 of ubiquitin SMAD (SMURF2). Such data reveal the potential of Ova in the treatment of breast cancer.

In 2017, Win et al., (2017) (57) after isolating 17 bicyclic diterpenoids from the *Curcuma amada* evaluated their antiproliferative activities against the lines MCF-7, HeLa, A549, PANC-1, and PSN-1 (human pancreatic cancer). In the present investigation, compounds 1 and 6 were not effective with any lineage, while compounds 2-4, 7, 8, 12, and 17 were found to be moderately active against the tested cells. Interestingly, (E)-14-hydroxy-15-norlabda-8(17),12-dien-16-al (11) selectively inhibited the proliferation of HeLa, PSN-1 and MCF-7 cells. Structure-activity relationship analyses against PANC-1 and PSN-1 cells suggested that the hydroxymethyl functionality at C-13 might be important to inhibit the proliferation of human pancreatic cancer cell lines, and may also be responsible for the effect on MCF-7 cells.

Triple-negative breast cancers (TNBCs) are considered irresponsible to current therapies because they are more aggressive, have early recurrence and metastases. Thus, Varghese et al., (2018) (58) when evaluating the antiproliferative activity of triptolide, isolated from *Tripterigium wilfordii*, on MDA-MB-231, MDA-MB-468, and MCF-

7, found that the compound was able to inhibit growth, being more evident in MDA-MB-231 after 72 hours of treatment ($IC_{50} > 0.3$ nM). Besides, there was a halt in the cell cycle in the sub-G0/G1 phase and a reduction in G0/G1, an increase in autophagy, and the treatment activated the caspase 3-dependent apoptotic pathway, thus promoting the death of this cell.

In the same year, Awasthee et al., (2018) (59) demonstrated that bharangin, a diterpene isolated from *Pigmacopremna herbacea*, also reduced the proliferation of MCF-7, MDA-MB-231, MDA-MB-453, MDA-MB-468, and T-47D cells. Also, treatment with this diterpene inhibited the migration and invasion of MDA-MB-231, altered the potential of the mitochondrial membrane, reduced proteins associated with cell survival (Bcl-2, Bcl-xL, and survivin), increased levels of Bax (pro-apoptotic) and promoted death by apoptosis, mediated by an increase in caspase-7 and 9. Also, the authors showed that bharangin acts in the MDA-MB-231 line by suppressing the activation of NF-κB and modulates the expression of lncRNAs (long non-coding RNA), a class of non- coding-protein transcripts, which aberrant expression can act as an oncogene.

In the same way, triptolide was investigated for its antiproliferative effects on tumor lines MCF-7 and MDA-MB-231, as well as for its antitumor action on BALB/c-nu+/nu+ female mice. *In vitro*, the tested compound has been shown to exert potent effects in inhibiting cell viability, mediated through the attenuation and overexpression of ERα in MCF-7 and MDA-MB-231, respectively. In the *in vivo* study, the mice xenografted with MCF-7 and MDA-MB-231 were able to reduce the weight and volume of the tumor, being more evident in MCF-7 (60).

Parvifloron F, a highly oxidized bioactive abiethane diterpene, and its synthetic intermediates were studied on MDA-MB- 231 and MCF-7 cells, besides A549, nasopharyngeal squamous cell carcinoma (KB) and underlines KB MDR overexpressing P glycoprotein (KB-VIN). Some of the molecules, including parvifloron F, presented good antiproliferative effects. The compounds containing methoxy groups exhibited moderate activity on the cell lines, and that the stereochemistry of molecules did not influence the activity. On the other side, the oxidation level of the abietane ring seemed to be important for the antiproliferative and selective activity of the active compounds (61).

4. Inhibition of tumor angiogenesis and metastasis by diterpenes

Metastasis is an important prognostic factor in breast cancer since around 90% of deaths are not associated with the primary tumor, but with metastasis to distant sites (62). Studies indicate that the cell adhesion to the extracellular matrix (ECM), the structural and functional changes in epithelial cells that permit their migration through the basement membrane, called epithelial-mesenchymal transition, and angiogenesis are

the main mechanisms involved in breast cancer metastasis. The angiogenesis is directly related to the availability of vascular endothelium growth factor (VEGF), which is essential for tumor neovascularization. Therefore, screening for compounds with the ability to control breast cancer metastasis is essential for improving breast cancer treatment (63). Some diterpenoids from plants have been studied about its capacity to inhibit the angiogenesis in breast cancer models, with promising results.

In this sense, Sun et al., (2015) (64) evaluated the anti-metastatic effect of jolkinolide B (JB), a compound isolated from *Euphorbia fischeriana* Steud, on MDA-MB-231, U251 (glioblastoma multiforme), DU145 (prostate cancer), MGC803 (gastric mucinous adenocarcinoma), K562 (erythroleukemic), A549 (lung carcinoma), Bcap37 (endocervical adenocarcinoma), and ACHN (Papillary renal cell carcinoma) cell lines. The authors demonstrated that the higher expression of β1-integrin (molecules that mediate tumor cell adhesion to ECM) and FAK (focal adhesion kinase) were more expressed in MDA-MB-231, however, after treatment with JB, cell adhesion and invasion were inhibited, in addition to positively regulating the expression of β1-integrin protein and blocking FAK phosphorylation. Thus, these data contribute to the development of new strategies for the treatment of breast cancer metastasis.

In the same way, Carnosol, a phenolic diterpene extracted from culinary herbs such as oregano and rosemary, presented *in vitro* antimetastatic action, mitigating the migration and invasion of breast cancer cells MDA-MB-231 by downregulating activity and reducing metalloproteinase 9 expressions. Also, carnosol is still able to inhibit the STAT3 signaling pathway, as it induces its proteasomal degradation in a manner dependent on reactive oxygen species. Thus, the reduction in both the activity of metalloproteinase 9 and STAT3 in vitro implies that carnosol may have a promising effect in reducing the degradation of the extracellular matrix, inhibiting the metastasis of breast cancers. Besides, carnosol-induced ROS production in breast cancer cells culminates in cell death from apoptosis and autophagy and is therefore a promising compound for the development of new therapeutic approaches in breast cancer (65).

Cembranoids are carbocyclic diterpenes widely present in the plants belonging to the genera *Nicotiana* (44). The cembranoid 1S,2E,4S,6R,7E,11E)-2,7,11-cembratriene-4,6-diol (CDO) isolated from *Nicotiana tabacum* presented significantly reduced VEGFR2 levels in TNBC MDA-MB-231 and BT-474 breast cancer cell lines and showed anti-migratory activity against the TNBC MDA-MB-231. *In vivo*, the intraperitoneal treatment of CDO (40 mg/kg, 3 times/week) significantly reduced the MDA-MB-231 cells breast tumor size in athymic nude mice, with significant downregulation of the vasculogenesis marker CD31 and suppression of VEGFR2-paxillin-FAK pathway. Similar results were found in the swiss albino mice-Matrigel model, which mimic the *in vivo* capillary formation

process, confirming the antiangiogenic potential of CDO. Chemically, CDO consists of 14-membered macrocyclic diterpene skeleton with hydroxyl, methyl, and isopropyl substituents. The docking studies showed that C-4 and C-6 hydroxyl groups are responsible for potent interactions with different amino acids of VEGFR2 (1Y6A and 3CJF). The C-19 and C-20 methyl groups of CDO also promoted favorable interactions with the predicted protein, promoting its inhibition (66).

Oridonin, an active diterpenoid compound isolated from *Rabdosia rubescens*, induced a significant reduction of the migration, invasion, and adhesion of MDA-MB-231 and 4T1 breast cancer cells, and inhibition of tube formation of human umbilical vein endothelial cells in a dose-dependent manner. Oridonin also caused increases in the expression levels of E-cadherin, and decreased expression of N-cadherin, vimentin, and snail, inhibiting the epithelial-mesenchymal transition. Besides that, oridonin exerted its anti-angiogenesis activity through significantly decreasing HIF-1α, VEGF-A, and VEGF receptor-2 protein expression. Furthermore, oridonin was demonstrated to decrease the micro-vessel density as evidenced by the decreased expression of cluster of differentiation 31, a marker for neovasculature. Thus, oridonin seems to be a good candidate for new studies, since it presented important anti-metastatic features (62).

Zebrafish model was used to study the effect against vein formation of eriocalyxin B (EriB), a natural *ent*-kaurane diterpenoid isolated from *Isodon eriocalyx var. laxiflora*. EriB induced alteration of several angiogenic genes, inhibiting the subintestinal vein formation in zebrafish embryos. In human umbilical vein endothelial cells (UVEC), EriB treatment (50, 100 nM) inhibited the VEGF-induced cell proliferation via suppression of VEGFR-2-mediated downstream signaling pathway, tube formation, cell migration, and cell invasion, together with G1 arrest via the down-regulation of p21-cyclin D1/CDK4-pRb pathway. The *in vivo* C57 mice-Matrigel model showed the further anti-angiogenic effect of EriB, with a reduction of blood vessels formation. Lastly, in BALB/c mouse 4T1 breast tumor model proved that Erib (5 mg/kg/day via intraperitoneal for 21 days) presented anti-tumor and anti-angiogenic activities by reduction on tumor weight, cell proliferation, cell growth, and microvessel density. Also, molecular docking studies showed that EriB could stably bind at the ATP-binding site of VEGFR-2, with seven amino acids actively involved. The findings indicated that the interactions of EriB to VEGFR-2 resulted in the competitive inhibition to ATP against VEGFR-2, leading to the prevention of VEGFR-2 phosphorylation. Therefore, EriB exhibited significant anti-angiogenesis activity through the modulation of the VEGFR-2 mediated signaling pathway both *in silico*, *in vitro,* and *in vivo* (67).

The diterpenoid lactone andrographolide (andro) isolated from *Andrographis paniculata* presented an inhibitory effect against MDA-MB-231, BT-549, MCF-7, MDA-

MB-361, and T47D cell lines. When investigated the mechanism of action of this diterpenoid it was found induction of apoptosis in both MDA-MB-231and MCF-7 cells by activation of cytochrome c and caspase-dependent apoptotic signaling pathway. Andro treatment *in vitro* also significantly downregulates the COX-2 expression and NF-κB signaling in MDA-MB-231 cells, and could significantly inhibit the migration, invasion, and tubulogenesis of HUVECs *in vitro*. To confirm its anti-angiogenic activity, human breast cancer xenograft nude mice model was established and the treatment (5 and 10 mg/kg) by intraperitoneal injection every 2 days for 15 days induced an important reduction of the tumor volume and weight, with concomitant reduction of COX-2, microvessel number and expression levels of CD31, when compared with the control group. Therefore, these results may indicate that andro inhibited breast cancer growth and tumor angiogenesis *in vivo* (68).

5. Induction of cell death mechanisms by diterpenes

Regulated cell death is a biological phenomenon resulting from natural homeostatic processes that replace senescent and damaged cells or as a result of diseases (69). On the other hand, the deregulation of the machinery of control and induction of cell death can allow cells with genomic lesions to survive, which initiates the process of carcinogenesis and permit its uncontrolled proliferation. Anticancer therapy is based on the principle of inhibiting cell proliferation and blocking / stimulating signaling pathways that culminate in the death of these aberrant cells (70). Thus, compounds with the ability to selectively induce the death of cancer cells are potential candidates for oncotherapy.

However, the high clinical, morphological, and biological heterogeneity of cancers makes the process of generating a new treatment extremely complex and laborious. Therefore, understanding how new compounds interact with cell signaling and the mechanism by which it induces death in these cells is fundamental (71).

A diterpenoid glycoside compound 6E,0E,14Z-(3S)-17-hydroxygeranyllinalool-17-O-β-d-glucopyranosyl-(1→2)-[α-l-rhamnopyranosyl-(1→6)]-β-d-glucopyranoside isolated from methanol extract of leaves *Blumea lacera* showed *in vitro* cytotoxic activity against two types of human breast cancer cell lines MCF-7 and MDA-MB-231 and the human stomach adenocarcinoma cell line AGS. Moreover, the compound showed low toxicity in healthy cell lines, such as NIH3T3 and VERO. In this study, the absence of the β-d-glucopyranose on the C-3 oxygen contributed to the significantly cytotoxic activity detected for the compound (72).

Parvifloron D (ParvD), 6,7-dehydroroyleanone (DeRoy,1), and 7-acetoxy-6-hydroxyroyleanone (Roy, 2) are abietan diterpenoid compounds found mostly in plants

of the genus *Plectranthus*, that have been promising in the *in vitro* treatment of breast cancer cells MCF-7, SkBr3, SUM159, and SUM159 sphere. Also, the *in silico* analysis showed that 1-3 was predicted as isozyme-selective PKC binders (73). PKC family has been intimately associated with proliferation, migration, differentiation, invasion, tumorigenesis, metastasis, and apoptosis of cancer cells (74) . Isca et al. 2020 showed that changes in the binding site of PKC isoform change the predicted interaction profiles of the ligands 1-3. Also, minor changes in 1-3 substitution patterns, such as a double substitution only with non-substituted phenyls, or hydroxybenzoate at position four that flips the binding mode, can increase the predicted interactions in certain PKC isoforms. Compound 3 presented the best-calculated interaction profile, given its good interactions of the core structure and amino acid residues in the PKC binding site, as well as experimental inhibition against all cell types, including the most aggressive form. Also, the authors found that substitution groups of the royleanone core (1 and 2), such as hydroxybenzoate on position 4, can provide a better docked binding pose, and they also suggested that further modification in the 1,1-methyl groups can improve its interaction with PKC residues (73). Corroborating with these data, another work showed that compound 1 still can induce apoptosis and arrest the cell cycle in the sub-G1 phase, in addition to reducing the invasive and migratory capacity of MDA-MB-231 cells (75).

Similarly, carnosic acid, a phenolic diterpene found in culinary herbs such as rosemary, has antiproliferative activity in MCF-7 breast cancer cell lines. When used concomitantly with tamoxifen, a standard compound used to treat estrogen receptor-positive breast cancer, carnosic acid was able to induce caspase-3-mediated apoptosis and downregulate the production of anti-apoptotic proteins like Bcl-xl and Bcl-2 and induce pro-apoptotic signals from Bax and Bad. Further, the carnosic acid treatment induced an increase in the activity of the p53 protein, which plays a central role in controlling the replication of aberrant cells, and tumor necrosis factor-related apoptosis-inducing ligand (TRAIL), which can quickly induce apoptosis in different types of cancer. Thus, the pro-apoptotic activity of carnosic acid is related to the induction of the TRAIL / p53 axis and activation of mitochondrial signaling that induces cell death. It is worth highlight that although *in vitro* monotherapy with carnosic acid induces apoptosis and activates death signaling molecules, tamoxifen co-treatment showed more marked and promising results. Besides, concomitant treatment of carnosic acid and tamoxifen inhibited tumor growth *in vivo* of xerographic models of breast cancer with apoptosis induction without generating toxicity (76).

Traditional Chinese medicine is widely used to treat cancer in China. In the herbs used in this type of treatment, oridonin (7,20-epoxy-ent-kauranes) is found in abundance and, therefore, several studies have used it in the development of new therapies for

cancer. About breast cancer, oridonin and oridonine phosphate (from Shifeng biocorporation) were able to inhibit the proliferation of cells of MDA-MB-436 and MDA-MB-231 lineages. Moreover, oridonine phosphate induced apoptosis of breast cancer cells MDA-MB-436, with downregulation of anti-apoptotic proteins such as Bcl-2 and upregulation of caspase-3 and Bax both pro-apoptotic, in addition to occurring caspase-9 activation. The treatment with oridonine phosphate also stimulated autophagy, with an increase in proteins related to the formation of autophagic vacuoles such as beclin-1 and LC-II, however when cells were treated with a 3-methyladenine autophagy inhibitor, the pro-apoptotic effect observed was abolished, indicating that oridonine phosphate induces autophagy-mediated apoptosis in breast cancer cell lines. The best effects found in the compound with the addition of phosphate groups can be explained because molecules attaching to phosphate groups could be easily transported into cells. Additionally, the phosphate group helps to maintain solubility, stability, and a longer half-life time (77).

In the same way, oridonin was also able to induce apoptosis in lung cancer 4T1 cells *in vitro* and inhibit tumor growth of these cells in a xerographic model of breast cancer in nude mice in a dose-dependent manner, significantly inhibiting the cell's invasive capacity by blocking the expression of Notch receptors 1 to 4. When the expression of Notch 1 receptors was hyperstimulated in cells by transfection with plasmids pEGFP-Notch 1, the effect of oridonine was less, indicating that its anti-tumor effect occurs by inhibiting Notch receptors (78).

Similarly, triptolide (from A.G. Scientific, Inc.), another natural compound extracted from herbs commonly used in traditional Chinese medicine, has antitumor activity *in vitro* and induces apoptosis in MCF-7 and MDA-MB-231 breast cancer cells when used concomitantly with a low dose of TNF-α. This effect was due to the induction of caspase-3 activation. Further, the combined triptolide and TNF-α therapy reduced the expression of IκB, XIAP, and cIAP1/2, which culminates in the activation of caspase-9, impairs the activation of the NF-κB signaling pathway, leading to apoptosis (79).

Another diterpene compound extracted from herbs (*Salvia corrugata*), 7β-acetoxy-20-hydroxy-19,20-epoxyroyleanone (AHE), presented an inhibitory effect against MCF10A, SKBR-3, and BT474 cell lines. Also, in SKBR-3 and BT474 cells, AHE induced a complex mechanism that involves cell cycle arrest in the G0/G1 phase, mitochondrial network collapse, induction of reactive oxygen species formation, and activation of ERK1/2 kinase pathway. These events lead to apoptotic death of both breast cancer cell lineages (80).

The use of diterpenic quinones (Cryptotanshinone, dihydrotanshinone I, tanshinone I, tanshinone II A) isolated from Danshen (*Radix Salviae Miltiorrhizae*) has

been studied about its therapeutic potential for the treatment of cancer, with an inhibitory effect *in vitro* on the growth of tumor cell lines, with a more prominent effect on breast cancer cells, such as MCF-7. Besides, treatment with diterpenic quinones induced the activation of caspase 3 and 9 and stimulated the caspase-mediated cleavage of Poly (ADP-ribose) polymerase (PARP), leading to its inactivation. PARP is a protein involved in DNA repair, genomic stability, and apoptosis control, plays an important role in oncogenesis, as it stabilizes the broken DNA strand for homologous recombination repair (HRR)-dependent repair. However, in HRR-defective cancer, classically those with BRCA1 and 2 mutations such as breast and ovarian cancer, PARP activity can prolong cell life and favor cancer development (81). On the other hand, the cleavage of PARP, as observed in the treatment with diterpenic quinones, leads to the separation of the protein into two subunits, one of which remains with the ability to bind to the injured DNA, but without its second subunit, it loses the ability to initiate DNA repair and acts as a pro-apoptotic stimulus (82). Treatment with diterpenic quinones further stimulated dose-dependent induction of p-JNK, caspase-12, and p-eif2α, and reduced ATF4, indicating the stress of the endoplasmic reticulum, leading to the progressive activation of the Apaf-1/caspase cascade resulting in apoptosis (83).

Yuanhuatine, a daphnane-type diterpene isolated from flowers of *Daphne genkwa*, has a significant inhibitory effect on the *in vitro* growth of breast cancer cells, with a more pronounced effect on MCF-7 cells positive for the alpha estrogen receptor (ERα). Treatment with yuanhuatine reduced the levels of pro-caspase-7 and PARP, increasing the active form of caspase-7, and the treatment also reduced the potential of mitochondrial membrane, induced the generation of reactive oxygen species and superoxide in the mitochondria, and increased Bax and reduced Bcl-2 levels, culminating in apoptosis due to mitochondrial dysfunction (84).

Also, computational molecular docking demonstrated that yuanhuatine forms key hydrophobic interactions in the hydrophobic pocket with some crucial lipophilic residues (Phe 404, Leu 391, Leu 387, Ala 350, Leu 346, Met 421 and Leu 525) as seen in ligand estradiol binding, which could overlap the ATP phosphate-binding region. Further, *in vitro* treatment with yuanhuatine reduces the production of ERα and down-regulated Akt/mTOR and MEK/ERK signaling, confirming that the compound inhibited ERα signaling pathway in MCF-7 cells since Akt/mTOR and MEK/ERK signaling molecules are important downstream molecules of ERα (84).

The natural compound andrographolide belonging to the group of diterpenic lactones, extracted from the plant *Andrographis paniculata* Nees, has been described to have antitumor activity, being three hydroxyls at C-3 (secondary), C-14 (allylic) and C-19 (primary) on the basic structural skeleton reported being responsible for its biological

activities. The *in vitro* treatment with andrographolide in MDA-MB-231 triple-negative breast cancer cell lines inhibited cell growth due to apoptosis triggered by the production of reactive oxygen species and reduced mitochondrial membrane potential. Moreover, the compound was also able to stimulate the production of Bax and reduce Bcl-2, such changes induced the release of cytochrome C in the cytosol, activation of Apaf-1, and consequent activation of caspase-9 and 3, culminating in apoptosis (85).

Similarly, an epoxy clerodane diterpene extracted from *Tinospora cordifolia*, was also able to reduce proliferation by inducing apoptosis in MCF-7 cells *in vitro*, without altering the viability of normal Vero and V79 cells. In MCF-7 cells, treatment induced the production of reactive oxygen species and altered the production of proteins related to cell death, with a reduction in anti-apoptotic (BCL-2, MDM-2 and PCNA), and an increase in pro-apoptotic (CYP1A, GPX, GSK3b, CDKN2A, RB1, BAX, CASP-8, CASP-9, P21, and P53) (61). Similarly, a *cis*-clerodane diterpene, called crispene E, extracted from plants of the same genus *Tinospora*, species *T. crispa*, showed important inhibitory activity of STAT3 dimerization, necessary for its activation and translocation to the nucleus to transcribe several genes related to proliferation and survival of cancer cells. MDA-MB-231 cells treated with crispene E significantly reduced cell viability, in addition to reducing the activation of STAT3 and its target genes bcl-2, cyclin D1, NNMT, and fascin. In this study, the molecular docking suggested that the molecule inhibits STAT3 by interacting with its SH2 domain (86).

Kopetdaghinane, a diterpene extracted from *Euphorbia kopetdaghi* plants, has demonstrated antitumor activity in vitro against MCF-7 cells by inducing caspase-6-mediated apoptosis, stimulating increased production of reactive oxygen species and reduced mitochondrial membrane potential, which culminated in the increased pro-apoptotic Bax protein activity and reduced Bcl-2 (87). Reactive oxygen species also seems to be pivotal to the anti-tumoral action of the diterpenoid Crassin, when tested against MDA-MB-231 and 4T1 cell lines. However, surprisingly, the inhibitory effects of Crassin were not related to common mechanisms of cell death (apoptosis, necrosis, necroptosis, and ferroptosis). The authors discuss that the mechanism of action of this compound could be cytostatic instead of cytotoxic (88).

Kahweol is a diterpene found in coffee beans, specifically *Coffea arabica*, and has antitumor activity in human epidermal growth factor receptor-2 (HER2)-overexpressing breast cancer cells in a caspase-3 dependent manner. Kahweol's antiproliferative activity also resulted in reduced Akt phosphorylation and its downstream signaling, mTOR, and cyclin D. Blocking Akt signaling by kahweol results in reduced expression of fatty acid synthase (FASN) and consequently inhibits cell proliferation (89).

Jatrophone, isolated from the root and stem of *Jatropha gossypiifolia*, showed antitumor activity in several cells of triple-negative breast cancer lineage (MDA-MB-231, HCC38, MDA-MB-157, and MDA-MB-468) by inhibiting the pathway signaling WNT/β-catenin, which is involved in the transcription of several genes related to cell proliferation, survival, development, and differentiation. Also, the Wnt/β-catenin pathway has been associated with the carcinogenesis of several types of cancer. The antitumor activity of the jatrophone occurs by inhibiting the downstream signaling triggered by the Wnt receptor complex, preventing the stabilization of β-catenin and its consequent translocation to the nucleus for transcription of genes such as AXIN2, HMGA2, MYC, PCNA, and CYCLIN D1, an inhibition demonstrated both at the transcriptomic and protein levels, which results in the induction of apoptosis. Thus, jatrophone interferes with triple-negative breast cancer cell proliferation based on the cancer cell line etiology-subtype, the known cellular chemoresistance status, and cell capacity to produce Wnt (90).

Eriocalyxin B (EriB), a diterpenoid with proven anti-angiogenic activity (described in section 4), was also tested against MCF-7 and MDA-MB-231 cell lines with good inhibitory activity, by inducing apoptosis accompanied by the activation of autophagy, which was evidenced by the increased accumulation of autophagosomes, acidic vesicular organelles formation, the microtubule-associated protein 1A/1B-light chain 3B-II (LC3B-II) conversion from LC3B-I and p62 degradation. In these cells, EriB treatment also inhibited the Akt/mTOR/p70S6K signaling pathway. The authors even showed that ROS played an essential role in EriB-induced cell death. Finally, it was shown that in the MDA-MB-231 xenograft breast tumor model, EriB also displayed a significant anti-tumor effect, with a reduction of tumor weight and activation of autophagy and apoptosis. Taken together, the findings demonstrated that EriB presents a potent anti-breast cancer effect both *in vitro* and *in vivo* (91).

6. Diterpenes as a therapeutic option in drug-resistant cell lineages

Multidrug resistance (MDR) is one of the main reasons for the fail of cancer treatments. It is characterized by broad cross-resistance to unrelated drugs that are different both in molecular structure and target specificity. The overexpression of P-glycoprotein (P-gp) is the most studied and common mechanism of MDR (92). P-gp is a plasma membrane-associated transport protein expressed in drug-resistant cancer cells, that recognizes chemotherapeutic drugs as substrates and extrude them out, besides to impair the immunesensitizing functions of the cells, leading to ineffective intracellular drug concentrations, reduced elimination by immune cells, and poor clinical outcomes following chemotherapy (92,93).

Jatrophanes are macrocyclic diterpenes with broad biological effects usually substituted for a variety of acyl groups (94). HU et al., (2018) isolated 15 different jatrophane diterpenoids from the fruits of *Euphorbia sororia* and evaluated its effects on multidrug-resistant MCF-7/ADR breast cancer cells with P-gp overexpression. Eight compounds showed good chemoreversal abilities compared to verapamil, a known P-gp inhibitor. From these, Euphosorophane A was the most promising molecule, with low cytotoxicity to normal cells (HEK293 cell line), high therapeutic index, inhibition of P-gp-mediated rhodamine123 efflux, and ability to reverse P-gp-mediated resistance to doxorubicin and other cytotoxic agents associated with MDR as docetaxel and vincristine. The authors further elucidated that the mechanism of action of this diterpene is involved with a competitive inhibition to DOX in the binding site of P-gp, resulting in increasing of intracellular DOX concentration, which culminates in resensitizing MCF-7/ADR to DOX. Also, some correlations of structure-actvity relationship were proposed, in which the acyloxyl at C-5 could modulate the reversal effects on DOX resistance. Furthermore, the authors hypothesized that the presence of an aromatic ester group (benzoyl) at C-14 has a positive role in the modulation of the drug accumulation in the MCF-7/ADR cells. Lastly, the presence of the carbonyl at C-14 instead of acetoxyl had little influence on the activity (95).

Similar effects were found when myrsinol diterpenes derived from *Euphorbia prolifera*, J196-9-4, and J196-10-1, were tested against MCF-7/ADR cells. Both compounds were non-toxic for cells at low concentrations (<50 μM) and could reverse the resistance to daunorubicin, vincristine, and topotecan by acting as P-gp substrate, inhibiting the P-gp mediated rhodamine 123 efflux, and stimulating the ATP hydrolysis. Thus, J196-9-4 and J196-10-1 also acted as a competitive inhibitor of P-gp and reverses MDR (96,97).

In the same way, XUE et al., (2016) isolated 27 *neo*-clerodane diterpenoids substituted with nicotinoyloxyl from *Scutellaria barbata*, which were tested against MCF-7/ADR cells. Among the tested molecules, four exhibited better chemoreversal abilities than verapamil, and the most potent compound, scutebatin A, reduced more than 45 times the IC_{50} value of DOX. Besides that, scutebatin A (10 and 20 μM) significantly increased DOX and rhodamine 123 accumulation in the cells, while decreased the P-gp expression level, and the docking simulations further confirmed scutebatin A is a competitive inhibitor of P-gp, by the interaction of benzoyloxy group at C-6 with residue Phe 974, besides interactions by hydrogen bonds that further stabilized the complex (98).

P-gp inhibition was also verified when MCF-7/ADR cells were treated with five series of 37 new acylate and epoxide derivatives of *Euphorbia* factor L3, a lathyrol diterpene isolated from *Euphorbia lathyris*, designed by modifying the hydroxyl moiety of C-3, C-5,

or C-15. Eight derivatives exhibited greater chemoreversal ability than verapamil against DOX resistance, from which the two most effective were able to effectively reverse the sensitivity to DOX by 34.4 and 28.6 fold, respectively, and exhibited effective efflux inhibition of rhodamine 123. From these experiments, it was proven that benzoylation of the OH-3 and OH-5 of lathyrol produced the best inhibitor. Molecular docking indicated the important influence of hydrophobic interactions and hydrogen bonds in the flexible cavity of P-gp for the compound effectiveness (99).

ERBB2 is a member of the epidermal growth factor (EGF) receptor is amplified and overexpressed in 20 % to 30 % of human breast cancers, and it is often associated with aggressive disease, poor prognosis, and Trastuzumab (Tz) resistance (100). The diterpene carnosic acid (CA) isolated from *Salvia somalensis* was tested against MCF7 and MDA-MB-231 (ERBB2$^-$), and also against SKBR-3, BT474 ERBB2$^+$ cell lines (Tz resistant). Firstly, CA significantly decreased the migratory capability of MDA-MB-231 and the survival of all cells compared to the non-treated control. The combination of Tz and CA in ERBB2$^+$ cells strongly enhanced the inhibitory effect by inducing cell cycle arrest in G0/G1 phases, reducing the fraction in G2/M, inhibiting ERBB2 signaling pathway, and cooperatively upregulating CDKN1B/p27KIP1 expression levels, suggesting a cooperative antitumor effect of the two drugs. Also, CA could partially restore Tz sensitivity in Tz-resistant SKBR-3 cells, which results from multiple mechanisms that ultimately cause cell cycle arrest and inhibition of the late stages of the autophagic flux (101).

Taking together, these works show that diterpenes isolates from plants have good potential to revert the drug resistance of breast cancer. However, most of the results are obtained from *in vitro* tests, therefore, further studies are necessary for a complete understanding of the action potential of diterpene compounds for a possible clinical application.

7. Nanotechnology as an enhancer of diterpenes activity

Nanotechnology has increasingly been a useful tool in the management of drugs with low solubility, high toxicity, and difficulty in administration, increasing the targeted and controlled delivery of a drug (102). In this sense, some diterpenes have been nanoencapsulated and studied for its anti-breast cancer potential.

Triptolide (TP) is a diterpenoid triepoxide extracted from the plant *Tripterygium wilfordii* with proven activity against many malignant tumors. However, its poor solubility and high toxicity are limited to its potential clinical application. For this, liposomes containing TP (TPLP) were formulated coated with hyaluronic acid (HA) and tested against MCF-7 and 4T1 breast cancer cell lines. Nanoparticulated TP (TPLP-HA) was

as effective as free TP against tumor lines, however, TPLP-HA presented a lower percentage of cells under late apoptosis and necrosis, which indicates less induction of local inflammation. TPLP-HA were also tested *in vivo* in 4T1 solid tumor-bearing BALB/c mice and the MCF-7 human breast cancer xenograft model in nude mice, both treated with 0.4 mg/kg via intravenous injection once every two days. After 17 days of treatment, it was observed that the TP and TPLP-HA had similar antitumor activity, and the effect on the MCF-7 model was better than 4T1 for both treatments. Also, TPLP-HA displayed lower toxicity than TP, with LD_{50} of 3.07 and 1.30 mg/kg, respectively, with low effects in the function of the liver and kidney, which indicated the selective tumor targeting of TPLP-HA. The nanoformulated TP also presented higher cellular uptake, which can explain the increase in efficacy while decreasing systemic toxicity (103).

Sclareol (SC) is another diterpene from natural origin with potential antitumor activity, but unfavorable bioavailability due to its poor aqueous solubility. To improve these features, SC was encapsulated in PLGA nanoparticles coated with HA and tested against MCF-7 and MDA-MB-468 breast cancer cell lines. The formulation containing SC coated with HA exerted a noticeable anticancer effect on both the cell lines (10 – 50 µM), promoting a greater decrease in their viability when compared to the uncoated formulation and the free SC. The HA coating of the PLGA nanoparticles favored a better interaction and uptake of particles by cells (104).

SC was also used to improve the cytotoxic effects of DOX, a commercial antitumoral drug from the anthracycline class. For this, OLIVEIRA et al., (2018) developed solid lipid nanoparticles (SLN) containing DOX and SC (SLN-DOX-SC), which were tested against MCF-7 and 4T1 cells. The release profiles revealed that the SLN-DOX-SC showed a controlled release of DOX at pH 7.4 with enhanced drug release at low pH, an important feature for cancer treatment. SLN-DOX-SC resulted in a dose-dependent increase in cell cytotoxicity, which was significantly higher than those observed for the blank SLN. Also, for 4T1cells, SLN-DOX-SC presented better cytotoxic effects than free DOX, which can be attributed to the combination of DOX and SC in SLN, since SLN-SC (with SC but without DOX) showed no inhibitory effect. The higher cytotoxicity observed for SLN-DOX-SC over free DOX in the 4T1 cell line is a huge achievement of the formulation, as this shows its capability of enhancing drug activity in DOX resistant cell lines (105).

The same research group showed that nanostructured lipid carrier (NLC) co-encapsulating DOX and SC (NLC-DOX-SC) presented a synergic effect on MDA-MB-231 and 4T1 cells in the molar ratio 1:1.9 (DOX: SC), with a significant reduction in the IC_{50} values when compared to free DOX and SC. Then, the formulation was tested *in vivo*, in a murine breast cancer model (4T1 tumor-bearing mice), and the treatment with NLC-DOX-SC presented a higher capacity to inhibit tumor growth than free DOX and

free SC. Both *in vitro* and *in vivo*, the effects of the association between DOX and SC were similar with or without the encapsulation, however, NLC-DOX-SC provoked a lower body weight loss and hematological alterations compared to free DOX + free SC, suggesting the ability of the NLC to reduce its toxicity (106).

The presented works show potential uses of nanoparticles as alternatives for targeting drugs and reducing toxicity. However, different results can be found when this approach is used for different cell lines. Therefore, studies are still needed to fully clarify the potential use of nanoparticles containing diterpenes for the treatment of breast cancer.

8.   Sites of interaction and structure-activity relationship

Some studies involving the activity of diterpenes directly relate structural changes to the activity of the compounds. Still, computational studies allow a predictive identification of targets, sites of interactions, and possible mechanisms of action of diterpenes. The works connecting these features that were presented throughout the chapter are described in Table 2. Also, the specific works on the relationship between structure and activity are described below.

Wada et a (2019) addressed the SAR of a lycoctonine-type C19 diterpenoid alkaloid. From the C-1 and C-14 esterifications 46 new derivatives were obtained (2–29, 2a, 3a, 5a - 7a, 9a, 13a, 13b, 14a, 14b, 16a, 17a, 24a, 32, 34a, 34b, 36a). The synthetic and natural compounds (obtained from the purification of the roots of *Aconitum yesoese* var. Macroyesoense), were evaluated for antiproliferative activity against five human tumor cell lines: pulmonary adenocarcinoma (A549), breast cancer (MDA-MB-231, MCF-7), cervical carcinoma HeLa derived cell line (KB), and vincristine-resistant KB subline (KB-VIN).

According to the results of the antiproliferative activity, the natural alkaloids Delcosine (1), 14-O-acetyldelcosine (31), and 14-O-acetylb-rowniine (33) were inactive ($IC_{50} > 20$ µM). However, acylation of the hydroxy group C-1 and/or C-14 of 1 (except with an acetyl group) led to varying degrees of antiproliferative activity. The esterified C-1 compounds, which showed greater potency in all five tumor cell lines tested, were 6 [1- (4-chloro-3-nitrobenzoyl) delcosine], 7 [1- (4-dichloromethylbenzoyl) delcosine], in addition to compounds 13a (pentafluorobenzoate in C-1 and C-14) and 13b (pentafluorobenzoate in C-1, acetate in C-14), with IC_{50} values ranging from 4.3 to 6.0 µM. All potent compounds, except 13a, caused the accumulation of sub-G1 cells within 24 h. 1-Acylation of 1 as a leader appears to be critical for producing antiproliferative activity in this alkaloid class (107).

The determination of the SAR using computational methods was presented by Da Costa et al., (2018) (108). From the isolation of kaurenoic acid (ent-kaur-16-en-19-oic acid) from *Copaifera* ssp, its analogs (ent-7α-hydroxy-kaur-16-en-19-oic acid, ent-15β-hydroxy-kaur-16-en-19-oic acid, methyl ent-7α,16β-dihydroxy-kaur-19-oate, and ent-7α, 11β-dihydroxy-kaur-16-en-19-oic acid) were obtained from the biotransformation process by the fungus *Aspergillus terreus* and tested against breast cancer cell lines (MCF-7), followed by the multivariate quantitative-structure activity relationship (QSAR) analysis where they presented IC_{50} of 145.40, 141.00, 505.90, 783.00, and 805.10 respectively. The results showed that the HOMO and HOMO-1 orbital energies and logP are related to the activity against MCF-7 breast cells. That is, the drug-receptor interactions for this class of compounds with carcinogenic activity are predominantly guided by the transferor displacement of charge, suggesting this displacement mainly from the substituent R1, which with the presence of more lipophilic substituents leads to the formation of more complex active compounds, adding to the molecules higher values of HOMO and HOMO-1 as well as logP.

Terpenoids isolated from *Euphorbia kansui* were evaluated according to their anti-proliferative potential in human cancer cells, showing the structure-activity relationship. In this work, twenty-five terpenoids were isolated from *E. kansui*, thirteen diterpenoids of the ingenane type, and eight of the jatrophane type (with two new compounds, kansuinin P and Q), and four triterpenoids. *In vitro* anticancer activity was performed by the MTS assay on five human cancer cell lines (human colorectal cancer Colo205 cells, human melanoma cells breast cancer MDA-MB-435 cells, human leukemia DAUDI cells, human prostate cancer PC3 cells, and human ovary cancer SKOV-3 cells). The results regarding the structure-activity relationship were performed for 12 ingenane-type diterpenoids in colorectal cancer Colo205 cells. The analysis of the structure-activity relationship showed that the presence of the acetoxy (-OAc), and hydroxyl group on position 20 were important for the activity of the compounds in Colo205 cells, while the in position 3 contributed to a more significant biological activity of the compounds both cells more than on position 5 (MDA-MB-435 and Colo205) (109).

Table 2 – Interactions predictions and structure-activity relationship between diterpenes and proteins involved in the breast cancer evolution.

Diterpene (and type)	Source	Interactions predictions/ structure-activity relationship	Ref.

Taicrypnacids A and B	*Taiwania cryptomerioides*	Presence of the hydroxycarbonyl group can play a crucial role in cytotoxicity, unaffected by the configurational changes in C-7 and C-14 in the compounds	(35)
Lipomesaconitine Lipoaconitine Lipomesaconitine (diterpenoid alkaloids)	*Aconitum japonicum*	The fatty acid ester at C-8 and the anisoyl group at C-14 may be important to the cytotoxic activity of aconitine-type C19-diterpenoid alkaloids against human tumor cell lines.	(36)
Barbatin H (neo-clerodane) and its analogs	*Scutellaria barbata*	Presence of two benzoyloxy groups in C-6 and C-7, associated with the strongest aromaticity in the benzene ring and biological action.	(37)
Siegesides A (diterpenoid glycosides)	*Siegesbeckia pubescens*	The presence of a 15S-16 vicinal diol was an effective group for the teaching of inhibitory activities, and the number, location, and orientation of hydroxyl groups may be essential for the inhibitory effects of diterpenoids against the invasion of MB-MDA-231 cells.	(41)
ent-2,3,7-trihydroxy-18-nor-rosa-1,3,5,7,15-pentane-6-one (C): ent-rosane. ent-11a,14a-dihydroxy-abieta-7(8),13(15)-dien-16,12a-olide (E), and ent-11a-hydroxy-8a,14a-epoxy-12-oxo-abieta-13(15)-en-16-oic acid methyl ester (H): ent-abietane	*Euphorbia fischeriana*	Primary consideration of the structure-activity relationship of the isolated compounds suggesting that an aromatic A-ring may be of benefit for the activity of ent-rosanes. However, details about the action of these bioactive diterpenoids are still under investigation.	(46)
Azorellanol (zorellane)	*Azorella compacta*	In the azorellanes, the beta acetate group at position C-7 in the skeleton increases the cytotoxic effect. The alpha position of the OH group at position C-13 further increases the effect.	(47)
Cyrtophyllones B, Uncinatone, 3-*O*-α-l-arabinopyranosyl olean-12-en-28-oic acid, 3-*O*-[β-d-glucopyranosyl(1-4)-α-l-arabinopyranosyl)]olean-12-en-28-oic acid, and 2α,3α,23-trihydroxyoleane-12-en-28-oic acid.	*Akebia quinata*	Presence of a COOH group at C-28 showed a significant increase in inhibitory activity against the PTP1B enzyme. Increased activity due to one less glucopyranosyl, linked to arabinopyranyl C-3′. The presence of an alcohol group at C-23 may decrease the inhibitory effects on PTP1B.	(54)
(E)-14-hydroxy-15-norlabda-8(17),12-dien-16-al (bicyclic diterpenoid)	*Curcuma amada*	The hydroxymethyl functionality at C-13 might be responsible for the effect.	(57)
Parvifloron F and the synthetic intermediates	genus *Plectranthus*	The oxidation level of the abietane ring may to be important for antiproliferative and selective activity .	(61)
(1S,2E,4S,6R,7E,11E)-2,7,11-cembratriene-4,6-diol (cembranoid)	*Nicotiana tabacum*	Complete shape fitting at the ATP binding pocket of VEGFR2 kinase domain, with important participation of C-4 and C-6 hydroxyl groups and C-19 and C-20 methyl groups.	(66)

Eriocalyxin B	*Isodon eriocalyx var. laxiflora*	Stably bind at the ATP-binding site of VEGFR-2, with seven amino acids actively involved.	(67)
6E,0E,14Z-(3S)-17-hydroxygeranyllinalool-17-O-β-d-glucopyranosyl-(1→2)-[α-l-rhamnopyranosyl-(1→6)]-β-d-glucopyranoside (glycoside)	*Blumea lacera*	Absence of the β-d-glucopyranose on the C-3 oxygen contributed for the significantly cytotoxic activity	(72)
Parvifloron D, 6,7-dehydroroyleanone and 7-acetoxy-6-hydroxyroyleanone	genus *Plectranthus*	Double substitution only with non-substituted phenyls, or hydroxybenzoate at position four, can increase the interactions in PKC. Substitution groups of the royleanone core, can provide a better docked binding pose.	(75)
Oridonin (7,20-epoxy-ent-kauranes)	Commercial, found in Chinese herbs	Addition of phosphate group provides better effects.	(77)
Yuanhuatine (daphnane)	*Daphne genkwa*	Hydrophobic interactions in the hydrophobic pocket with some crucial lipophilic residues (Phe 404, Leu 391, Leu 387, Ala 350, Leu 346, Met 421, and Leu 525).	(84)
Crispene E (clerodane-type)	*Tinospora crispa*	The inhibition of STAT3 might be by hydrophobic interactions with its SH2 domain.	(86)
Euphosorophane A (jatrophane)	*Euphorbia sororia*	High binding affinity toward the DOX recognition site of P-gp	(95)
Scutebatin A (*neo*-clerodane)	*Scutellaria barbata*	The benzoyloxy group at C-6 interacted with residue Phe 974 of P-gp, with possible roles in the binding pocket. The interaction of scutebatin A with Tye 949 and Gln 721 further stabilized the complex.	(98)
Euphorbia factor L3 (lathyrane)	*Euphorbia lathyris*	Influence of hydrophobic interactions and hydrogen bonds in the flexible cavity formed by two bundles of six transmembrane helices of P-gp.	(99)
1-(3,5-dichlorobenzoyl) delcosine and 1-(4-dichloromethylbenzoyl) delcosine (lycoctonine-type)	*Aconitum yesoense var. macroyesoense*	C-1 esterified compounds caused an increase in the number of cells in phases S and G2/M followed by the accumulation of sub-G1	(107)
ent-kaur-16-en-19-oic acid, *ent*-7α-hydroxy-kaur-16-en-19-oic acid, *ent*-15β-hydroxy-kaur-16-en-19-oic acid, *ent*-7α,11β-dihydroxy-kaur-16-en-19-oic acid, and methyl *ent*-7α,16β-dihydroxy-kaur-19-oate (kaurane)	*Copaifera ssp*	The drug-receptor interactions are predominantly guided by the transfer or displacement of charge, mainly from the R1 substituent, which with the presence of more lipophilic substituents there is the formation of more active compounds.	(108)
CI-(1-13) (ingenane)	*Euphorbia kansui*	The presence of the substituent in position 3 contributed to a more significant biological activity.	(109)

We described here the works addressing the structure-activity relationship of plant diterpenes, identifying the structural changes where an increase in antitumor activity was

described when compared to the initial compound, as well as the works where this improvement was not observed. From these studies, it is possible to infer that compounds modified via classical synthesis or from the fungal biotransformation process tend to present a significant improvement in the antitumor activities.

However, some authors do not address the structure-activity relationship but perform an analysis of the molecular interaction with the active site in addition to its therapeutic viability from computational or experimental screening. In these works, it was observed strong interactions of the diterpene molecules with amino acid residues from different breast cancer cell proteins. It is worth mentioning that a large part of the studies did not directly indicate which portion of the molecule or the interaction site was responsible for the biological effects described, which does not diminish the importance and quality of the respective works, showing important results about to the action of diterpenes in the context of breast cancer.

9. Conclusions

In this chapter, it was described the recent discovery diterpenes from plant sources were described by its anti-breast cancer activity, besides the compounds in which the action mechanisms were proved, namely: the antiproliferative action, the inhibition of tumor angiogenesis and metastasis, and induction of cell death. The chapter also covered the diterpenes studied by its effect in drug-resistant breast cancer cell lineages and the use of nanotechnology as an enhancer of its activity. From the structure-activity relationship studies, it was possible to infer that most compounds modified via classical synthesis or from biotransformation process had improved antitumor activities. Thus, we conclude that studies related to diterpenes can be constantly explored since obtaining from natural sources is a vast field and several even more active derivatives can be obtained from structural modification processes, and therefore, diterpenes from plants have an important potential in drug discovery for breast cancer treatment.

10. References

1. Guerriero G, Berni R, Muñoz-Sanchez JA, Apone F, Abdel-Salam EM, Qahtan AA, et al. Production of plant secondary metabolites: Examples, tips and suggestions for biotechnologists. Vol. 9, Genes. MDPI AG; 2018. p. 309.

2. Isah T. Stress and defense responses in plant secondary metabolites production. Vol. 52, Biological research. NLM (Medline); 2019. p. 39.

3. Hiruma K. Roles of plant-derived secondary metabolites during interactions with pathogenic and beneficial microbes under conditions of environmental stress.

Vol. 7, Microorganisms. MDPI AG; 2019.

4. Cardoso JC, de Oliveira MEBS, Cardoso F de CI. Advances and challenges on the in vitro production of secondary metabolites from medicinal plants. Hortic Bras. 2019 Apr;37(2):124–32.

5. Liu K, Abdullah AA, Huang M, Nishioka T, Altaf-Ul-Amin M, Kanaya S. Novel Approach to Classify Plants Based on Metabolite-Content Similarity. Biomed Res Int. 2017;2017.

6. Rishton GM. Natural Products as a Robust Source of New Drugs and Drug Leads: Past Successes and Present Day Issues. Am J Cardiol [Internet]. 2008 May 22 [cited 2020 Sep 24];101(10 SUPPL.). Available from: https://pubmed.ncbi.nlm.nih.gov/18474274/

7. Kabera JN, Semana E, Mussa; AR, Xin; H. Plant Secondary Metabolites: Biosynthesis, Classification, Function and Pharmacological Classification, Function and Pharmacological Properties Ethnobotanical survey of medicinal plants with pesticides properties and their potential use in Rwanda View pro. 2014.

8. Nagel R, Schmidt A, Peters RJ. Isoprenyl diphosphate synthases: the chain length determining step in terpene biosynthesis. Vol. 249, Planta. Springer Verlag; 2019. p. 9–20.

9. Rabi T, Bishayee A. Terpenoids and breast cancer chemoprevention. Vol. 115, Breast Cancer Research and Treatment. Springer; 2009. p. 223–39.

10. Hemmerlin A, Harwood JL, Bach TJ. A raison d'être for two distinct pathways in the early steps of plant isoprenoid biosynthesis? Prog Lipid Res. 2012;51(2):95–148.

11. Berthelot K, Estevez Y, Deffieux A, Peruch F. Isopentenyl diphosphate isomerase: A checkpoint to isoprenoid biosynthesis. Vol. 94, Biochimie. Elsevier; 2012. p. 1621–34.

12. Lanzotti V. Diterpenes for therapeutic use. In: Natural Products: Phytochemistry, Botany and Metabolism of Alkaloids, Phenolics and Terpenes [Internet]. Springer Berlin Heidelberg; 2013 [cited 2020 Oct 28]. p. 3173–91. Available from: https://link.springer.com/referenceworkentry/10.1007/978-3-642-22144-6_192

13. Pasdaran A, Hamedi A. Natural Products as Source of New Antimicrobial Compounds for Skin Infections. In: The Microbiology of Skin, Soft Tissue, Bone and Joint Infections. Elsevier; 2017. p. 223–53.

14. Cheuka PM, Mayoka G, Mutai P, Chibale K. The role of natural products in drug discovery and development against neglected tropical diseases [Internet]. Vol. 22, Molecules. MDPI AG; 2017 [cited 2020 Sep 24]. Available from:

https://pubmed.ncbi.nlm.nih.gov/28042865/

15.   Pertino MW, Vega C, Rolón M, Coronel C, De Arias AR, Schmeda-Hirschmann
        G. Antiprotozoal activity of triazole derivatives of dehydroabietic acid and
        oleanolic acid. Molecules [Internet]. 2017 Mar 1 [cited 2020 Sep 24];22(3).
        Available from: /pmc/articles/PMC6155273/?report=abstract

16.   Montesino NL, Schmidt TJ. Salvia species as sources of natural products with
        antiprotozoal activity [Internet]. Vol. 19, International Journal of Molecular
        Sciences. MDPI AG; 2018 [cited 2020 Sep 24]. Available from:
        /pmc/articles/PMC5796210/?report=abstract

17.   Islam MT, Ali ES, Uddin SJ, Islam MA, Shaw S, Khan IN, et al. Andrographolide,
        a diterpene lactone from Andrographis paniculata and its therapeutic promises in
        cancer [Internet]. Vol. 420, Cancer Letters. Elsevier Ireland Ltd; 2018 [cited 2020
        Sep 24]. p. 129–45. Available from: https://pubmed.ncbi.nlm.nih.gov/29408515/

18.   Yuan XL, Mao XX, Du YM, Yan PZ, Hou XD, Zhang ZF. Anti-tumor activity of
        cembranoid-type diterpenes isolated from Nicotiana tabacum L. Biomolecules
        [Internet]. 2019 Jan 1 [cited 2020 Sep 24];9(2). Available from:
        /pmc/articles/PMC6406568/?report=abstract

19.   Reddy P, Guthridge K, Vassiliadis S, Hemsworth J, Hettiarachchige I,
        Spangenberg G, et al. Tremorgenic mycotoxins: Structure diversity and
        biological activity [Internet]. Vol. 11, Toxins. MDPI AG; 2019 [cited 2020 Sep 24].
        Available from: /pmc/articles/PMC6563255/?report=abstract

20.   Hammami S, Snène A, El Mokni R, Faidi K, Falconieri D, Dhaouadi H, et al.
        Essential Oil Constituents and Antioxidant Activity of Asplenium Ferns. J
        Chromatogr Sci [Internet]. 2016 Sep 1 [cited 2020 Sep 24];54(8):1341–5.
        Available from: https://academic.oup.com/chromsci/article/54/8/1341/2196931

21.   Gómez-Rivera A, González-Cortazar M, Herrera-Ruíz M, Zamilpa A, Rodríguez-
        López V. Sessein and isosessein with anti-inflammatory, antibacterial and
        antioxidant activity isolated from Salvia sessei Benth. J Ethnopharmacol
        [Internet]. 2018 May 10 [cited 2020 Sep 24];217:212–9. Available from:
        https://pubmed.ncbi.nlm.nih.gov/29458147/

22.   Ba Vinh L, Thi Minh Nguyet N, Young Yang S, Hoon Kim J, Thi Vien L, Thi
        Thanh Huong P, et al. A new rearranged abietane diterpene from Clerodendrum
        inerme with antioxidant and cytotoxic activities. Nat Prod Res [Internet]. 2018
        Sep 2 [cited 2020 Sep 24];32(17):2001–7. Available from:
        https://www.tandfonline.com/doi/full/10.1080/14786419.2017.1360885

23.   Li D, Han T, Liao J, Hu X, Xu S, Tian K, et al. Oridonin, a promising ent-kaurane
        diterpenoid lead compound [Internet]. Vol. 17, International Journal of Molecular

Sciences. MDPI AG; 2016 [cited 2020 Sep 24]. Available from: https://pubmed.ncbi.nlm.nih.gov/27563888/

24.   Alves JM, Leandro LF, Senedese JM, Castro PT de, Pereira DE, Resende FA, et al. Antigenotoxicity properties of Copaifera multijuga oleoresin and its chemical marker, the diterpene (−)-copalic acid. J Toxicol Environ Heal - Part A Curr Issues. 2018 Mar 4;81(5):116–29.

25.   Pfeifer Barbosa AL, Wenzel-Storjohann A, Barbosa JD, Zidorn C, Peifer C, Tasdemir D, et al. Antimicrobial and cytotoxic effects of the Copaifera reticulata oleoresin and its main diterpene acids. J Ethnopharmacol. 2019 Apr 6;233:94–100.

26.   Chen HY, Liu TK, Shi Q, Yang XL. Sesquiterpenoids and diterpenes with antimicrobial activity from Leptosphaeria sp. XL026, an endophytic fungus in Panax notoginseng. Fitoterapia [Internet]. 2019 Sep 1 [cited 2020 Sep 24];137. Available from: https://pubmed.ncbi.nlm.nih.gov/31226283/

27.   Hou S, Dai J. Transcriptome-based signature predicts the effect of taxol in serous ovarian cancer. PLoS One [Internet]. 2018 Mar 1 [cited 2020 Sep 24];13(3). Available from: https://pubmed.ncbi.nlm.nih.gov/29494610/

28.   Zhu L, Chen L. Progress in research on paclitaxel and tumor immunotherapy. Cell Mol Biol Lett [Internet]. 2019 Jun 13 [cited 2020 Sep 24];24(1). Available from: https://pubmed.ncbi.nlm.nih.gov/31223315/

29.   Akram M, Iqbal M, Daniyal M, Khan AU. Awareness and current knowledge of breast cancer [Internet]. Vol. 50, Biological Research. BioMed Central Ltd.; 2017 [cited 2020 Oct 3]. p. 33. Available from: /pmc/articles/PMC5625777/?report=abstract

30.   Harbeck N, Gnant M. Breast cancer [Internet]. Vol. 389, The Lancet. Lancet Publishing Group; 2017 [cited 2020 Oct 3]. p. 1134–50. Available from: https://pubmed.ncbi.nlm.nih.gov/27865536/

31.   Hassan HM, Rateb ME, Hassan MH, Sayed AM, Shabana S, Raslan M, et al. New antiproliferative cembrane diterpenes from the Red Sea Sarcophyton species. Mar Drugs [Internet]. 2019 [cited 2020 Sep 28];17(7). Available from: /pmc/articles/PMC6669714/?report=abstract

32.   Subik K, Lee JF, Baxter L, Strzepek T, Costello D, Crowley P, et al. The expression patterns of ER, PR, HER2, CK5/6, EGFR, KI-67 and AR by immunohistochemical analysis in breast cancer cell lines. Breast Cancer Basic Clin Res [Internet]. 2010 [cited 2020 Sep 28];4(1):35–41. Available from: http://www.la-press.com.

33.   Jacobo-Herrera N, Pérez-Plasencia C, Castro-Torres VA, Martínez-Vázquez M,

González-Esquinca AR, Zentella-Dehesa A. Selective Acetogenins and Their Potential as Anticancer Agents. Front Pharmacol. 2019 Jul;10:783.

34. Kamel MR, Nafady AM, Hassanein AMM, Hassan AR, Shimizu K, Ibrahim RR, et al. Ent-trachylobane-3β-hydroperoxide, a new diterpene from the root bark of Chrozophora oblongifolia (Fam.; Euphorbiaceae). Nat Prod Res [Internet]. 2019 [cited 2020 Sep 29]; Available from: https://pubmed.ncbi.nlm.nih.gov/31691590/

35. Wang WL, Zhu DR, Chen C, Zhu TY, Han C, Liu FY, et al. Taicrypnacids A and B, a Pair of C37 Heterodimeric Diterpenoid Stereoisomers from Taiwania cryptomerioides. J Nat Prod [Internet]. 2019 Aug 23 [cited 2020 Sep 29];82(8):2087–93. Available from: https://pubmed.ncbi.nlm.nih.gov/31347365/

36. Wada K, Yamashita H. Cytotoxic effects of diterpenoid alkaloids against human cancer cells [Internet]. Vol. 24, Molecules. MDPI AG; 2019 [cited 2020 Sep 29]. Available from: https://pubmed.ncbi.nlm.nih.gov/31234546/

37. Wang M, Ma C, Chen Y, Li X, Chen J. Cytotoxic Neo-Clerodane Diterpenoids from Scutellaria barbata D.Don. Chem Biodivers [Internet]. 2019 Feb 1 [cited 2020 Sep 29];16(2). Available from: https://pubmed.ncbi.nlm.nih.gov/30444060/

38. Ke LY, Zhang Y, Xia MY, Zhuo JX, Wang YH, Long CL. Modified Abietane Diterpenoids from Whole Plants of Selaginella moellendorffii. J Nat Prod [Internet]. 2018 Feb 23 [cited 2020 Sep 29];81(2):418–22. Available from: https://pubmed.ncbi.nlm.nih.gov/29412669/

39. Zhang X, Li W, Shen L, Wu J. Four new diterpenes from the mangrove Ceriops tagal and structure revision of four dolabranes with a 4,18-epoxy group. Fitoterapia [Internet]. 2018 Jan 1 [cited 2020 Sep 29];124:1–7. Available from: https://pubmed.ncbi.nlm.nih.gov/28964872/

40. Lun BS, Shao LW, Wang Y, Li CC, Yu H, Wang CH, et al. Taxanes from Taxus wallichiana var. mairei cultivated in the southern area of the Yangtze River in China. Nat Prod Res [Internet]. 2017 [cited 2020 Sep 29];31(20):2341–7. Available from: https://pubmed.ncbi.nlm.nih.gov/28322597/

41. Wang J, Xie K, Duan H, Wang Y, Ma H, Fu H. Isolation and characterization of diterpene glycosides from Siegesbeckia pubescens. Bioorganic Med Chem Lett [Internet]. 2017 [cited 2020 Sep 29];27(8):1815–9. Available from: https://pubmed.ncbi.nlm.nih.gov/28302401/

42. Farimani MM, Taleghani A, Aliabadi A, Aliahmadi A, Esmaeili MA, Sarvestani NN, et al. Labdane diterpenoids from Salvia leriifolia: Absolute configuration, antimicrobial and cytotoxic activities. Planta Med [Internet]. 2016 Apr 19 [cited 2020 Sep 29];82(14):1279–85. Available from: https://pubmed.ncbi.nlm.nih.gov/27280932/

43. Wang J, Duan H, Wang Y, Pan B, Gao C, Gai C, et al. ent-strobane and ent-pimarane diterpenoids from Siegesbeckia pubescens. J Nat Prod [Internet]. 2017 Jan 27 [cited 2020 Sep 29];80(1):19–29. Available from: https://pubmed.ncbi.nlm.nih.gov/28009521/

44. Yulianto W, Andarwulan N, Giriwono PE, Pamungkas J. HPLC-based metabolomics to identify cytotoxic compounds from Plectranthus amboinicus (Lour.) Spreng against human breast cancer MCF-7Cells. J Chromatogr B Anal Technol Biomed Life Sci [Internet]. 2016 Dec 15 [cited 2020 Sep 29];1039:28–34. Available from: https://pubmed.ncbi.nlm.nih.gov/27816313/

45. Zheng YD, Guan XC, Li D, Wang AQ, Ke CQ, Tang CP, et al. Novel diterpenoids from the twigs of Podocarpus nagi. Molecules [Internet]. 2016 Oct 1 [cited 2020 Sep 29];21(10). Available from: https://pubmed.ncbi.nlm.nih.gov/27681713/

46. Kuang X, Li W, Kanno Y, Yamashita N, Kikkawa S, Azumaya I, et al. Euphorins A–H: bioactive diterpenoids from Euphorbia fischeriana. J Nat Med [Internet]. 2016 Jul 1 [cited 2020 Sep 29];70(3):412–22. Available from: https://pubmed.ncbi.nlm.nih.gov/27000121/

47. Bórquez J, Bartolucci NL, Echiburú-Chau C, Winterhalter P, Vallejos J, Jerz G, et al. Isolation of cytotoxic diterpenoids from the Chilean medicinal plant Azorella compacta Phil from the Atacama Desert by high-speed counter-current chromatography. J Sci Food Agric [Internet]. 2016 Jun 1 [cited 2020 Sep 29];96(8):2832–8. Available from: https://pubmed.ncbi.nlm.nih.gov/26425819/

48. Zhao M, Onakpa MM, Chen WL, Santarsiero BD, Swanson SM, Burdette JE, et al. 17-norpimaranes and (9βH)-17-norpimaranes from the tuber of Icacina trichantha. J Nat Prod [Internet]. 2015 Apr 24 [cited 2020 Sep 29];78(4):789–96. Available from: https://pubmed.ncbi.nlm.nih.gov/25782063/

49. Meesakul P, Ritthiwigrom T, Cheenpracha S, Sripisut T, Maneerat W, MacHan T, et al. A new cytotoxic clerodane diterpene from casearia graveolens twigs. Nat Prod Commun. 2016 Jan 23;11(1):13–5.

50. Ma J, Yang X, Zhang Q, Zhang X, Xie C, Tuerhong M, et al. Cytotoxic clerodane diterpenoids from the leaves of Casearia kurzii. Bioorg Chem [Internet]. 2019 Apr 1 [cited 2020 Sep 29];85:558–67. Available from: https://pubmed.ncbi.nlm.nih.gov/30807898/

51. He Y, Zhang D, West LM. Delphatisine D and Chrysotrichumine A, two new diterpenoid alkaloids from Delphinium chrysotrichum. Fitoterapia [Internet]. 2019 Nov 1 [cited 2020 Sep 29];139. Available from: https://pubmed.ncbi.nlm.nih.gov/31705949/

52. Wang Y gai, Ren J, Ma J, Yang J bo, Ji T, Wang A guo. Bioactive cembrane-

type diterpenoids from the gum-resin of Boswellia carterii. Fitoterapia [Internet]. 2019 Sep 1 [cited 2020 Sep 29];137. Available from: https://pubmed.ncbi.nlm.nih.gov/31295512/

53.   Mofidi Tabatabaei S, Salehi P, Moridi Farimani M, Neuburger M, De Mieri M, Hamburger M, et al. A nor-diterpene from Salvia sahendica leaves. Nat Prod Res [Internet]. 2017 [cited 2020 Sep 29];31(15):1758–65. Available from: https://pubmed.ncbi.nlm.nih.gov/28278660/

54.   An JP, Ha TKQ, Kim J, Cho TO, Oh WK. Protein tyrosine phosphatase 1B inhibitors from the stems of Akebia quinata. Molecules [Internet]. 2016 Aug 1 [cited 2020 Sep 29];21(8). Available from: https://pubmed.ncbi.nlm.nih.gov/27548130/

55.   Win NN, Ito T, Aimaiti S, Imagawa H, Ngwe H, Abe I, et al. Kaempulchraols A-H, Diterpenoids from the Rhizomes of Kaempferia pulchra Collected in Myanmar. J Nat Prod [Internet]. 2015 May 22 [cited 2020 Sep 29];78(5):1113–8. Available from: https://pubmed.ncbi.nlm.nih.gov/25919052/

56.   Lu KT, Wang BY, Chi WY, Chang-Chien J, Yang JJ, Lee H Te, et al. Ovatodiolide inhibits breast cancer stem/progenitor cells through SMURF2-mediated downregulation of Hsp27. Toxins (Basel) [Internet]. 2016 May 1 [cited 2020 Sep 28];8(5). Available from: https://pubmed.ncbi.nlm.nih.gov/27136586/

57.   Win NN, Ito T, Ngwe H, Win YY, Prema, Okamoto Y, et al. Labdane diterpenoids from Curcuma amada rhizomes collected in Myanmar and their antiproliferative activities. Fitoterapia [Internet]. 2017 Oct 1 [cited 2020 Sep 28];122:34–9. Available from: https://pubmed.ncbi.nlm.nih.gov/28827004/

58.   Varghese E, Samuel SM, Varghese S, Cheema S, Mamtani R, Büsselberg D. Triptolide decreases cell proliferation and induces cell death in triple negative MDA-MB-231 breast cancer cells. Biomolecules [Internet]. 2018 Dec 1 [cited 2020 Sep 28];8(4):163. Available from: /pmc/articles/PMC6315979/?report=abstract

59.   Awasthee N, Rai V, Verma SS, Sajin Francis K, Nair MS, Gupta SC. Anti-cancer activities of Bharangin against breast cancer: Evidence for the role of NF-κB and lncRNAs. Biochim Biophys Acta - Gen Subj. 2018 Dec 1;1862(12):2738–49.

60.   Li H, Pan GF, Jiang ZZ, Yang J, Sun LX, Zhang LY. Triptolide inhibits human breast cancer MCF-7 cell growth via downregulation of the ERα-mediated signaling pathway. Acta Pharmacol Sin [Internet]. 2015 May 1 [cited 2020 Sep 28];36(5):606–13. Available from: https://pubmed.ncbi.nlm.nih.gov/25864647/

61.   Saito Y, Goto M, Nakagawa-Goto K. Total Synthesis of Antiproliferative Parvifloron F. Org Lett [Internet]. 2018 Feb 2 [cited 2020 Sep 28];20(3):628–31.

Available from: https://pubmed.ncbi.nlm.nih.gov/29345474/

62. Li C, Wang Q, Shen S, Wei X, Li G. Oridonin inhibits vegf-a-associated angiogenesis and epithelial-mesenchymal transition of breast cancer in vitro and in vivo. Oncol Lett [Internet]. 2018 Aug 1 [cited 2020 Sep 23];16(2):2289–98. Available from: /pmc/articles/PMC6036431/?report=abstract

63. Artacho-Cordón F, Ríos-Arrabal S, Lara PC, Artacho-Cordón A, Calvente I, Núñez MI. Matrix metalloproteinases: Potential therapy to prevent the development of second malignancies after breast radiotherapy [Internet]. Vol. 21, Surgical Oncology. 2012 [cited 2020 Sep 23]. p. e143–51. Available from: https://linkinghub.elsevier.com/retrieve/pii/S0960740412000321

64. Sun C, Cui H, Yang H, Du X, Yue L, Liu J, et al. Anti-metastatic effect of jolkinolide B and the mechanism of activity in breast cancer MDA-MB-231 cells. Oncol Lett [Internet]. 2015 [cited 2020 Sep 28];10(2):1117–22. Available from: /pmc/articles/PMC4509074/?report=abstract

65. Alsamri H, El Hasasna H, Al Dhaheri Y, Eid AH, Attoub S, Iratni R. Carnosol, a natural polyphenol, inhibits migration, metastasis, and tumor growth of breast cancer via a ROS-dependent proteasome degradation of STAT3. Front Oncol [Internet]. 2019 [cited 2020 Sep 28];9(AUG). Available from: https://pubmed.ncbi.nlm.nih.gov/31456939/

66. Hailat MM, Ebrahim HY, Mohyeldin MM, Goda AA, Siddique AB, El Sayed KA. The tobacco cembranoid (1S,2E,4S,7E,11E)-2,7,11-cembratriene-4,6-diol as a novel angiogenesis inhibitory lead for the control of breast malignancies. Bioorganic Med Chem [Internet]. 2017 Aug [cited 2020 Sep 22];25(15):3911–21. Available from: https://linkinghub.elsevier.com/retrieve/pii/S0968089617305497

67. Zhou X, Yue GGL, Liu M, Zuo Z, Lee JKM, Li M, et al. Eriocalyxin B, a natural diterpenoid, inhibited VEGF-induced angiogenesis and diminished angiogenesis-dependent breast tumor growth by suppressing VEGFR-2 signaling. Oncotarget [Internet]. 2016 [cited 2020 Sep 23];7(50):82820–35. Available from: /pmc/articles/PMC5347735/?report=abstract

68. Peng Y, Wang Y, Tang N, Sun D, Lan Y, Yu Z, et al. Andrographolide inhibits breast cancer through suppressing COX-2 expression and angiogenesis via inactivation of p300 signaling and VEGF pathway 11 Medical and Health Sciences 1112 Oncology and Carcinogenesis. J Exp Clin Cancer Res [Internet]. 2018 Oct 12 [cited 2020 Sep 23];37(1). Available from: /pmc/articles/PMC6186120/?report=abstract

69. Galluzzi L, Vitale I, Aaronson SA, Abrams JM, Adam D, Agostinis P, et al. Molecular mechanisms of cell death: Recommendations of the Nomenclature

Committee on Cell Death 2018 [Internet]. Vol. 25, Cell Death and Differentiation. Nature Publishing Group; 2018 [cited 2020 Oct 3]. p. 486–541. Available from: /pmc/articles/PMC5864239/?report=abstract

70.   Patterson AD, Gonzalez FJ, Perdew GH, Peters JM. Molecular Regulation of Carcinogenesis: Friend and Foe [Internet]. Vol. 165, Toxicological Sciences. Oxford University Press; 2018 [cited 2020 Oct 3]. p. 277–83. Available from: /pmc/articles/PMC6154271/?report=abstract

71.   Harbeck N, Gnant M. Breast cancer [Internet]. Vol. 389, The Lancet. Lancet Publishing Group; 2017 [cited 2020 Oct 2]. p. 1134–50. Available from: http://www.thelancet.com/article/S0140673616318918/fulltext

72.   Akter R, Uddin SJ, Tiralongo J, Grice ID, Tiralongo E. A new cytotoxic diterpenoid glycoside from the leaves of Blumea lacera and its effects on apoptosis and cell cycle. Nat Prod Res [Internet]. 2016 [cited 2020 Sep 28];30(23):2688–93. Available from: https://pubmed.ncbi.nlm.nih.gov/26982796/

73.   Isca VMS, Sencanski M, Filipovic N, Dos Santos DJVA, Gašparović AČ, Saraíva L, et al. Activity to breast cancer cell lines of different malignancy and predicted interaction with protein kinase C isoforms of royleanones. Int J Mol Sci [Internet]. 2020 May 2 [cited 2020 Nov 11];21(10):3671. Available from: /pmc/articles/PMC7279380/?report=abstract

74.   Bessa C, Soares J, Raimundo L, Loureiro JB, Gomes C, Reis F, et al. Discovery of a small-molecule protein kinase Cδ-selective activator with promising application in colon cancer therapy article. Cell Death Dis [Internet]. 2018;9(2). Available from: http://dx.doi.org/10.1038/s41419-017-0154-9

75.   Saraiva N, Costa JG, Reis C, Almeida N, Rijo P, Fernandes AS. Anti-migratory and pro-apoptotic properties of parvifloron d on triple-negative breast cancer cells. Biomolecules [Internet]. 2020 Jan 1 [cited 2020 Sep 28];10(1). Available from: https://pubmed.ncbi.nlm.nih.gov/31963771/

76.   Han N na, Zhou Q, Huang Q, Liu K jiang. Carnosic acid cooperates with tamoxifen to induce apoptosis associated with Caspase-3 activation in breast cancer cells in vitro and in vivo. Biomed Pharmacother [Internet]. 2017 May 1 [cited 2020 Sep 28];89:827–37. Available from: https://pubmed.ncbi.nlm.nih.gov/28282784/

77.   Li Y, Wang Y, Wang S, Gao Y, Zhang X, Lu C. Oridonin phosphate-induced autophagy effectively enhances cell apoptosis of human breast cancer cells. Med Oncol [Internet]. 2015 [cited 2020 Sep 28];32(1):1–8. Available from: https://pubmed.ncbi.nlm.nih.gov/25491140/

78.   Xia S, Zhang X, Li C, Guan H. Oridonin inhibits breast cancer growth and

metastasis through blocking the Notch signaling. Saudi Pharm J [Internet]. 2017 May 1 [cited 2020 Sep 28];25(4):638–43. Available from: https://pubmed.ncbi.nlm.nih.gov/28579904/

79.   Cheng X, Shi W, Zhao C, Zhang D, Liang P, Wang G, et al. Triptolide sensitizes human breast cancer cells to tumor necrosis factor-α-induced apoptosis by inhibiting activation of the nuclear factor-κB pathway. Mol Med Rep [Internet]. 2016 Apr 1 [cited 2020 Sep 28];13(4):3257–64. Available from: https://pubmed.ncbi.nlm.nih.gov/26935527/

80.   Cortese K, Marconi S, D'Alesio C, Calzia D, Panfoli I, Tavella S, et al. The novel diterpene 7β-acetoxy-20-hydroxy-19,20-epoxyroyleanone from Salvia corrugata shows complex cytotoxic activities against human breast epithelial cells. Life Sci [Internet]. 2019 Sep 1 [cited 2020 Sep 28];232:116610. Available from: https://linkinghub.elsevier.com/retrieve/pii/S0024320519305363

81.   Curtin NJ, Szabo C. Therapeutic applications of PARP inhibitors: Anticancer therapy and beyond [Internet]. Vol. 34, Molecular Aspects of Medicine. Mol Aspects Med; 2013 [cited 2020 Sep 28]. p. 1217–56. Available from: https://pubmed.ncbi.nlm.nih.gov/23370117/

82.   Doetsch M, Gluch A, Poznanović G, Bode J, Vidaković M. YY1-Binding Sites Provide Central Switch Functions in the PARP-1 Gene Expression Network. PLoS One [Internet]. 2012 Aug 28 [cited 2020 Sep 28];7(8). Available from: https://pubmed.ncbi.nlm.nih.gov/22937159/

83.   Shen L, Lou Z, Zhang G, Xu G, Zhang G. Diterpenoid Tanshinones, the extract from Danshen (Radix Salviae Miltiorrhizae) induced apoptosis in nine human cancer cell lines. J Tradit Chinese Med = Chung i tsa chih ying wen pan [Internet]. 2016 Aug 1 [cited 2020 Sep 28];36(4):514–21. Available from: https://pubmed.ncbi.nlm.nih.gov/28459519/

84.   Zhang YY, Shang XY, Hou XW, Li LZ, Wang W, Hayashi T, et al. Yuanhuatine from Daphne genkwa selectively induces mitochondrial apoptosis in estrogen receptor α-positive breast cancer cells in vitro. Planta Med [Internet]. 2019 [cited 2020 Sep 28];85(16):1275–86. Available from: https://pubmed.ncbi.nlm.nih.gov/31627219/

85.   Banerjee M, Chattopadhyay S, Choudhuri T, Bera R, Kumar S, Chakraborty B, et al. Cytotoxicity and cell cycle arrest induced by andrographolide lead to programmed cell death of MDA-MB-231 breast cancer cell line. J Biomed Sci [Internet]. 2016 Apr 16 [cited 2020 Sep 28];23(1). Available from: https://pubmed.ncbi.nlm.nih.gov/27084510/

86.   Mantaj J, Rahman SMA, Bokshi B, Hasan CM, Jackson PJM, Parsons RB, et al.

Crispene E, a cis-clerodane diterpene inhibits STAT3 dimerization in breast cancer cells. Org Biomol Chem [Internet]. 2015 Apr 7 [cited 2020 Sep 28];13(13):3882–6. Available from: https://pubmed.ncbi.nlm.nih.gov/25721973/

87. Riahi F, Dashti N, Ghanadian M, Aghaei M, Faez F, Jafari SM, et al. Kopetdaghinanes, pro-apoptotic hemiacetialic cyclomyrsinanes from Euphorbia kopetdaghi. Fitoterapia [Internet]. 2020 Oct 1 [cited 2020 Sep 28];146. Available from: https://pubmed.ncbi.nlm.nih.gov/32464255/

88. Richards CE, Vellanki SH, Smith YE, Hopkins AM. Diterpenoid natural compound C4 (Crassin) exerts cytostatic effects on triple-negative breast cancer cells via a pathway involving reactive oxygen species. Cell Oncol [Internet]. 2018 Feb 1 [cited 2020 Sep 28];41(1):35–46. Available from: https://pubmed.ncbi.nlm.nih.gov/29134467/

89. Oh SH, Hwang YP, Choi JH, Jin SW, Lee GH, Han EH, et al. Kahweol inhibits proliferation and induces apoptosis by suppressing fatty acid synthase in HER2-overexpressing cancer cells. Food Chem Toxicol [Internet]. 2018 Nov 1 [cited 2020 Sep 28];121:326–35. Available from: https://pubmed.ncbi.nlm.nih.gov/30205135/

90. Fatima I, El-Ayachi I, Taotao L, Lillo MA, Krutilina R, Seagroves TN, et al. The natural compound Jatrophone interferes with Wnt/β-catenin signaling and inhibits proliferation and EMT in human triple-negative breast cancer. PLoS One [Internet]. 2017 Dec 1 [cited 2020 Sep 28];12(12). Available from: https://pubmed.ncbi.nlm.nih.gov/29281678/

91. Zhou X, Yue GGL, Chan AML, Tsui SKW, Fung KP, Sun H, et al. Eriocalyxin B, a novel autophagy inducer, exerts anti-tumor activity through the suppression of Akt/mTOR/p70S6K signaling pathway in breast cancer. Biochem Pharmacol [Internet]. 2017 Oct 15 [cited 2020 Sep 29];142:58–70. Available from: https://pubmed.ncbi.nlm.nih.gov/28669564/

92. Vtorushin S V, Khristenko KY, Zavyalova M V, Perelmuter VM, Litviakov N V, Denisov E V, et al. The phenomenon of multi-drug resistance in the treatment of malignant tumors. Experimental Oncology. 2014;36:144–56.

93. Kopecka J, Godel M, Dei S, Giampietro R, Belisario C, Akman M, et al. Insights into P-Glycoprotein Inhibitors: New Inducers of Immunogenic Cell Death. Cells [Internet]. 2020 [cited 2020 Sep 22];(9):1033. Available from: www.mdpi.com/journal/cells

94. Fattahian M, Ghanadian M, Ali Z, Khan IA. Jatrophane and rearranged jatrophane-type diterpenes: biogenesis, structure, isolation, biological activity and SARs (1984–2019) [Internet]. Vol. 19, Phytochemistry Reviews. Springer;

2020 [cited 2020 Sep 22]. p. 265–336. Available from:
https://doi.org/10.1007/s11101-020-09667-8

95. Hu R, Gao J, Rozimamat R, Aisa HA. Jatrophane diterpenoids from Euphorbia sororia as potent modulators against P-glycoprotein-based multidrug resistance. Eur J Med Chem [Internet]. 2018 Feb 25 [cited 2020 Sep 21];146:157–70. Available from: https://linkinghub.elsevier.com/retrieve/pii/S0223523418300278

96. Chen X, Chen X, Liu X, Wink M, Ma Y, Guo Y. A myrsinol diterpene isolated from Euphorbia prolifera reverses multidrug resistance in breast cancer cells. Pharmazie. 2016 Sep 1;71(9):537–9.

97. Wang H, Chen X, Li T, Xu J, Ma Y. A myrsinol diterpene isolated from a traditional herbal medicine, LANGDU reverses multidrug resistance in breast cancer cells. J Ethnopharmacol [Internet]. 2016 Dec 24 [cited 2020 Sep 22];194:1–5. Available from: https://pubmed.ncbi.nlm.nih.gov/27566201/

98. Xue GM, Xia YZ, Wang ZM, Li LN, Luo JG, Kong LY. Neo-Clerodane diterpenoids from Scutellaria barbata mediated inhibition of P-glycoprotein in MCF-7/ADR cells. Eur J Med Chem. 2016 Oct 4;121:238–49.

99. Jiao W, Wan Z, Chen S, Lu R, Chen X, Fang D, et al. Lathyrol diterpenes as modulators of P-glycoprotein dependent multidrug resistance: Structure-activity relationship studies on Euphorbia factor L3 derivatives. J Med Chem [Internet]. 2015 May 14 [cited 2020 Sep 22];58(9):3720–38. Available from: https://pubs.acs.org/doi/abs/10.1021/acs.jmedchem.5b00058

100. Gaviraghi M, Rabellino A, Brand M, Bagnato P, Feudis G De, Raimondi A, et al. ERBB2 activation leads to an anti-oncogenic signalling. Ital J Anat Embryol. 2018;123(1):1.

101. D'Alesio C, Bellese G, Gagliani MC, Aiello C, Grasselli E, Marcocci G, et al. Cooperative antitumor activities of carnosic acid and Trastuzumab in ERBB2+ breast cancer cells. J Exp Clin Cancer Res [Internet]. 2017 Nov 3 [cited 2020 Sep 24];36(1):154. Available from: http://jeccr.biomedcentral.com/articles/10.1186/s13046-017-0615-0

102. Tomiotto-Pellissier F, Miranda-Sapla MM, Machado LF, Bortoleti BT da S, Sahd CS, Chagas AF, et al. Nanotechnology as a potential therapeutic alternative for schistosomiasis. Acta Trop [Internet]. 2017;174:64–71. Available from: http://dx.doi.org/10.1016/j.actatropica.2017.06.025

103. Zheng W, Wang C, Ding R, Huang Y, Li Y, Lu Y. Triptolide-loaded nanoparticles targeting breast cancer in vivo with reduced toxicity. Int J Pharm [Internet]. 2019 Dec 15 [cited 2020 Sep 21];572:118721. Available from: https://linkinghub.elsevier.com/retrieve/pii/S0378517319307665

104. Cosco D, Mare R, Paolino D, Salvatici MC, Cilurzo F, Fresta M. Sclareol-loaded hyaluronan-coated PLGA nanoparticles: Physico-chemical properties and in vitro anticancer features. Int J Biol Macromol [Internet]. 2019 Jul 1 [cited 2020 Sep 21];132:550–7. Available from: https://linkinghub.elsevier.com/retrieve/pii/S0141813019311821

105. Oliveira MS, Lima BHS, Goulart GAC, Mussi SV, Borges GSM, Oréfice RL, et al. Improved Cytotoxic Effect of Doxorubicin by Its Combination with Sclareol in Solid Lipid Nanoparticle Suspension. J Nanosci Nanotechnol [Internet]. 2018 Feb 20 [cited 2020 Sep 21];18(8):5609–16. Available from: http://www.ingentaconnect.com/content/10.1166/jnn.2018.15418

106. Borges GSM, Silva J de O, Fernandes RS, de Souza ÂM, Cassali GD, Yoshida MI, et al. Sclareol is a potent enhancer of doxorubicin: Evaluation of the free combination and co-loaded nanostructured lipid carriers against breast cancer. Life Sci [Internet]. 2019 Sep 1 [cited 2020 Sep 21];232:116678. Available from: https://linkinghub.elsevier.com/retrieve/pii/S0024320519306046

107. Wada K, Goto M, Shimizu T, Kusanagi N, Mizukami M, Suzuki Y, et al. Structure–activity relationships and evaluation of esterified diterpenoid alkaloid derivatives as antiproliferative agents. J Nat Med [Internet]. 2019 Sep 13 [cited 2020 Sep 24];73(4):789–99. Available from: https://doi.org/10.1007/s11418-019-01331-6

108. da Costa RM, Bastos JK, Costa MCA, Ferreira MMC, Mizuno CS, Caramori GF, et al. In vitro cytotoxicity and structure-activity relationship approaches of ent-kaurenoic acid derivatives against human breast carcinoma cell line. Phytochemistry [Internet]. 2018 Dec 1 [cited 2020 Sep 24];156:214–23. Available from: https://pubmed.ncbi.nlm.nih.gov/30321792/

109. HOU JJ, SHEN Y, YANG Z, FANG L, CAI LY, YAO S, et al. Anti-proliferation activity of terpenoids isolated from Euphorbia kansui in human cancer cells and their structure-activity relationship. Chin J Nat Med. 2017 Oct 1;15(10):766–74.

6.3. PARECER DA COMISSÃO DE ÉTICA DE NO USO DE ANIMAIS

Universidade Estadual de Londrina

COMISSÃO DE ÉTICA NO USO DE ANIMAIS

OF. CIRC. CEUA Nº 103/2016   Londrina, 01 de Junho de 2016.
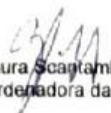
Prezado Pesquisador,

Certificamos que o projeto intitulado "**Ação do flavonóide quercetina nos eventos iniciais da infecção experimental de camundongos Balb/c por Leishmania amazonensis** ", protocolo CEUA n° **8286.2016.60** sob a responsabilidade de **Wander Rogério Pavanelli**, que envolve a produção, manutenção e/ou utilização de animais pertencentes ao filo Chordata, subfilo Vertebrata (exceto o homem), para fins de pesquisa científica (ou ensino), encontra-se de acordo com os preceitos da Lei nº 11.794, de 8 de outubro de 2008, do Decreto nº 6.899, de 15 de julho de 2009, e com as normas editadas pelo Conselho Nacional de Controle da Experimentação Animal (CONCEA), foi **aprovado** pela Comissão de Ética no Uso de Animais da Universidade Estadual de Londrina (CEUA/UEL), em reunião realizada em **24/05/2016**.

O objetivo do projeto é avaliar os períodos iniciais da infecção experimental por *Leishmania amazonensis* e a ação do flavonoide quercetina como modulador da resposta inflamatória induzida por este parasito em camundongos BALB/c e C57BL/6. Para isso os camundongos serão infectados no coxim plantar de ambas as patas traseiras, via subcutânea, com 1×10^5 formas promastigotas de *L. amazonensis* em fase estacionária de crescimento (5 dias pós-repique). Neste experimento, será avaliada a diferença entre os estágios iniciais da infecção de camundongos BALB/c e C57BL/6 e a ação da quercetina sobre camundongos BALB/c infectados com L. amazonensis, nos momentos iniciais da infecção e após o estabelecimento da lesão. Os períodos definidos para as análises serão 6, 24, 72, 144 e 240h pós-infecção e após o aparecimento da lesão (5 semanas pós-infecção). Os grupos experimentais serão: controle sem infecção, que receberá apenas salina via oral (v.o.); controle infectado no coxim plantar de ambas as patas traseiras, via subcutânea, com 1×10^5 formas promastigotas de L. amazonensis; e grupos tratados que, além da infecção com 1×10^5 formas promastigotas de L. amazonensis, serão tratados por via oral com microcápsulas inertes suspensas em salina (100 mg/kg), quercetina (10 e 100mg/kg, solubilizadas com 10% de tween 80 e 90% de salina) e microcápsulas de quercetina (10 e 100mg/kg, solubilizadas em salina). Em relação ao ovino, o animal será contido em decúbito lateral para coleta do sangue, serão coletados 20 mL de sangue que serão transferidos para frascos de vidro estéreis contendo pérolas de vidro seguido de agitação manual destes frascos durante aproximadamente 15 minutos para o processo de desfibrinização do sangue necessário para o preparo do meio de cultura ágar sangue, necessário para o cultivo do protozoário *Leishmania*. Ao longo dos 3 anos de projeto, será utilizado até 160 mL de sangue (20 mL por coleta). GI 1.

Vigência do Projeto	15/05/2016 a 15/04/2019
Espécie/linhagem	Camundongo isogênico / BALB/c e C57BL/6 Ovino / Ovis aries
Nº de animais	197 BALB/c, 53 C57BL/6 e 1 Ovino
Peso/Idade	Camundongos: 25g / 6 a 8 semanas Ovino: Indeterminado
Sexo	Machos e Fêmeas
Origem	Camundongos: Biotério Fiocruz/Curitiba Ovino: Fazenda Escola / UEL
Amostras a serem coletadas	Camundongos: Plasma, patas, linfonodo poplíteal, estômago, fígado. Ovino: Sangue

Cumpre orientar que caso pretendam-se quaisquer alterações no protocolo experimental aprovado, deve-se submeter o novo protocolo à apreciação da CEUA/UEL anteriormente à execução das modificações.

Coloco-me á disposição para quaisquer esclarecimentos que se fizerem necessária. Sem mais para o momento, subscrevo, cordialmente,

Profa. Dra. Glaura Scantamburlo Alves Fernandes
Coordenadora da CEUA/UEL

Ilmo. Sr.
Prof. Dr. Wander Rogério Pavanelli
Coordenador do Projeto
Departamento de Ciências Patológicas / Centro de Ciências Biológicas
Com cópia para Diretor da Fazenda Escola/UEL, Chefe do Departamento de Ciências Patológicas e Diretor(a) do Centro de Ciências Biológicas

Campus Universitário: Rodovia Celso Garcia Cid (PR 445) km 380   Fone (043) 3371 4000 PABX   Fax 3328 4440   Caixa Postal 10.011   CEP 86057 970   Internet http://www.uel.br
LONDRINA   PARANÁ   BRASIL